

**KANSAS GEOLOGICAL SURVEY
OPEN-FILE REPORT 93-7**

**STREAM-AQUIFER MODELING AND PRELIMINARY MINERAL
INTRUSION ANALYSIS OF THE LOWER RATTLESNAKE CREEK
BASIN WITH EMPHASIS ON THE QUIVIRA NATIONAL WILDLIFE
REFUGE, KANSAS**

by

**Marios Sophocleous
Samuel P. Perkins**

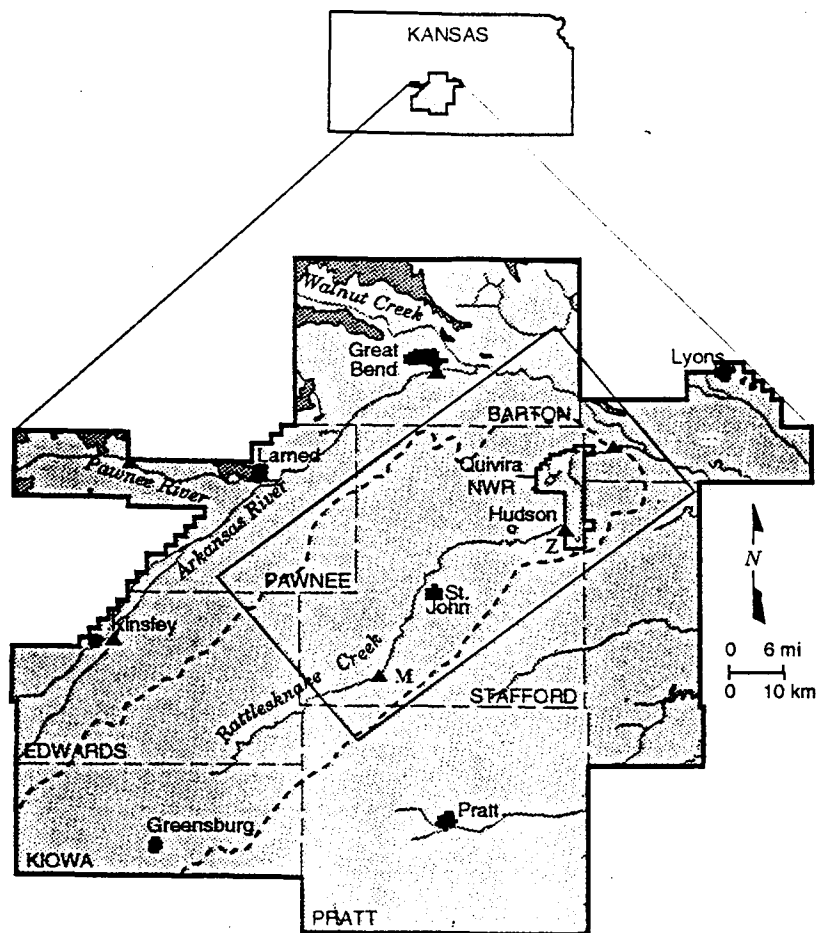
Disclaimer

The Kansas Geological Survey does not guarantee this document to be free from errors or inaccuracies and disclaims any responsibility or liability for interpretations based on data used in the production of this document or decisions based thereon. This report is intended to make results of research available at the earliest possible date, but is not intended to constitute final or formal publications.

Kansas Geological Survey
1930 Constant Avenue
University of Kansas
Lawrence, KS 66047-3726

Kansas Geological Survey

Stream-aquifer modeling and preliminary mineral intrusion analysis of the lower Rattlesnake Creek basin with emphasis on the Quivira National Wildlife Refuge, Kansas



Marios Sophocleous
and Samuel P. Perkins

Open-File Report 93-7

GEOHYDROLOGY



Stream-aquifer modeling and preliminary mineral intrusion analysis of the lower Rattlesnake Creek basin with emphasis on the Quivira National Wildlife Refuge

by

Marios Sophocleous and Samuel P. Perkins
Kansas Geological Survey

Open-File Report 93-7
May 1993

Contents

Abstract	1
I. Statement of the problem	1
II. Purpose and objectives	8
III. Hydrogeology and Pleistocene history of the Great Bend Prairie with emphasis on the study area	9
IV. Methodology and data analysis results	18
Compilation and analysis of existing information	18
Bedrock and predevelopment water table maps	18
Soils	18
Water rights	21
Rattlesnake Creek streamflows	24
Climate	24
Water table maps	30
Field data collection	30
Water-level survey	30
Geophysical logging	32
Drilling	32
Saltwater-freshwater interface monitoring	39
Water quality of the Quivira marsh	39
Numerical modeling	42
Calibration	44
Regression problem	45
Sources of error in ground-water data	47
Numerical regression solution procedure	48
Assumptions for the regression analysis	50
V. Model implementation and calibration	51
Grid selection	51
Boundary conditions	51

Model stresses	53
Groundwater pumpage	53
Incoming streamflows	53
Aquifer-related data	55
Aquifer base	55
Predevelopment and other water levels	56
Hydrogeologic properties	56
Recharge data	56
Ground-water evapotranspiration	57
Stream-related data	57
Calibration	57
Steady-state calibration	58
Transient-state calibration	58
VI. Initial simulation results and model analysis	60
Predevelopment (steady-state) conditions	60
Water budget	65
Transient-state simulations for the stream-aquifer system	69
Sensitivity analysis and initial predictive runs	81
Sensitivity of ground-water levels to changing aquifer and input parameters	84
Sensitivity of streamflows to changing aquifer, input, and stream parameters	84
VII. Revised simulation results and model analysis	90
Further sensitivity analysis	106
Refined-grid modeling of the Quivira National Wildlife Refuge	109
VIII. Management alternatives	109
Climatic fluctuations set of scenarios	111
Stream corridor set of scenarios	111
IX. Summary and conclusions	122
Acknowledgments	124
References	125
Appendices	129
Appendix 1. Ground-water rights in the Rattlesnake Creek study area	129
Appendix 2. Well records for the Sittner and Figger sites	161
Appendix 3. Chemical analyses of the waters of the Quivira National Wildlife Refuge	164
Appendix 4. X-ray analyses of rock and sediment samples from the Big Salt Marsh and the bedrock outcrop	166
Appendix 5. Revised model ground-water and streamflow sensitivities to varying stream-aquifer and input parameters	168
Appendix 6. Refined-grid modeling of the immediate vicinity of the Quivira National Wildlife Refuge	189

Figures

- Figure 1. Study area. 3
- Figure 2. (a) Annual precipitation and Arkansas River streamflows at Great Bend. (b) Appropriated cumulative ground-water rights in the GMD5. (c) Two long-term observation well hydrographs. 4
- Figure 3. Average annual streamflows of Rattlesnake Creek at the Macksville, Zenith, and Raymond gaging stations and annual precipitation at Hudson. 5
- Figure 4. Bedrock geology of the Great Bend Prairie. 11
- Figure 5. Geologic cross section passing through the Big Salt Marsh. 13
- Figure 6. Specific-conductance survey along Rattlesnake Creek. 15
- Figure 7. Bedrock contour map of the study area and inferred paleochannels. 17
- Figure 8. Predevelopment water table map of the study area. 19
- Figure 9. Soil association map of the study area. 20
- Figure 10. Ground-water rights map of the study area and vicinity. 22
- Figure 11. Ground-water rights issued in the study area versus time. 23
- Figure 12. Average annual streamflows of Rattlesnake Creek at the (a) Macksville, (b) Zenith, and (c) Raymond gaging stations. 25
- Figure 12a. Average monthly streamflows and minimum desirable streamflows for the Rattlesnake Creek at Macksville gaging station. 26
- Figure 12b. Average monthly streamflows and minimum desirable streamflows for the Rattlesnake Creek at Zenith gaging station. 27
- Figure 12c. Baseflow separation for the Rattlesnake Creek at Macksville gaging station using three baseflow separation techniques (fixed interval; local minimum; and sliding interval). 28
- Figure 12d. Baseflow separation for the Rattlesnake Creek at Zenith gaging station using three baseflow separation techniques (fixed interval; local minimum; and sliding interval). 29
- Figure 13. Average (1980–1990) annual precipitation contour map of the study area and vicinity. 31
- Figure 14. January 1991 water table contour map of the study area and vicinity. 33
- Figure 15. January 1991 depth to water-table contour map of the study area and vicinity. 34
- Figure 16. Observed ground-water level changes from predevelopment (c. 1955) to January 1991. 35

- Figure 17. Location of saltwater-freshwater interface monitoring wells and water-quality sampling stations. 36
- Figure 18. Lithology and gamma-ray log of the Sittner observation well. 37
- Figure 19. Lithology and gamma-ray log of the Figger observation well. 38
- Figure 20. Specific-conductance depth profile at the Sittner and Figger wells. 40
- Figure 21. Finite-difference grid of the model area. 52
- Figure 22. Model stresses versus time. 54
- Figure 23. Hydraulic conductivity zonation of the model area. 59
- Figure 24. Ground-water recharge zonation of the model area. 61
- Figure 25. Ground-water evapotranspiration zonation of the model area. 62
- Figure 26. Comparison of observed and simulated steady-state water table contours. 64
- Figure 27. Steady-state residuals versus predicted hydraulic head. 66
- Figure 28. Contours of steady-state residuals. 67
- Figure 29. Probability plot of steady-state residuals. 68
- Figure 30. Comparison of observed and model-predicted January 1991 water table contours. 70
- Figure 31. 1990 residuals versus predicted hydraulic head. 71
- Figure 32. Contours of 1990 residuals. 72
- Figure 33. Probability plot of 1990 residuals. 73
- Figure 34. Comparison of predicted Rattlesnake Creek baseflow and streamflow at the Zenith gaging station versus time. 74
- Figure 35. Model-predicted 1990 gaining and losing stretches of Rattlesnake Creek. 77
- Figure 36. Time distribution of the water-balance components during the 1955–1990 simulation period. 79
- Figure 37. Water table profiles near Macksville, Hudson, and Big Salt Marsh. 80
- Figure 38. Water table profiles near St. John and in between the Little and Big Salt Marsh. 82
- Figure 39. Simulated ground-water-flow vectors for predevelopment (1955) and present-day conditions (1990). 83
- Figure 40. Sensitivity plots of drawdown with changing pumpage, recharge, storativity, hydraulic conductivity, and ground-water evapotranspiration near Hudson. 85

- Figure 41. Sensitivity plots of drawdown with changing pumpage, recharge, storativity, hydraulic conductivity, and ground-water evapotranspiration near St. John. 86
- Figure 42. Sensitivity plots of drawdown with changing pumpage, recharge, storativity, hydraulic conductivity, and ground-water evapotranspiration north of Zenith. 87
- Figure 43. Sensitivity plots of stream baseflow with changing input, aquifer, and stream-related parameters near Zenith stream-gaging station. 88
- Figure 44. Sensitivity plots of stream baseflow with changing input, aquifer, and stream-related parameters southwest of St. John. 89
- Figure 45. Model-predicted stream-baseflow declines during the 1991–2010 period. 91
- Figure 46. Ground-water evapotranspiration zonation of the model area. 93
- Figure 47. 1955–1990 temporal evolution of water-balance components of the revised simulation. 96
- Figure 48. Predevelopment and present-day water budgets for the original and revised simulations of the Rattlesnake Creek–Quivira model area. 98
- Figure 49. Appropriated ground-water-rights density throughout the model grid. 100
- Figure 50. Comparison of revised model results for observed and simulated predevelopment water table contours. 101
- Figure 51. Comparison of revised model results for observed and simulated developed-conditions water table contours for January 1991. 102
- Figure 52. Comparisons of revised model results for observed and simulated water table contours for January 1978. 103
- Figure 53. Comparison of measured and averaged (model input) streamflows versus model-simulated streamflows of the Rattlesnake Creek at the Zenith gaging station for the original and revised simulations. 104
- Figure 54. Model-predicted Rattlesnake Creek streamflow declines during the 1991–2010 period for the original and revised simulations. 105
- Figure 55. Areal variation in transient-state model scaled recharge sensitivities for the intermediate and high recharge zones. 107
- Figure 56. Areal variation in transient-state model scaled hydraulic conductivity sensitivities for the intermediate zone and scaled storativity sensitivities. 108
- Figure 57. Base-case water table drawdown versus time. 110
- Figure 58. Flood-drought and drought-flood-cycle streamflows at the model entry point and the Zenith streamgaging station. 112
- Figure 59. Effect of streamflow climatic cycles on aquifer near St. John and Hudson. 113

- Figure 60. Effect of streamflow climatic cycles on aquifer near St. John and Hudson assuming complete pumping moratorium for the next 20 years. 114
- Figure 61. Predicted effect of different management scenarios on Rattlesnake Creek streamflows at Zenith gaging station. 115
- Figure 62. Predicted effect of reach-by-reach Rattlesnake Creek streamflow recovery for the case of complete pumpage moratorium for the 1991–2010 period. 118
- Figure 63. Three-mile and 5-mile stream corridors around Rattlesnake Creek within the model area. 119
- Figure 64. Predicted reach-by-reach Rattlesnake Creek streamflow gains or losses with time for the base or status quo case, 3-mile, and 5-mile stream corridors with pumping moratoria. 120
- Figure 65. Predicted effect of additional management options on Rattlesnake Creek streamflows at Zenith gaging station. 121

Tables

- Table 1. Generalized columnar section of geologic units and their water-bearing properties. 10
- Table 2. Selected chemical characteristics of the Quivira National Wildlife Refuge waters. 41
- Table 3. Stress periods employed in the model. 55
- Table 4. Steady-state analysis results. 63
- Table 5. Volumetric water budget for model area under predevelopment conditions (c. 1955). 75
- Table 6. Transient 1955–1990 analysis results. 75
- Table 7. Volumetric water budgets for the last stress period (1988–1990) of the transient 1955–1990 simulation. 76
- Table 8. Revised steady-state analysis results. 92
- Table 9. Revised volumetric budget for entire model area under predevelopment conditions (c. 1955). 94
- Table 10. Revised transient 1955–1990 analysis results. 95
- Table 11. Revised volumetric water budgets for the last stress period (1988–1990) of the transient 1955–1990 simulations. 95
- Table 12. Management alternatives considered for the lower Rattlesnake Creek model area. 116
- Table 13. Management scenarios for enhancing streamflows in Rattlesnake Creek. 117

Stream-aquifer and mineral intrusion modeling of the lower Rattlesnake Creek basin with emphasis on the Quivira National Wildlife Refuge

by

Marios Sophocleous and Samuel P. Perkins
Kansas Geological Survey

Open-File Report 93-7
May 1993

Abstract

We address the problem of declining streamflows in interconnected stream-aquifer systems and explore possible management options to address the problem for the lower Rattlesnake Creek–Quivira National Wildlife Refuge area. The approach we followed was to implement, calibrate, and partially validate a stream-aquifer numerical model combined with a parameter estimation package and sensitivity analysis. Hydrologic budgets for both predevelopment and developed conditions indicate significant differences in the hydrologic components of the study areas resulting from development. The predevelopment water budgets give an estimate of natural ground-water recharge, whereas the developed-conditions budgets give an estimate of induced recharge, indicating that major ground-water development changes the recharge-discharge regime of the model area with time. Such stream-aquifer models link proposed actions to hydrologic effects, as clearly demonstrated by the effects of various management alternatives on the streamflows of Rattlesnake Creek. Thus we show that a possible means of restoring specified streamflows in the area is to implement protective stream corridors with restricted ground-water extraction.

I. Statement of the problem

Many regions of western and central Kansas have experienced significant ground-water and streamflow declines, especially during the last two decades (Sophocleous, 1981; Sophocleous and McAllister, 1987, 1990; among others). According to the Kansas Water Office (KWO), extensive ground-water appropriations in the Big Bend Prairie (fig. 1) have contributed to extreme

low flows in the Arkansas River and Rattlesnake Creek (Water Research Needs Conference, Wichita, Kansas, Nov. 14, 1984). Also, according to the Kansas Department of Wildlife and Parks, fish and wildlife resources in and along the Arkansas River, the Smoky Hill River, the Pawnee River, Rattlesnake Creek, and other streams in western and south-central Kansas have been significantly affected because of losses of baseflows (Water Research Needs Conference, Wichita, Kansas, Nov. 14, 1984).

Figures 2 and 3 summarize the general hydrologic state of the Great Bend Prairie region. Figure 2 depicts annual streamflows of the Arkansas River at Great Bend together with annual precipitation in Great Bend (fig. 2a), the number of ground-water rights issued in the Big Bend Groundwater Management District No. 5 (GMD5) over time (fig. 2b), and two long-term ground-water-level observation well hydrographs in the area (fig. 2c). Figure 3 depicts the Rattlesnake Creek annual streamflows for the period of record at the Macksville and Zenith gaging stations together with the annual precipitation at Hudson, in northeast Stafford County. Both figs. 2 and 3 indicate streamflow and ground-water declines with time, with precipitation patterns and amounts showing no corresponding declines and ground-water rights showing a dramatic increase over the same period of time.

In 1983 the Kansas legislature passed the minimum instream flow law, which requires that minimum desirable streamflows be maintained in different streams in Kansas, including Rattlesnake Creek. According to the Kansas Water Plan document (Kansas Water Plan, subsection: Minimum Desirable Streamflows, FY1990; KWO, July 1988): "The safe yield policy of Groundwater Management District No. 5 has not protected low flows in the [Rattlesnake] Creek." Implementation of this law certainly requires a better understanding of the stream-aquifer system. According to the Division of Water Resources (Water Research Needs Conference, Wichita, Kansas, Nov. 14, 1984), a more thorough understanding of this stream-aquifer relationship would allow quantitative determination of the effect of ground-water withdrawals on streamflows and would be valuable in the administration of the minimum desirable streamflow program.

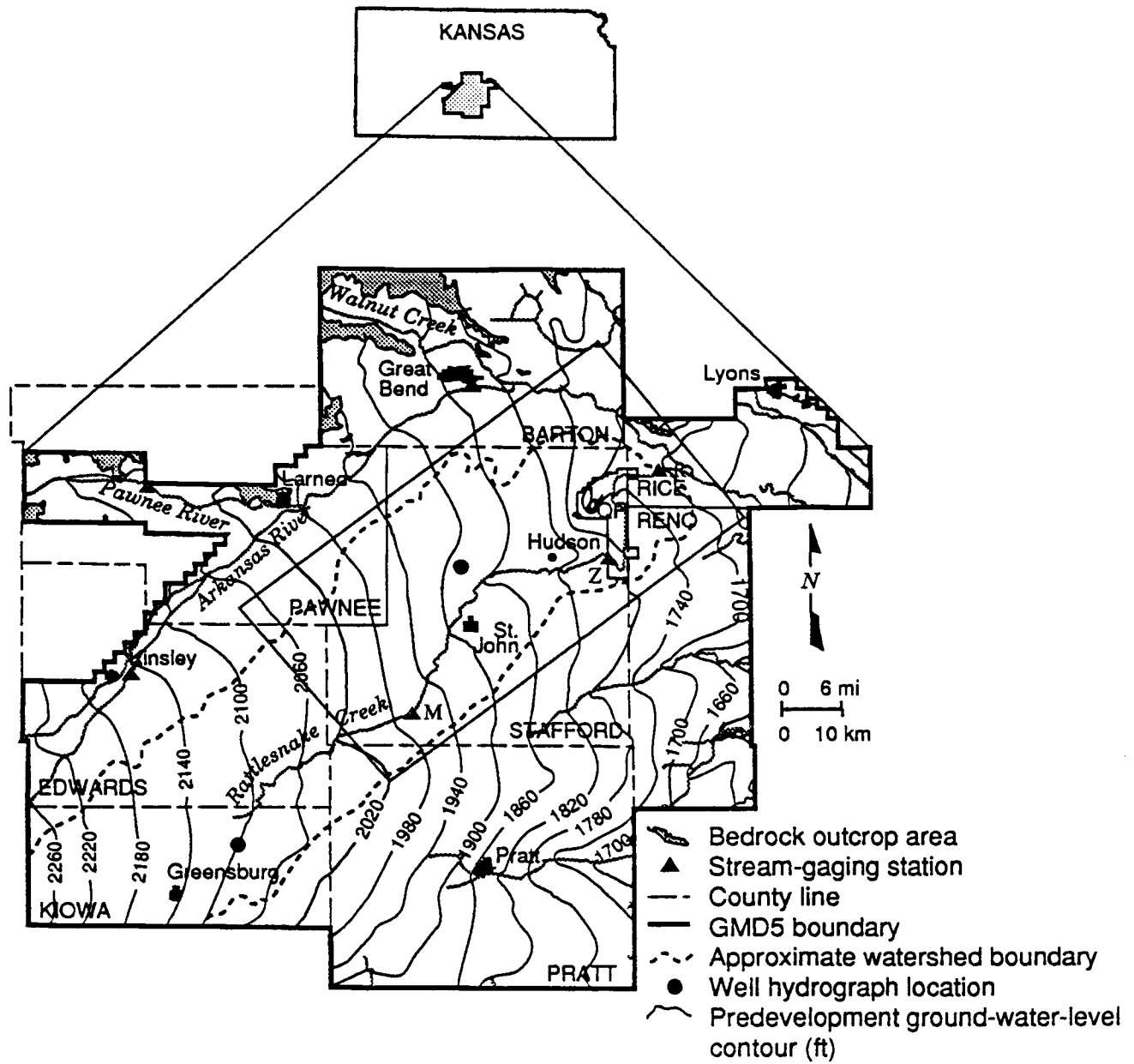


Figure 1. Study area. Diagonal box encompasses the model area. Uppercase letters denote stream-gaging stations (M, Macksville; Z, Zenith; R, Raymond). Contours represent the predevelopment (1940's and 1950') water table elevation in feet above mean sea level.

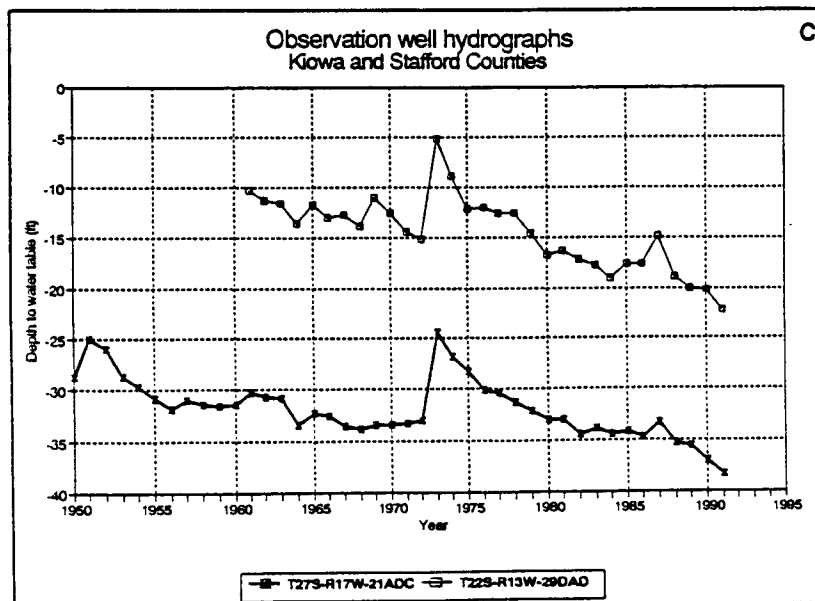
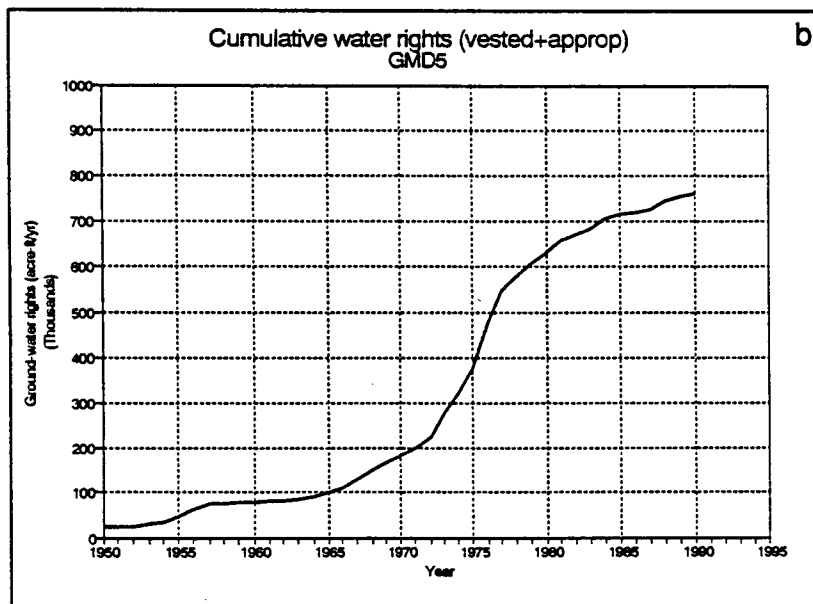
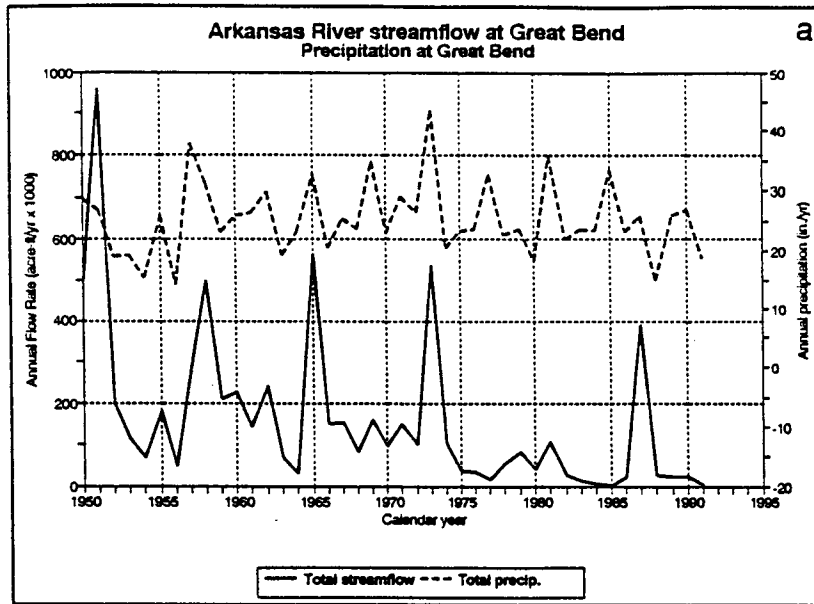


Figure 2. (a) Annual precipitation and Arkansas River streamflows at Great Bend. (b) Appropriated cumulative ground-water rights in GMD5. (c) Two long-term observation well hydrographs in the study area (see fig. 1 for well locations).

Rattlesnake Cr Strflows & Hudson Precip
 Macksville, Zenith, Raymond Gaging Sta.

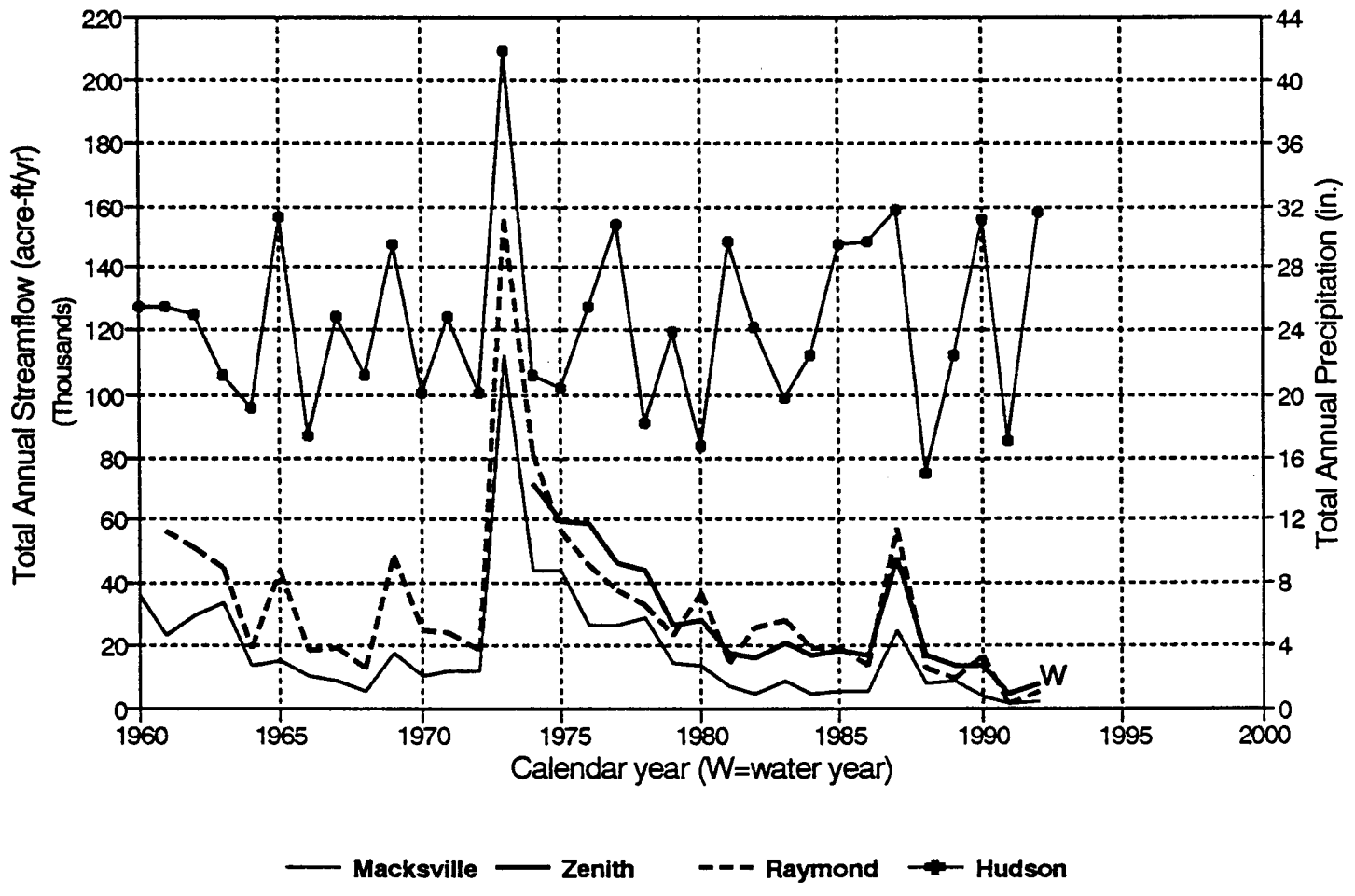


Figure 3. Average annual streamflows of Rattlesnake Creek at the Macksville, Zenith, and Raymond gaging stations and annual precipitation at Hudson, west of the Little Salt Marsh.

The two major central Kansas wetlands—the Cheyenne Bottoms Wildlife Area and the Quivira National Wildlife Refuge, both of which are classified as "outstanding natural resource areas of unique significance" [KAR 28-16c(3)]—are being threatened because of decreasing water supplies and probably deteriorating water quality. The quality of ground and surface waters is deteriorating mainly because of suspected increased natural nonpoint mineral intrusion from underlying geologic formations; this increased mineral intrusion is considered to be a consequence of freshwater declines in the Quaternary alluvial aquifers of central Kansas. Natural conditions, such as low streamflows and mineral intrusion, result in violations of the dissolved oxygen, chloride, fluoride, and metals criteria for streams during the summer months in several parts of Kansas. According to Fromm and Wilk (1988), streams in central Kansas overlying the Permian red beds and Wellington Formation have elevated levels of metals and selenium. In addition to natural conditions, past and current oil and gas production activities have increased the mineral content of some streams. According to the same report (Fromm and Wilk, 1988), the monitoring station on Rattlesnake Creek at Raymond indicates that the 35.4 river miles of the creek governed by that monitoring station are threatened because of the high concentrations of fecal coliform and salt, which are due to agricultural non-point-source pollution and natural saltwater intrusion.

The Quivira National Wildlife Refuge (NWR), which covers approximately 21,280 acres in northeast Stafford County, is a major stopover point for migratory birds in the Central Flyway. The refuge was established in 1955 and obtained a permit to divert up to 22,000 acre-ft of water per year from Rattlesnake Creek (presumably this water right has not yet been verified). A review of existing water rights in the Rattlesnake Creek basin as of December 31, 1966 (Stramel, 1967), indicated that more water rights had already been filed in the basin than there was water in the stream, and the applications for irrigation rights were increasing. According to Stramel (1967):

Development of groundwater in Rattlesnake Creek basin will theoretically, in time, reduce the Creek to a wet weather stream. This results because ground water that normally flows to Rattlesnake Creek will be intercepted by pumping and the base flow of the stream will be intercepted.... Irrigators have already decided to develop the groundwater, and much additional irrigation is expected.... It will be impossible to

fully develop the groundwater resources of Rattlesnake Creek basin and not dry up the baseflow of the Creek.... Thus, the drying of Rattlesnake Creek is inevitable. You simply cannot have one without the other. (p. 10–13)

However, the Rattlesnake Creek is the source of water for the Quivira NWR, a critical habitat for several endangered species of birds and, as mentioned, a major stopover point for thousands of migratory birds. Any major changes in the quantity or quality of river flow can upset the delicate balance necessary for the survival of the Quivira ecological system. Furthermore, a Rattlesnake Creek fish investigation by the Kansas Department of Wildlife and Parks (Ray and Coslett, 1972) concluded that

inadequate flow appears to be the most important limiting factor in establishing and maintaining a sport fishery in Rattlesnake Creek.... If the Rattlesnake Creek sport fishery is to survive, effective legislation restricting present use and limiting further exploitation of ground-water supplies within the basin must be enacted. A detailed ground-water and hydrologic study is needed to provide information upon which the design of a balanced water-use schedule can be developed so that adequate stream flow is insured. (p. 27)

This study was undertaken to address some of these water issues affecting the Quivira NWR. The study area encompasses an approximately 560-square-mile area of the lower Rattlesnake Creek watershed predominantly in Stafford County but also includes portions of other counties, such as Pawnee, Barton, Rice, and Reno (fig. 1). The study area encompasses all three existing stream-gaging stations on the Rattlesnake Creek, namely, the Macksville, Zenith, and Raymond stations.

The remainder of this report is organized into eight parts: (1) purpose and objectives, (2) brief hydrogeology of the study region, (3) methodology employed and basic data analysis, (4) model implementation and calibration, (5) numerical modeling results and related analysis, (6) revised simulation results and model analysis, (7) management alternatives, and (8) summary and conclusions. The more technical, mathematical parts of section IV can be skipped without a loss of continuity.

II. Purpose and objectives

The availability of adequate amounts of water of suitable quality directly affects the future of the Quivira NWR and the economic development of the Rattlesnake Creek basin and hence the welfare of the people living in the region. It should be noted that most of the developable water in Kansas has already been developed, and the future water management in Kansas will depend heavily on obtaining more mileage from existing supplies. Sustaining solutions must be based on fundamentally sound hydrologic endeavors and related technology. Therefore the broad goals of this proposed research are to provide information and analysis to make better use of scarce water resources and to preserve or improve existing water quality. These two goals can be accomplished only through a basic understanding of the long-term behavior of the stream-aquifer system and development of an effective management policy. The specific objectives of this research are:

1. Analysis of the effects of overall regional appropriations and various pumping patterns on streamflows and aquifer water levels and a preliminary analysis of the effects of mineral intrusion from underlying geologic formations. Such analyses will involve development and application of a stream-aquifer numerical model for predicting streamflows and ground-water levels, given various pumping and drought scenarios; it will also involve field monitoring of the saltwater-freshwater interface.
2. Evaluation of the outlook for available surface-water and ground-water supplies to the Quivira NWR and development of strategies to maintain or enhance these supplies. The impacts on the Quivira refuge of recently established minimum streamflows in Rattlesnake Creek and continued water rights appropriations will be analyzed, especially if the Rattlesnake streamflows are less than the current or projected water requirements for properly managing the wetland.
3. Evaluation of the hydrologic effectiveness of management alternatives, including the determination of protective corridors around Rattlesnake Creek for possible water rights restrictions if streamflows fall below established minima or if drought conditions develop. We will test the hydrologic effectiveness of the protective corridor idea to see whether it will appreciably enhance the available water supplies for the refuge.

Because such management-oriented studies affect people's livelihoods, they are controversial. Therefore we believe that it is important to combine state-of-the-art parameter estimation procedures (inverse modeling; to be discussed later) with predictive modeling to obtain consistent, objective, and repeatable results against which to judge possible conflicting claims. In addition, these modeling procedures will enable managers and researchers to make intelligent use of all available data and information.

III. Hydrogeology and Pleistocene history of the Great Bend Prairie with emphasis on the study area

Knowing the geologic history, composition, and structure of the study area is a prerequisite to understanding the water-bearing and water-yielding properties of the modeled stream-aquifer system.

The Great Bend Prairie is covered with a veneer of loess deposits and sand dunes, with underlying Pleistocene alluvium forming the major aquifer of the area (Latta, 1950; Fader and Stullken, 1978). This alluvium was deposited by the ancestral Arkansas River and a small number of local streams and is composed of undifferentiated early Pleistocene sediments (the Meade formation, which consists of interbedded lenses of unconsolidated gravel, sand, and silt; caliche is common throughout the formation) and late Pleistocene sediments (the Sanborn formation, which consists of silt, sandy silt, and fine sand that locally contains lenses of coarse sand and gravel; Latta, 1950). The Pleistocene alluvium overlies Cretaceous and Permian bedrock. A generalized columnar section of the geologic units and their water-bearing properties is given in table 1 [from Fader and Stullken (1978)], and a bedrock geology map of the region is shown in fig. 4. The lower reaches of the Rattlesnake Creek and the Quivira Refuge represent a natural groundwater discharge area of both the unconsolidated Great Bend Prairie aquifer and the underlying bedrock aquifers.

Most of the Tertiary deposits that make up the Ogallala Formation were removed by erosion before Pleistocene material was deposited. The stratigraphy of the Quaternary alluvium in

Table 1. Generalized columnar section of geologic units and their water-bearing properties [from Fader and Stullken (1978)].

System	Geologic unit	Maximum thickness, in feet	Physical character	Remarks
Quaternary	Undifferentiated Pleistocene deposits	360	Unconsolidated deposits of sand and gravel with interbedded lenses of clay, silt, and caliche. Windblown silt (loess) and dune sand occur at the surface over most of the area. Stream-laid deposits (alluvium) of late Quaternary age ranging from clay to gravel occur along the principal stream valleys.	Comprises principal aquifer. Water generally is of good chemical quality but may be of poor chemical quality in the northeastern part of the area and in deep buried valleys in the southeastern part. Yields as much as 2,000 gal/min to wells.
	Ogallala Formation (Pliocene deposits)	65	Unconsolidated deposits of silt and fine sand with interbedded caliche. Some interbedded sand and gravel.	
Cretaceous	Undifferentiated Lower Cretaceous rocks	380	Upper unit (Dakota Formation) brown to gray fine- to medium-grained sandstone interbedded with gray sandy shale and varicolored shale. Middle unit (Kiowa Shale) dark gray to black shale interbedded with tan and gray sandstone. Lower unit (Cheyenne Sandstone) gray and brown fine- to medium-grained sandstone interbedded with dark gray shale.	Water probably of poor chemical quality. Yields 10 to 100 gal/min to wells locally in the western part of the area.
Permian	Undifferentiated Permian rocks	350	Interbedded reddish shale, siltstone, and sandstone with some beds of dolomite and anhydrite. Includes, in descending order, Whitehorse Formation, Dog Creek Formation, Blaine Formation, and Flower-pot Formation.	Water generally of poor chemical quality. May yield as much as 10 gal/min to wells.
	Cedar Hills Sandstone	200	Reddish shale, siltstone, silty shale and sandstone.	Sandstone may contribute highly mineralized water to the principal aquifer where the two units are in contact.
	Salt Plains Formation	300	Reddish-brown sandy siltstone and fine-grained sandstone.	May contribute highly mineralized water to the principal aquifer where the two units are in contact.
	Harper Sandstone	250	Brownish-red siltstone and silty shale with a few thin beds of silty sandstone. Kingman sandstone member is near the top of the formation.	Water may be of poor chemical quality. May yield no water or as much as 100 gal/min to wells in the eastern part of area.
	Stone Corral Formation	20	White and light-gray anhydrite and dolomite.	Not known to yield significant amounts of water to wells in the area.
	Ninnescah Shale	400	Red and grayish-green shale siltstone and very fine grained silty sandstone.	May yield water of fair to poor chemical quality to wells in the outcrop areas.
	Wellington Formation	550	Calcerous gray and blue shale containing several thin beds of limestone, gypsum, and anhydrite. The Hutchinson Salt Member, when present, is near the middle of the formation.	Not known to yield significant amounts of water to wells in the area.

*Chemical quality of water is classed as good if the concentration of dissolved solids is less than 500 mg/L (milligrams per liter) or the concentrations of chloride and sulfate are less than 250 mg/L, fair if dissolved solids are 500 to 1,000 mg/L or chloride and sulfate are 250 to 500 mg/L, and poor if dissolved solids are greater than 1,000 mg/L or chloride and sulfate are greater than 500 mg/L.

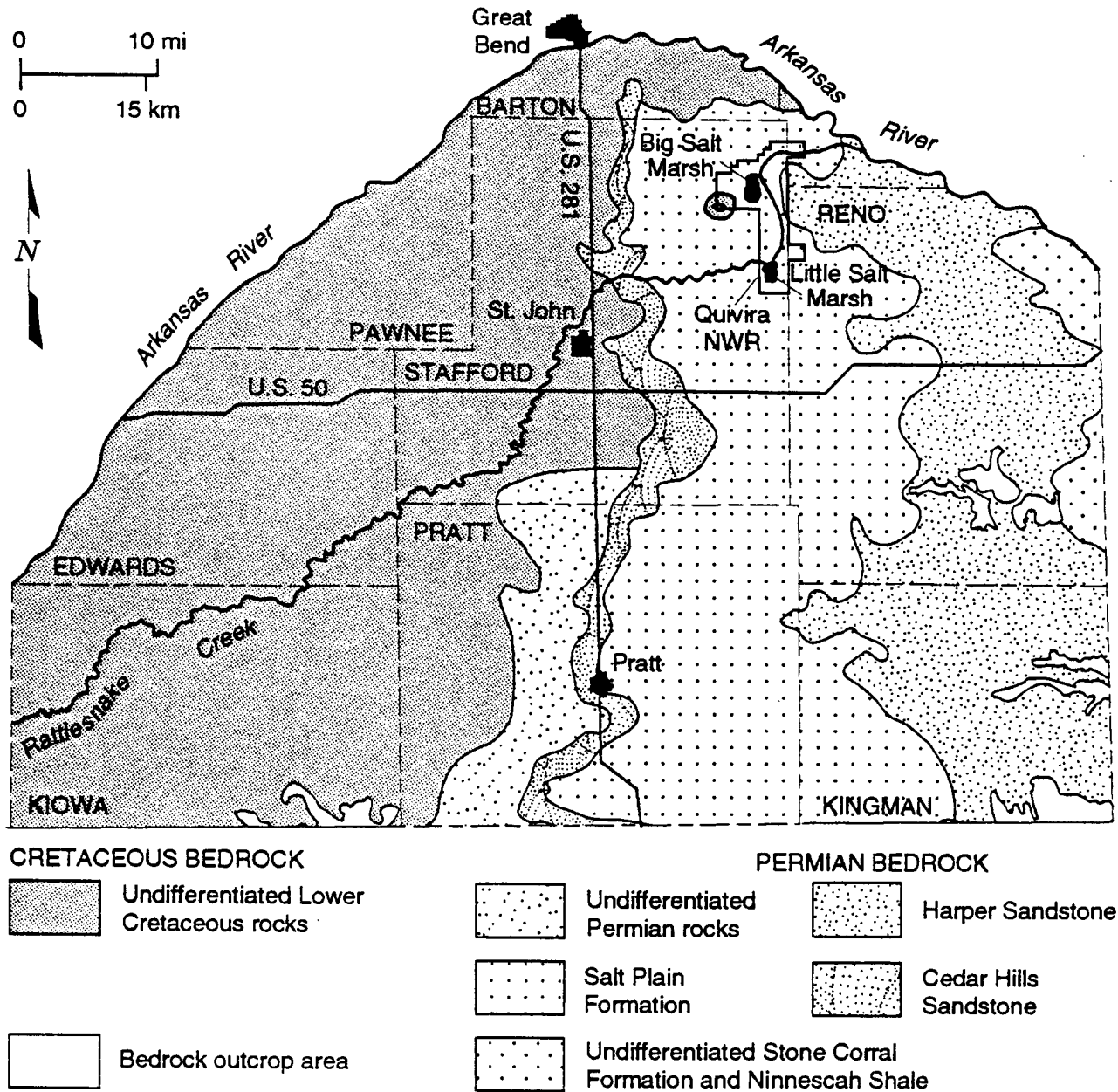


Figure 4. Bedrock geology of the Great Bend Prairie [adapted from Fader and Stullken (1978)].

descending order is generally (1) sand dunes; (2) a relatively continuous near-surface silt-clay bed, probably a loess deposit; (3) alternating sequences of fining-upward sandy silt-clay, and sand and gravel lenses (not always present); (4) a basal sand and gravel bed of fluvial origin; and (5) bedrock (Rosner, 1988).

The alluvium in the Rattlesnake Creek valley is relatively thin, probably less than 20 ft thick everywhere. It is composed chiefly of poorly sorted sand and gravel that was derived from the Meade formation. The alluvium is underlain by thick deposits of the Meade formation.

The flat areas of the Big and Little Salt Marshes in northeastern Stafford County are underlain by unconsolidated marsh deposits consisting of clay, silt, sand, and fine to medium gravel that were derived mostly from dune sand but also from the Meade formation and the Kiowa Shale. The maximum thickness of these deposits probably does not exceed 15 ft. The upper 1–2 ft consists of fossiliferous sand, silt, and clay, below which are layers of poorly sorted, silty and clayey, fine to coarse sand containing only minor amounts of fine to medium gravel (Latta, 1950).

A ridge of beach sand having a maximum thickness of 15 ft occurs along the eastern and southeastern sides of the intermittent lake that occupies the central part of the Big Salt Marsh. The beach sands are composed of fine to medium sand and are lithologically similar to the dune sand from which they were derived. They are not as well sorted as the dune sand and contain a larger amount of silt, clay, and coarse sand. Some medium to fine gravel is also found locally in the beach sands. The surface of the Big Salt Marsh, although seemingly flat, slopes gently toward an intermittent lake near the center of the marsh. The size of this lake depends entirely on the elevation of the water table. A geologic cross section passing through the Big Salt Marsh in an east to west direction is shown in fig. 5, from Latta (1950). A bedrock ridge trending roughly north-south beneath the Big Salt Marsh and the resulting thinning of the permeable water-bearing material is a major factor in the discharge of ground water there, according to Latta (1950).

The Permian bedrock subcrops along an approximately north-south trend near US–281 and constitutes a source of poor-quality (saline) water east of US–281 in northeast Stafford County (fig. 4). The Permian formations in the area, known as red beds, consist of reddish-brown

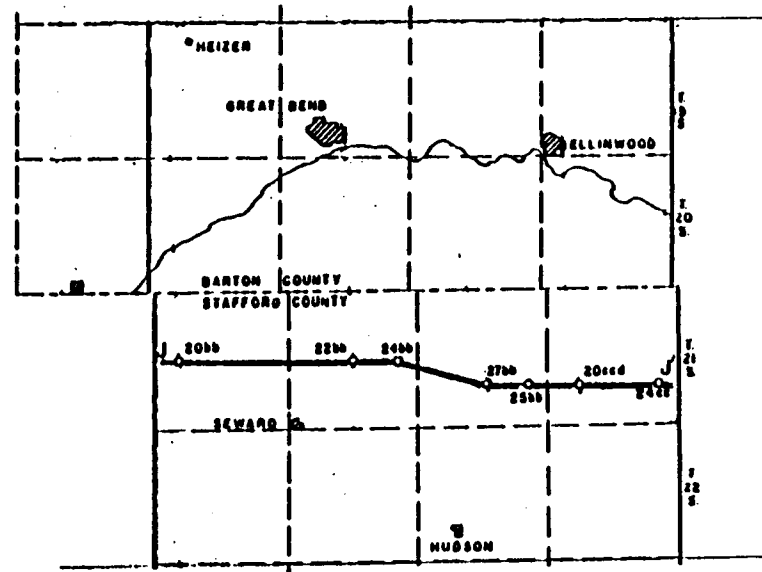
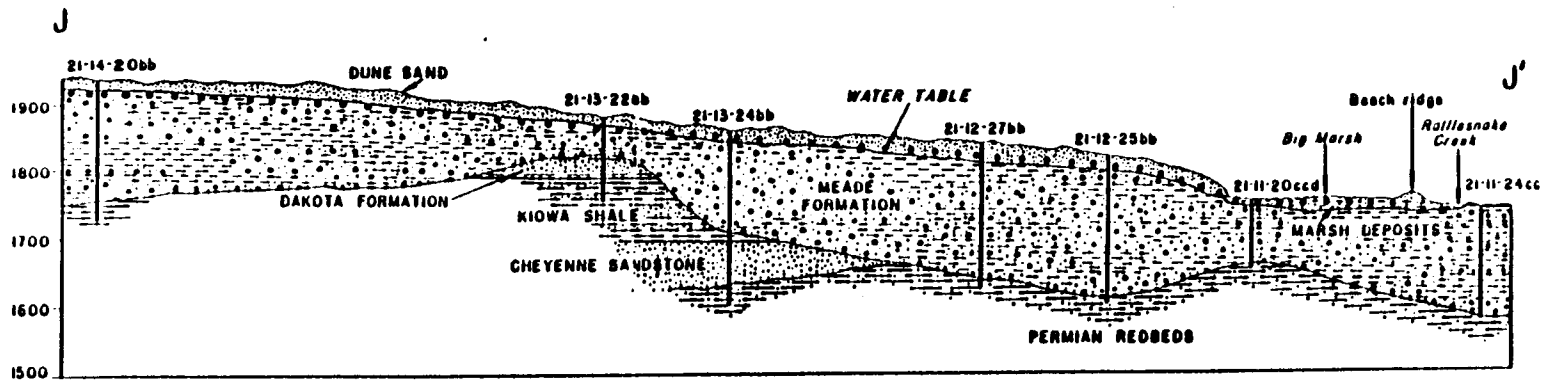


Figure 5. Geologic cross section passing through the Big Salt Marsh [from Latta (1950)].

sandstone, siltstone, shale, salt, gypsum, anhydrite, and limestone. The Permian deposits and especially the Late Permian red beds are a source of poor-quality water, which rises upward and increases the salinity of the water in the unconsolidated aquifer in the lower reaches of Rattlesnake Creek, in particular, the Quivira NWR area.

The mechanical details of the subsurface hydraulic relationships of the consolidated and unconsolidated deposits are not clearly understood. The average chloride load of flow in Rattlesnake Creek at its mouth is about 130 ton/d (U.S. Army Corps of Engineers, 1966). The water near the salt marshes is believed to be a natural occurrence of artesian saltwaters encountered deeper to the west. The saltwater flows from the edges of the bedrock formation into the overlying sediments and rises to the surface in the low areas, primarily along Rattlesnake Creek. The upper reaches of Rattlesnake Creek yield fairly good quality water with little chloride pollution from natural sources. A 1983 electrical conductivity survey of Rattlesnake Creek (Bidleman, 1983) (fig. 6) indicates that conductivity from eastern Edwards County to just northeast of St. John ranged from 350 $\mu\text{S}/\text{cm}$ to approximately 625 $\mu\text{S}/\text{cm}$. An abrupt rise in conductivity was observed within a 3-mi distance, 1 mi east of where Rattlesnake Creek crosses US-281, with values leveling off at 3,000–4,000 $\mu\text{S}/\text{cm}$. Note that the brine-saturated Permian bedrock directly subcrops the Great Bend Prairie aquifer from here eastward. Where the creek enters the Quivira NWR, another rise in conductivity occurs, with an abrupt increase to values exceeding 20,000 $\mu\text{S}/\text{cm}$ within a 2-mi stretch (fig. 4). Before discharging into the Arkansas River, however, the creek's conductivity drops to 3,141 $\mu\text{S}/\text{cm}$. Most of the pollution is from small seeps or marshes in and near the streambed.

Rocks of Cretaceous age form the bedrock surface in the western part of the Great Bend Prairie. These rocks consist of interbedded shales, sandy shales, and fine- to coarse-grained sandstones (Fader and Stullken, 1978). Of the three Cretaceous units (see table 1), only the lower unit (Cheyenne Sandstone) is a potential source of water to large-capacity wells, but the water is believed to be highly mineralized (Fader and Stullken, 1978). The Kiowa Shale is the oldest formation exposed in the Rattlesnake Creek watershed (in the northwestern part of T. 22 S.,

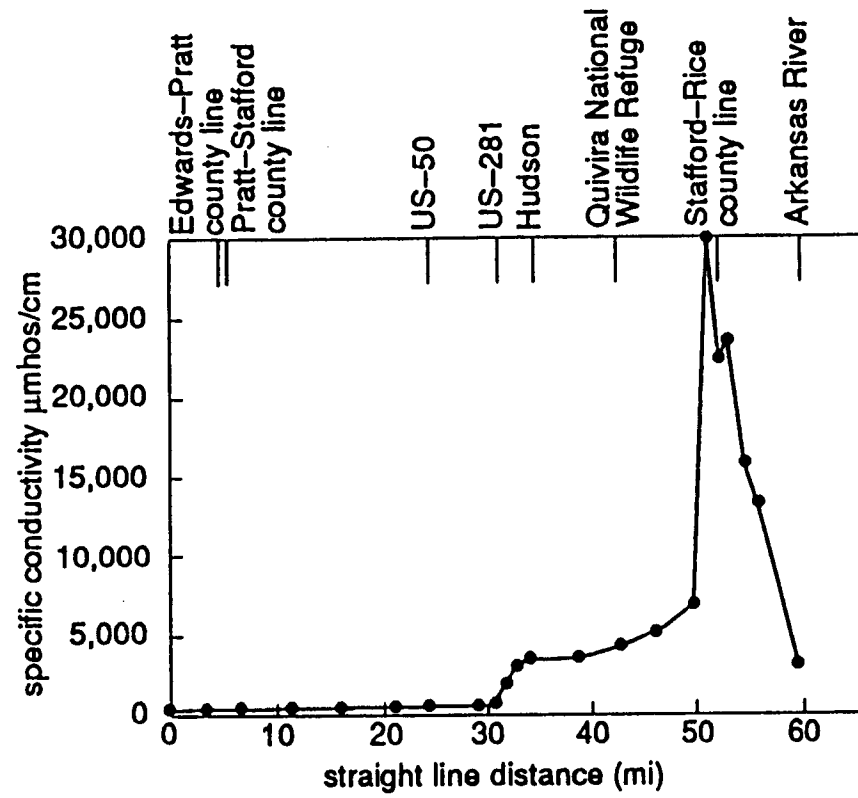


Figure 6. Specific conductance survey along Rattlesnake Creek [adapted from Bidleman (1983)].

R. 11 W., northeastern Stafford County), where it consists of dark fossiliferous shale and rusty sandstone. The overlying Dakota Formation is not exposed in the study area.

In general, the present drainage system of central Kansas is the result of events that took place during the Pleistocene Epoch. The Pleistocene history of the area is complex and is marked by the cutting and filling of deep valleys and by major changes in drainage (Fent, 1950; Frye and Leonard, 1952). During early Pleistocene time, the ancestral Arkansas River, instead of following its present course around the great bend, probably flowed eastward or southeastward across south-central Kansas. This can be seen on the bedrock map of the area (Sophocleous et al., 1990), in which a number of west-east paleodrainage channels progress from south to north throughout the basin, as is shown in fig. 7.

The Pleistocene drainage patterns of central Kansas record the history of the northeastward migration of through-flowing streams from the Rocky Mountain area. According to Fent (1950), this migration was caused by successive captures of the southern trunk of the ancestral stream by its own northern tributaries. The captures seem to have resulted from the difference in the debris load available in the headwater areas of the streams. Throughout the Pleistocene, through-flowing streams originating from the Rocky Mountains, such as the Arkansas River, filled their channels with coarse gravel and sandy alluvium derived from igneous rocks. This material built up the surface over which the streams flowed, causing stream avulsions and the consequent spreading of alluvial material over wide areas. In contrast, the northern tributaries to the southern trunk stream carried only the finer grained, less permeable sediment load obtained by downcutting in their immediate headwater areas. The silt and fine-grained sand of local origin in the northern Great Bend Prairie, with its low permeability, favored runoff and consequently more erosion and downcutting to below the level of the through-flowing streams; this downcutting led to the eventual capture of the through-flowing streams. This is evident in the relative abundance of northern tributaries to the Arkansas River in central Kansas (Fent, 1950).

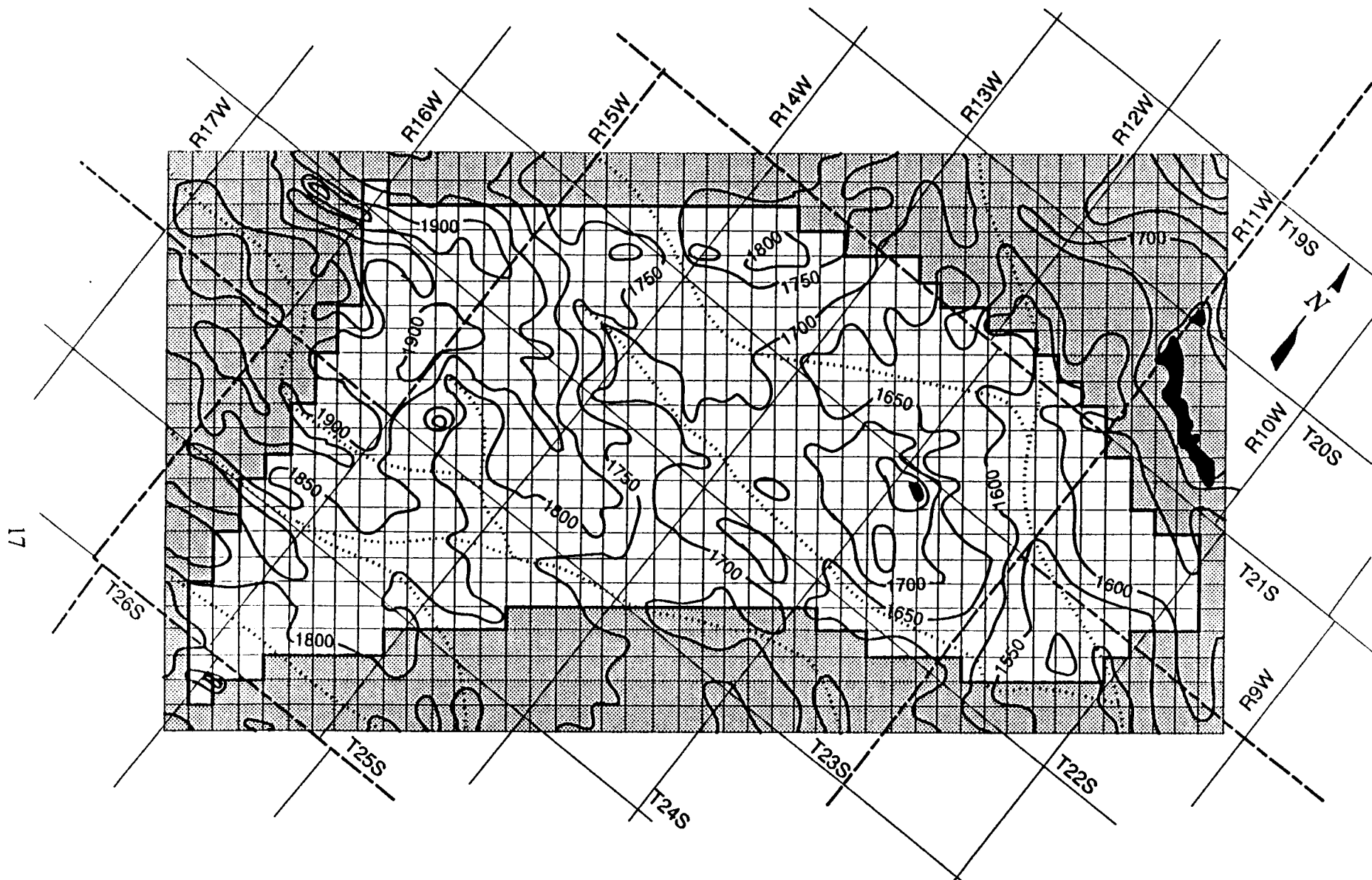


Figure 7. Bedrock contour map of the study area. Contour interval 50 ft. Dotted lines indicate inferred paleochannel traces.

IV. Methodology and data analysis results

The methodology we employed in this study consists of three approaches: (1) compilation and analysis of existing information, (2) limited field data collection, and (3) numerical modeling. A brief summary of the main components of each approach together with some basic data analysis follows.

Compilation and analysis of existing information

Bedrock and predevelopment water table maps

A comprehensive bedrock and predevelopment water table map for the Great Bend Prairie region (in which the study area belongs) based on all data accessible or known to us has been prepared and documented by Sophocleous et al. (1990). A bedrock map and a predevelopment water table map of the study area [extracted from Sophocleous et al. (1990)] are shown in figs. 7 and 8, respectively. A number of inferred paleochannels are noted on the bedrock surface map (Sophocleous et al., 1990), the geologic origin of which was outlined in section III. The inferred paleochannels within the model region are also indicated in fig. 7.

Soils

A soils map of the lower Rattlesnake Creek watershed from near the Macksville stream-gaging station to the confluence with the Arkansas River has been constructed based on Soil Conservation Service (SCS) digitized GIS soil coverages (STATSGO) (fig. 9). The soils of the watershed formed in several different kinds and ages of parent material, such as sand, loess, and Pleistocene and Holocene sediments.

In early Pleistocene time, alluvium (Meade formation) was deposited over most of the watershed. Soils formed in this old wind-modified alluvium include the Farnum, Blanket, and Lubbock soils (Roth, 1973). Carwile soils also formed in old alluvium.

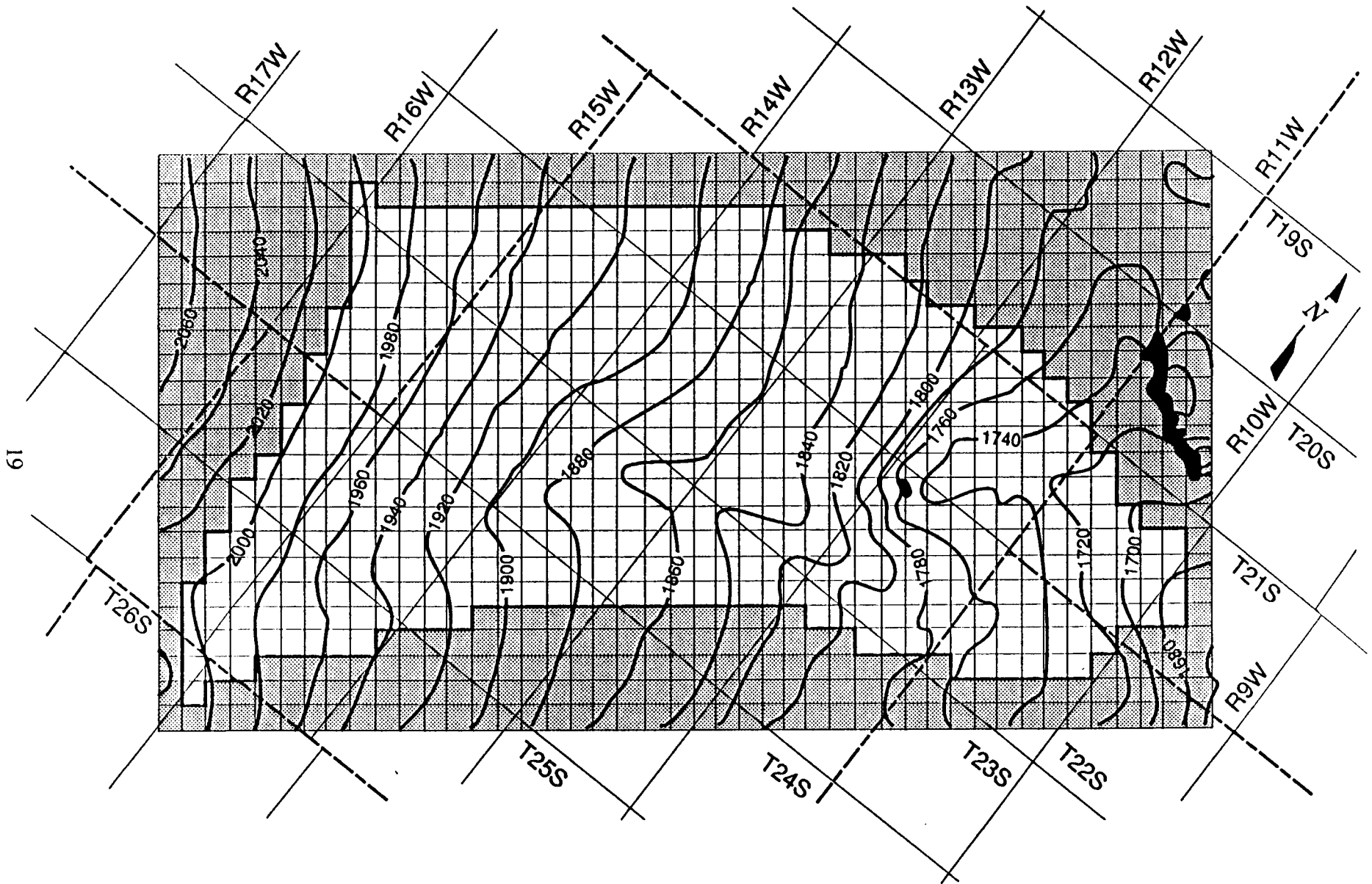


Figure 8. Predevelopment water table map of the study area. Contour interval 20 ft.

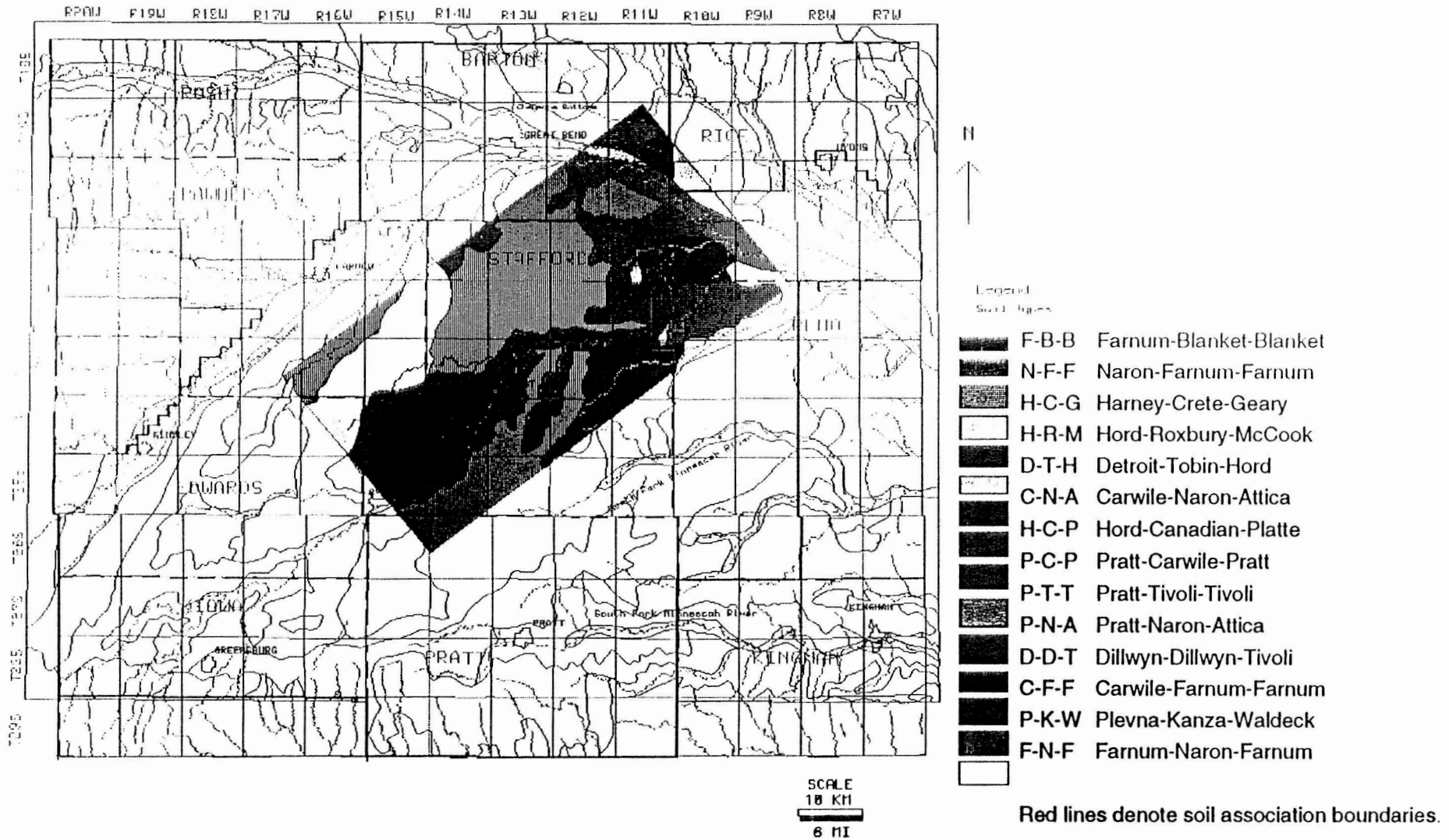


Figure 9. Soil Association map of the study area.

The loess deposits consist of relatively sand-free silty material that was deposited by wind in late Pleistocene time. The dominant soils formed in this parent material are the Harney, Holdrege, and Uly soils.

Eolian material with a high sand content is the major parent material of the soils in the sand hills. Most of this material was deposited during the Holocene, after the Pleistocene loess was deposited (Roth, 1973). Tivoli soils formed in fine sand, Attica and Pratt soils in loamy fine sand, and Naron soils in fine sandy loam. Tivoli and Pratt soils occur in areas of undulating to dunelike topography. Attica, Naron, and Pratt soils occur in areas of nearly level to undulating topography next to sand dune areas.

The alluvium that was deposited during the Holocene ranges from sand to clay loam. The dominant soils in this parent material are the Hord and Zenda soils and soils of the Plevna-Kanza-Waldeck association. The latter soils were formed on floodplains and stream terraces along Rattlesnake Creek and in the Big and Little Salt Marsh areas.

The hydrologic properties of these soils are outlined in the SCS Soil Survey county reports and were used by Sophocleous and McAllister (1987, 1990) in constructing a water budget model for the entire Rattlesnake watershed. The soil hydrologic characteristics are also used in this study to obtain initial qualitative recharge-potential estimates.

Water rights

All current water rights (as of 1990) for the Great Bend Prairie region were obtained on tape from the Division of Water Resources, Kansas State Board of Agriculture, and the ground-water rights have been processed and displayed on a 1:250,000 map (Sophocleous, 1990, unpublished map). Figure 10 displays the ground-water rights in the study area, and fig. 11 depicts the number of ground-water rights issued in the study area versus time (a), the corresponding appropriated (cumulative) amounts (b), and the year-by-year incremental appropriations (c). A listing of the water rights is included in Appendix 1. Because of water

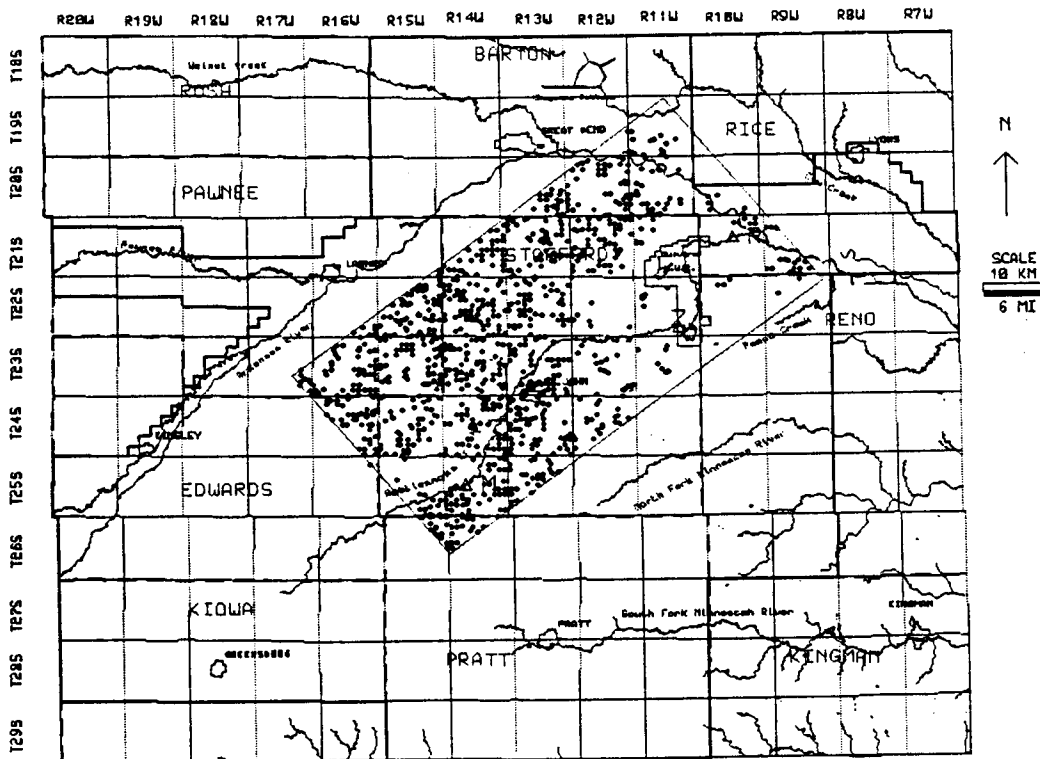


Figure 10. Ground-water rights map of the study area and vicinity.

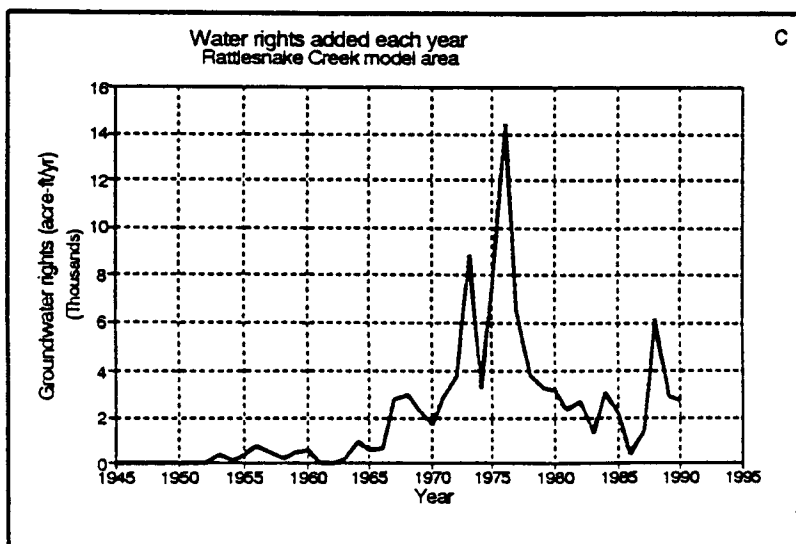
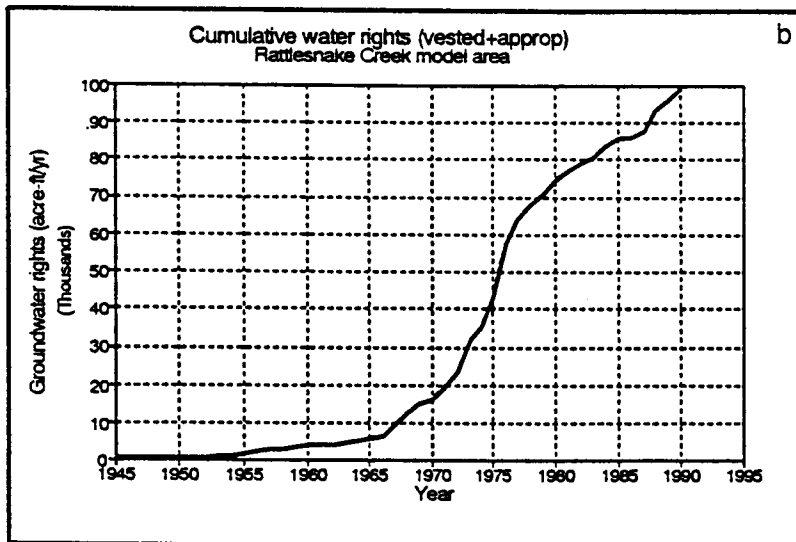
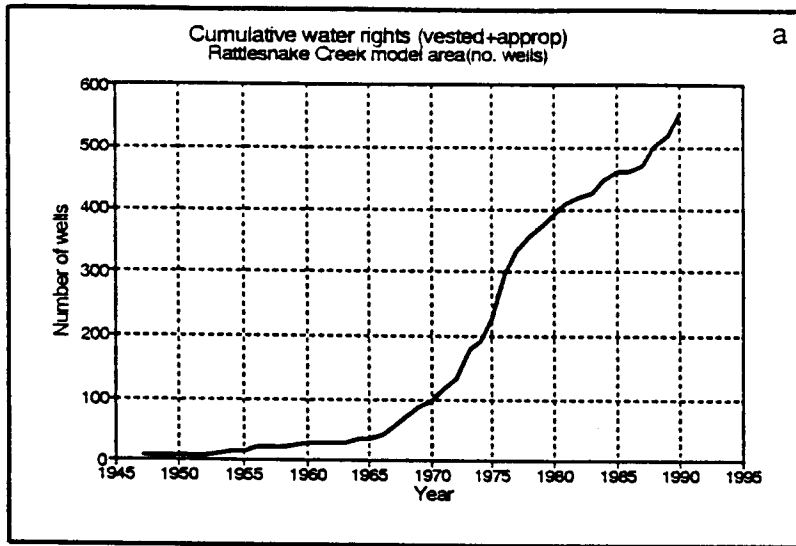


Figure 11. Ground-water rights issued in the study area versus time.

salinity problems, water rights are minimal along the lower Rattlesnake Creek reaches and the Quivira marsh region (fig. 10).

Rattlesnake Creek streamflows

Current and historical streamflow data for the area streams have been compiled and analyzed. Total annual streamflows of the Rattlesnake Creek at the Macksville, Zenith, and Raymond stream-gaging stations are shown in fig. 12. As can be seen in fig. 12, the streamflows at all gaging stations have been generally declining since the flood of 1973. Other stream-related data, such as stream widths and stream slopes, were obtained from area visits and from topographic and other maps.

Figures 12a and 12 b display the established monthly minimum desirable streamflows (MDS) for the Rattlesnake Creek at Macksville and Zenith gaging stations, respectively, together with the observed mean monthly streamflows at these stations for the period of record. The increasing violations of those MDS since the early 1980's is obvious from the figures.

The Rattlesnake Creek is a predominantly "baseflow" stream, that is most of its flow is contributed by ground-water seepage. A USGS streamflow separation program (White and Sloto, 1990) using three baseflow separation techniques (fixed-interval, sliding interval, and local minimum) was applied to the Rattlesnake Creek streamflow data. Figures 12c and 12d display the streamflow hydrograph separation for Macksville and Zenith gaging stations, respectively. It is evident from these figures that approximately 70% of the total streamflow, on average, is contributed by ground-water seepage to Rattlesnake Creek.

Climate

Climatic data were obtained from existing National Oceanic and Atmospheric Administration (NOAA) climatic stations in Kansas and from a Groundwater Management District No. 5-Kansas Geological Survey (GMD5-KGS) cooperative study on recharge assessment in

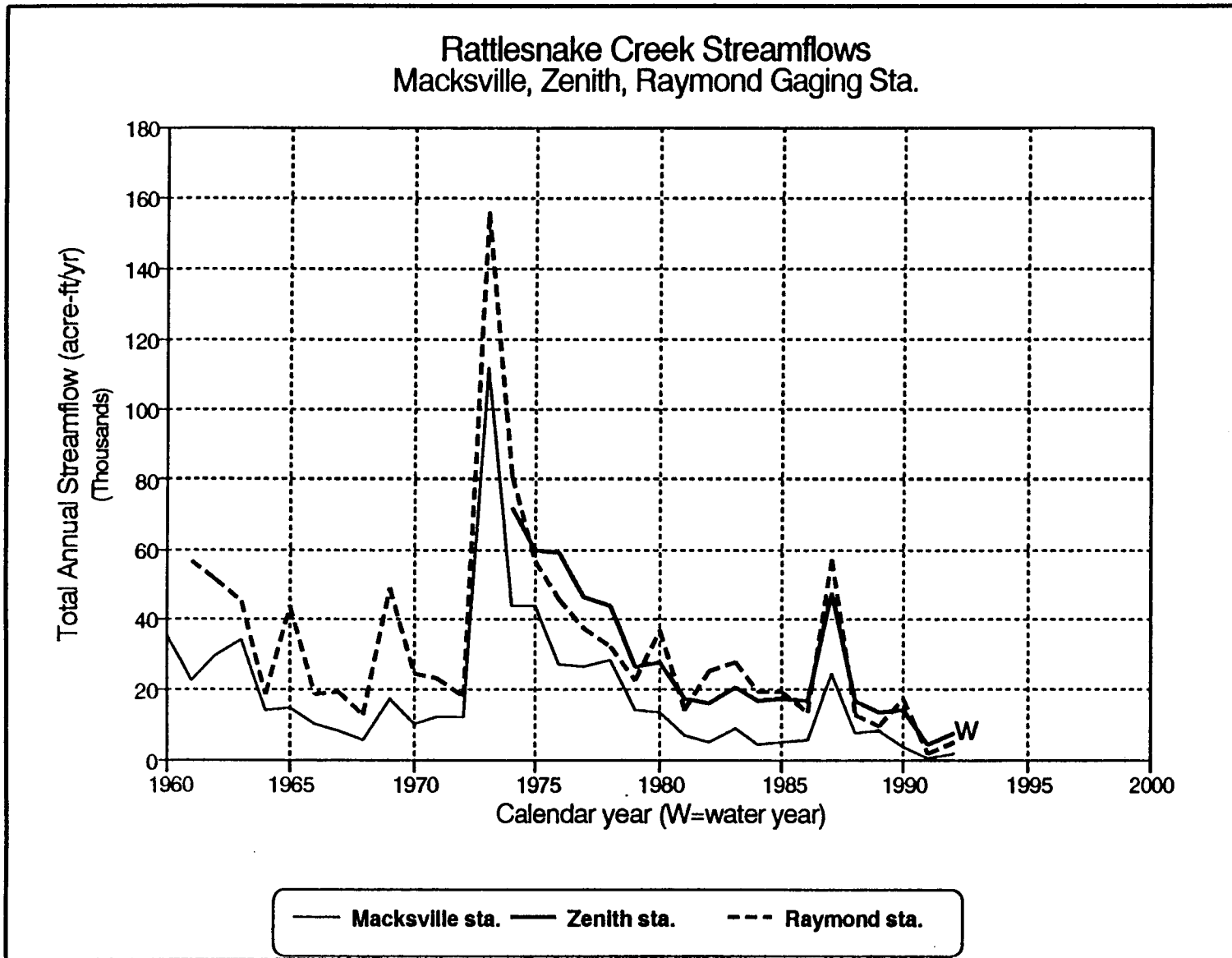


Figure 12. Average annual streamflows of Rattlesnake Creek at the (a) Macksville, (b) Zenith, and (c) Raymond gaging stations.

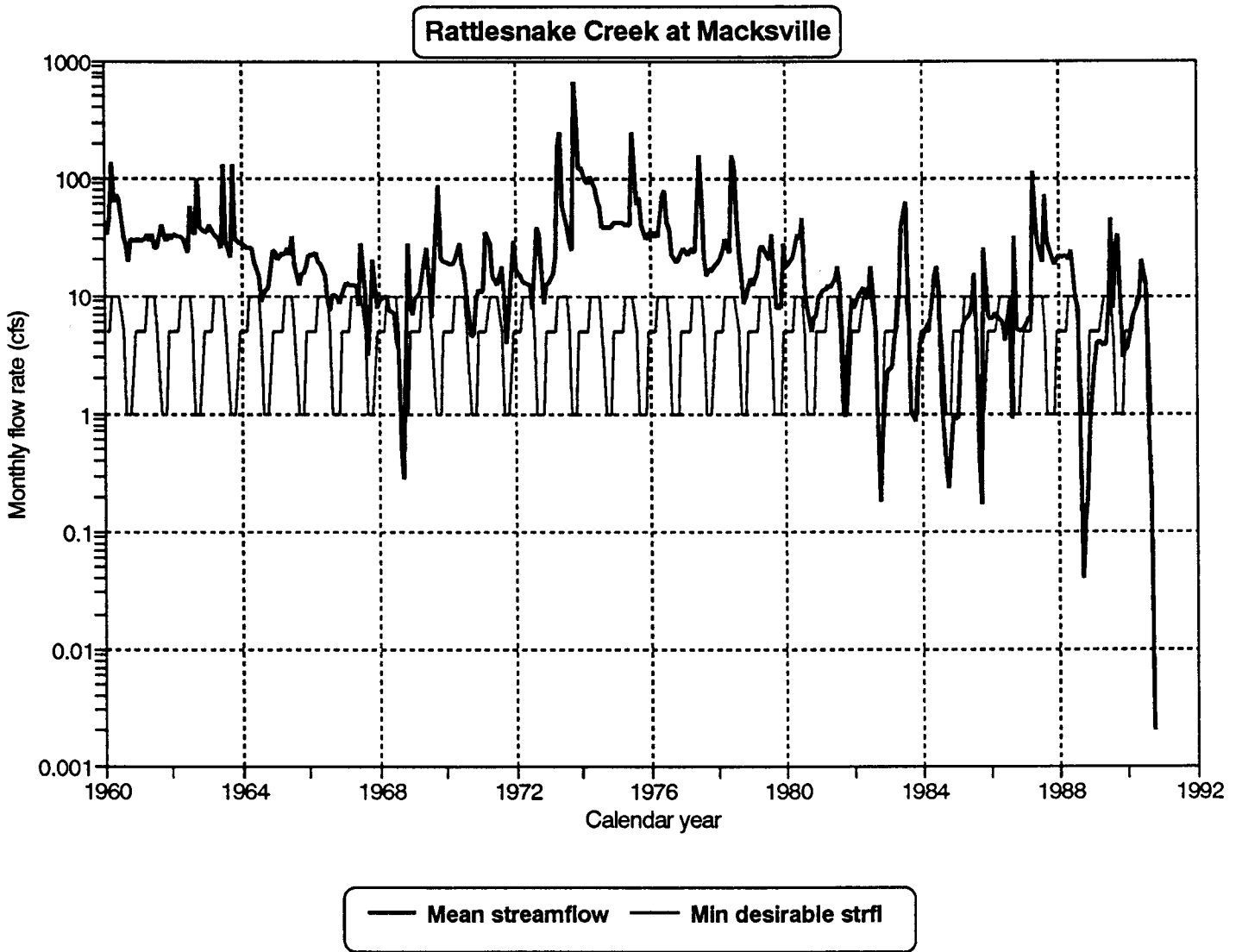


Figure 12a. Average monthly streamflows and minimum desirable streamflows for the Rattlesnake Creek at Macksville gaging station.

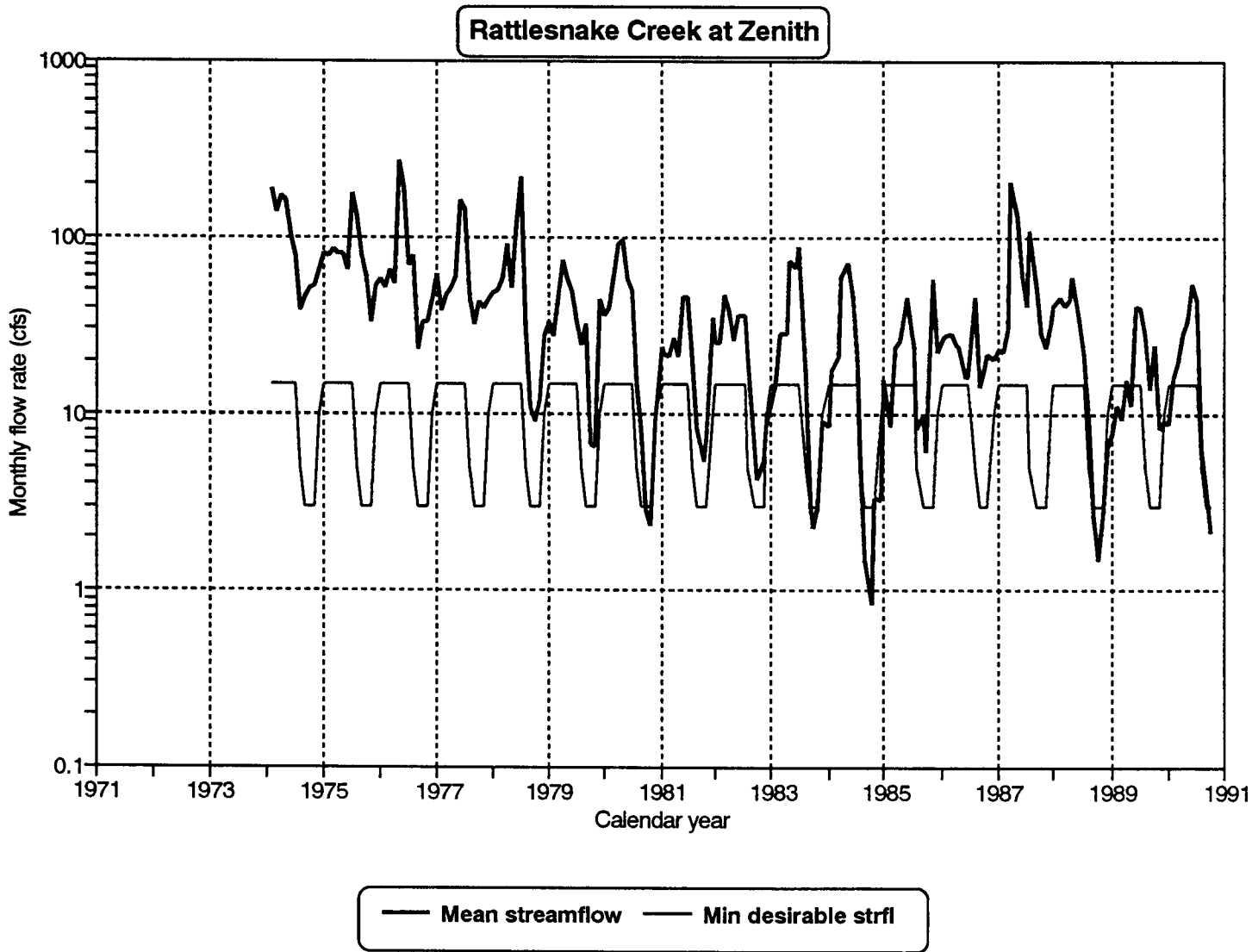


Figure 12b. Average monthly streamflows and minimum desirable streamflows for the Rattlesnake Creek at Zenith gaging station.

Macksville streamgaging station Baseflow separation

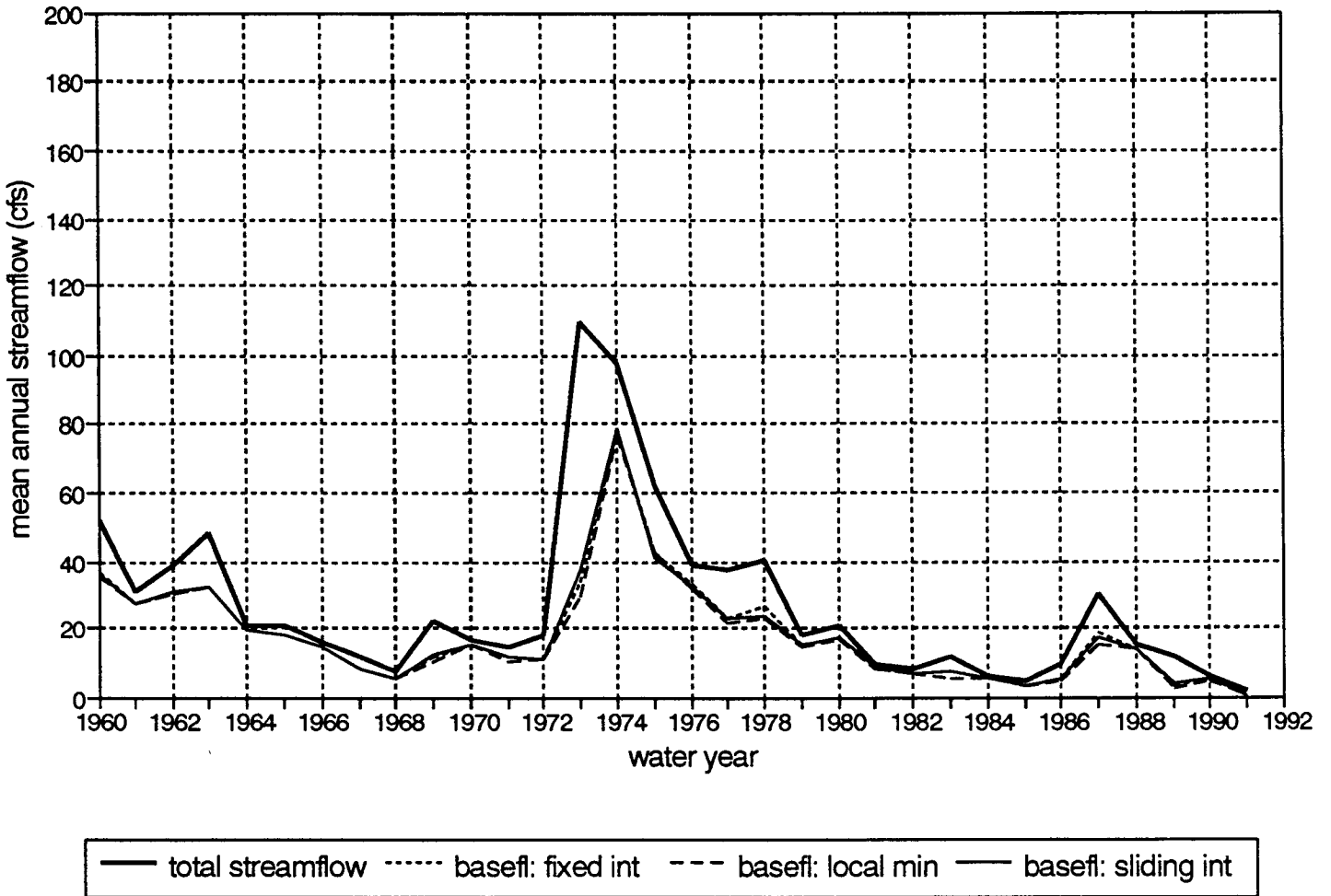


Figure 12c. Baseflow separation for the Rattlesnake Creek at Macksville gaging station using three baseflow separation techniques (fixed interval; local minimum; and sliding interval).

Zenith streamgaging station Baseflow separation

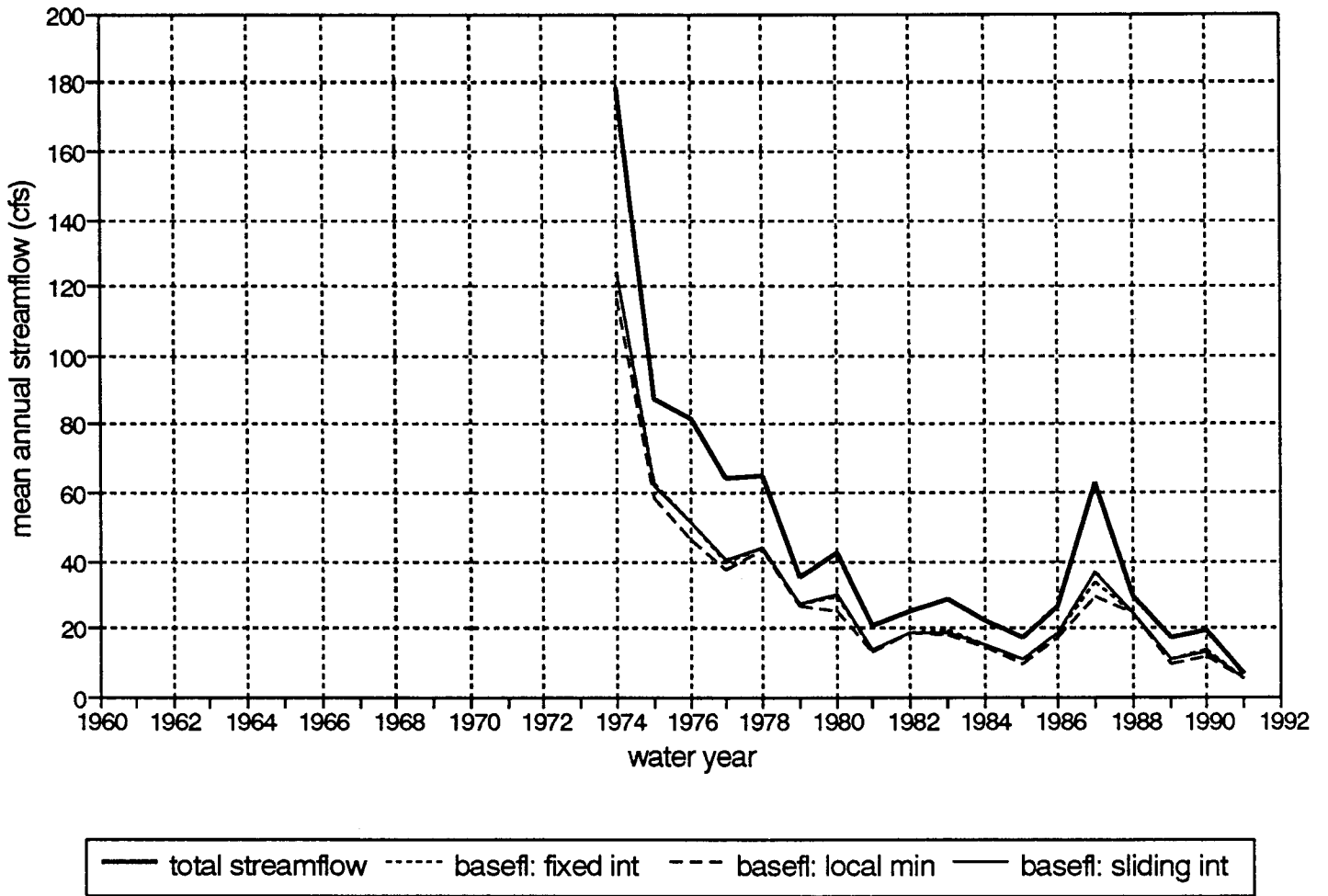


Figure 12d. Baseflow separation for the Rattlesnake Creek at Zenith gaging station using three baseflow separation techniques (fixed interval; local minimum; and sliding interval).

GMD5, which encompasses most of the Great Bend Prairie region, including the study area. The available 1980–1990 average annual precipitation data for all the stations have been compiled and a precipitation contour map of the Great Bend Prairie has been prepared (fig. 13). As can be seen from fig. 13, the Quivira refuge falls in the 23–25-in. average annual precipitation category.

The Great Bend Prairie has a typical continental climate: dry and relatively cold winters, warm to hot summers, a late spring–early summer precipitation maximum, moderate surface winds, and large daily and annual variations in temperature. Two climate controls contribute to the precipitation pattern in the Great Bend Prairie. The Rocky Mountains are effective in producing a rain shadow over western Kansas. The Gulf of Mexico is the principal source of moisture for precipitation in the area. From west to east the average annual amount of precipitation increases by approximately 1 in. for each 17 mi of distance (Bark, 1961). Average annual precipitation in the Great Bend Prairie ranges from 20 in. at the western border to 29 in. near the eastern border. Approximately 75% of the annual precipitation occurs in the growing season of April through September. May and June have the highest average number of rainy days per month and the highest average amounts of precipitation. Most of the total annual precipitation comes from convective shower activity, usually in the evening or at night (Bark, 1978).

Water table maps

Water-level data from the Great Bend aquifer for predevelopment conditions and for various years since the 1970's (unpublished records) have been examined and analyzed to delineate ground-water flow lines that can be used to select boundary flow lines separating the lower Rattlesnake Creek watershed study area from the rest of the Great Bend aquifer.

Field data collection

Water-level survey

During January and February 1991 a ground-water-level survey in GMD5 encompassing the study area was conducted by GMD5 personnel. These data combined with the annual water-

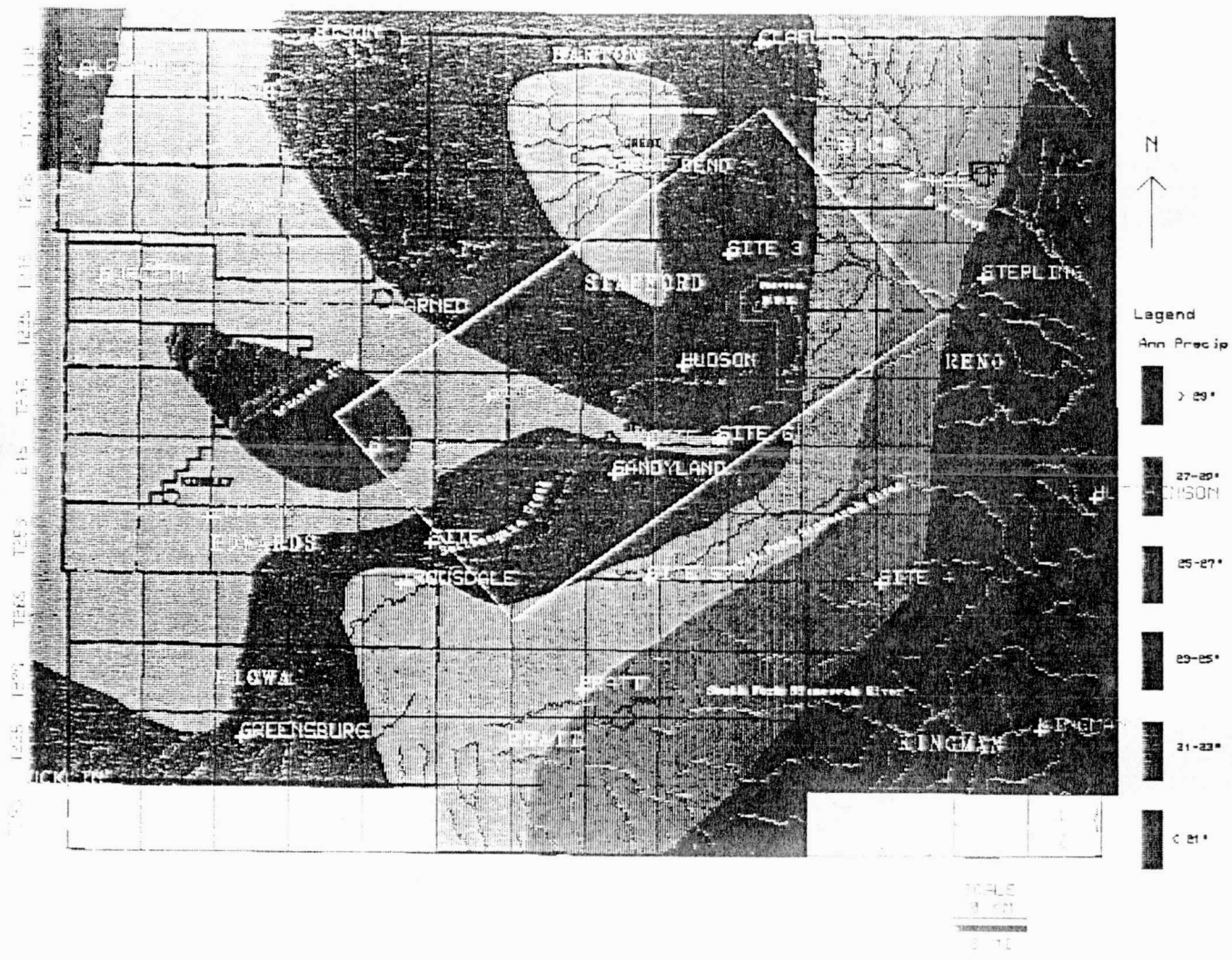


Figure 13. Average 1980-1990 annual precipitation in the study area and vicinity

level measurements taken by the Division of Water Resources in cooperation with the U.S. Geological Survey were used to produce the January 1991 water-level and depth to water table maps of the study area (figs. 14 and 15). A comparison of the January 1991 point-by-point water level measurements with the corresponding predevelopment water-level data for the study area (boxed area in figs. 14 and 15) is shown in fig. 16, where the largest declines (more than 20 ft) are observed near the western Stafford County border. Although a few data points show no decline or a water table rise, most of the data points in the study area show appreciable water-level declines.

Geophysical logging

A geophysical logging survey of a limited number of existing wells in the study region was conducted in April and May 1990 using a rented U.S. Geological Survey logging vehicle. The purpose of this survey was to locate the saltwater-freshwater interface below the Great Bend aquifer and to pinpoint locations for detailed study. Despite equipment deficiencies, which resulted in only a qualitative logging survey, the results were helpful in locating the approximate extent of the saltwater-freshwater interface in specific areas and in siting appropriate locations for drilling monitoring wells. The inferred depths to the saltwater-freshwater interface ranged from approximately 130 ft below ground surface east of St. John to approximately 40–45 ft west of the Big Salt Marsh and near the Stafford-Barton county line.

Drilling

Two locations near the Quivira marsh, known as the Sittner and Figger sites, were selected for drilling monitoring wells to track the location and temporal variations of the saltwater-freshwater interface. The locations of these monitoring wells are shown in fig. 17. After permission was obtained from landowners and other clearances were secured, two 5-in. fully screened wells down to bedrock were drilled, installed, developed, and logged (lithology and gamma-ray) by the Kansas Geological Survey in May and June 1990. The lithology and gamma-ray logs are shown in figs. 18 and 19; the well record forms are included in Appendix 2. Note that

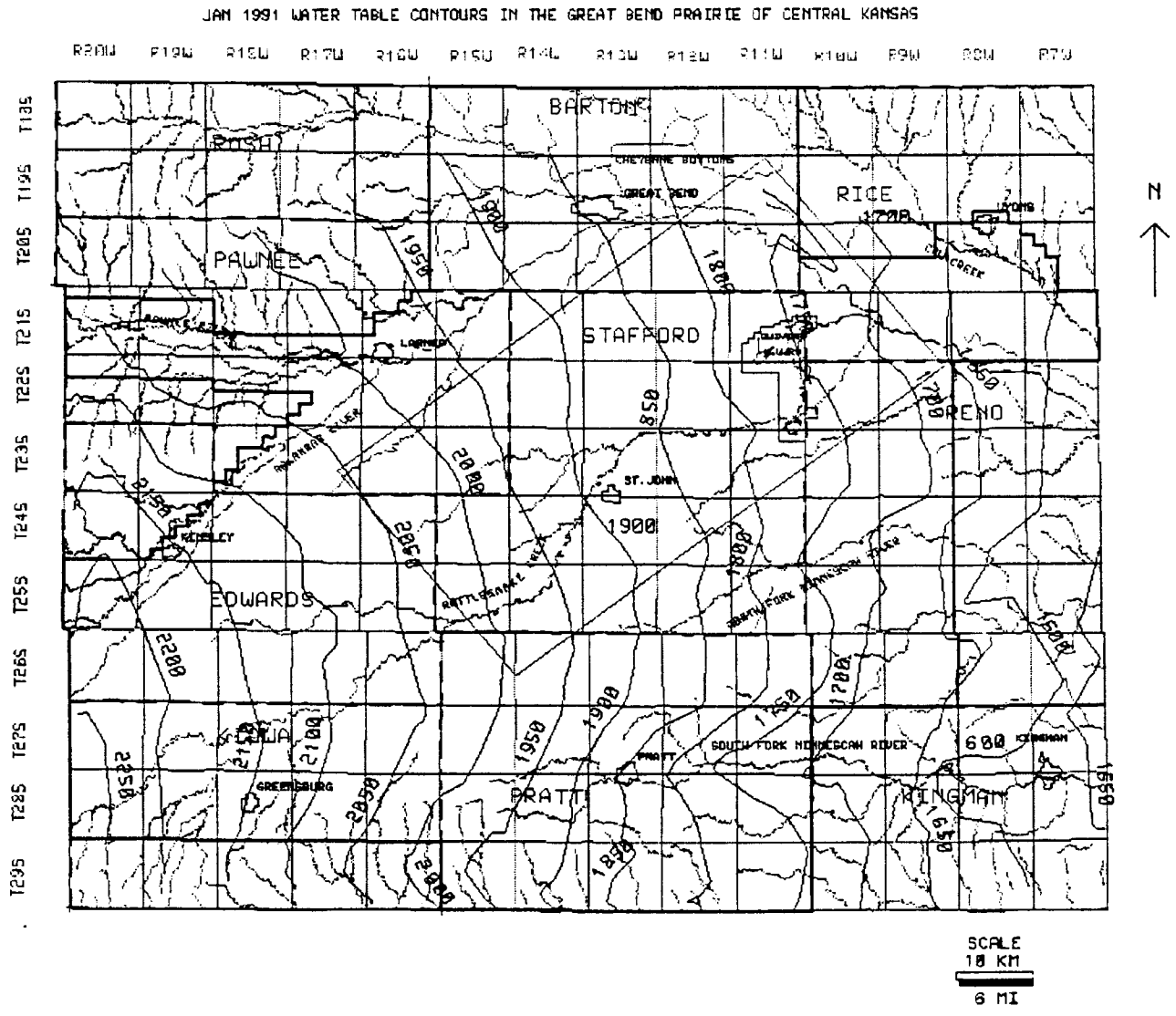


Figure 14. January 1991 water table contour map of the study area and vicinity.



Figure 1. January 1991 depth contours and bathymetry of the study area and location of the study area in the Gulf of Mexico.

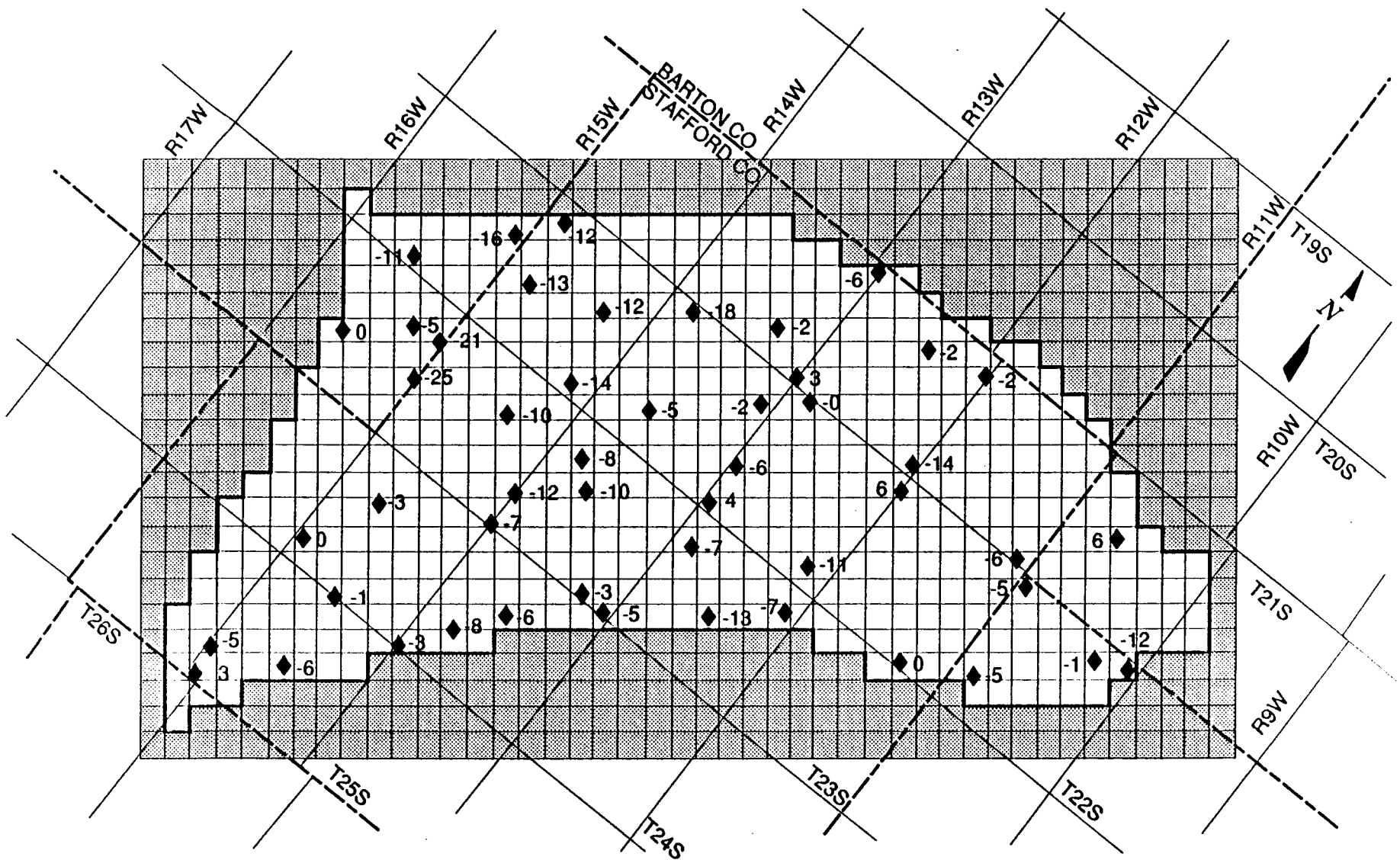
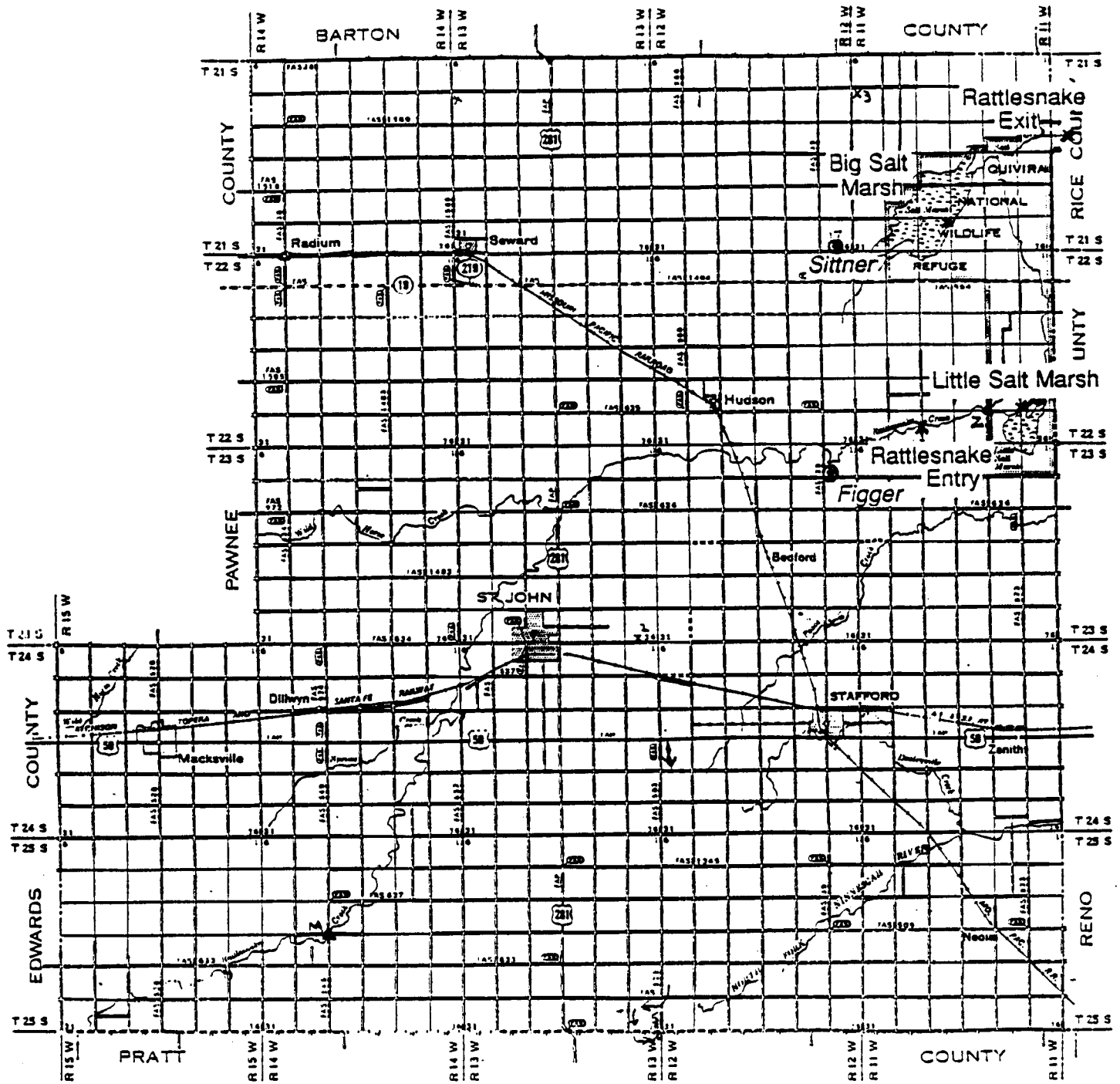


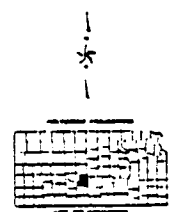
Figure 16. Observed ground-water-level changes from predevelopment (c. 1955) to January 1991.
Negative values indicate water-level declines.



LEGEND

- ROADS AND ROADWAY FEATURES**
- UNPAVED ROAD
 - GRAVEL OR STONE ROAD
 - GRAVEL OR STONE ROAD - NOT GRADED OR CHAINED
 - GRAVEL AND ASPHALT
 - GRAVEL AND ASPHALT WITH STABILIZED SURFACE
 - INTERCHANGE
 - DIVIDED HIGHWAY
 - DIVIDED HIGHWAY WITH FULL CONTROL OF ACCESS AND INTERCHANGE

- OTHER FEATURES**
- FEDERAL AND STATE HIGHWAY
 - FEDERAL AND STATE HIGHWAY - LIMITED ACCESS
 - INTERSTATE NUMBERED HIGHWAY
 - U.S. NUMBERED HIGHWAY
 - STATE HIGHWAY
 - TOWN ROAD
 - RAILROAD
 - CANAL
 - RIVER
 - LAKE
 - DAM
 - POWER PLANT
 - WINDMILL
 - WATER TOWER
 - TELEPHONE TOWER
 - AIRPORT
 - SCHOOL
 - CHURCH
 - GYMNASIUM
 - HALL
 - STORE
 - RESTAURANT
 - MOTEL
 - HOTEL
 - COTTAGE
 - HOUSE
 - GARAGE
 - DRIVEWAY
 - FENCE
 - POST
 - SIGN
 - LIGHT
 - TOWER
 - ANTENNA
 - WINDMILL
 - WATER TOWER
 - TELEPHONE TOWER
 - AIRPORT
 - SCHOOL
 - CHURCH
 - GYMNASIUM
 - HALL
 - STORE
 - RESTAURANT
 - MOTEL
 - HOTEL
 - COTTAGE
 - HOUSE
 - GARAGE
 - DRIVEWAY
 - FENCE
 - POST
 - SIGN
 - LIGHT
 - TOWER
 - ANTENNA



**GENERAL HIGHWAY MAP
STAFFORD COUNTY
KANSAS**

Prepared by the
**STATE HIGHWAY COMMISSION OF KANSAS
DEPARTMENT OF PLANNING AND DEVELOPMENT**

in cooperation with the
**U. S. DEPARTMENT OF TRANSPORTATION
FEDERAL HIGHWAY ADMINISTRATION**

1974

Figure 17. Location of saltwater-freshwater interface monitoring wells and water-quality sampling stations.

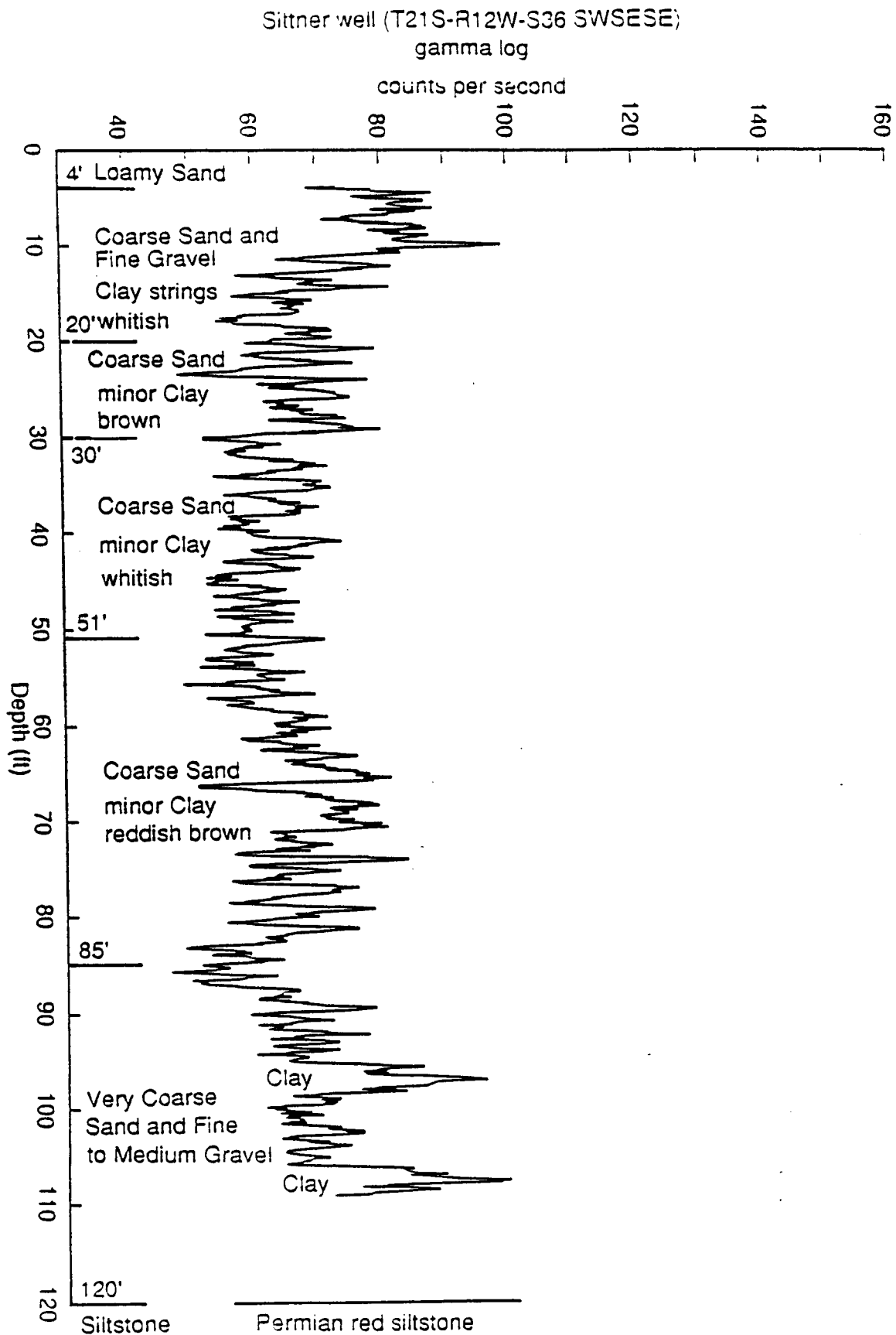


Figure 18. Lithology and gamma-ray log of the Sittner observation well.

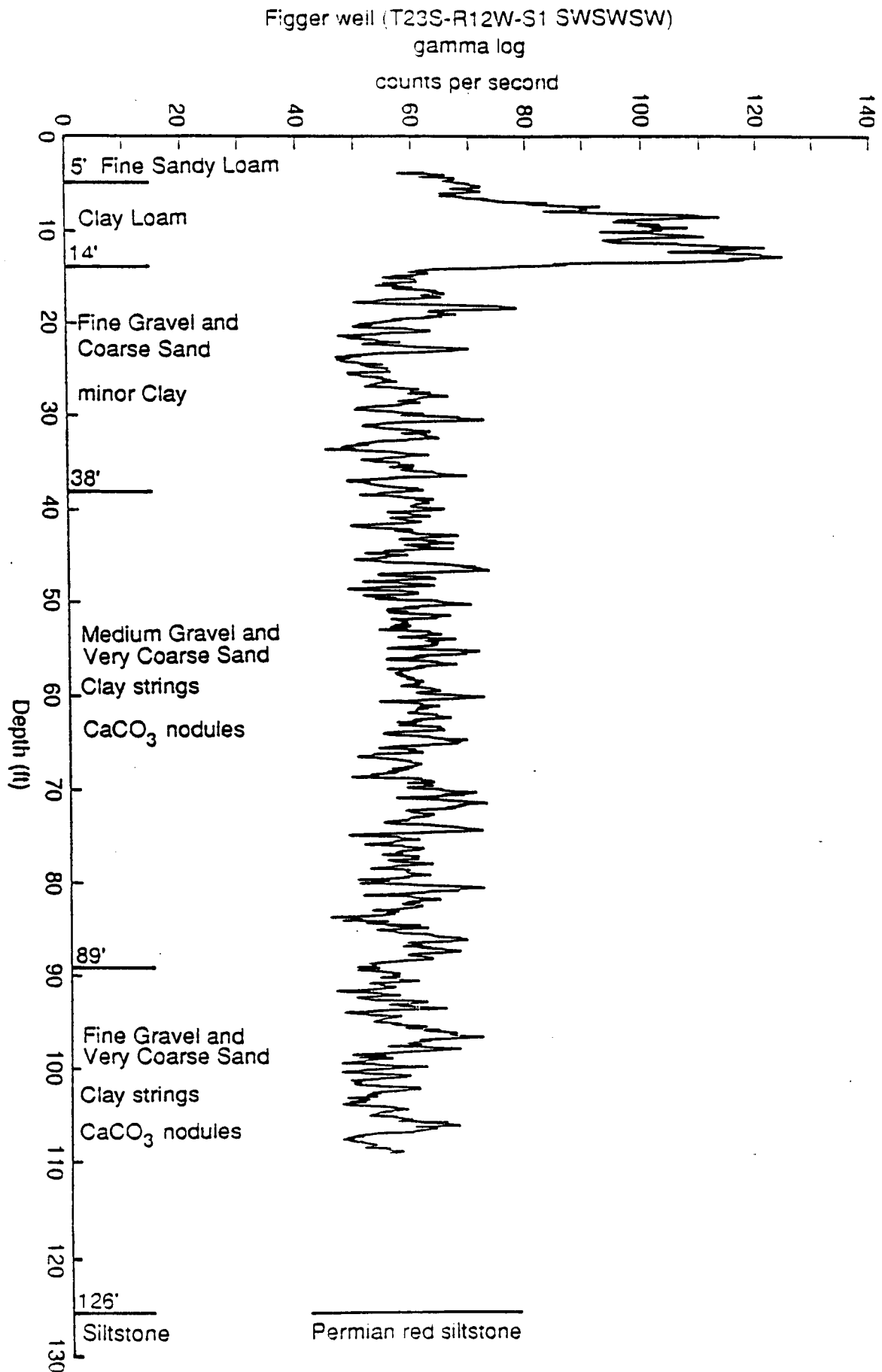


Figure 19. Lithology and gamma-ray log of the Figger observation well.

the coarse sand and gravel deposits of the aquifer directly overlie the Permian red siltstone bedrock in both boreholes without major intervening clay layers.

Saltwater-freshwater interface monitoring

Two conductivity recording probes, one with an electronic data acquisition system (Hydrolab's Datasonde III) and the other with a recording chart, were selected and purchased by the KGS. These probes were checked, adapted to our field situation by rewiring some circuits for extended battery operation, calibrated, and installed in the field in August 1990. Periodic field maintenance and instrumentation adjustment were conducted in cooperation with Quivira NWR personnel.

Results from the saltwater-freshwater interface monitoring sites indicate that the interface is extremely sharp at the Sittner site west of the Big Salt Marsh (within 1 ft the specific conductance increases from 700 $\mu\text{S}/\text{cm}$ to 24,000 $\mu\text{S}/\text{cm}$; fig. 20) and fluctuates appreciably (with a range of 55–90 ft below ground surface) with very small changes in water table levels (less than 0.5 ft in most cases). The saltwater-freshwater interface at the Figger monitoring site west of the Little Salt Marsh and near Rattlesnake Creek is more diffuse (fig. 20) and does not fluctuate as much as at the Sittner site. These results indicate that the behavior of the saltwater-freshwater interface in the study area is complex and poorly understood; thus concentrated study of saltwater behavior in the region is needed.

Water quality of the Quivira marsh

Several water-quality surveys of the waters entering and leaving the Quivira marsh and of the Little and Big Salt Marshes were conducted in late 1990 and in 1991, including surveys specifically conducted for trace element analyses. The location of the regular sampling sites are indicated in fig. 17.

The waters of the Quivira NWR are typical sodium chloride waters, the detailed chemical analyses of which are included in Appendix 3. One significant aspect of these chemical analysis

Depth Profiles of Water Salinity Sittner & Figger Monitoring Wells

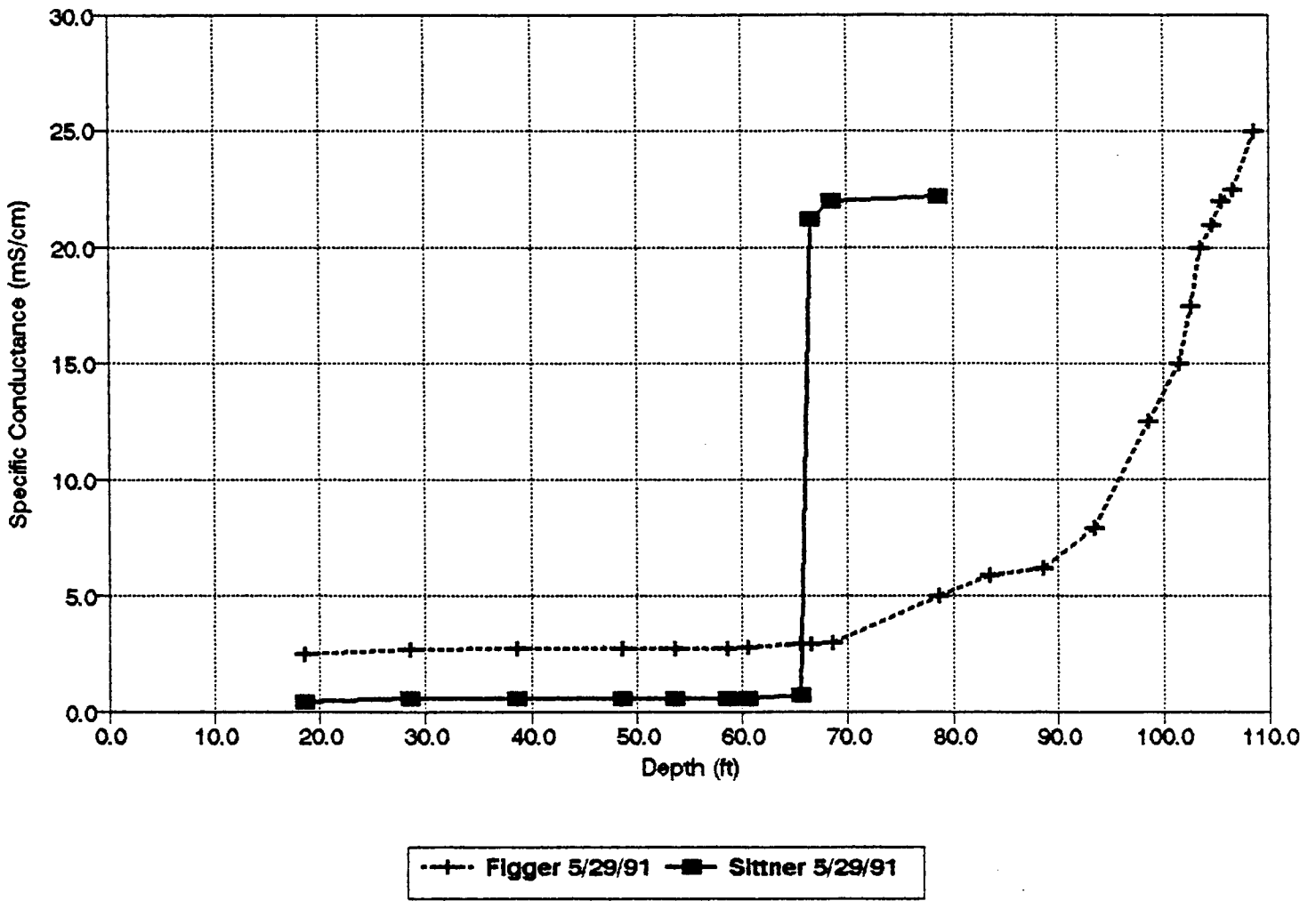


Figure 20. Specific-conductance depth profile at the Sittner and Figger wells.

results is the relatively high concentrations of selenium in the Big Salt Marsh and in Rattlesnake (or Salt) Creek exiting the refuge. Selenium is an essential trace nutrient for terrestrial and aquatic organisms; however, proper selenium levels in biota fall within narrow ranges (U.S. Environmental Protection Agency, 1987). Selenium has received attention because high levels of selenium borne by irrigation return flows have caused serious problems for fish and wildlife (Ohlendorf, 1989; Saiki and Lowe, 1987). Table 2 summarizes the specific conductance, pH, and chloride and selenium concentrations of the major sampling stations at different times. The Environmental Protection Agency (EPA) limits for chronic and acute selenium concentrations for aquatic life are 8.4 and 11.2 µg/l, respectively. The measured selenium concentrations of the Big Salt Marsh and the Rattlesnake Creek exit usually exceed the acute exposure limits.

It was reported by Anderson et al. (1961) that Cretaceous shales in the midcontinent and elsewhere contain appreciable amounts of selenium. Therefore the Cretaceous bedrock outcrop southwest of the Big Salt Marsh, which consists predominantly of the Kiowa Shale, was suspected of being the source of the excess selenium. However, x-ray analysis of six rock and sediment samples from the Big Salt Marsh and the bedrock outcrop (see Appendix 4) indicated that the selenium level was below detection (10 ppm).

Table 2. Selected chemical characteristics of the Quivira National Wildlife Refuge waters.

Sampling time	Specific conductance (µS/cm)				pH				Chloride (mg/l)			Selenium (µg/l)			
	Aug 90	Mar 91	Aug 91	Sept 91	Aug 90	Mar 91	Aug 91	Sept 91	Mar 91	Aug 91	Sept 91	Aug 90	Mar 91	Jun 91	Sept 91
Rattlesnake entry to refuge	9,570	7,580	7,130	14,700 ^a	7.95	8.15	8.55	8.20	2,220	2,110	4,820	1	3	5	5
Little Salt Marsh	9,020	9,020	8,420	dry	8.45	8.00	8.30	—	2,980	2,470	—	14	4	5	—
Big Salt Marsh	14,460	16,500	18,400	49,900 ^b	8.90	8.05	9.65	8.40	5,250	6,020	19,700	21	4	11	19
Rattlesnake exit from refuge	22,300	22,600	24,200	18,700 ^a	7.50	7.95	8.00	8.75	7,480	7,920	6,170	51	28	8	15

a. Standing water (stream not flowing).
b. Big Salt Marsh significantly shrunk.

Numerical modeling

A two-dimensional areal model combining stream-pond-aquifer interaction modeling and saltwater-freshwater sharp interface modeling has been developed and tested against analytical and other numerical solutions; this work is documented elsewhere (Sophocleous and Birdie, 1990). However, because of data deficiencies related to the saltwater aspects, the model has not been fully implemented. Instead, the well-known MODFLOW model, which is equivalent to our freshwater stream-aquifer model module and a parameter estimation model (MODINV; Doherty, 1990) have been implemented for the Rattlesnake Creek watershed. Because MODFLOW deals only with freshwater aspects and has associated pre- and postprocessors, we preferred to use it in this phase of the analysis to expedite processing and analysis.

The major thrust of this study is to implement and analyze an appropriate stream-aquifer numerical model for the study area. The simulation model chosen to evaluate the lower Rattlesnake Creek stream-aquifer system is a modified two-dimensional version of the popular modular three-dimensional finite-difference ground-water model (MODFLOW) of McDonald and Harbaugh (1988) with the streamflow routing capabilities of Prudic (1989). MODFLOW solves the three-dimensional ground-water flow equation using finite-difference approximations and includes the effects of such processes as areal recharge, rivers, drains, evapotranspiration, and pumpage. The finite-difference procedure requires that the aquifer be divided into cells. The aquifer properties in each cell are assumed to be uniform. The unknown head in each cell is calculated at a point or node at the center of the cell. The head is calculated by iterating through the finite-difference equations for all nodes until the maximum head change in any cell between the previous iteration and the current iteration is less than a specified small value. Once this criterion is met, the program advances to a new time step and the process of computing heads at each node is repeated.

Streams superimposed on the aquifer are divided into *reaches* and *segments*. A segment consists of one or more reaches. Each reach corresponds to an individual cell in the finite-difference equation used to simulate ground-water flow. Streamflow is specified for the first reach in each segment that enters the model area; streamflow to adjacent downstream reaches in each

segment is calculated as equal to inflow in the upstream reach plus or minus leakage from or to the aquifer in the reach. Leakage is calculated for each reach on the basis of the head difference between the stream and aquifer and a conductance term:

$$Q_{\ell} = C_{\text{str}} (H - h), \quad (1)$$

where Q_{ℓ} is the leakage to or from the aquifer through the streambed, H is the head in the stream, h is the head in the aquifer side of the streambed, and C_{str} is the conductance of the streambed, which is the hydraulic conductivity of the streambed times the product of the width of the stream reach and its length divided by the thickness of the streambed.

The stage in each reach can be computed by using the Manning formula under the assumption of a rectangular stream channel:

$$Q = \frac{c}{n} \left(AR^{2/3} S_0^{1/2} \right), \quad (2)$$

where Q is the stream discharge, n is Manning's roughness coefficient, A is the cross-sectional area of the stream, R is the hydraulic radius, S_0 is the slope of the stream channel, and c is a constant, which is 1.486 for units of cubic feet per second (cfs). The cross-sectional area A and the hydraulic radius R for a rectangular channel are

$$A = wd, \quad (3)$$

$$R = wd/(w + 2d), \quad (4)$$

where d is the depth of the water in the stream and w is the width of the channel.

The amount of leakage in each reach either into or out of the aquifer is incorporated into the ground-water flow model by adding appropriate terms to the finite-difference equation. Recharge to the aquifer in a reach ceases when all the streamflow in the upstream reaches has leaked into the aquifer and the stream is dry. A stream is permitted to flow again in the downstream reaches when the head in the aquifer is above the elevation of the streambed.

For simulation of stream-aquifer interaction, the ground-water flow model with the streamflow-routing package has an advantage over the analytical solution because it can be used to simulate complex systems that cannot be readily solved analytically.

Required input data for the stream-aquifer model include (1) the areal distribution of aquifer-related parameters, such as transmissivity or hydraulic conductivity, storativity, and natural recharge; (2) water levels in the aquifer and the stream(s); (3) bedrock and land surface elevations; (4) the input stream and tributary hydrograph; (5) stream width, slope, streambed elevations, and Manning's roughness coefficients; (6) streambed conductance (i.e., hydraulic conductivity of streambed or canal and ditch sediments divided by their thickness); (7) location and pumping rate of wells; and (8) initial and boundary conditions.

Calibration

One of the most important steps in setting up a ground-water model is calibration. Development of the computer model as a predictive tool is based on the premise that, if historic hydrologic phenomena can be satisfactorily approximated by the model, then so should future conditions. Calibration involves adjusting model input parameters, based on field data, to accurately predict real-world cause-and-effect relationships. The task of manually adjusting parameter and past recharge values over different parts of the aquifer until the model nearly replicates previously measured water-level measurements in a set of observation wells is an arduous one requiring many model runs. Adjustments are often made in a hit-or-miss fashion until the fit between the model and the observed water levels is acceptable. This process is often time-consuming and expensive and sometimes can result in no answer. Also, questions about whether or not the derived solution is the optimum one and how many other solutions are equally good are difficult to answer when trial-and-error methods are used. To avoid problems related to manual calibration, one can use a parameter estimation computer program that uses the MODFLOW program as its forward processor to obtain an optimum set of parameter or input values. The process by which solutions are found for one or more of the model parameters or inputs is known as *inverse*

modeling (or the *inverse problem*). Once the parameters or inputs to the model are known (e.g., hydraulic conductivity, storativity, recharge), it is a relatively simple matter to obtain model outputs (such as heads or water levels in the aquifer). This modeling process is known as the *forward problem* or *forward modeling*. In this study we used a parameter optimization method for MODFLOW, known as MODINV (for *modflow inverse*). Using MODINV, we can optimize the specific values taken by any parameter type that MODFLOW can read as a two-dimensional data array such that model-generated heads are as well matched as possible to those observed in the field. Steady-state and transient-state, single-layer and multilayer, and confined and unconfined models can all be calibrated in this manner. MODINV adjusts the parameter and/or recharge values pertaining to a set of constant-value zones chosen by the modeler (based on field data) for each parameter type until the optimum fit between the observed and the model heads is obtained. MODINV then provides the covariance matrix, which indicates the reliability or uncertainty levels of the parameter estimates. Model and observed heads are matched according to the weighted least-squares criterion, and optimization is achieved using the Gauss-Newton-Marquardt method (Draper and Smith, 1981).

Regression problem

The calibration or parameter estimation problem can be viewed as a classical nonlinear regression problem with a solution of the appropriate flow equation forming the regression equation and all unknown quantities (e.g., hydrogeologic parameters, sources, sinks, and boundary fluxes) serving as parameters (Sophocleous, 1984). The measured hydraulic heads are observations of the dependent variable for which a set of least-squares estimates is to be obtained. This regression problem finds the parameters of a given model that produce the best fit of the calculated hydraulic head (dependent) variable to the observed dependent variable and allows implementation of other methods and tests that analyze on a probabilistic basis the propagation of data errors in the estimates of parameters and the predictive capability of the model (Draper and Smith, 1981).

The basic equation to be fitted to the observed hydraulic head data is the general form of the two-dimensional ground-water flow equation (which the MODFLOW program is designed to solve):

$$\frac{\partial}{\partial x} \left(T_{xx} \frac{\partial h}{\partial x} \right) + \frac{\partial}{\partial y} \left(T_{yy} \frac{\partial h}{\partial y} \right) + R(H - h) + W + \sum_{\ell=1}^N \delta(x - a_{\ell}) \delta(y - b_{\ell}) Q_{\ell} = S \frac{\partial h}{\partial t}, \quad (5)$$

where $T_{xx} (= K_{xx}b)$ and $T_{yy} (= K_{yy}b)$ are the transmissivities in the x and y directions, respectively; K_{xx} and K_{yy} are the hydraulic conductivities of the aquifer in the x and y directions, respectively; $b(x, y)$ is the saturated thickness of the aquifer; $R(x, y)$ is the hydraulic conductance of the streambed, which is the hydraulic conductivity of the streambed times the product of the width of the stream and its length divided by the thickness of the streambed; $H(x, y, t)$ is the head in the stream; $h(x, y, t)$ is the hydraulic head in the aquifer; and $W(x, y, t)$ is a source-sink term (positive for a source, such as recharge) distributed areally. The expression $\sum_{\ell=1}^N \delta(x - a_{\ell}) \delta(y - b_{\ell}) Q_{\ell}$ is the Dirac delta designation for N wells, each one pumping at rate $Q_{\ell}(t)$ (positive for injection) and located at coordinates (a_{ℓ}, b_{ℓ}) . S is the storativity (storage coefficient or specific yield); x and y are the Cartesian coordinates; and, finally, t is time.

To approximate the variability of a given parameter, the region of interest is subdivided into zones; the parameter is assumed to be constant within each zone. Zones of one type of parameter, such as hydraulic conductivity, do not necessarily correspond to zones for another type of parameter, such as recharge.

Boundary conditions, such as lateral model inflow rate or constant head levels, are often considered part of the model itself, being neither an input nor a parameter. Along internal discontinuities in hydraulic conductivity the hydraulic head and flux normal to the boundary remain unchanged as the boundary is crossed.

The classical problem of ground-water hydrology is to solve Eq. (5) and its associated boundary conditions (including the initial head at $t = 0$) for the hydraulic head $h = h(x, y, t)$ in the aquifer, whereas an inverse solution involves solving Eq. (5) and its boundary conditions for one or more of the parameters, such as T , K , S , or W .

Sources of error in ground-water data

Numerous problems involving ground-water flow modeling of real field systems exist because the data necessary for the direct or inverse solutions are usually lacking. Head distribution is never known exactly because measurements do not exist at all points and because, where the measurements do exist, they are not exact. Estimates of the parameters either are completely unknown or have been obtained by spot measurements, few of which are directly useful for constructing appropriate effective values for use in Eq. (5). It should be clear that modeling problems in ground-water hydrology involve an incomplete combination of several types of data in which error and error propagation are important considerations.

Some major potential sources of random error in head data with respect to the model [Eq. (5)] have been enumerated by Cooley (1979):

1. Areal ground-water models assume that the head used is the average over the vertical, but wells may not be open over the entire interval modeled, and, if they are, they may not measure the average.
2. Hydraulic conductivity varies from point to point, which causes water levels to vary from values they would have if hydraulic conductivity were uniform. However, models usually do not take this detailed variation into account.
3. Water levels measured in wells in use may contain unknown amounts of residual drawdown. In addition, unused wells may be near wells that are in use, with resulting unknown drawdown in the unused well.
4. Measurement of well-head elevation may be in error.
5. Measurement of water levels may be in error [although usually of the order of 0.1–0.2 ft (0.03–0.06 m)].

Actual total error from the listed sources is highly problem dependent, but it is easy to imagine errors of several feet. In addition, interpolation errors are also of the order of several feet

(Sophocleous, 1983). Major model errors in Eq. (5) and its associated boundary conditions can be detected relatively easily and can be eliminated by analysis of model results.

Because there are several different parameters to be considered and because each parameter can be estimated or measured in several different ways, numerous sources of error exist in the parameter data. Some examples of errors in parameter data have been given by Cooley and Naff (1985):

1. Too few estimates of parameters are available to compute stable estimates of statistics such as mean and variance.
2. Results of point sampling are often biased because a large amount of data does not necessarily allow computation of nearly true or effective values of a parameter and its variance. For example, permeability values from core analyses often are not representative of regional values because flow through large fractures is not reproduced by core analyses.
3. Transmissivities estimated from specific capacity data collected by drillers are subject to numerous sources of error. Common sources include mismeasured water levels or pumping rates, recovery of water level after bailing, clogging the slots or screen, and inaccurate reporting. A persistent source of bias results because drillers drill wells in favorable locations and screen only the most productive zones.
4. Transmissivities and storativities estimated from pumping-test analyses are subject to many of the same errors in item 3, but the more carefully controlled tests should reduce their frequency and magnitude. In addition, a single test may not be representative of an entire hydrostratigraphic unit.
5. Transmissivities and storativities estimated from lithologic data are usually biased to an unknown extent.

Numerical regression solution procedure

To form the regression problem, Eq. (5) must be solved subject to the appropriate boundary conditions. For the present study the regression solution is based on a numerical solution of Eq. (5) described in detail by McDonald and Harbaugh (1988). In matrix form the solution can be written

$$D \mathbf{h} = \mathbf{q}, \quad (6)$$

where D is a square coefficient matrix involving parameters T_{ij} and R of order m , the number of nodes used to discretize the model region; \mathbf{h} is the hydraulic head vector of order m ; and \mathbf{q} is the known vector involving parameters W , Q , specified head, and boundary fluxes.

The set of optimal parameters is defined as the set that minimizes the objective function

$$SS = \mathbf{e}^T \mathbf{w} \mathbf{e} = (\mathbf{h}^{\text{obs}} - \mathbf{h})^T \mathbf{w} (\mathbf{h}^{\text{obs}} - \mathbf{h}), \quad (7)$$

where \mathbf{h}^{obs} is the vector of observed heads, \mathbf{h} is a vector of predicted heads, $\mathbf{e} = (\mathbf{h}^{\text{obs}} - \mathbf{h})$ is the residual vector consisting of the deviations of calculated heads from observed heads, superscript T indicates transpose, and \mathbf{w} is a diagonal weight matrix that describes the reliability of \mathbf{h}^{obs} at each node. If for observation l , $w_l = 0$, then there is no observed head at that node. SS is the weighted sum of squared deviations of calculated heads from observed heads and is to be minimized. Using the objective function [Eq. (7)] is equivalent to minimizing the error variance.

If the parameters to be computed (such as all the different values of K_{xx} , K_{yy} , S , and W) are designated vector \mathbf{b} , then the normal equations (Draper and Smith, 1981) derived by minimizing Eq. (7) with respect to each parameter can be written

$$\mathbf{e}^T \mathbf{w} \frac{\partial \mathbf{e}}{\partial \mathbf{b}} = 0. \quad (8)$$

The necessary elements of \mathbf{e} and their derivatives are obtained by applying a Gauss-Marquardt linearization scheme to Eq. (6). The technique yields a regression equation, which can be written

$$\Delta \mathbf{b}_i = -N^{-1} \mathbf{f}_i, \quad (9)$$

where $\Delta \mathbf{b}_i = \mathbf{b}_{i+1} - \mathbf{b}_i$, i is the iteration number, N is the normal matrix ($J^T \mathbf{w} J$) consisting of the derivatives of the elements of \mathbf{h} with respect to each of the elements of \mathbf{b} , and \mathbf{f}_i is the gradient of the objective function (i.e., the weighted sum of squared head differences between the model and the observed heads).

The sensitivity coefficients J_{ij} , or simply sensitivities, indicate the change in the value of head h_i for a unit change in parameter b_j . The regression algorithm uses only observed values of head in the criterion SS for the best fitting solutions.

Assumptions for the regression analysis

The nonlinear model—assumed to be the true model—represented by the solution of Eq. (6) for \mathbf{h} , which is the subset of \mathbf{h}_m that applies at nodes that are observation nodes, can be written for observation ℓ as

$$\mathbf{h}_\ell^{\text{obs}} = f(\xi_\ell, \beta) + \varepsilon_\ell, \quad (10)$$

where f indicates a function that is the solution of Eq. (6); ξ_ℓ is a vector of independent variables that is an undetermined but observable function of coordinates x, y , the problem geometry and boundary conditions; β is the vector of true parameters; and ε_ℓ is an error in observation.

To analyze statistically the results of and the predictions made by the regression model, we assume (Draper and Smith, 1981) that

$$E(\varepsilon_\ell) = 0, \quad (11)$$

$$\text{Var}(\varepsilon_\ell) = \sigma^2, \quad (12)$$

$$\text{Cov}(\varepsilon_\ell, \varepsilon_m) = 0, \quad \ell \neq m, \quad (13)$$

where E , Var , and Cov are the expected value, variance, and covariance operators, respectively. These assumptions indicate that ε_ℓ is a random variable with zero mean and constant variance σ^2 and that ε_ℓ and ε_m ($\ell \neq m$) are uncorrelated. In addition, it is often assumed that ε_ℓ is normally distributed with mean 0 and variance σ^2 (I is an identity matrix, and $I\sigma^2$ is a scalar diagonal matrix-covariance matrix) such that

$$\varepsilon \sim N(0, I\sigma^2). \quad (14)$$

This means that the elements of ϵ are independent and uncorrelated and allow the use of statistical tests and measures involving the F and t distributions (Draper and Smith, 1981).

Because β is unknown, ϵ is not observable and the assumptions cannot be checked directly. However, they can often be checked indirectly, after the regression and model analysis have been performed, as demonstrated later.

V. Model implementation and calibration

Grid selection

The study area consists of a 44×23 mi rectangle oriented in a southwest to northeast direction; it includes Rattlesnake Creek from west of the Macksville stream-gaging station to the confluence with the Arkansas River (fig. 21). This rectangle is divided into 1,012 squares or cells, each being 1 square mile in area, thus forming a rectangular cell-centered finite-difference grid used by MODFLOW. A total of 562 grid cells form the active area within the boundaries of the model region.

Boundary conditions

The model boundaries for the study area, as shown in fig. 21, were arrived at by drawing bounding flow lines on water table maps, as mentioned previously, and using them as no-flow boundaries (because no-flow lines can cross each other) along the northwest and southeast sides. These bounding flow lines coincide approximately with the Rattlesnake Creek watershed boundaries. The southwest boundary was cut along the 2,000-ft water-level contour passing through Macksville, whereas the northeast boundary was taken along the Arkansas River by the confluence with Rattlesnake Creek, thus forming assumed constant-head end boundaries. Examination of the 2,000-ft contour over time from water table maps of the GMD5 over different years (KGS unpublished maps) since predevelopment time indicates that this contour did not change appreciably over time. That constant-head boundary is far away from the main area of interest in this study, that is the Quivira NWR.

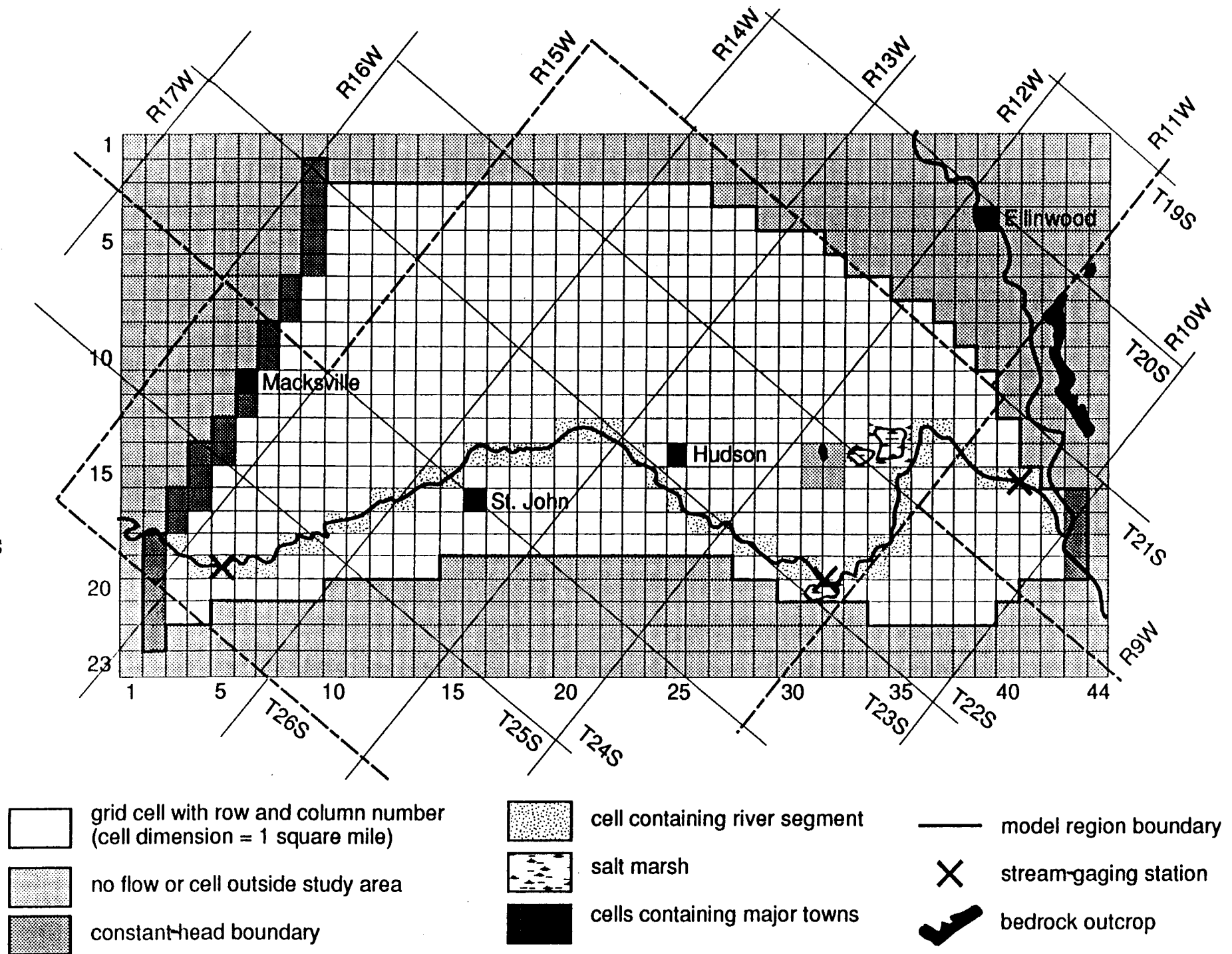


Figure 21. Finite-difference grid of the model area.

Model stresses

The period of simulation is divided into a series of stress periods within which specified stress parameters are constant. Each stress period, in turn, is divided into a series of yearly time steps. A system of finite-difference equations of the form of Eq. (6) is formulated and solved to yield the head at each node at the end of each time step.

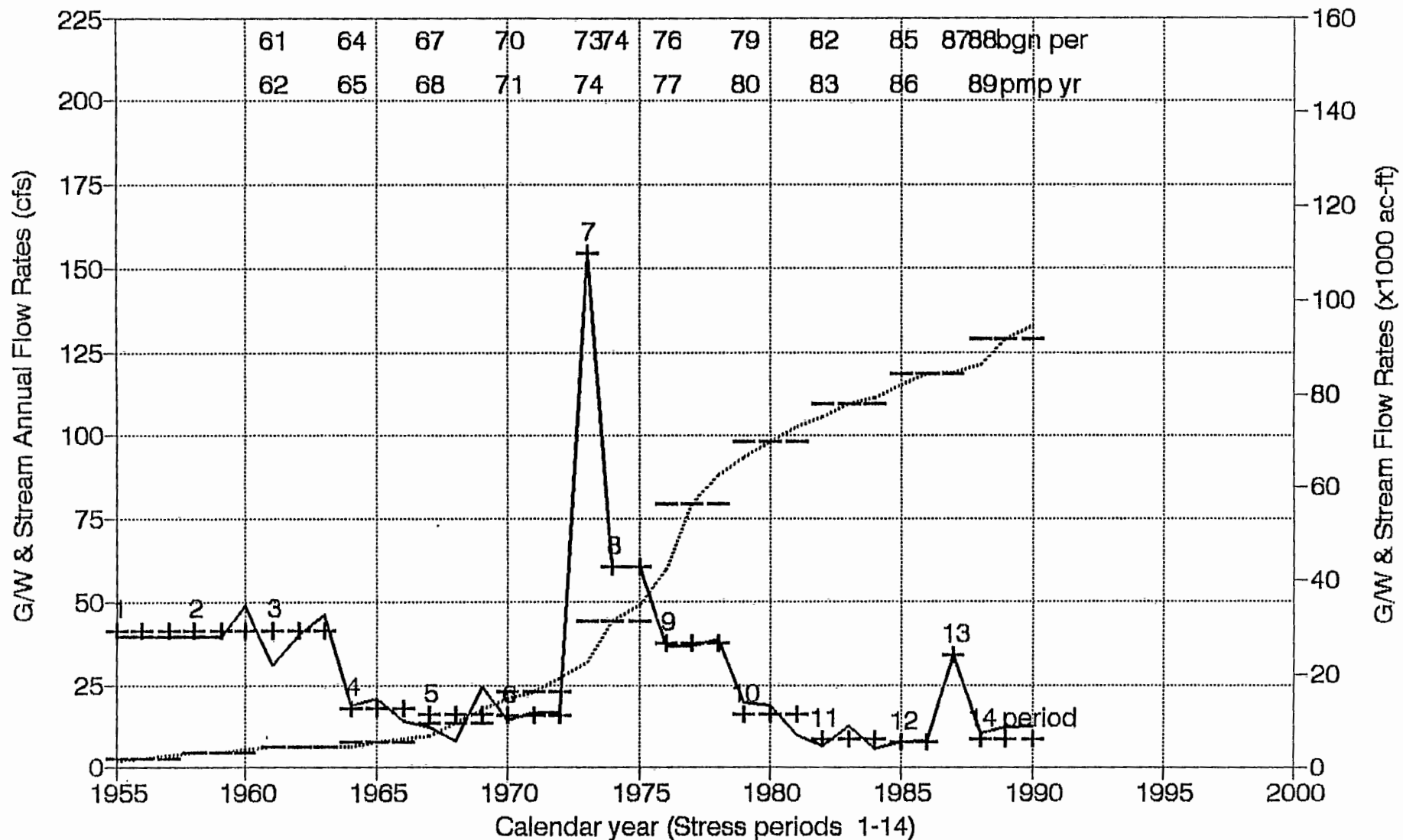
Groundwater pumpage

A computer program was written to read and reformat the water rights tape obtained from the Division of Water Resources and to sort water rights according to year, application number, or legal location. See fig. 10 for a plot of all ground-water rights versus year of issue in the model area. By the end of 1990 ground-water appropriations for the model area totaled 96,457 acre-ft. To simplify matters and to avoid excessive input files to the model, we decided to approximate this curve by dividing it into 3-year segments of uniform number and distribution of wells starting in 1955, which is considered an indicator year of predevelopment conditions. Thus the time period from 1955 to 1957 is represented by the 1956 ground-water rights distribution, the 1958–1960 period by the 1959 ground-water rights distribution, and so on, as shown by the dash lines in fig. 22. Pumping-well matrices for the different pumping stress periods, as indicated by the chosen index years 1956, 1959, 1962, 1965, 1968, 1971, 1974, 1977, 1980, 1983, 1986, and 1989, were prepared as input to the model (table 3).

Incoming streamflows

Another stress to the model system is the fluctuating amount of streamflow coming into the model area from Rattlesnake Creek, as monitored at the Macksville station. To simplify matters in a way similar to that done for the pumping stresses, we divided the average annual incoming streamflows at Macksville into variable year periods of relatively uniform incoming streamflows (fig. 22). These periods and the average Rattlesnake Creek streamflows are shown in table 3. The progressive decline in incoming streamflow is clearly evident from these data and in fig. 22.

Rattlesnake streamflow and water rights Macksville station and total pumping



Ave Annual strmflow
 Stress inflow, strm
 Annual pumping
 Stress outflow,pump

Figure 22. Model stresses (incoming streamflows and ground-water pumping) versus time.

Table 3. Stress periods employed in the model.

Pumping period	Mid-interval appropriated ground-water pumpage in model area (acre-ft/yr)	Incoming streamflow averaging period	Average annual streamflow (cfs)	Stress period
1955–1957	1,829	1960–1963	41.72 ^a	1
1958–1960	3,252	1960–1963	41.72 ^a	2
1961–1963	4,345	1960–1963	41.72	3
1964–1966	5,505	1964–1966	17.80	4
1967–1969	9,627	1967–1969	16.25	5
1970–1972	16,693	1970–1972	15.89	6
1973–1975	32,250	1973	154.58	7
1973–1975		1974–1975	60.31	8
1976–1978	57,483	1976–1978	37.47	9
1979–1981	71,051	1979–1981	16.06	10
1982–1984	79,273	1982–1984	8.23	11
1985–1987	85,889	1985–1986	7.63	12
1985–1987		1987	33.98	13
1988–1990	93,628	1988–1990	8.21	14

a. Average streamflows assumed equal to the ones in the 1960–1963 period.

Because the Macksville stream-gaging station has been operational only since 1960, all previous streamflows were assumed to be equal to the average streamflow during the 1960–1963 period.

Therefore, by combining the pumping and incoming streamflow stress periods, we obtained 14 pumping and stream stress periods and therefore 14 corresponding input data matrices for the model in simulating stream-aquifer conditions from 1955 to 1990. Table 3 details these 14 stress periods.

Aquifer-related data

Aquifer base

The aquifer base was extracted from the compiled bedrock map (Sophocleous et al., 1990) by superimposing the model grid on that map and reading (or interpolating) a bedrock elevation value at the center of each cell block (see fig. 7).

Predevelopment and other water levels

The same procedure as that used to define the aquifer base was followed for the predevelopment water-level map (see fig. 8). Water levels from the 1991 survey (see fig. 14) were used to create an observed water-level matrix for comparison with corresponding simulated results.

Hydrogeologic properties

Several existing values of hydrogeologic properties from previous reports, such as Fader and Stullken's (1978), were considered for initial parameter values. For example, analysis of specific capacities of 235 irrigation wells in the Great Bend Prairie by Fader and Stullken (1978) indicated an aquifer transmissivity range of 2,500–35,000 ft²/d, which, assuming a saturated thickness of 125 ft, translates to a range of hydraulic conductivities of 20–280 ft/d.

We know that the study area is characterized by a number of high-transmissivity buried channels (Sophocleous et al., 1990; Sophocleous, 1991b) (see fig. 7). We also know that a Cretaceous bedrock outcrop (Kiowa Shale) occurs west of the Big Salt Marsh, implying low aquifer transmissivity in the area surrounding the outcrop. Thus the study area was initially zoned into (1) different hydraulic conductivity regions based on the existence of buried channels, (2) a low hydraulic conductivity region near the bedrock outcrop and (3) the remaining aquifer region.

Values of aquifer storativity are more difficult to come by. However, typical values of storativity for sand range from 0.01 to 0.46 and for gravel from 0.13 to 0.44 (Morris and Johnson, 1967). Because of the limited number of storativity values in the study region, the area was zoned as a single storativity region.

Recharge data

Recharge data from a recently completed study on ground-water recharge assessment of the GMD5 (Sophocleous, 1991a; 1992a, c), a previous study of the Rattlesnake watershed (Sophocleous and McAllister, 1987, 1990), and a recent U.S. Geological Survey study (Hansen, 1991) have been used as initial estimates of the recharge in the study area. Based on those studies,

recharge in the study area ranges from approximately 0 to less than 6 in. per year and it averages 1 to 2 in. per year. Because the Big Salt Marsh is a discharge zone for the area and because the region around the bedrock outcrop is characterized by low transmissivities, that combined region is zoned as a very low (minimal) recharge zone for the model. A second recharge zone was established based on the bulging water table contours in the region (see fig. 8) between Rattlesnake Creek and the bedrock outcrop, implying relatively high recharge. The rest of the study area was considered a mixed zone containing low, high, and intermediate recharge values.

Ground-water evapotranspiration

As indicated in the January 1991 depth to water table map (see fig. 15), the area around the Quivira NWR is generally characterized by very shallow depths to the water table (less than 6–10 ft) from which ground water can easily be lost from the aquifer by evapotranspiration. Thus that region was considered a ground-water evapotranspiration zone, and the evaporation modules of the MODFLOW program were activated.

Stream-related data

Stream widths and slopes for the model area were estimated, as mentioned previously, from site visits and from topographic and other maps. Streambed hydraulic conductance was approximated based on the knowledge of the area's geology. Manning's coefficients were obtained from tables (Chow, 1959; White, 1979) based on our knowledge of the area streams.

Calibration

Calibration involves adjustment of model input using alternative combinations of parameter values and zones to obtain reasonable agreement with measured data. The model was calibrated for both steady-state and transient-state conditions. For this study we adhered to the *principle of parsimony*, according to which in a choice among competing hypotheses, other things being

equal, the simplest hypothesis (i.e., the one with the smallest possible number of parameters for adequate representation) is preferable.

Steady-state calibration

Because of the relatively large number of data points used in the construction of the predevelopment water-level map (Sophocleous et al., 1990) and the minimal amount of external stresses (e.g., pumpage) imposed on the aquifer, the interpolated predevelopment water levels for each active cell of the model grid were considered of similar accuracy to the actually measured ones. Thus all active model grid cells are considered cells with observed (measured) values that are identical with the initial (starting) water-level cell entries in the model.

Initially, the model area was divided into several hydraulic conductivity zones, as mentioned previously. Using this K zonation and the recharge and evapotranspiration zonation mentioned previously, we ran the MODINV model to optimize the hydraulic conductivity values using the predevelopment (steady-state) conditions, as exemplified by the predevelopment water levels and the 1955 irrigation well distribution. However, when we reran the simulation using fewer buried-channel hydraulic conductivity zones, the results and the sum of squares of the deviations between simulated and observed heads progressively improved until only two buried-channel zones remained. Therefore only two K buried-channel zonations (indicated in fig. 23) were adopted. Using no buried-channel K zones increased the sum of squares of the deviations significantly, and thus this option was not adopted. (The parameter zonations for recharge and evapotranspiration are shown in the next section.) The final result of these parameter optimization iterations is shown in section VI.

Transient-state calibration

To ensure that the transient-state model will simulate future conditions in the real system, we found it necessary to first simulate with reasonable accuracy as much hydrologic history as practical. Therefore the transient-state calibration was run from 1955 to 1990 using yearly time

Hydraulic Conductivity Zonation

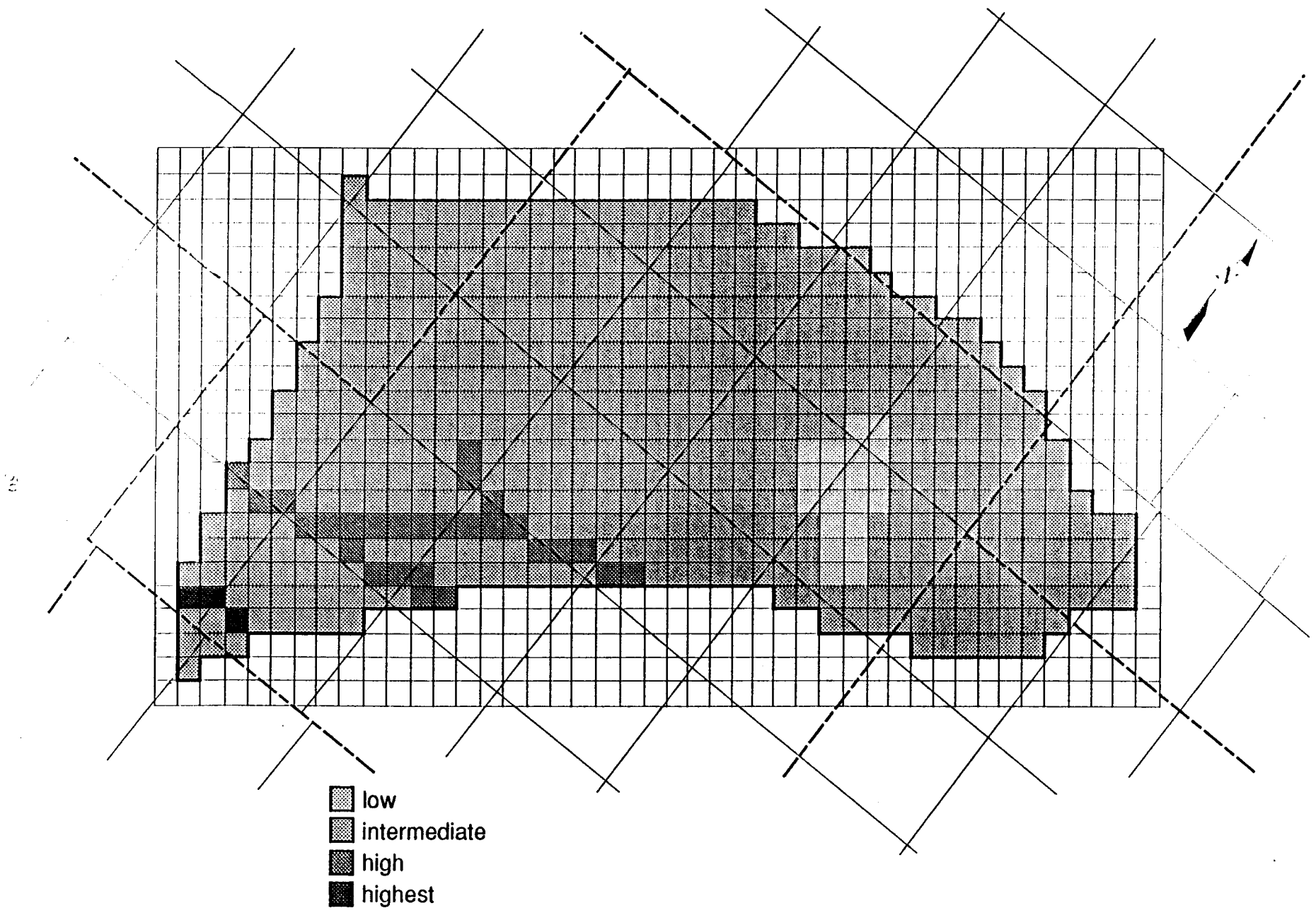


Figure 23. Hydraulic conductivity zonation of the model area.

steps and the stress history outlined in table 3. When the model is thus calibrated, it can be used to project stream-aquifer responses to hydrologic conditions.

Starting with the optimized parameter estimates from the steady-state calibration and employing the stress periods indicated in the "Model Stresses" section, we ran the MODINV parameter estimation program to optimize, in sequence or simultaneously, storativity, recharge, and evapotranspiration, keeping the already optimized hydraulic conductivity values constant. Employing two or more zones of storativity, based on geologic reasoning, versus one zone did not result in any significant difference in the sum of squares of deviations between simulated and observed values of hydraulic head, and thus a single storativity zone was used. The final recharge and evapotranspiration parameter zonations are shown in figs. 24 and 25, respectively. In the transient runs the ground-water pumpage was held at 80% of the appropriated amounts. We judged that 80% of the appropriated water rights was closer to the one actually used, and therefore all transient-state runs were performed under this assumption.

VI. Initial simulation results and model analysis

As mentioned previously, the calibration or parameter estimation problem is in essence a regression problem, and the various methods and tests that have been developed to analyze regression problems also can be applied to ground-water flow models. Many of these procedures are used in the following steady-state and transient-state model analyses.

Predevelopment (steady-state) conditions

The results of the steady-state analysis are shown in table 4, in which the fit of simulated and observed values of head is very good, as indicated by the high value of the correlation coefficient ($R = 0.9994$). The standard error of the estimate for the i th parameter [given by the square root of the i th diagonal component of the parameter variance-covariance (or simply covariance) matrix] is a measure of the range over which the parameter can be varied to produce a solution for the dependent variable (i.e., hydraulic head) that is similar to the solution obtained

Recharge Zonation

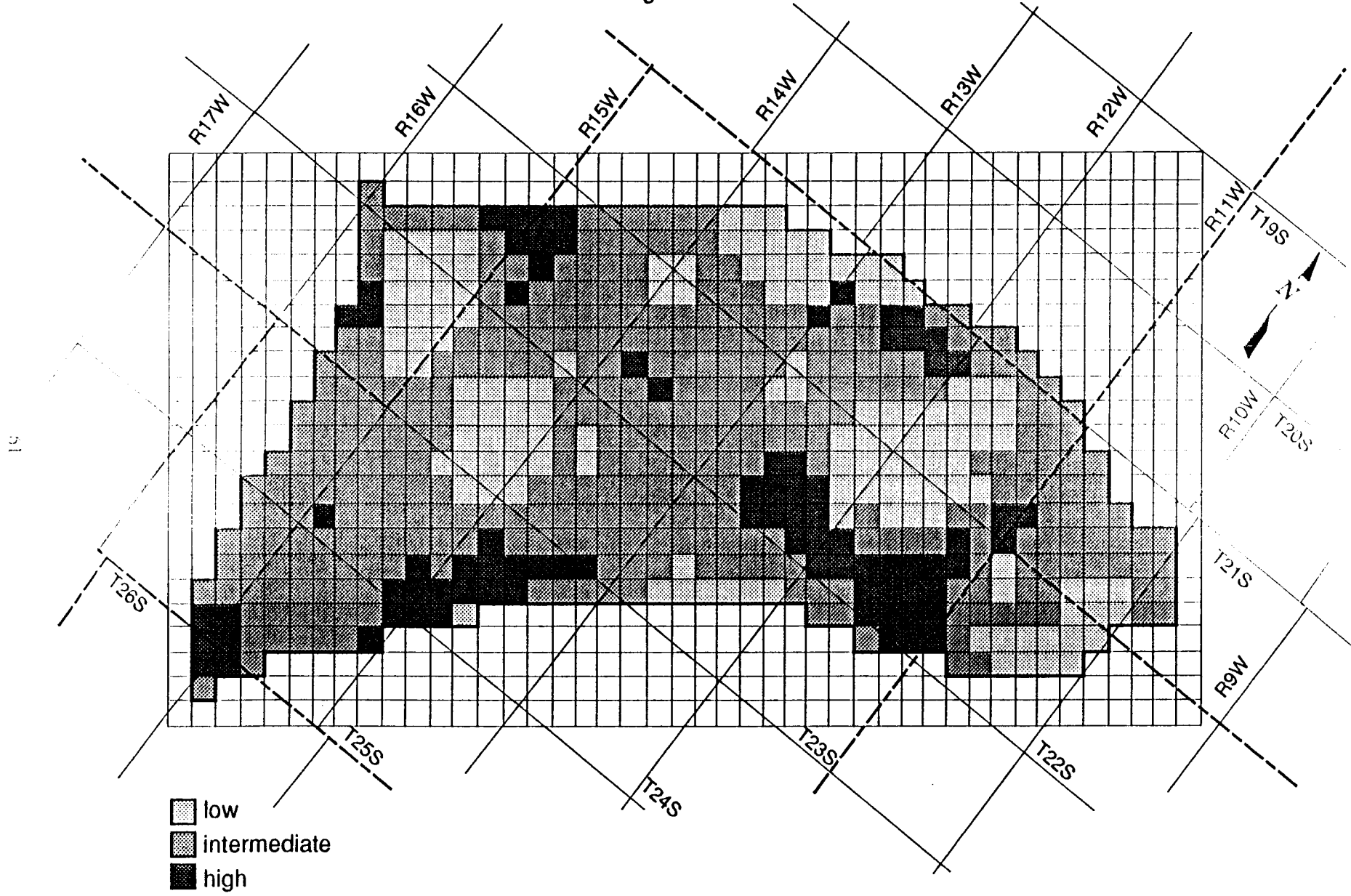


Figure 24. Ground-water recharge zonation of the model area.

Groundwater Evapotranspiration Zonation

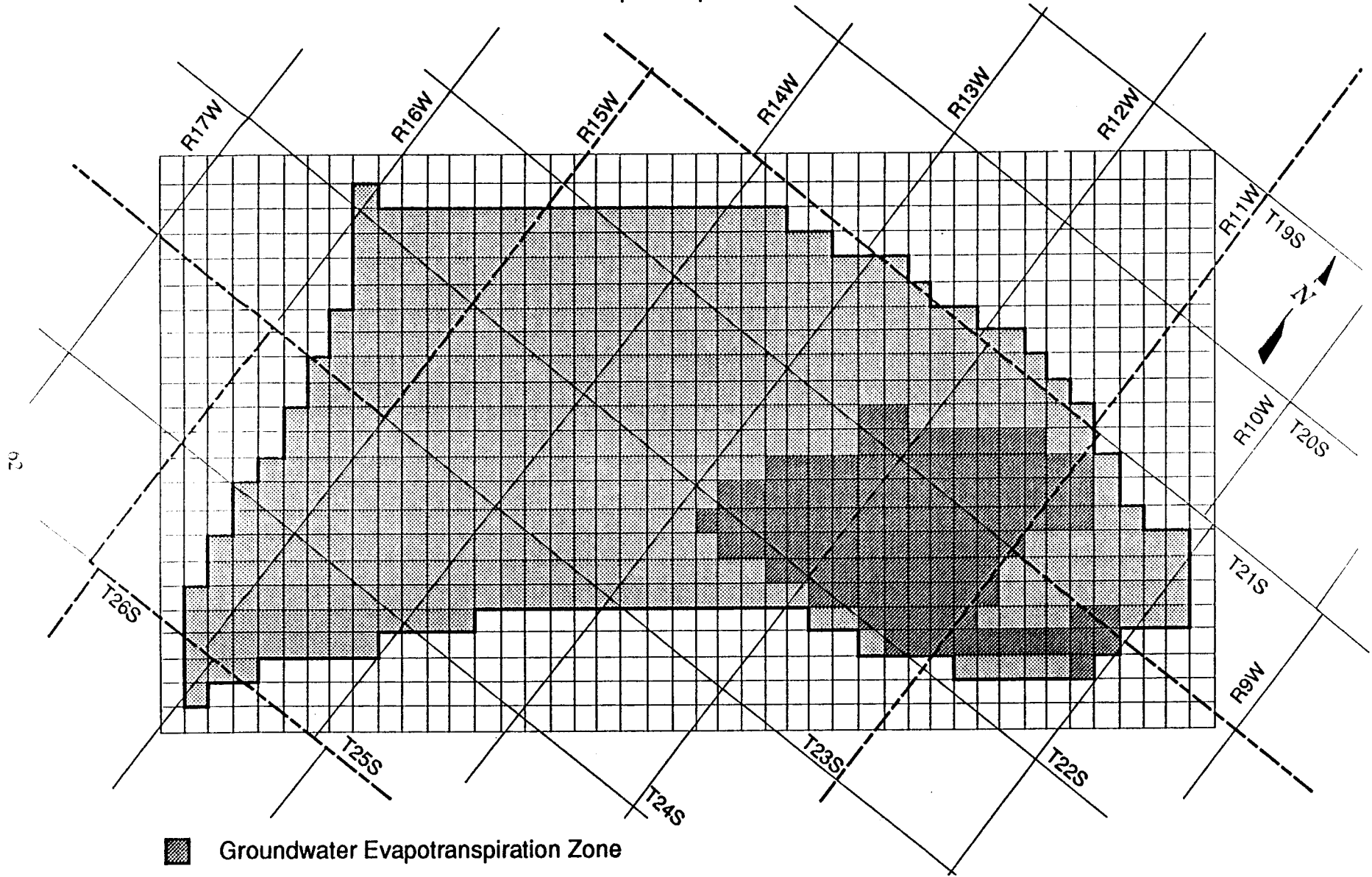


Figure 25. Ground-water evapotranspiration zonation of the model area.

Table 4. Steady-state analysis results.

Zone	K (ft/d)	Std. error	Zone	Recharge (in./yr)	Std. error	Zone	ET (in./yr)	Std. error
1	21	2.2	i	0.001	0.038	(1)	2.86	0.304
2	10	12.9	ii	0.54	0.052			
3a	50	9.5	iii	5.33	0.646			
4a	78	71.7						

Square root of the error variance (s) = 2.85 ft.

Correlation between simulated and observed water levels (R) = 0.9994.

Number of observations (N) = 492.

Weighted sum of squares of the deviations between simulated and observed values of head (SS) = 3,904 ft².

$s/\Delta h = 0.0085$ ($\Delta h = 335$ ft).

Std. error = $\sigma/N^{1/2}$.

a. Paleochannel zones.

using the estimated parameter. Standard errors are indications of the precision of the determined parameters. Converting such standard errors into a confidence interval requires assuming a probability distribution for these errors. For example, if the central limit theorem holds, a 95% confidence interval for the parameter values will be given by $\hat{b} \pm 1.96\sigma_E$, where \hat{b} is the estimated value of the parameter and σ_E is the standard error. The final hydraulic conductivity, recharge, and evapotranspiration zonations of the model area are shown in figs. 23, 24, and 25, respectively.

The error variance s^2 of the hydraulic head values is another measure of overall goodness of fit of the model. [It is calculated as the ratio of the weighted sum of squares of the deviations between simulated and observed values of head (SS) over the number of observation points minus the number of estimated parameters.] A good overall fit between modeled and measured heads indicates that the head measurement standard deviations (i.e., the square root of the error variance) are small. The value of the ratio of the square root of the error variance over the difference between the highest and the lowest value of head in the model region ($s/\Delta h$) is 0.0085 (table 4), a relatively small value; thus errors in the model are considerably less than the model response, as indicated by the maximum head loss (Δh) of 335 ft in the model area. A comparison of observed and model simulated water table contours, shown in fig. 26, indicates a satisfactory match.

Observed and predicted predevelopment water levels

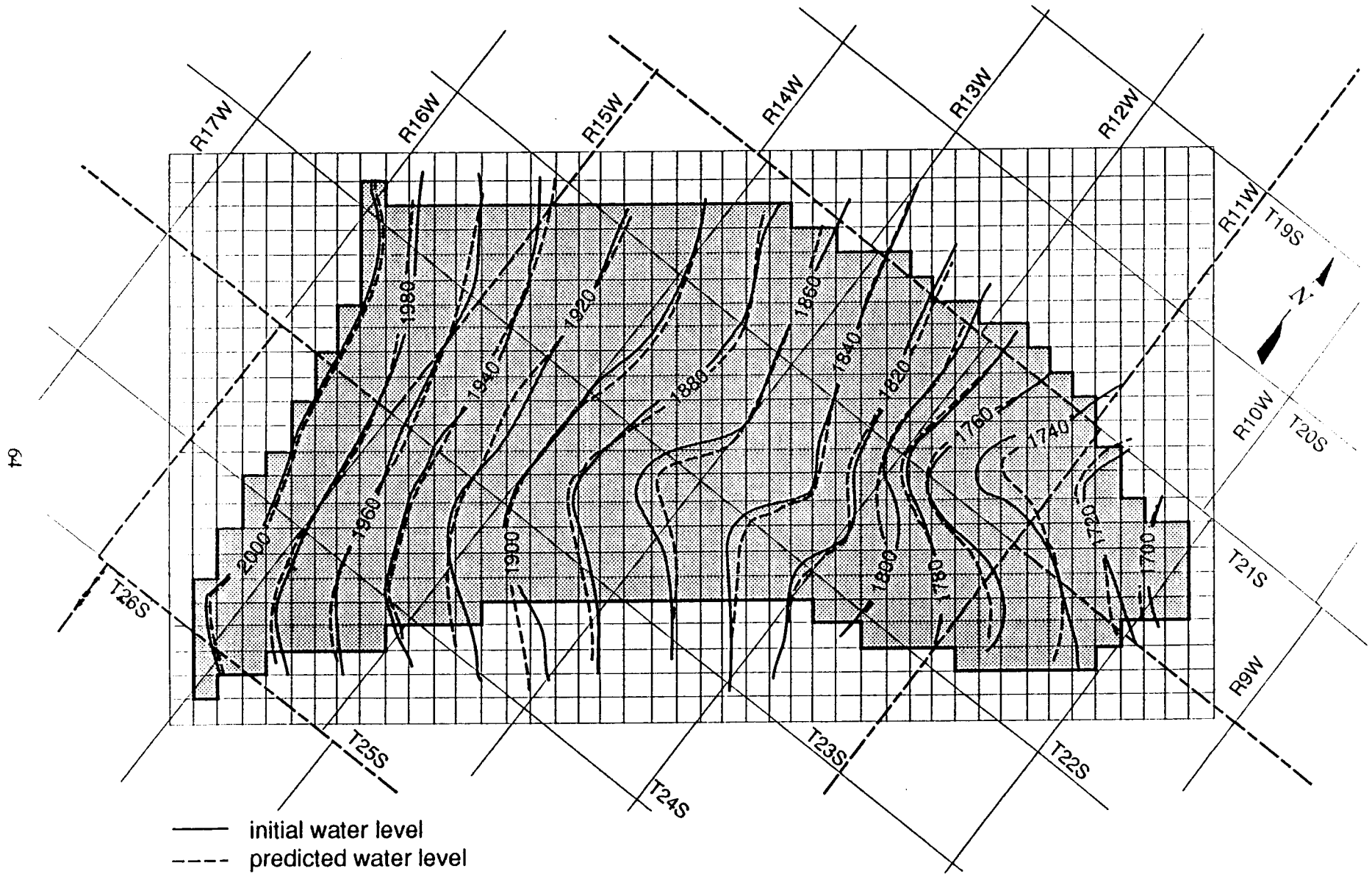


Figure 26. Comparison of observed and simulated steady-state water table contours.

The main reasons for analyzing residuals are to examine the validity of the various assumptions concerning their distribution [Eqs. (11)–(14)] and to investigate the correctness of the model. Aspects that could be investigated include evidence of spatial nonrandomness and evidence that the residuals are not approximately normally distributed (Sophocleous, 1984). Draper and Smith (1981) give a number of methods for examining residuals, and they emphasize that graphical procedures are valuable tools for detecting nonrandomness because violations of assumptions serious enough to require corrective action generally are apparent on the various plots. In fig. 27 residuals are plotted against values of estimated head. Under the given assumptions the plot should display a roughly horizontal band of residuals having no apparent trend, and this is exactly how the plotted residuals in fig. 27 behave. The residuals were also plotted in Cartesian coordinates and contoured (fig. 28). The residuals show no obvious systematic variation of significant degree over the map area, indicating that this model is probably adequate for these data.

To check whether the residuals are normally distributed, we plotted them on normal probability paper (fig. 29). A relatively good-fitting straight line can be drawn through the bulk of the points, indicating that the calculated residuals are approximately normally distributed. For the parameters derived from the least-squares analysis as maximum-likelihood estimates of the true parameters (i.e., parameter estimates that give the greatest probability of obtaining the observed data), residuals must be normally distributed.

Water budget

A summary of all inflows and outflows to a region is generally called a water budget. Because in the model program the water budget is calculated independently of the equation solution process, it provides independent evidence of a valid solution. The difference between total inflow and outflow is given as a percent error, calculated using the formula

$$D = \frac{100(\text{In} - \text{Out})}{(\text{In} + \text{Out})/2}, \quad (15)$$

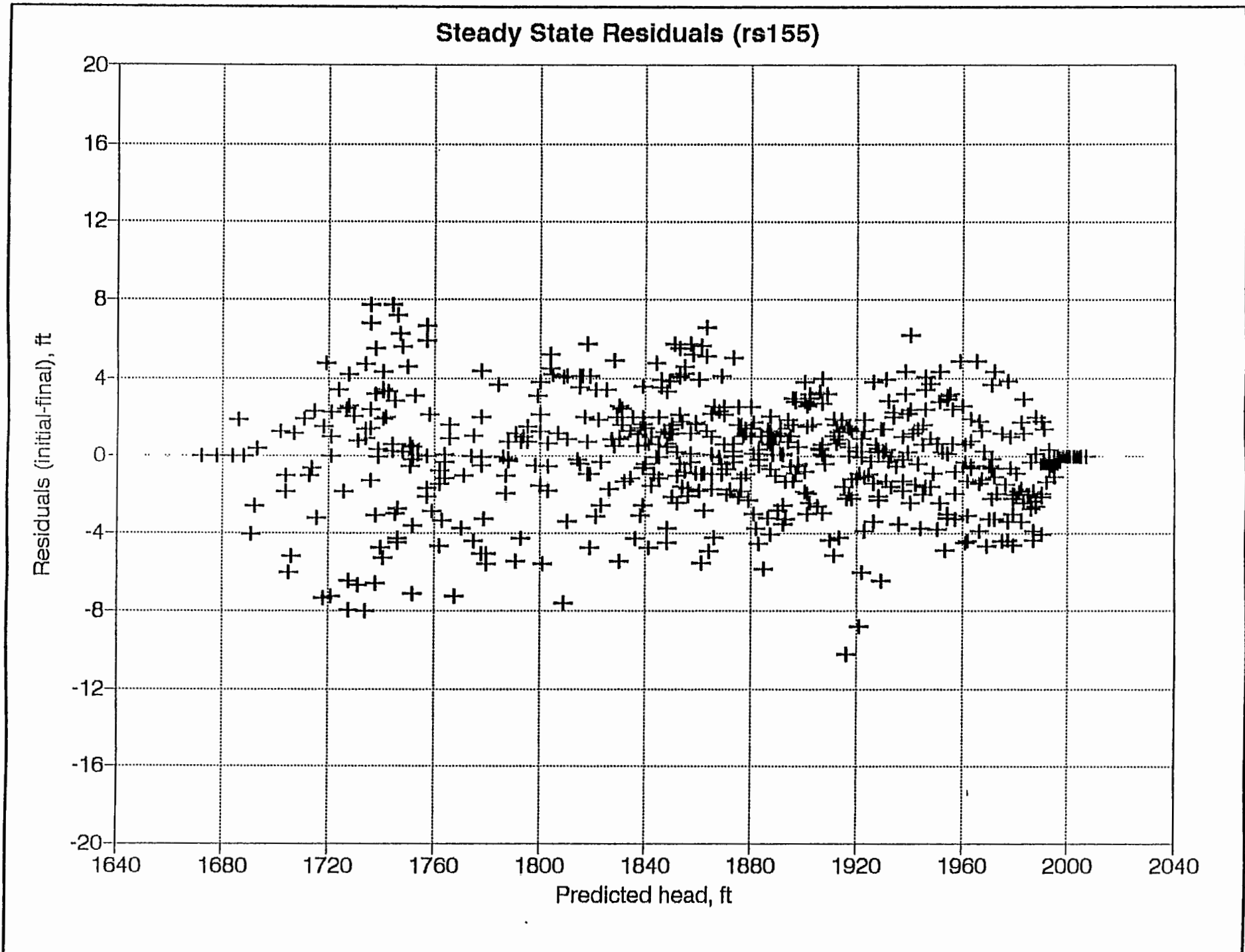
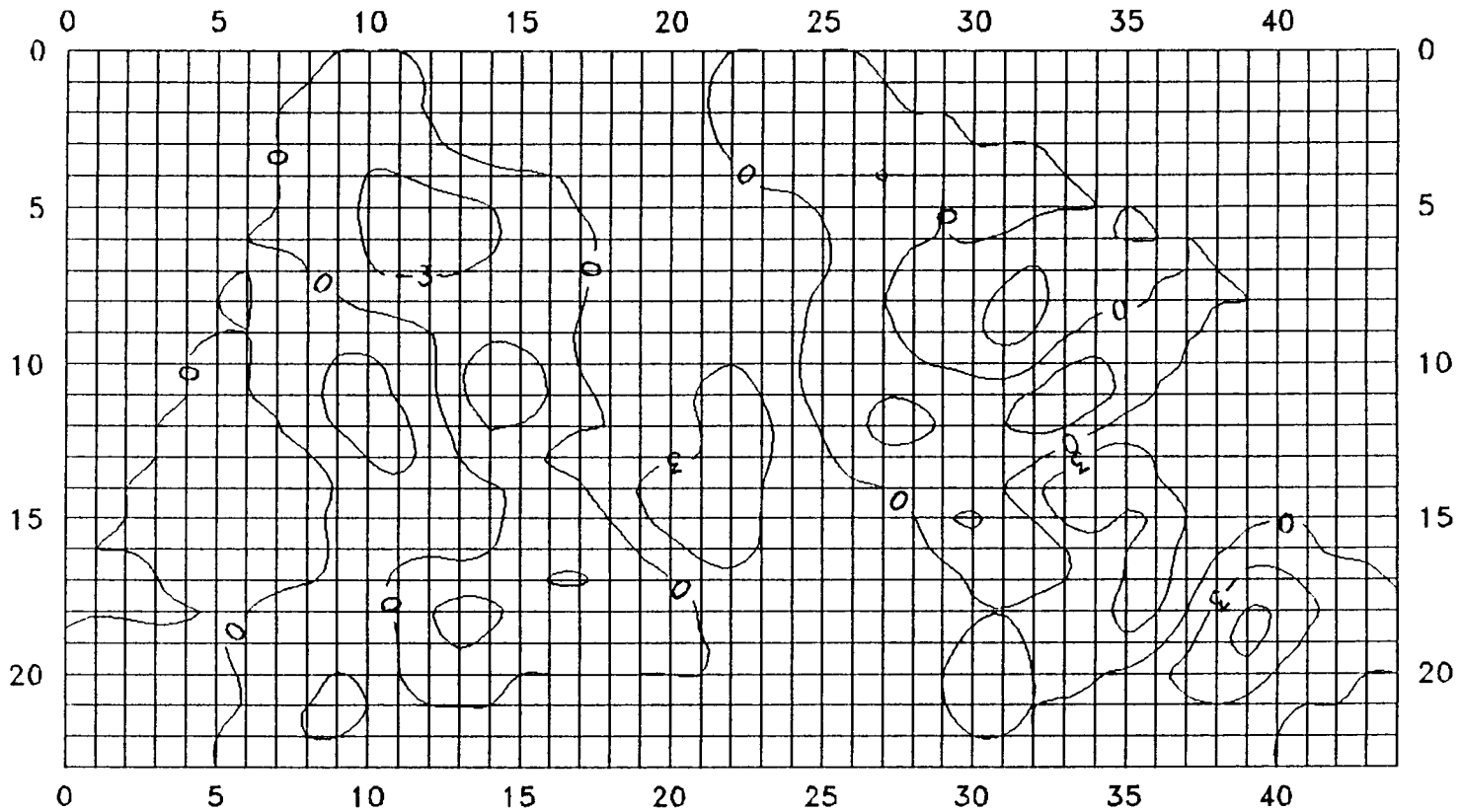


Figure 27. Steady-state residuals (differences between observed and simulated water table values) versus predicted hydraulic head

Steady State Residuals (rs155)



67

Figure 28. Contours of steady-state residuals. Contour interval 3 ft.

Probability plot for normal distribution, 1955 residuals

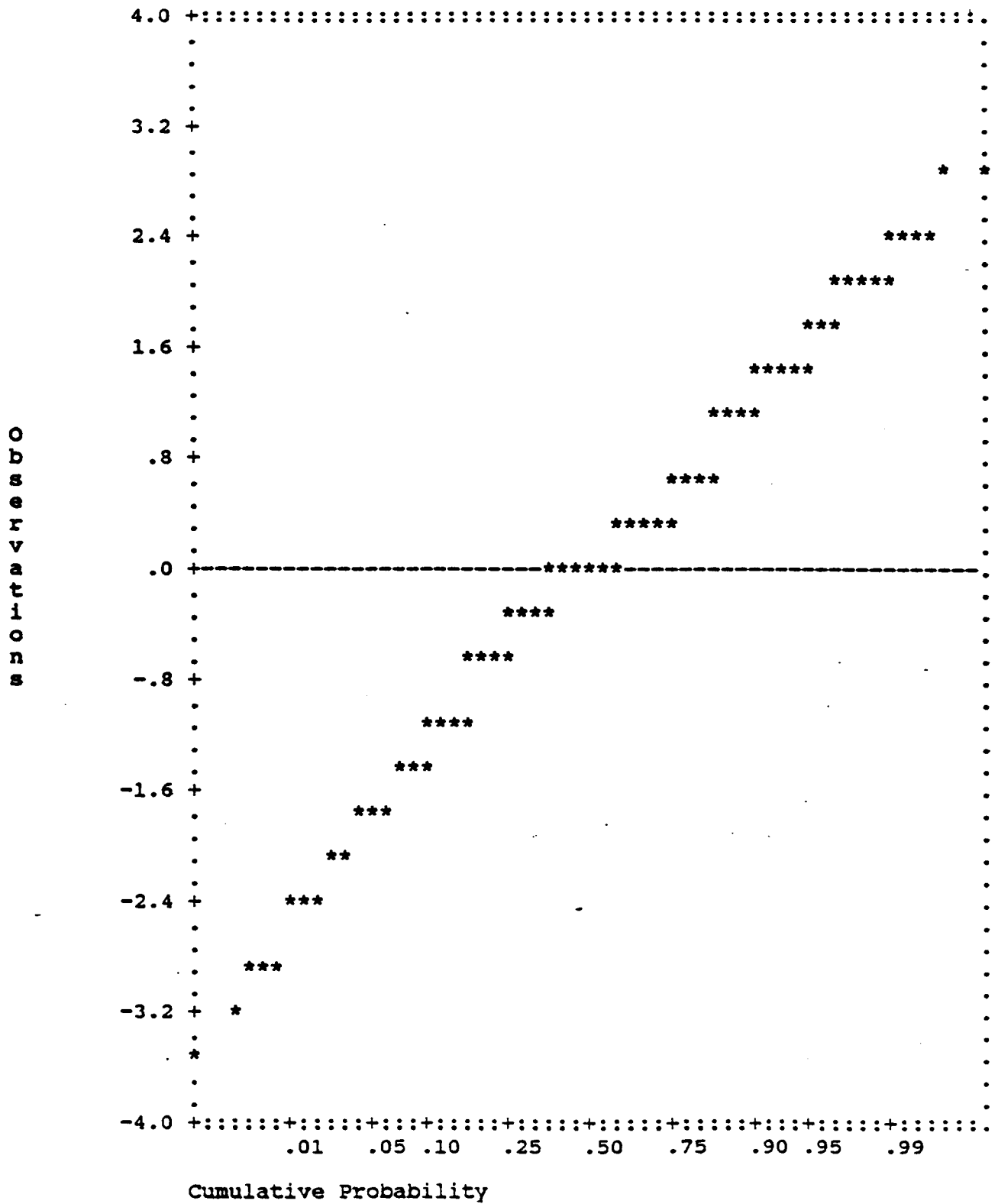


Figure 29. Probability plot of steady-state residuals.

where In is the total inflow to the system, Out is the total outflow, and D is the percent error term. If the model equations are solved correctly, the percent error should be small. The overall model water budget is presented to check the acceptability of the solution and to provide summarized information on the flow system. The volumetric water budget for the model area under predevelopment conditions is presented in table 5. It is evident from the table that the bulk input to the stream-aquifer system is ground-water recharge and that the largest outflows from the system are evapotranspiration losses and baseflow contributions to streamflows. Note that the irrigation pumpage is a minor element of total system outflow for the considered period.

Transient-state simulations for the stream-aquifer system

The results of the transient-state simulations from 1955 to 1990 are shown in table 6. The value of the ratio $s/\Delta h$ (0.0127) is still relatively small, indicating that errors in the model are considerably less than the model response, as indicated by the maximum head loss. Comparisons of predicted versus observed values of hydraulic head, depicted in fig. 30 (for 1990 and January 1991) are satisfactory. A plot of the residuals versus predicted values of hydraulic head for the 1955–1990 period (fig. 31) and a contouring of residual values (fig. 32) reveal that no relationship of significant concern is obvious, indicating that this model is probably adequate for these data. A normal probability plot of the residuals for the 1955–1990 period (fig. 33) reveals a well-fitting straight line through most of the plotted points, indicating that the residuals are approximately normally distributed.

Comparison of predicted ground-water discharge and observed average annual streamflow for the 1955–1990 simulation period near the Zenith stream-gaging station shows a satisfactory match, as indicated in fig. 34. As can be seen from that figure, the model underpredicts ground-water discharge during periods of high streamflow because the model does not simulate overland runoff. During periods of low flow, however, most streamflow is derived from ground-water discharge.

Observed and Predicted water levels (Jan 1991)

70

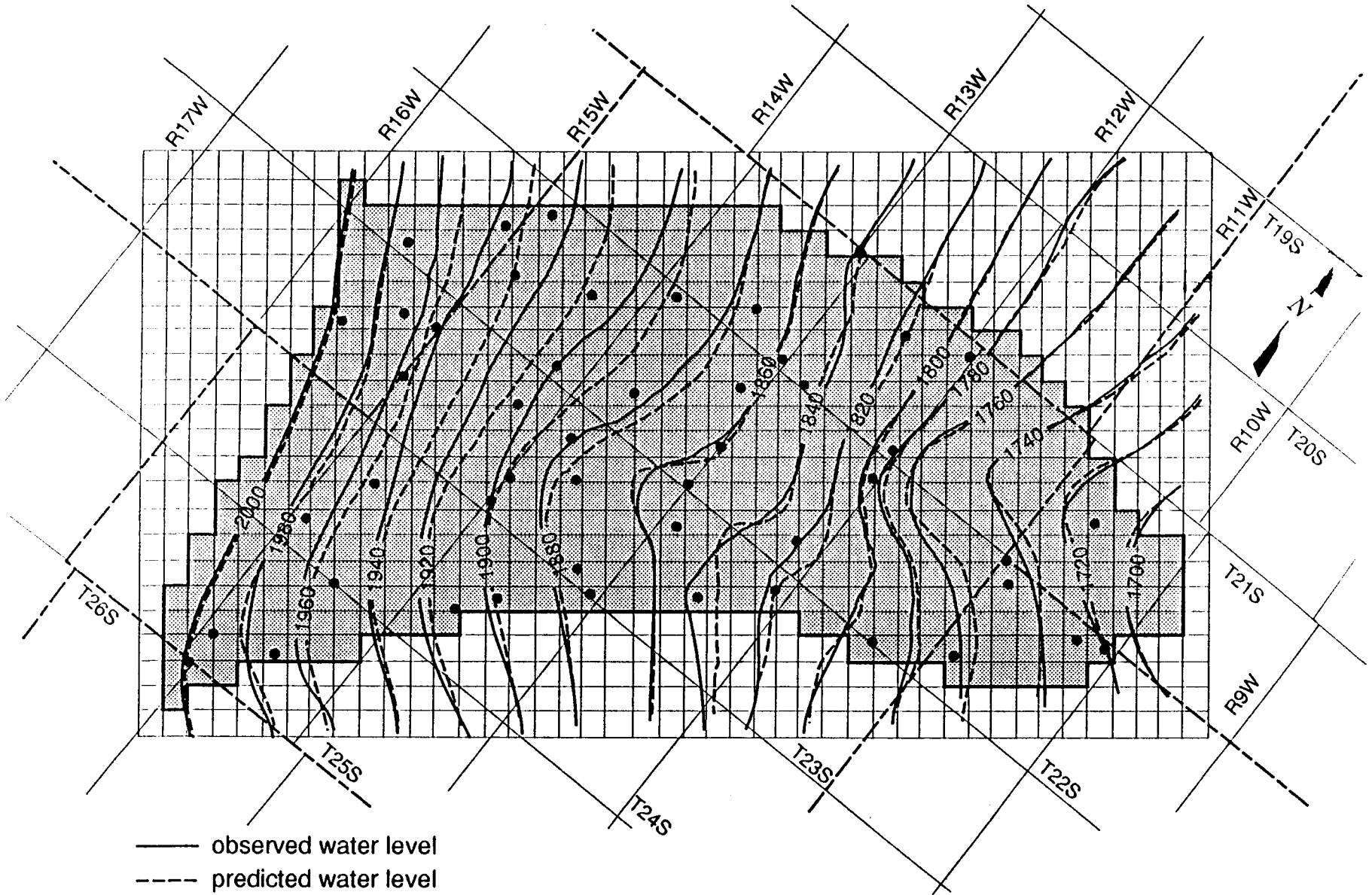


Figure 30. Comparison of observed and model-predicted January 1991 water table contours.

rs1wl91: 51 observed water levels (Jan)
Residual(obs.-pred.) mean 0, ss 1472

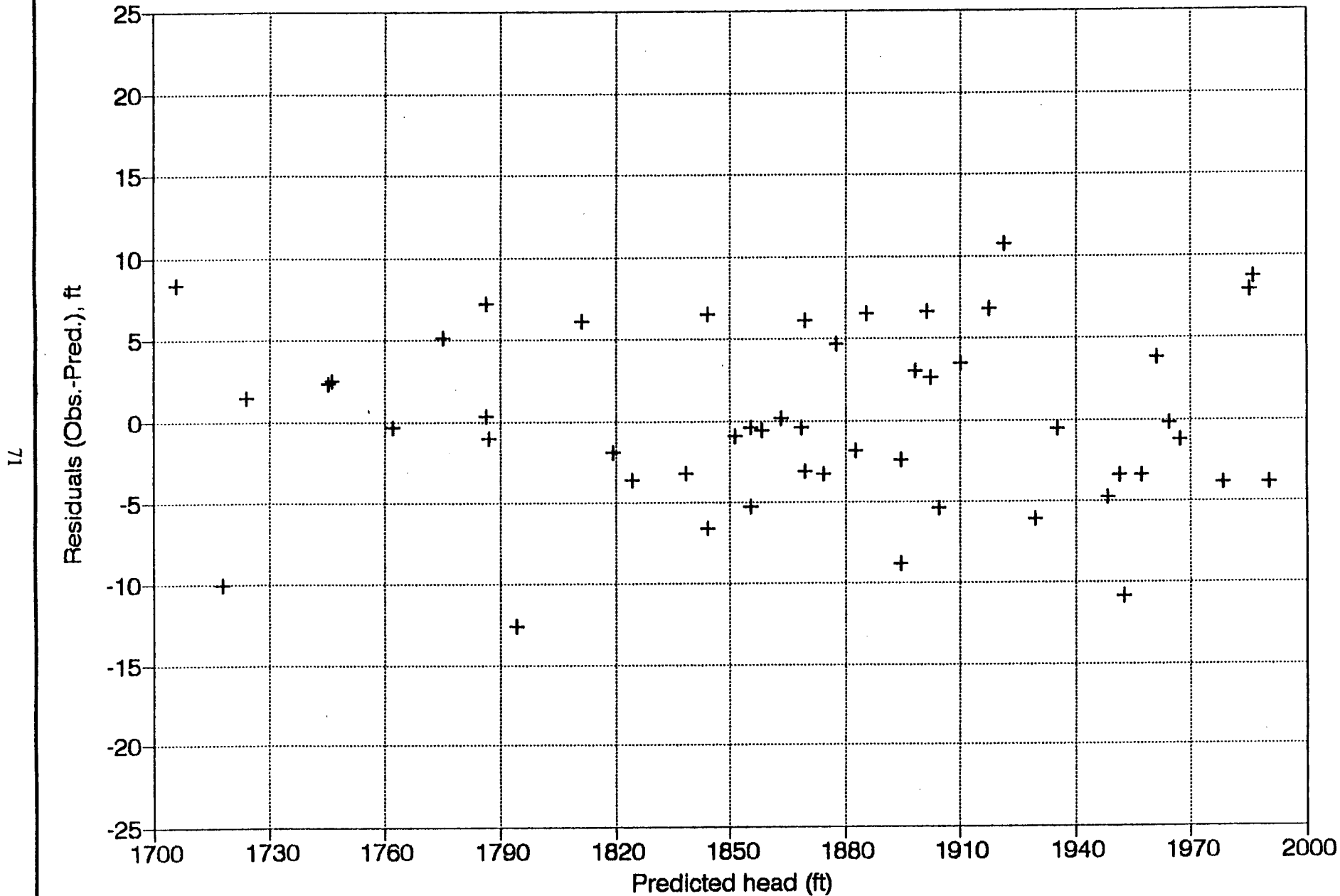


Figure 31. 1990 residuals versus predicted hydraulic head.

Rattlesnake 1990 residuals

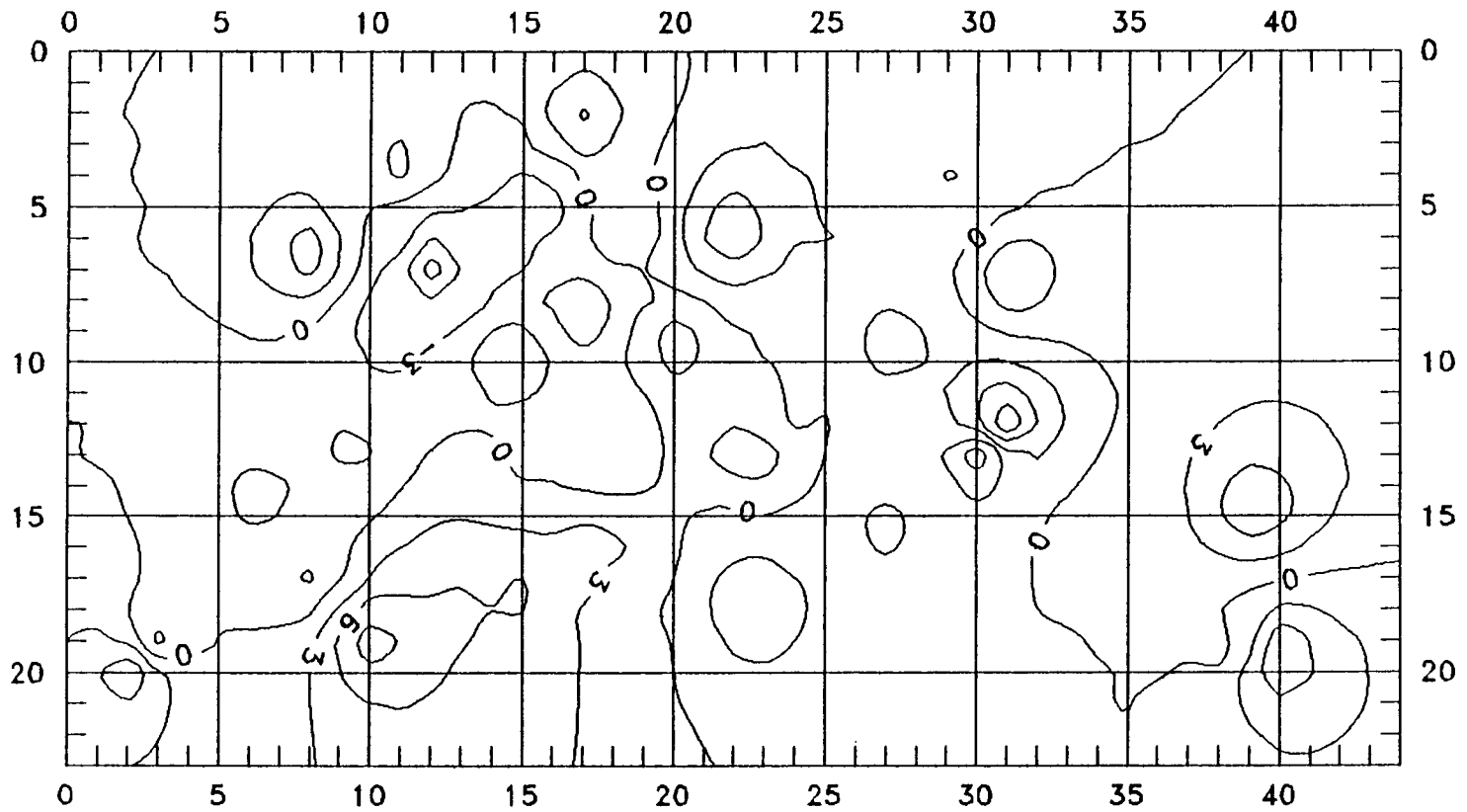


Figure 32. Contours of 1990 residuals. Contour interval 3 ft.

Probability plot for normal distribution, 1990 residuals

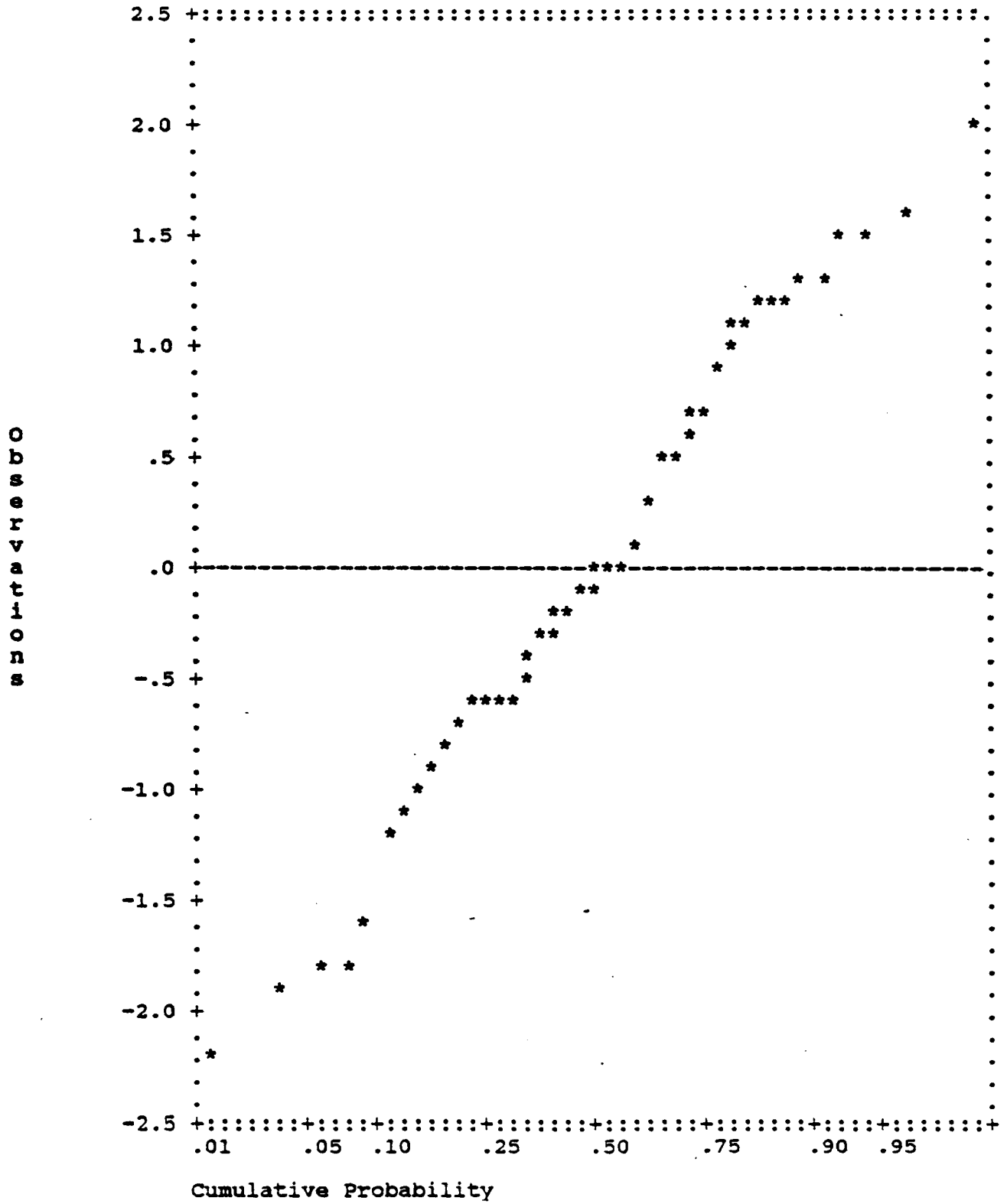


Figure 33. Probability plot of 1990 residuals.

Rattlesnake Creek annual streamflow Node (19,31) near Zenith, KS

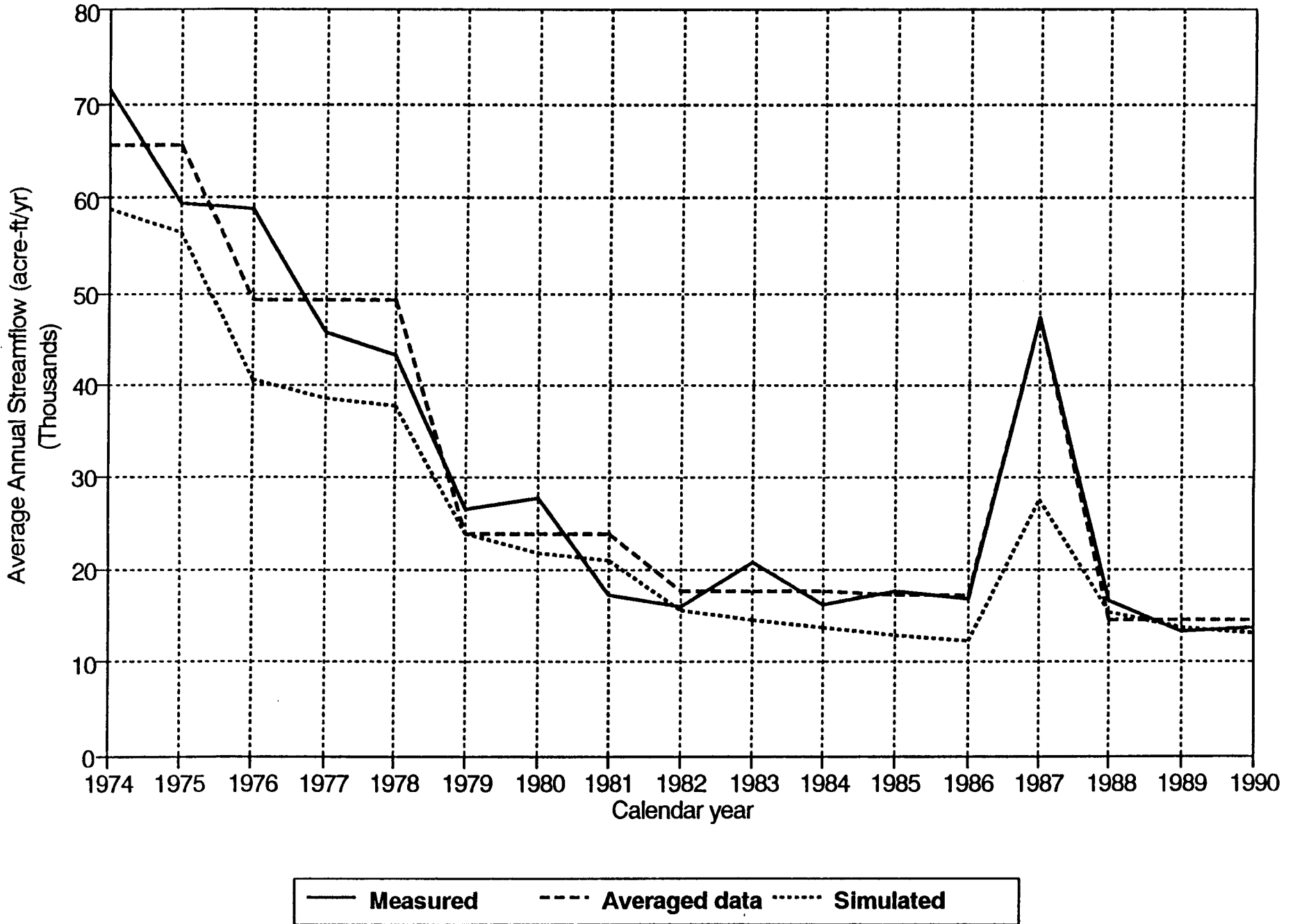


Figure 34. Comparison of predicted Rattlesnake Creek baseflow and streamflow at the

Table 5. Volumetric budget for entire model area under predevelopment conditions (c. 1955).

Water-balance component	Volumetric rate (acre-ft/yr)
Inflows	
Constant head (underflow into study area)	4,800
Recharge	22,603
Stream leakage	998
Total inflows	28,401
Outflows	
Constant head (underflow out of study area)	760
Pumping wells	1,820
Evapotranspiration	13,695
Stream leakage (net ground-water discharge to stream)	12,133
Total outflows	28,408
Discrepancy = 0.00%	

Table 6. Transient 1955–1990 analysis results.

Zone	Recharge (in./yr)	Std. error	Zone	ET (in./yr)	Std. error	Zone	Storativity
i	0.001	0.273	a	2.167	0.437	a	0.25
ii	1.681	0.155					
iii	3.001	0.435					

Square root of the error variance (s) = 4.27 ft.

Correlation between simulated and observed water levels (R) = 0.9974.

Number of observations (N) = 42.

Weighted sum of squares of the deviations between simulated and observed values of head (SS) = 710.9 ft².

$s/\Delta h = 0.0127$. ($\Delta h = 335$ ft).

Std. error = $\sigma/N^{1/2}$.

Under natural conditions the water table gradient slopes toward the river, and ground water discharges from the aquifer into the river. This can be seen by the curvature of the water-level contours pointing upstream (see fig. 8). However, under drought or pumping conditions, the water table gradient decreases and ground-water discharge to the stream is reduced. If pumping is of sufficient volume and duration, the gradient may be reversed and water from the stream will move by induced infiltration through the streambed into the alluvial aquifer. During

predevelopment times (circa 1955), the part of Rattlesnake Creek within the study area was entirely a gaining stream. At present, however, the model results indicate that the stream has both gaining and losing reaches, as indicated by the negative and positive seepage values, respectively, in fig. 35. (Each reach corresponds to a 1-mi grid.) The major losing stream segments are (1) between the Little Salt Marsh and the RCA structure, that is, in T. 22 S., R. 11 W., and (2) from south of US-50 to northwest of St. John. The major gaining segment of Rattlesnake Creek, according to our model results, are (1) after the juncture with Salt Creek exiting the Big Salt Marsh and (2) from the confluence with Wild Horse Creek up to southeast of Hudson.

The overall volumetric water budget for the model area during the last stress period (1988–1990) of the 1955–1990 transient-state simulation is presented in table 7. The convention followed in MODFLOW is that flow into or out of storage is considered part of the overall budget inasmuch as accumulation in storage effectively removes water from the flow system and storage release effectively adds water to the flow, even though neither process in itself involves the transfer of water into or out of the ground-water regime (McDonald and Harbaugh, 1988).

Table 7. Volumetric water budgets for the last stress period (1988–1990) of the transient 1955–1990 simulation.

Water-balance component	Volumetric rate (acre-ft/yr)
<u>1988–1990 Inflows</u>	
Release from storage	48,347
Constant head (underflow into study area)	6,264
Recharge	42,041
Stream leakage	1,574
Total inflows	98,226
<u>1988–1990 Outflows</u>	
Uptake to storage	38
Constant head (underflow out of study area)	743
Pumping	74,893
Evapotranspiration	11,731
Stream leakage (net groundwater discharge to stream)	10,820
Total outflows	98,225
Discrepancy = 0.00%	

Rattlesnake stream 1990 Flow into aquifer from stream (cfs)

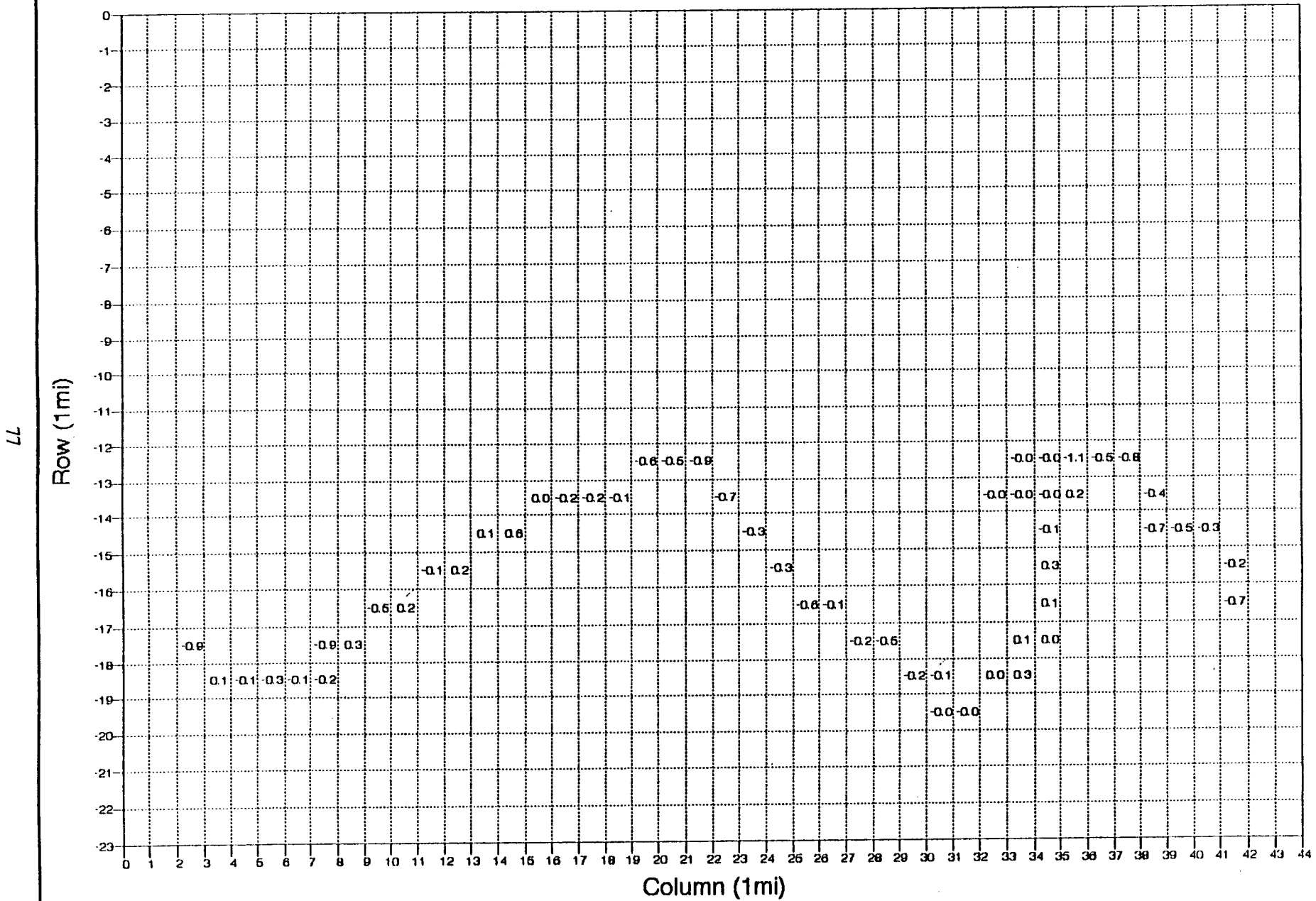


Figure 35. Model-predicted 1990 gaining (negative water fluxes) and losing (positive water fluxes) stretches of Rattlesnake Creek.

The time distribution of the water balance components during the 1955–1990 period is shown in fig. 36, in which it is evident that since the mid-1970's aquifer storage depletion (storage curve) has been taking place. This storage depletion coincides with an accelerated irrigation pumping period (pumpage curve). Baseflow contributions to streamflow are also decreasing (stream leakage curve). Constant-head underflow denotes the net subsurface inflow in the model area through the constant-head boundaries; net recharge denotes the total recharge minus total evapotranspiration in the model area. The water balance for the last stress period (1988–1990) of the 1955–1990 transient-state simulation is shown in table 7. The major inflow and outflow for the transient period is ground-water recharge and pumping, respectively.

In contrast to what was the case during the 1950's and early 1960's, the present-day dominant outflow component from the aquifer is ground-water pumpage for irrigation, which is a new discharge superimposed on the predevelopment (steady-state) system. This irrigation pumpage must be balanced by (1) an increase in the aquifer recharge (by increased induced leakage from streams, drainage of the dewatered aquifer sediments, irrigation return flows, capture of previously "rejected" recharge as surface runoff by increased hydraulic gradients between recharge areas and areas with significant irrigation well development, and increased recharge from below, i.e., from saltwater intrusion from the Permian formations), (2) a decrease in the old natural discharge (by decreased baseflow contributions to streams, decreased outflows to seeps and springs, decreased ground-water evapotranspiration), (3) loss of water storage in the aquifer as manifested by long-term ground-water-level declines, or (4) a combination of these changes. Indeed, a combination of all three types of change is indicated in the water budget of the model area, which shows an increase in recharge, a loss of water in storage, and a decrease in baseflow contributions to streamflows and decreased evapotranspiration losses compared with the predevelopment water budget (see table 5).

A 35-mi-long southwest to northeast water table profile along a model cell row (row 13, fig. 21) passing through or near the towns of Macksville and Hudson and also through the Big Salt Marsh is shown in fig. 37. The thickness of the profile line is proportional to the simulated change

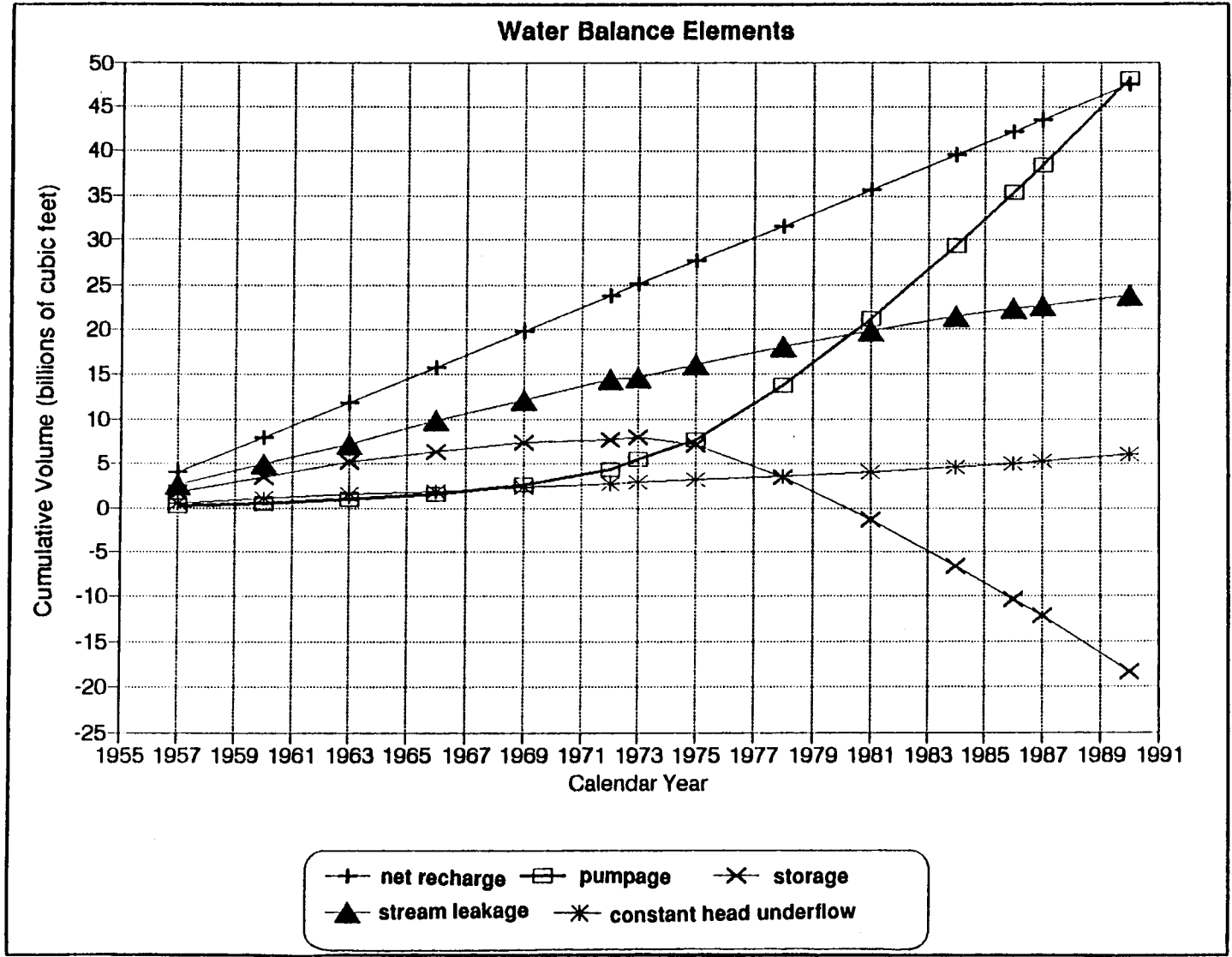


Figure 36. Time distribution of the water balance components during the 1955-1990 simulation period.

Rattlesnake predicted water levels
'55-'90 along rs1 row 13

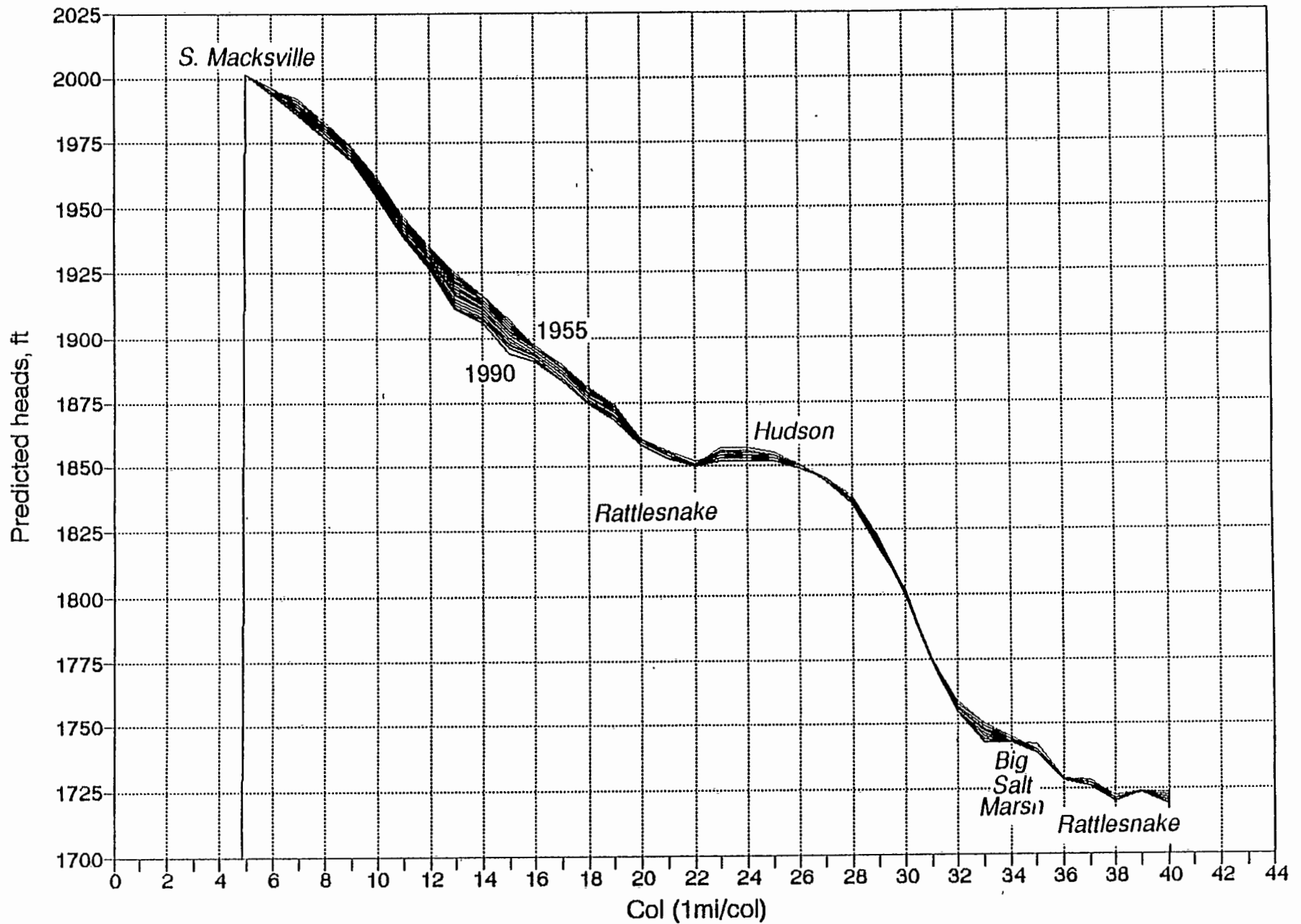


Figure 37 Water table profiles along row 13 passing near Macksville, Hudson, and Big Salt Marsh.

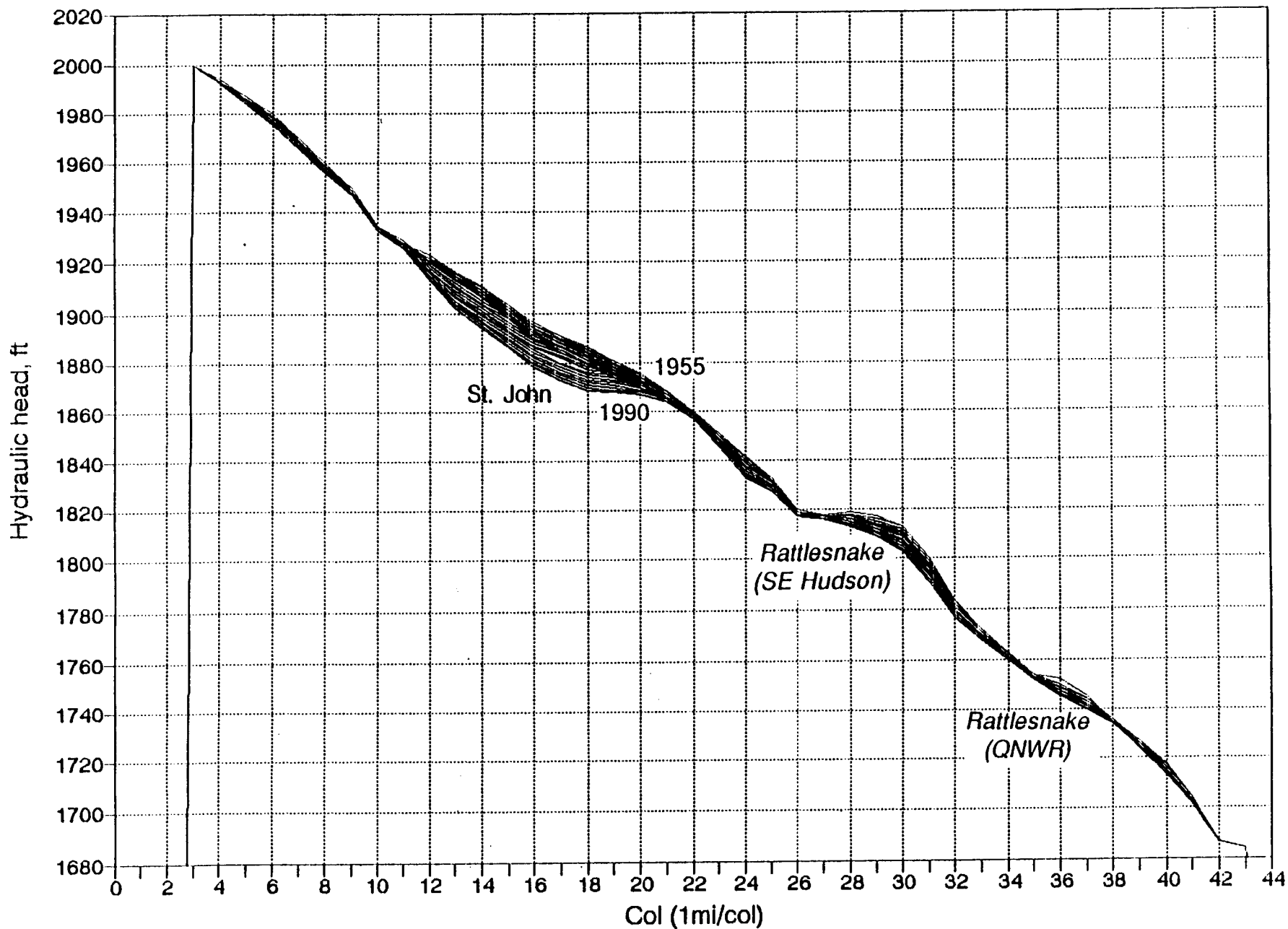
in the water table over the 1955–1990 period. It is clear from the figure that (1) the water table elevation declines from the southwest to the northeast, (2) the water table declines the most in the area between Macksville and northeast of St. John, along this chosen row, (3) the water table slope flattens out near the Rattlesnake Creek and Hudson areas, (4) the water table steepens abruptly and declines the least from northeast of Hudson to near the Big Salt Marsh, and (5) the water table flattens out again at the Big Salt Marsh and Rattlesnake Creek northeast of the marsh. Another similar profile (40 mi long) along model cell row 17 (see fig. 21) passing through southeast St. John and midway between the Little Salt Marsh and the Big Salt Marsh is shown in fig. 38; the largest water table declines are in the area around St. John. The predevelopment groundwater fluxes (fig. 39a) are much more pronounced and contributed to Rattlesnake streamflows and the Quivira marsh more water than the present-day conditions indicate (fig. 39b).

A plot of the simulated ground-water flow vectors (fig. 39) indicates that ground water flows to the Quivira marsh from the northwest, west, and southwest and that it flows around the Cretaceous bedrock outcrop. The largest ground-water fluxes to the marsh are from the west-northwest feeding into the Big Salt Marsh area. A strong ground-water flow component toward Rattlesnake Creek is also evident, especially after the confluence with Wild Horse Creek and at the Rattlesnake stream course southwest of St. John. Predevelopment ground-water fluxes (fig. 39a) were much more pronounced and contributed more water to Rattlesnake streamflows and the Quivira marsh than present fluxes contribute (fig. 39b).

Sensitivity analysis and initial predictive runs

Sensitivity analysis, which quantifies the model's response to input parameter changes, gives insight into mechanisms and dependencies. Therefore an analysis was made to determine the sensitivity of the model to variations in the values of selected parameters on both the aquifer and the stream. The input and aquifer parameters considered were pumpage, recharge, hydraulic conductivity, and storativity. The stream parameters considered were conductance of the streambed, Manning's roughness coefficient, stream slope, and stream width. Sensitivity to each

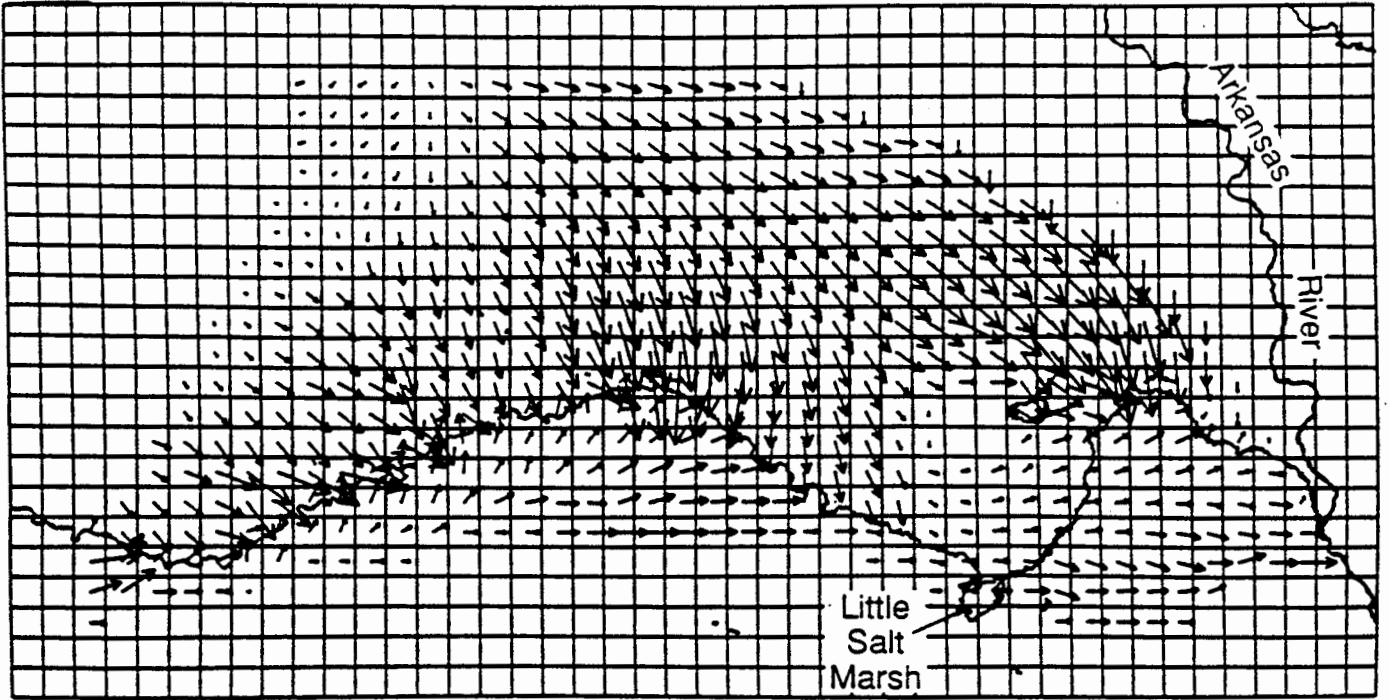
Rattlesnake '55-'90 hydrograph Head along row 17



82

Figure 38. Water table profiles along row 17 passing near St. John and in between the Little and Big Salt Marshes

a



b

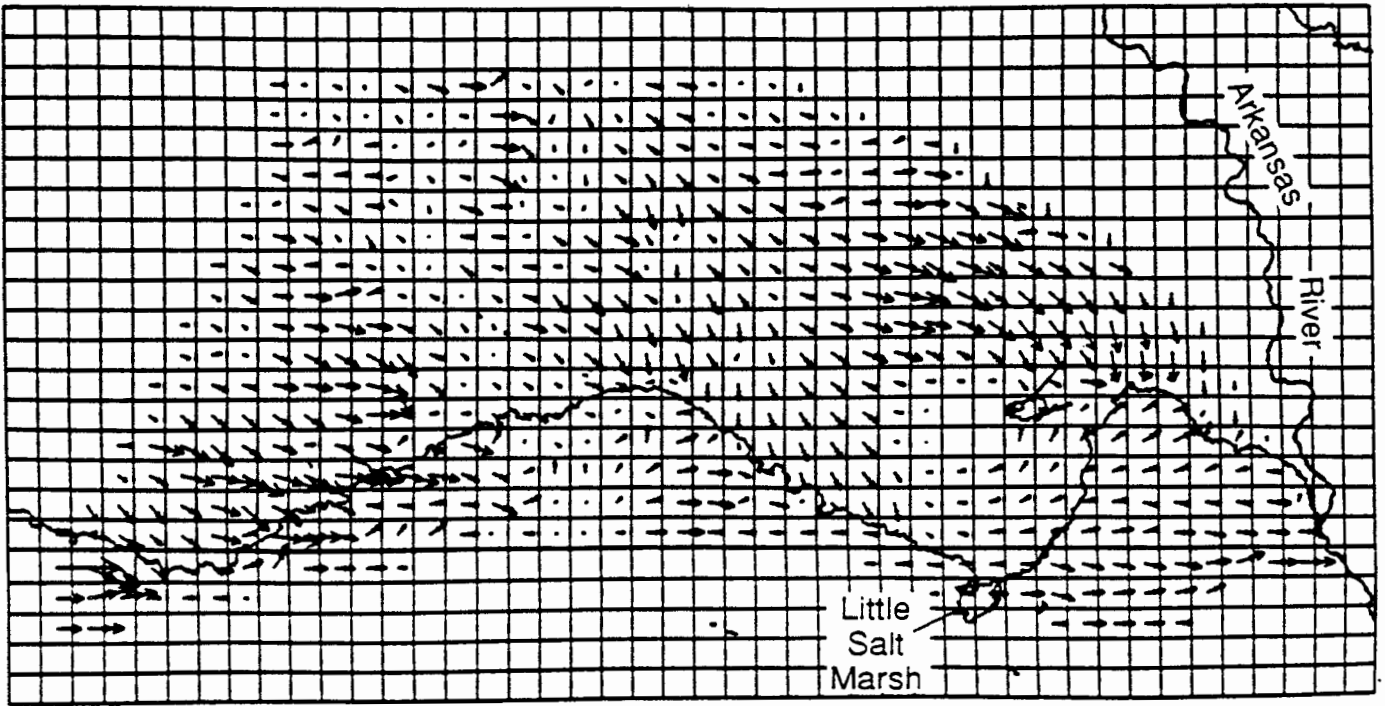


Figure 39. Simulated ground-water-flow vectors for (a) predevelopment (1955) and (b) present-day conditions (1990). Flow-vector scale is one grid cell length to 0.5 ft³/s or 362 acre-ft/yr.

parameter was determined by running the model with the optimized parameters for 1990 in a predictive mode from 1990 to 2010 and by varying (increasing and decreasing) each parameter by 50%. Corresponding changes in ground-water hydraulic heads or drawdown were observed, tabulated, and graphed at typical nodes near Hudson [node at row 12, column 24, (12, 24)], near St. John [node (16, 14)], and approximately 3 mi north of the Zenith gaging station [node (17, 31)] (figs. 40–42); the corresponding changes in streamflow (ground-water runoff or baseflow) were displayed for Rattlesnake Creek near the Zenith stream-gaging station [node (19, 31)] and for southwest of St. John [node (17,11)] (figs 43–44).

Sensitivity of ground-water levels to changing aquifer and input parameters

Examination of figs. 40 and 41 indicates that ground-water pumpage has the largest effect on aquifer water levels (note that the 50% change in pumpage is taken over the assumed 80% water appropriation use). For example, a sustained 50% change in the considered pumpage would cause an approximately 7-ft change in water table drawdown by the year 2010. The water levels are also highly sensitive to the amount of ground-water recharge, followed by aquifer storativity or aquifer hydraulic conductivity. However, different parts of the aquifer respond differently in absolute amount to changing parameters, with the relative significance of some parameters altered in some instances. For example, in the area north of the Zenith gaging station and southeast of the bedrock outcrop [node (17, 31)], where irrigation pumping is nonexistent and the depth to the water table is shallow, water levels are most sensitive to recharge and evapotranspiration followed by hydraulic conductivity and storativity with no sensitivity to pumpage (fig. 42).

Sensitivity of streamflows to changing aquifer, input, and stream parameters

Examination of figs. 43 and 44 indicates that, similar to what was observed with regard to water levels, streamflows respond differently to various parameters. The aquifer and aquifer input-related parameters in this case have a much more pronounced effect on streamflows than do stream-related parameters. For example, ground-water pumpage and recharge are more sensitive

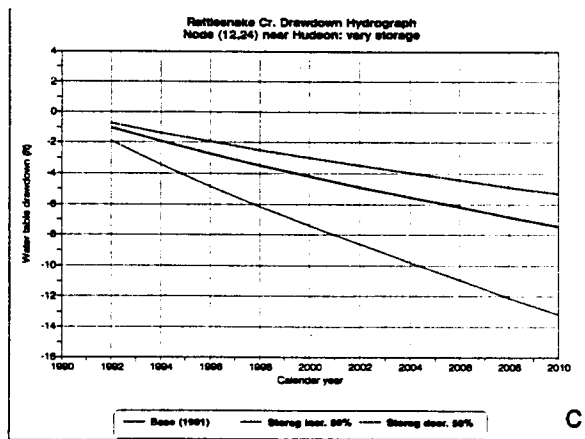
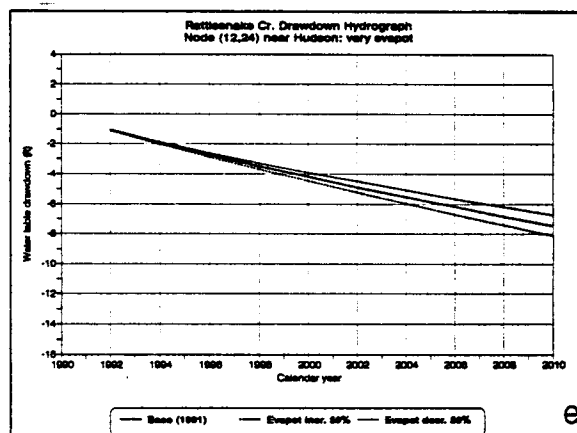
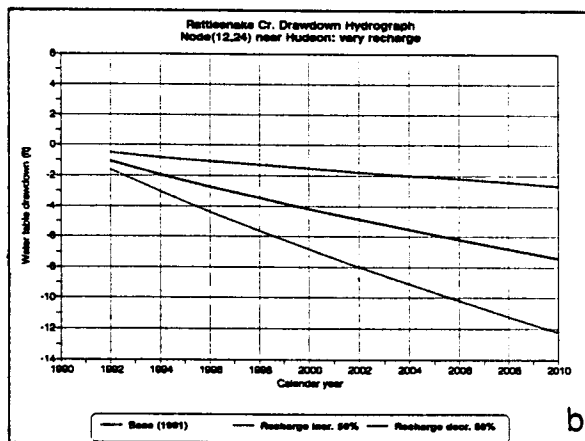
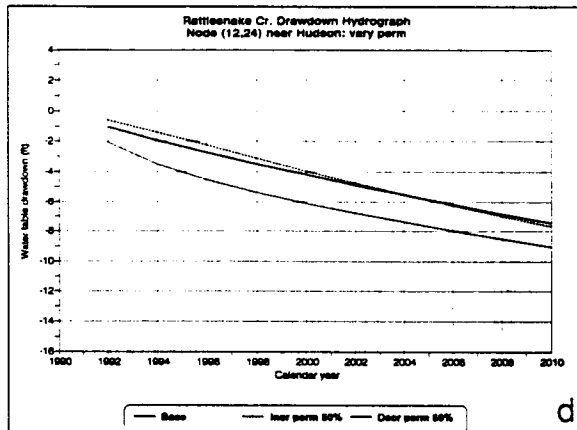
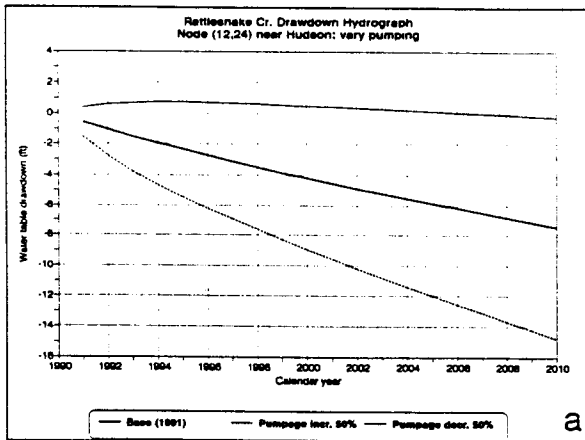


Figure 40. Sensitivity plots of drawdown with changing pumpage, recharge, storativity, hydraulic conductivity, and ground-water evapotranspiration at node (12, 24) (row column) near Hudson.

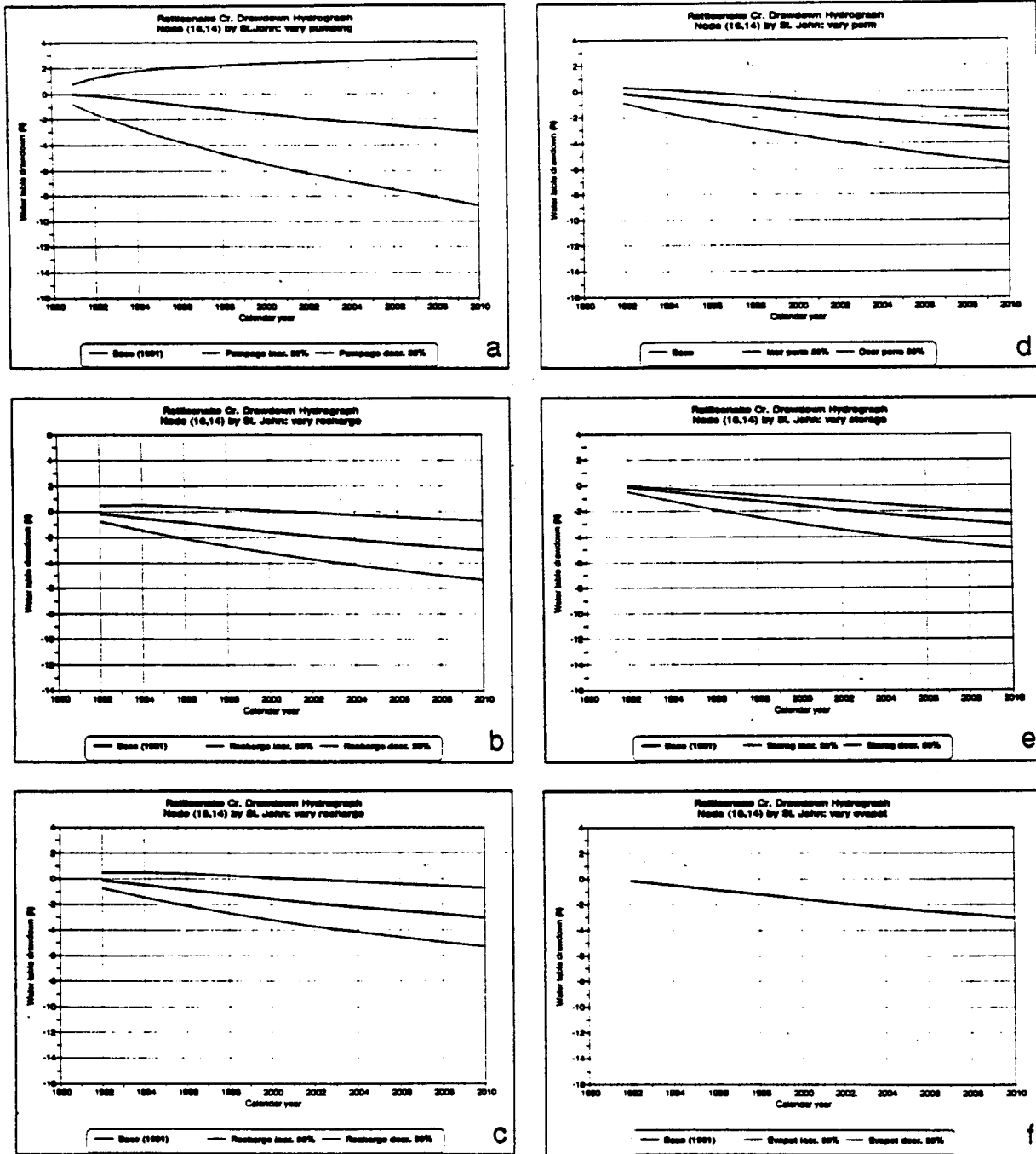


Figure 41. Sensitivity plots of drawdown with changing pumpage, recharge, storativity, hydraulic conductivity, and ground-water evapotranspiration at node (16, 14) (row, column) near St. John.

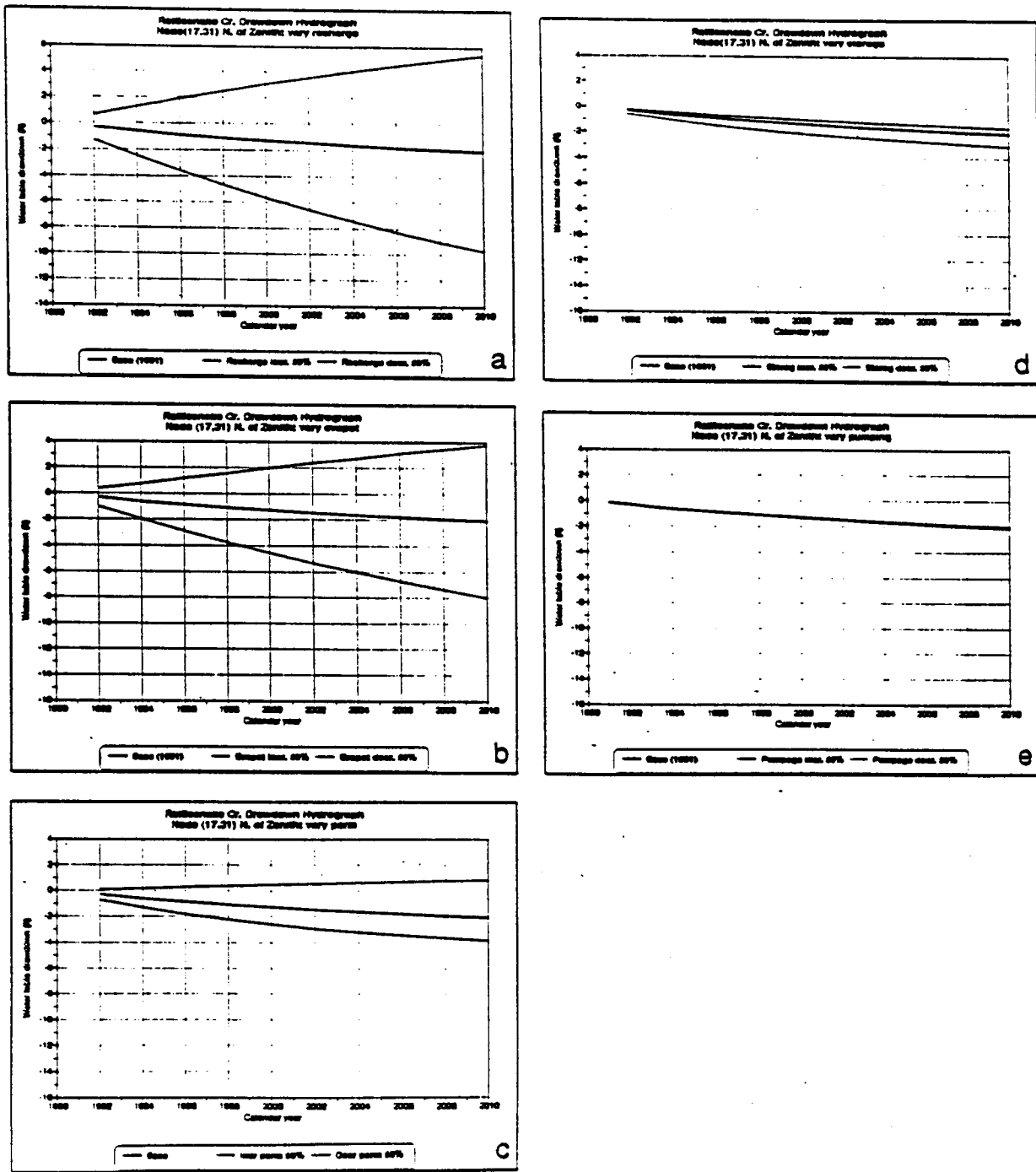


Figure 42. Sensitivity plots of drawdown with changing pumpage, recharge, storativity, hydraulic conductivity, and ground-water evapotranspiration at node (17, 31) (row, column) north of Zenith.

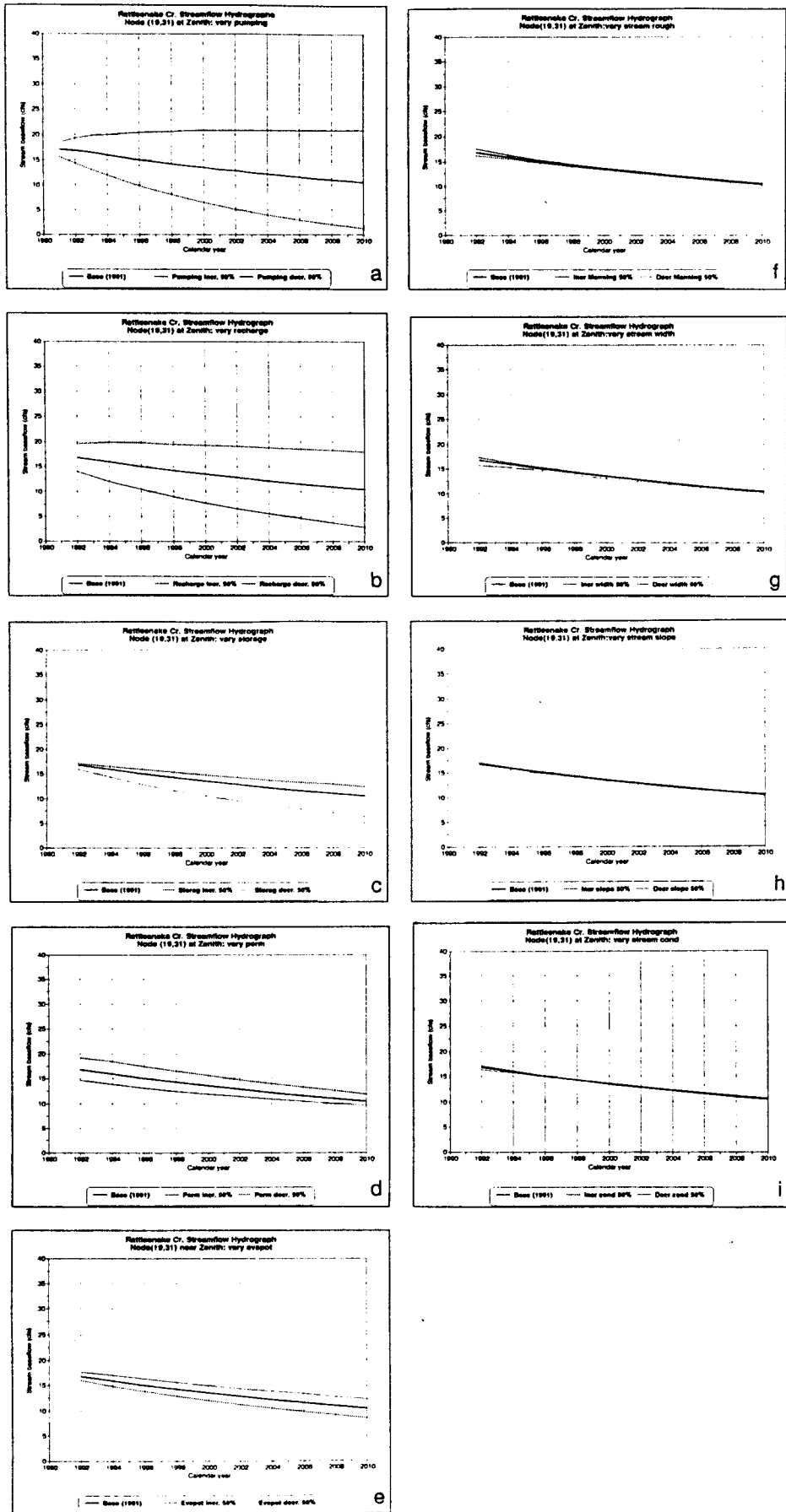


Figure 43. Sensitivity plots of stream baseflow with changing input-, aquifer-, and stream-related parameters at node (19, 31) (row, column) near the Zenith stream-gaging station.

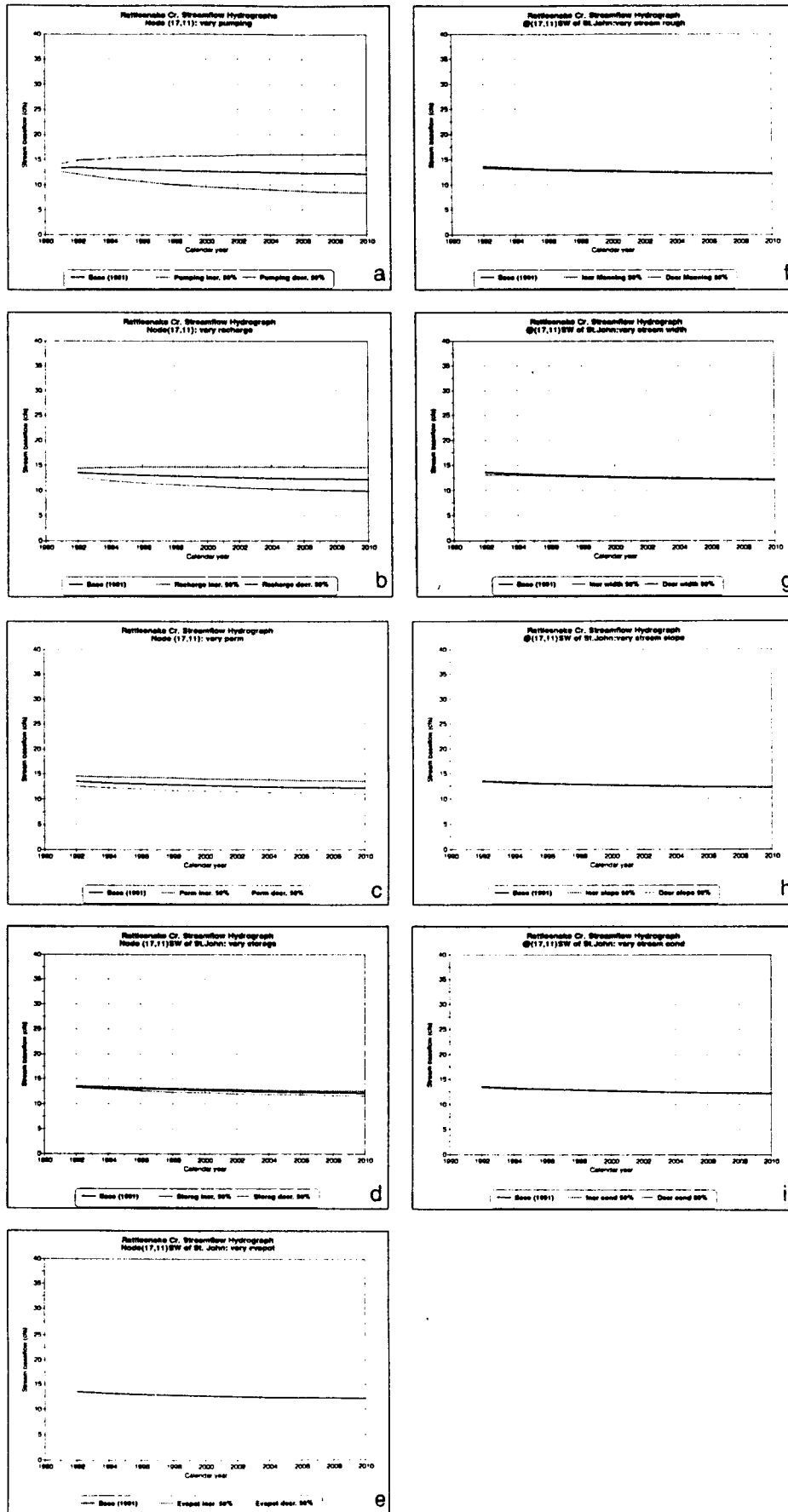


Figure 44. Sensitivity plots of stream baseflow with changing input-, aquifer-, and stream-related parameters at node (17, 11) (row, column) southwest of St. John.

parameters than aquifer storativity, hydraulic conductivity, or aquifer evapotranspiration, but all these aquifer variables are much more sensitive parameters than streambed conductance, Manning's roughness coefficient, stream slope, or stream width.

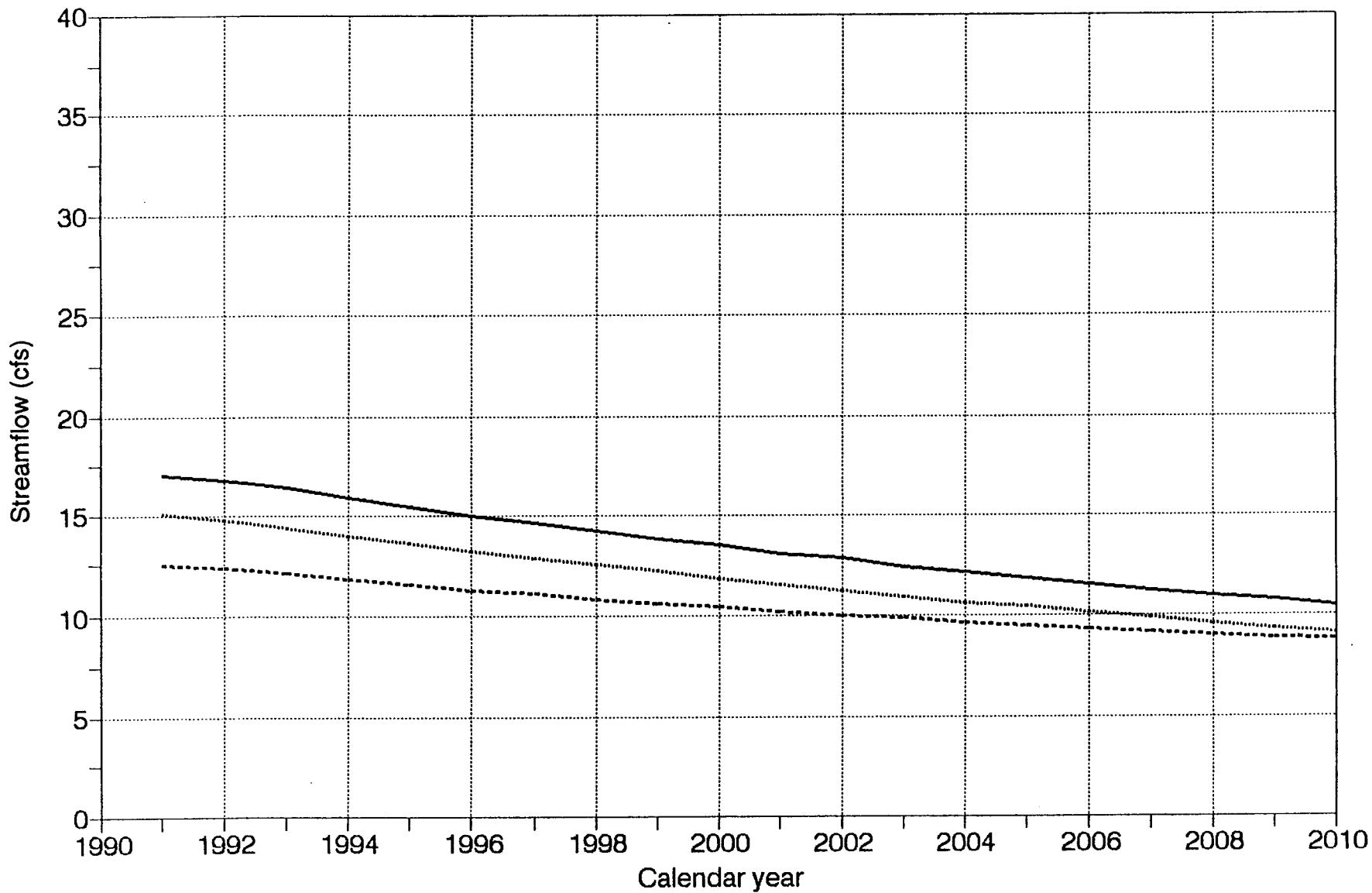
A model prediction of baseflows, assuming that present conditions (pumpage, recharge, evapotranspiration, incoming streamflows at the Macksville gaging station) persist throughout the 1990–2010 period, is shown in fig. 45 for three Rattlesnake Creek locations near Macksville, St. John, and the Zenith gaging station. In all three areas future baseflows will be declining, with the steepest decline of approximately 40% by the year 2010 occurring at the Zenith gaging station near the entrance to the Quivira NWR.

VII. Revised simulation results and model analysis

As mentioned earlier, the reported values of measured or estimated hydraulic conductivity for the Great Bend Prairie aquifer, including the highly transmissive Arkansas River alluvium (which is outside the model region), range from 20 to 280 ft/day. These values are mostly based on existing irrigation wells that normally tap the most productive parts of the aquifer, so this reported range is probably biased toward the higher values. The model-optimized hydraulic conductivity values for the four hydraulic conductivity zones of the model area in this study range from 10 ft/day (for the region surrounding the Cretaceous bedrock outcrop southwest of the Big Salt Marsh) to 78 ft/day. The resulting standard deviation of the ground-water levels for the predevelopment conditions, based on the optimized hydraulic conductivity values, is 2.84 ft, a relatively small value (compared with the 335-ft difference between the highest and the lowest values of observed heads within the model area) indicating a satisfactory fit.

Because the optimized hydraulic conductivity values fell in the lower part of the range of the expected values and because sensitivity analysis indicated that the hydraulic conductivity is not a highly sensitive parameter, the optimized values were increased through trial-and-error to the highest degree possible for a stable solution with a satisfactory match to the observed predevelopment water levels. The values for all zones, except the lowest hydraulic conductivity

Rattlesnake Cr. Streamflow Hydrographs 1991-2010 baseline



— Zenith Sta (19,31) - - - - - Near St John(14,17) SW of Hudson(14,23)

Figure 45. Model-predicted stream baseflow declines during the 1991–2010 period.

zone by the bedrock outcrop, could be approximately doubled before results became unsatisfactory (i.e., either no model solution or a rapid increase in error variance). These higher values resulted in a slightly worse (ground-water-level standard deviation: 3.08 ft) but still satisfactory fit than in the original predevelopment case. The trial-and-error fit of the four hydraulic conductivity zones of the model area ranged from 11 to 130 ft/day. Effects on post-development model fit are discussed in what follows.

Ground-water evapotranspiration was originally restricted to the lower half of the model region, where the water table was shallow (less than 6–10 ft below ground surface); deeper depths to the water table have minimal or no effect on ground-water evapotranspiration. To take into account the riparian zone along the stream banks, we expanded the ground-water evapotranspiration zone by adding a second zone to encompass all model grid cells through which Rattlesnake Creek passes (fig. 46). Incorporating this additional change to the simulation results in a standard deviation of the predevelopment ground-water levels of 3.14 ft, which is still a satisfactory result. Although this model fit is slightly worse than the original simulation, the model fit may be more physically satisfying in that it better represents observational experience; however, because of the coarseness of the model grid (1-mi² grid cells) compared to the much smaller dimensions of the riparian zone area around the stream banks, this refinement may be unnecessary. The modified steady-state analysis results are presented in table 8, and the predevelopment water balance is shown in table 9.

Table 8. Revised steady-state analysis results.

Zone	<i>K</i> (ft/d)	Std. error(ft/d)	Zone	Recharge (in./yr)	Std. error (in./yr)	Zone	<i>ET</i> (in./yr)	Std. error (in./yr)
1	41	8.9	i	0.001	0.091	(1)	3.33	0.720
2	11	2.5	ii	0.98	0.207	(2)	1.86	1.172
3 ^a	106	35.3	iii	7.83	1.730			
4 ^a	130	139.4						

Square root of the error variance (s) = 3.15 ft.

Number of observations (N) = 492.

Weighted sum of squares of the deviations between simulated and observed values of head (SS) = 4,786 ft².

$s/\Delta h = 0.0094$ ($\Delta h = 335$ ft).

Std. error = $\sigma/N^{1/2}$.

a. Paleochannel zones.

Groundwater Evapotranspiration Zonation

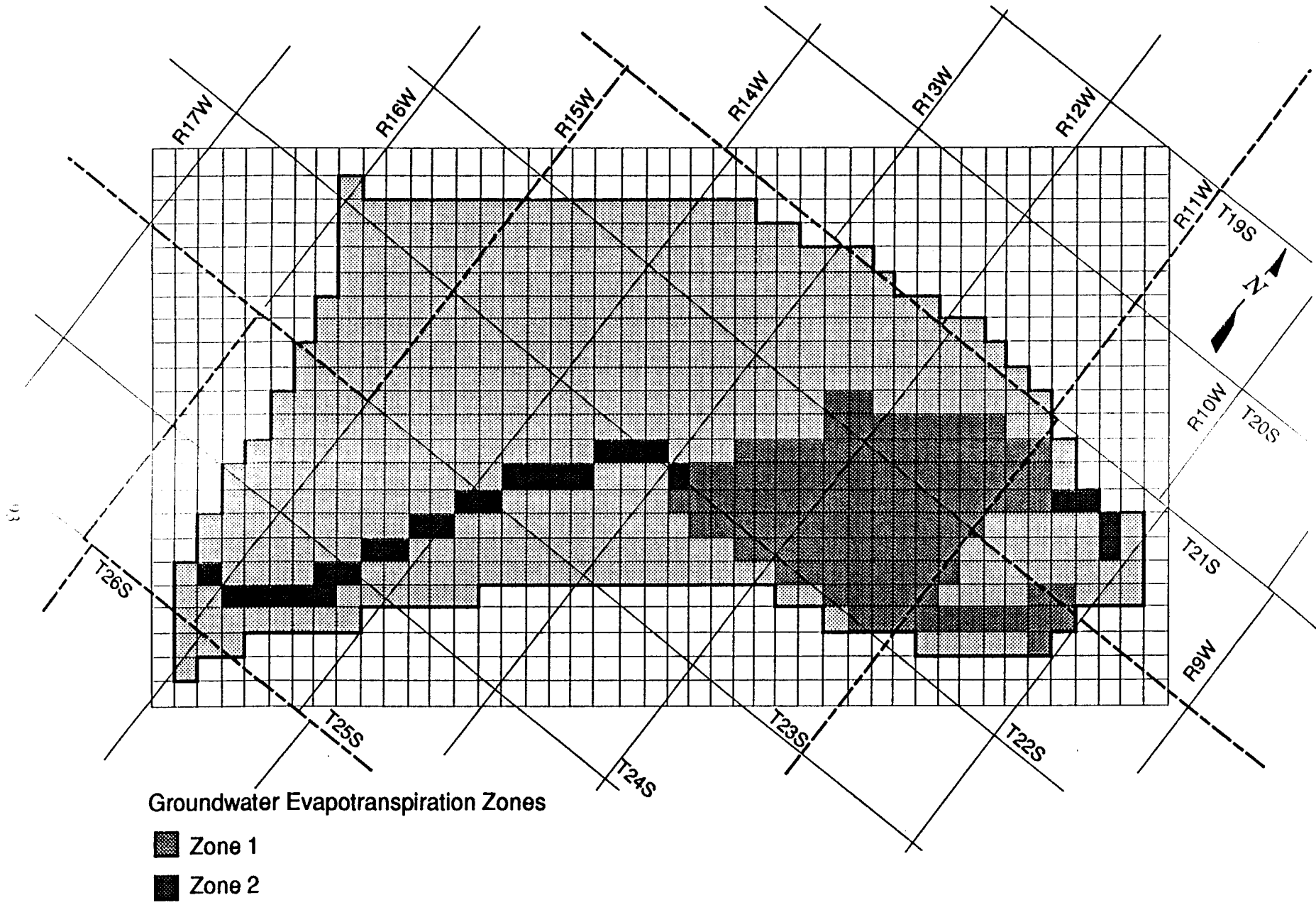


Figure 46. Ground-water evapotranspiration zonation of the model area.

Table 9. Revised volumetric budget for entire model area under predevelopment conditions (c. 1955).

Water-balance component	Volumetric rate (acre-ft/yr)
Inflows	
Constant head (underflow into study area)	9,087
Recharge	36,109
Stream leakage	1,898
Total inflows	47,094
Outflows	
Constant head (underflow out of study area)	1,270
Pumping wells	1,828
Evapotranspiration	20,388
Stream leakage (net groundwater discharge to stream)	23,607
Total outflows	47,093
Discrepancy = 0.00%	

The revised hydraulic conductivity values and expanded ground-water evapotranspiration zones were adopted for the transient developed-conditions simulations. We also reduced the actual amount of irrigation pumpage for the transient simulations from 80% of the appropriated amounts to 70%. These combined changes resulted in a significantly improved model fit compared with the original transient simulations. The resulting optimized average value of aquifer specific yield was 18%, which agrees with the expected value for the Great Bend aquifer. The standard deviation of the present-day ground-water levels in the predictive simulation from predevelopment to present-day conditions is only 3.22 ft compared with the original transient simulation fit of 4.27 ft. However, as will be shown later, the revised simulated Rattlesnake Creek streamflows generally overpredict observed flows compared with the original transient simulations, which underpredict observed streamflows. The modified transient analysis results are presented in table 10, where it can be seen that the ratio of hydraulic head standard error to the maximum head loss in the model area is small ($s/\Delta h = 0.0096$), indicating a good overall model fit.

The water balance results for the last stress period (1988–1990) of the revised model are shown in table 11, and the 1955–1990 temporal evolution of the water balance components of this

Table 10. Revised transient 1955–1990 analysis results.

Zone	Recharge (in./yr)	Std. error (in./yr)	Zone	ET (in./yr)	Std. error (in./yr)	Zone	Storativity	Std. error
i	0.001	0.358	(1)	3.23	0.573	a	0.183	0.001
ii	1.97	0.188	(2)	1.11	2.437			
iii	4.59	0.605						

Square root of the error variance (s) = 3.22 ft.

Number of observations (N) = 42.

Weighted sum of squares of the deviations between simulated and observed values of head (SS) = 372.4 ft².

$s/\Delta h = 0.0096$. ($\Delta h = 335$ ft).

Std. error = $\sigma/N^{1/2}$.

Table 11. Revised volumetric water budgets for the last stress period (1988–1990) of the transient 1955–1990 simulation.

Water-balance component	Volumetric rate (acre-ft/yr)
<u>1988–1990 Inflows</u>	
Release from storage	34,616
Constant head (underflow into study area)	11,552
Recharge	53,812
Stream leakage	2,668
Total inflows	102,668
<u>1988–1990 Outflows</u>	
Uptake to storage	0
Constant head (underflow out of study area)	1,334
Pumping	65,540
Evapotranspiration	18,911
Stream leakage (net groundwater discharge to stream)	16,887
Total outflows	102,672
Discrepancy = 0.00%	

transient simulation is depicted in fig. 47 for both cumulative water volumes and volumetric flow rates. The results are similar to the original simulation (see fig. 36).

The revised model was also successful in predicting observed events that were different from those used in the calibration or that reflected some change in the system, for example, different pumping stresses. Thus comparison of observed and predicted water levels during the end of 1977 (and beginning of 1978) resulted in a head standard error of 3.69 ft, which is a

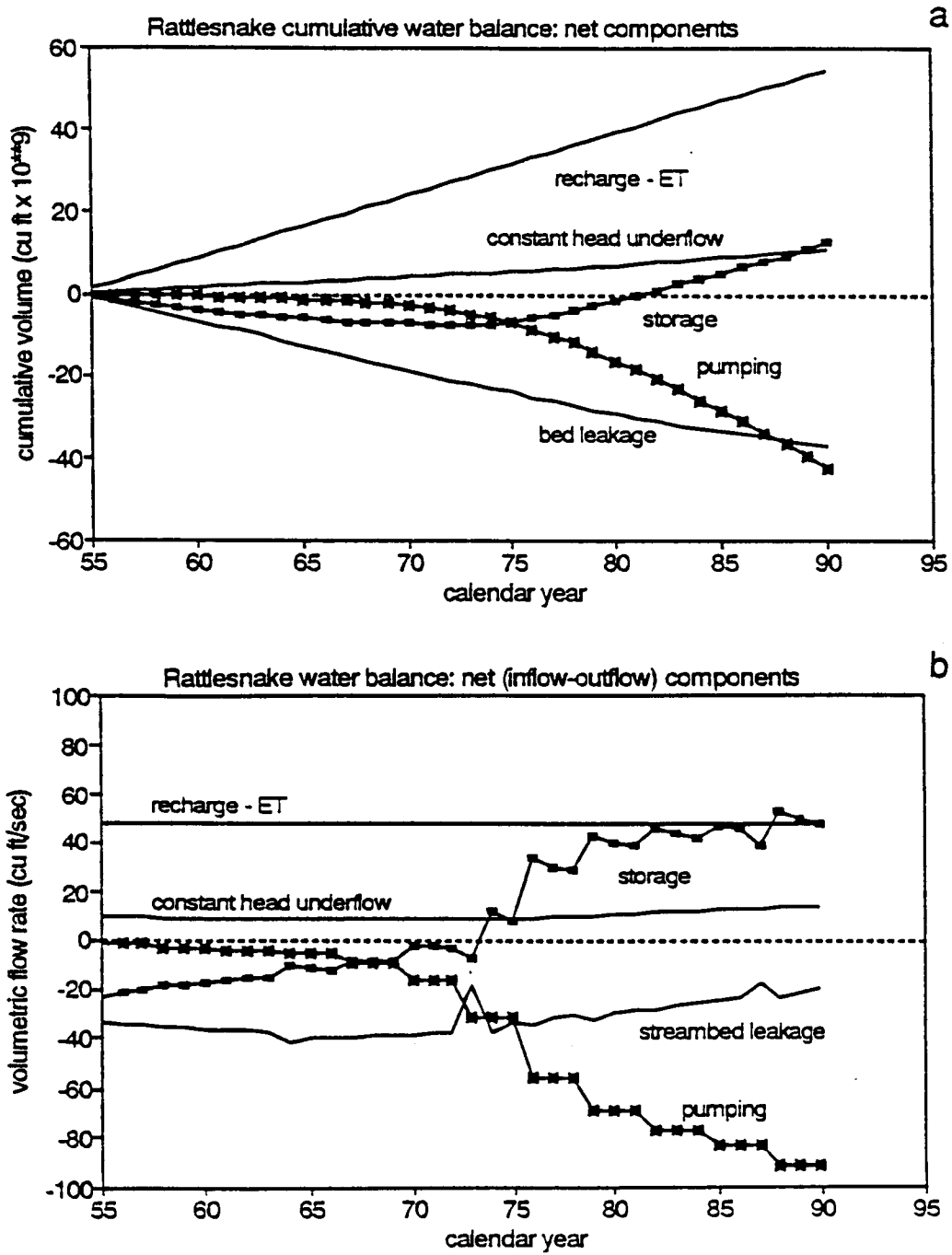


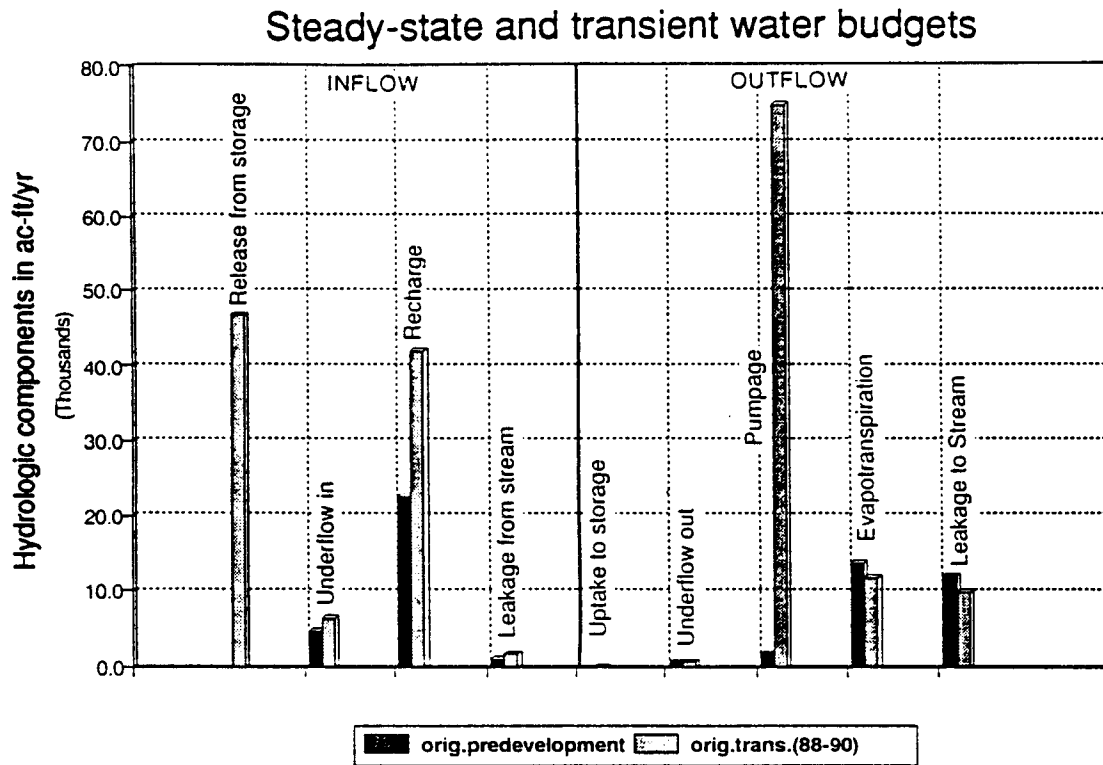
Figure 47. 1955–1990 temporal evolution of water balance components of the revised simulation expressed in both (a) cumulative volumes and (b) volumetric flow rates.

satisfactory result. A comparison of observed and simulated contours for this case will be shown further later (see fig. 52).

The following figures make some of the salient features of the revised simulations clearer. Figure 48a depicts the ground-water budget for the original predevelopment and developed-conditions simulations, and fig. 48b displays the same information for the revised simulations. Note that in the original transient-state simulations it was assumed that the actual pumpage was 80% of the appropriated amounts, whereas for the revised simulations the pumpage is assumed to be 70%. The hydrologic budgets for both predevelopment and developed conditions indicate significant differences in the hydrologic components resulting from development. For example, the revised predevelopment natural ground-water recharge across the model area was estimated as 1.3 in./yr (0.8 in./yr in the original simulations), whereas the induced recharge under development conditions was estimated as 1.9 in./yr (1.5 in./yr in the original simulations). These recharge estimates are in agreement with other independent recharge estimates in the region (Sophocleous, 1992c). The employed stream-aquifer model treats ground-water recharge as total aquifer replenishment, including irrigation return flows [see also Sophocleous (1992b) for additional information].

Such computer simulations provide insight into the changes in recharge and discharge resulting from development. The predevelopment budgets give us an estimate of natural recharge, that is, water moving through the ground-water system under the boundary conditions imposed by natural topography, geology, and climate, whereas the developed-conditions budgets give us an estimate of induced recharge, that is, water added to the natural ground-water system in response to artificial boundary conditions imposed at irrigation well fields, farm ponds, drains, etc. Although natural recharge balances natural discharge as baseflow to streams and outflow to springs and wetlands, induced recharge (including irrigation return flow) and ground-water storage (fig. 48) are the two sources of water to balance artificial ground-water withdrawals. A decrease in baseflow contributions to streamflows and decreased ground-water evapotranspiration losses are

a



b

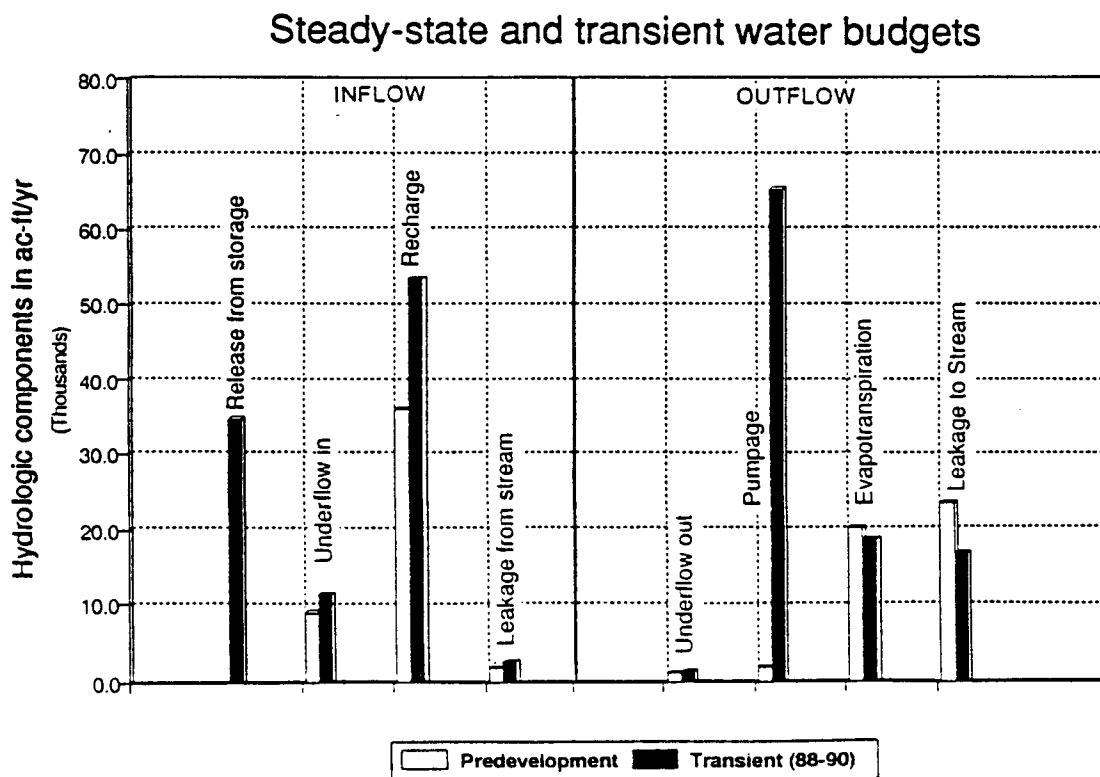


Figure 48. Predevelopment and present-day water budgets for the (a) original and (b) revised simulations of the Rattlesnake Creek–Quivira model area.

also a consequence of artificial ground-water withdrawals. Irrigation development along the lower reaches of Rattlesnake Creek close to the Quivira NWR has been minimal (fig. 49) because of salinity problems, resulting in relatively small decreases in baseflow contributions to streamflow (leakage to stream in fig. 48) and in evapotranspiration losses (see fig. 48).

Figures 50–52 depict comparisons of simulated and observed ground-water levels for both predevelopment and present-day conditions using the revised model. Figure 50 and 51 indicate calibrated results from the parameter estimation-optimization program for both predevelopment and developed present-day conditions, respectively, and fig. 52 is a verification run to check model performance for intermediate years (between the calibrated predevelopment and end of 1977 conditions); the results are satisfactory.

Figure 53 depicts Rattlesnake Creek streamflows at the Zenith gaging station as simulated by the original and revised models. Although, as mentioned earlier, the original simulations usually underpredict streamflows and the revised ones usually overpredict them, the predicted streamflow trends by both models closely follow the observed ones. This ability to reproduce dynamic behavior lends confidence to the appropriateness of the modeling approach we followed.

Finally, fig. 54 compares streamflow predictions using the original and the revised simulations for the next 20 years at several locations along Rattlesnake Creek, assuming that present-day climatic and streamflow conditions remain constant and ground-water pumpage stays at current levels. Both simulations predict that the declining streamflow trends observed since the mid-1970's will continue unabated for the entire 20-year prediction period. If undesirable effects of low streamflow are the primary concern, use of the original model will provide more conservative results. On the other hand, use of the revised model can provide an effective estimate of the minimum efforts required to stabilize or increase streamflow, as will be shown later.

The results of both the original and revised simulations represent reasonable ranges of possible outcomes and give an approximate measure of the range of uncertainty in model simulations. The revised model results make no qualitative difference in the general conclusions, which demonstrate the reality of stream-aquifer declines and expected declining trends. The

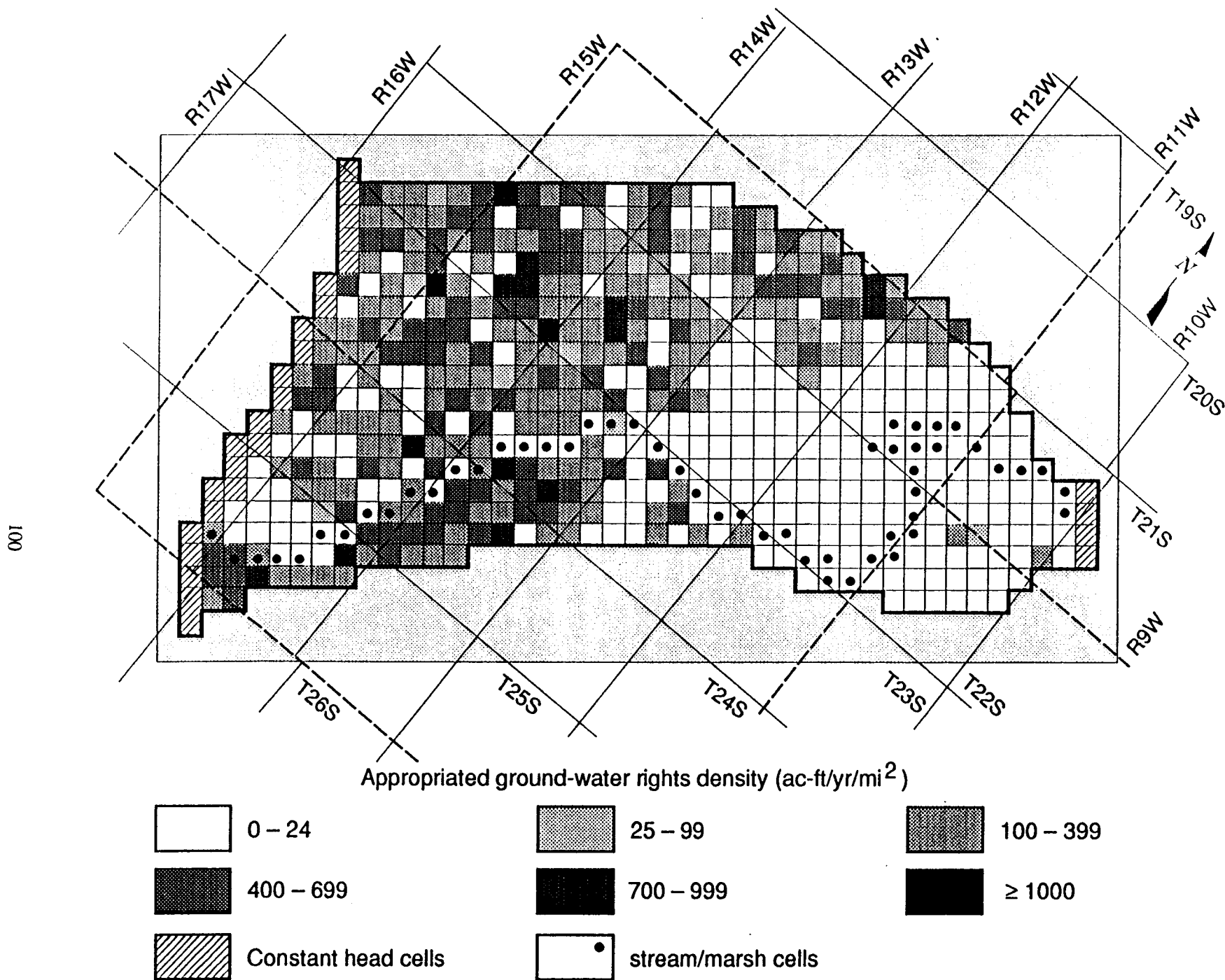


Figure 49. Appropriated ground-water rights density in acre-ft/yr/mi² throughout the model grid.

Observed and simulated predevelopment (1955) water levels.

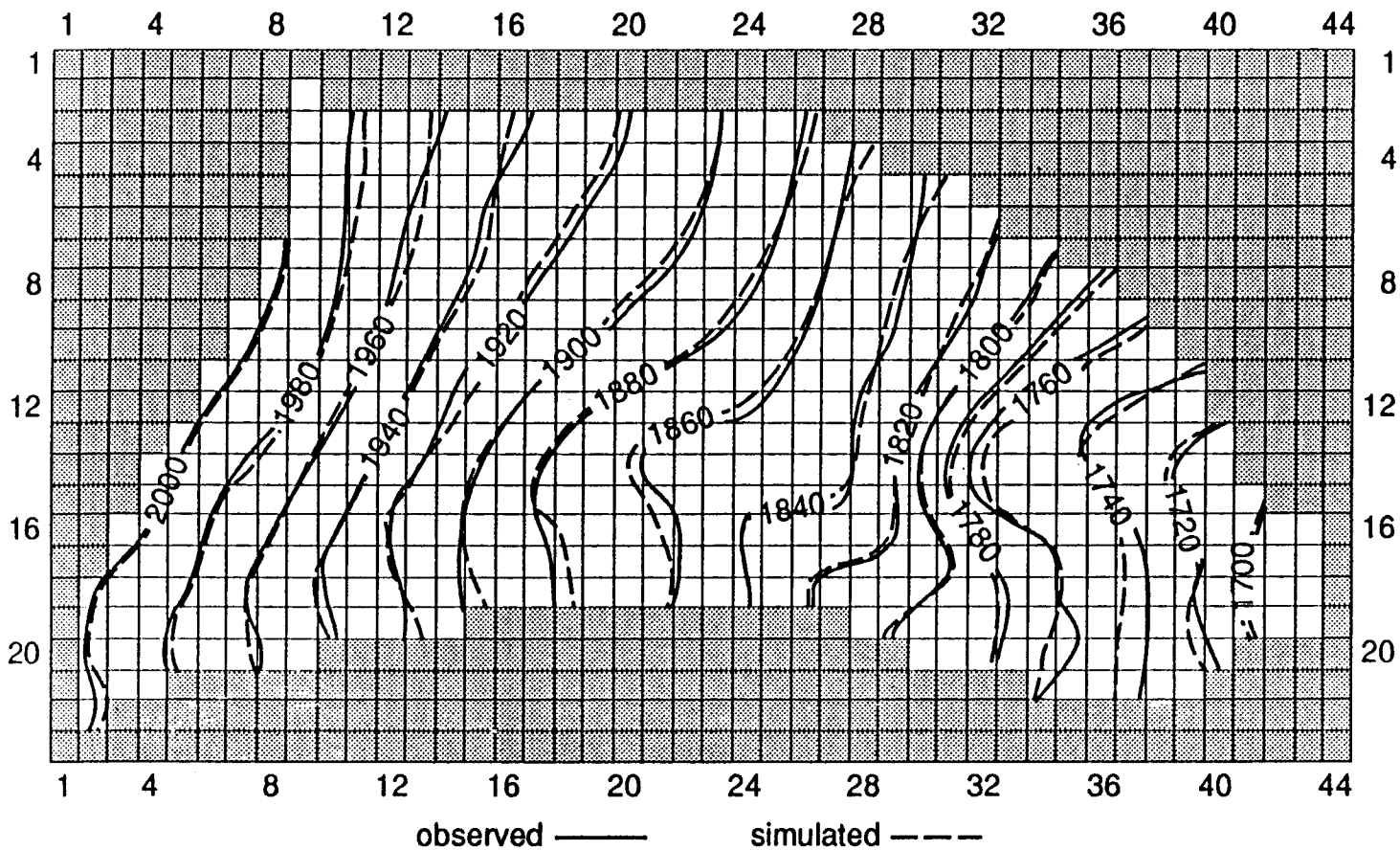


Figure 50. Comparison of revised model results for observed and simulated predevelopment water table contours.

Observed and simulated January 1991 water levels.

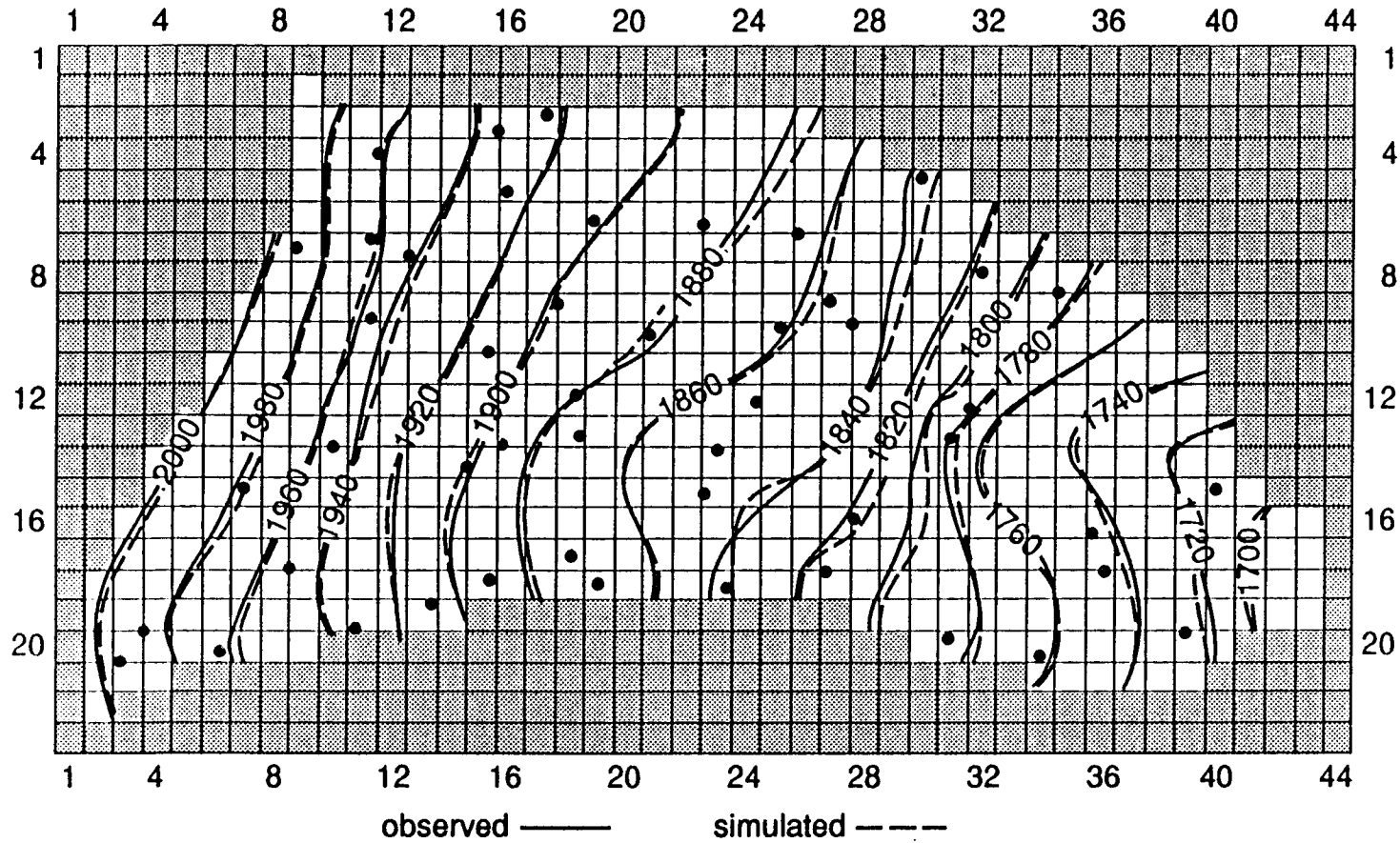


Figure 51. Comparison of revised model results for observed and simulated developed-conditions water table contours for January 1991.

Observed and simulated January 1978 water levels.

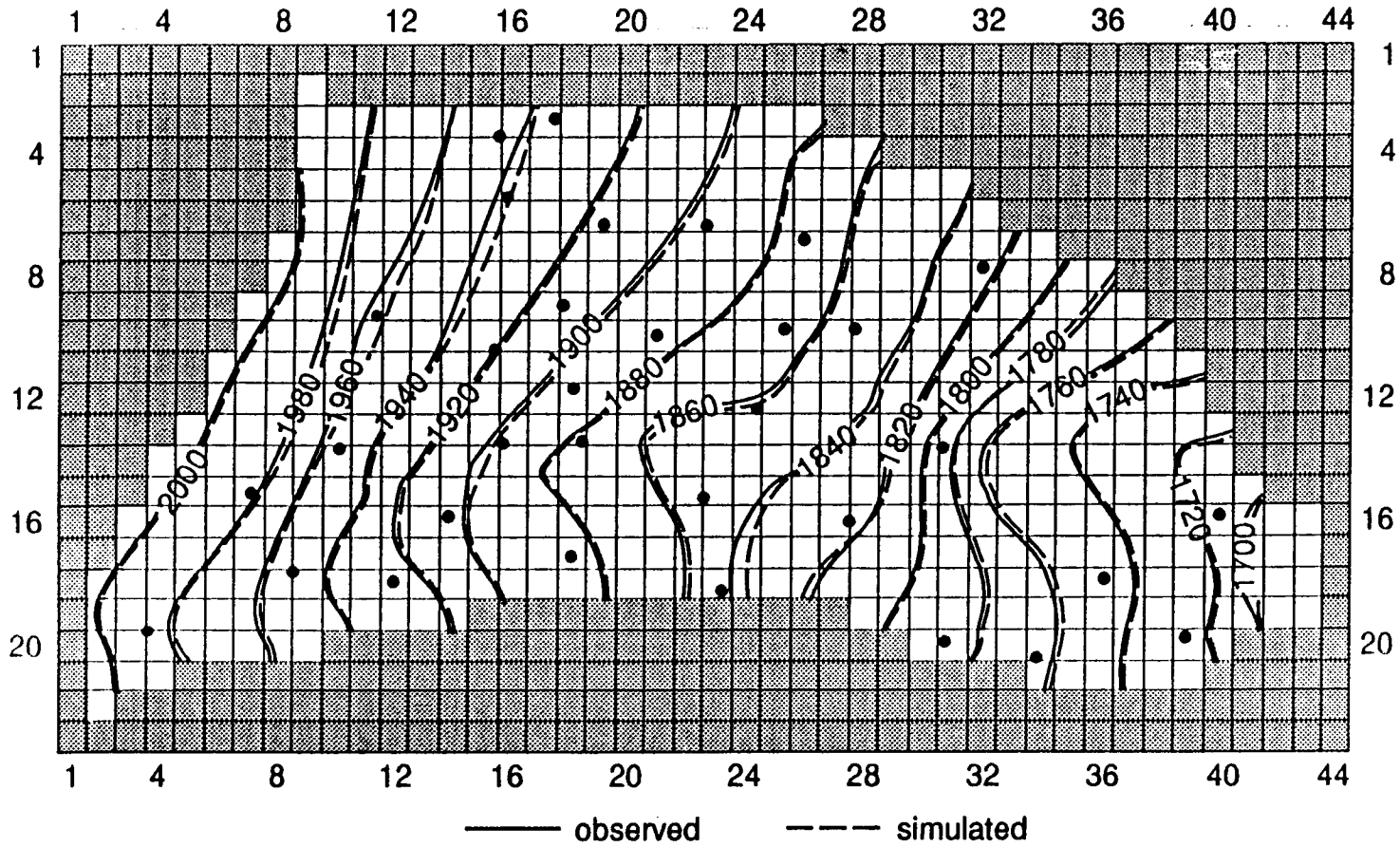


Figure 52. Comparisons of revised model results for observed and simulated water table contours for January 1978.

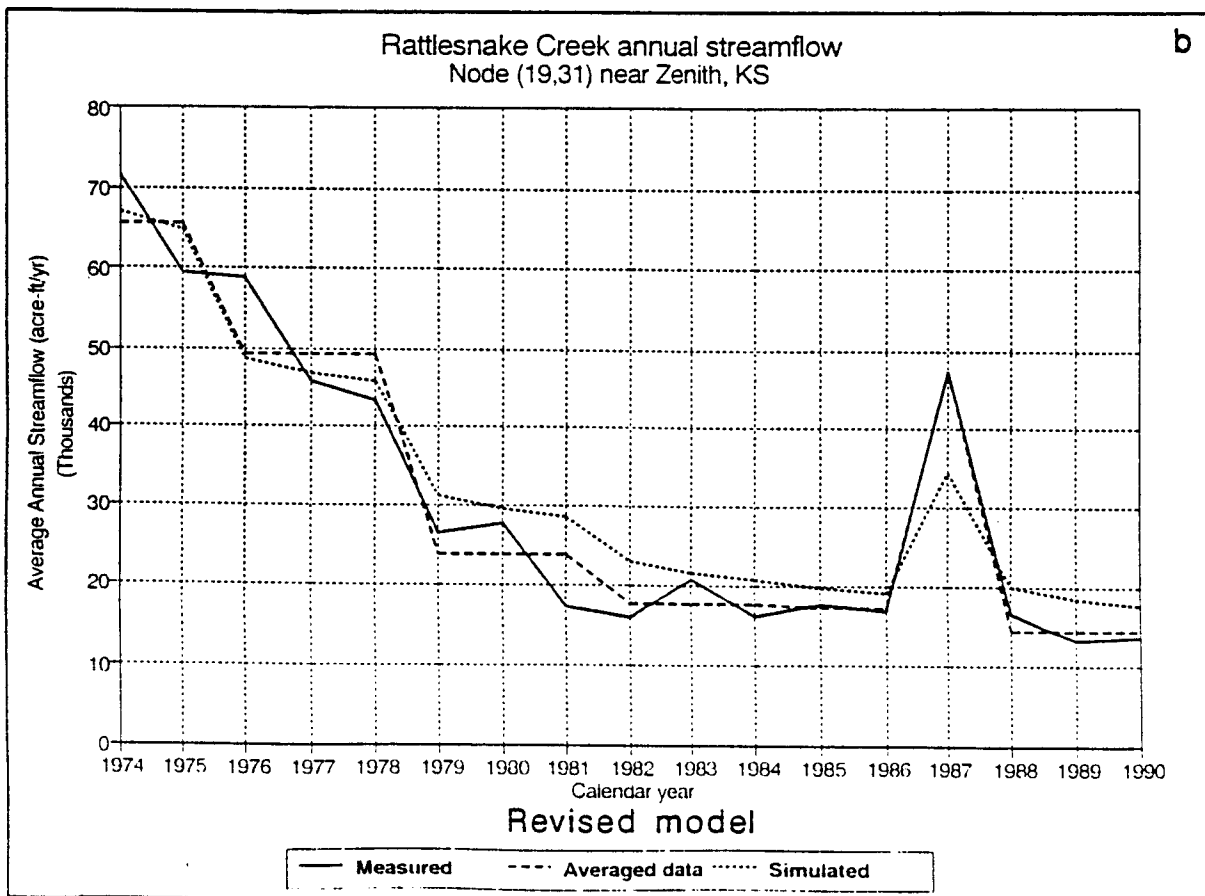
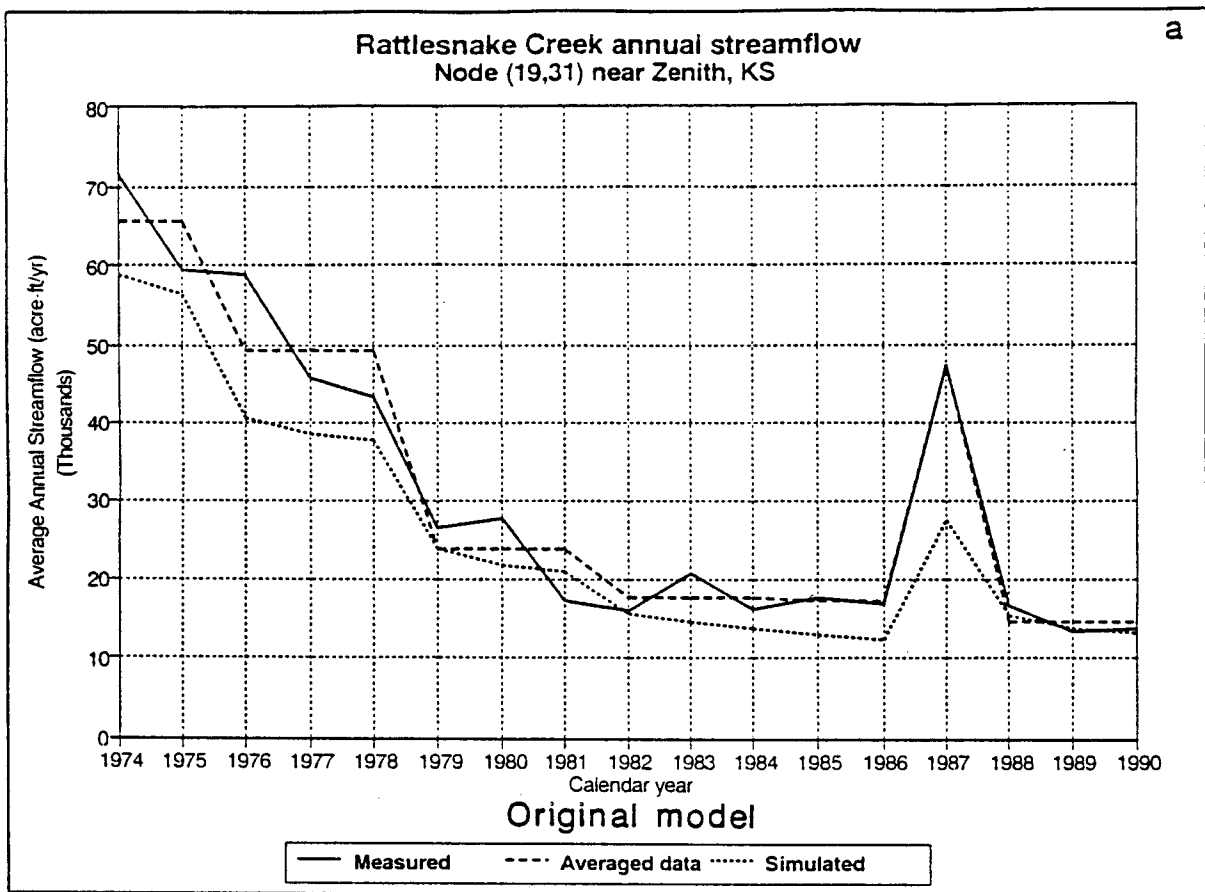


Figure 53. Comparison of measured and averaged (model input) streamflows versus model-simulated streamflows of the Rattlesnake Creek at the Zenith gaging station for the (a) original and (b) revised simulations.

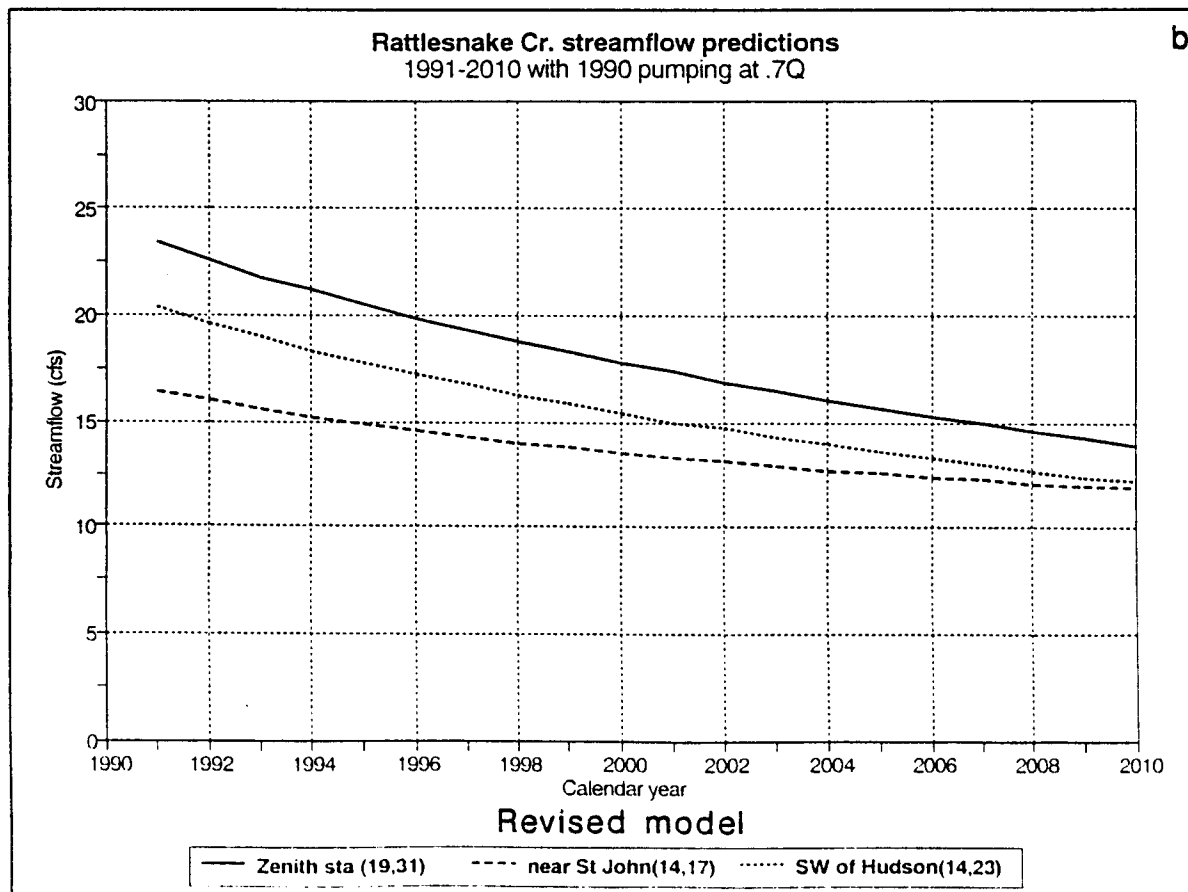
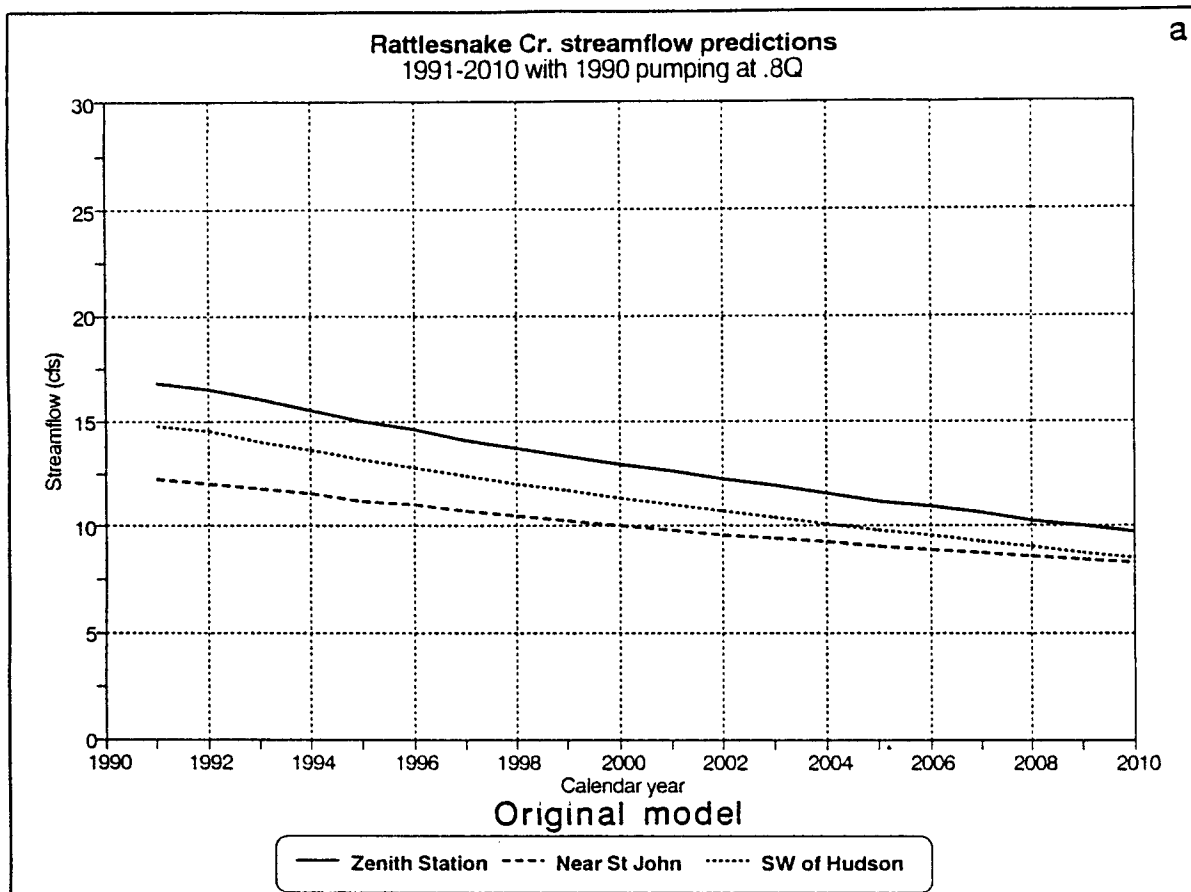


Figure 54. Model-predicted Rattlesnake Creek streamflow declines during the 1991–2010 period for the (a) original and (b) revised simulations.

original sensitivity analysis is reinforced by the results of the revised simulations and provides an effective way to evaluate model performance. It is highly probable that the "true" values of various parameters fall within the range defined by the original and revised model runs.

Further sensitivity analysis

As also noted by Yager (1991), simulation models can be used to estimate values for hydrogeologic properties if two conditions are met: (1) The simulation is sensitive to these properties and (2) the observed heads are measured at locations corresponding to areas in the model that are sensitive to these properties. Model calibration cannot be used to estimate parameters to which the model is insensitive. The sensitivity of the revised model to the change in value of a given parameter is measured by the resulting change in head or drawdown, as exemplified by node (12, 24) near Hudson (Appendix 5, figs. A5-1 through A5-5), and streamflow, as exemplified by node (19, 31) near the Zenith stream-gaging station (Appendix 5, figs. A5-6 through A5-14). The results are similar to those described in section VI. In addition to the previously discussed sensitivity analysis, we scaled (by the respective optimized parameters) and contoured the sensitivity components of the sensitivity (Jacobian) matrix, which are calculated in the inverse model procedure. Sensitivity of the model to changes in the respective parameter values can thus be compared directly from contour plots of scaled sensitivities.

The resulting lateral variation of model sensitivity is illustrated in figs. 55 and 56. Both figures show changes in head distribution that result from changes in parameters to which the model is most sensitive; specifically, fig. 55 depicts recharge for the intermediate and high recharge zones, whereas fig. 56 displays hydraulic conductivity (K) for the intermediate K zone, and storativity. The areal scaled sensitivities for the rest of parameters and zones are included in Appendix 5 (figs. A5-15 through A5-20). Examination of figs. 55 and 56 shows that there is considerable variation in sensitivity, indicating that additional data points in high-sensitivity areas would improve model results. The area of greatest model sensitivity to all displayed parameters in figs. 55 and 56 is the northwest model region in northwest Stafford County. The model was least

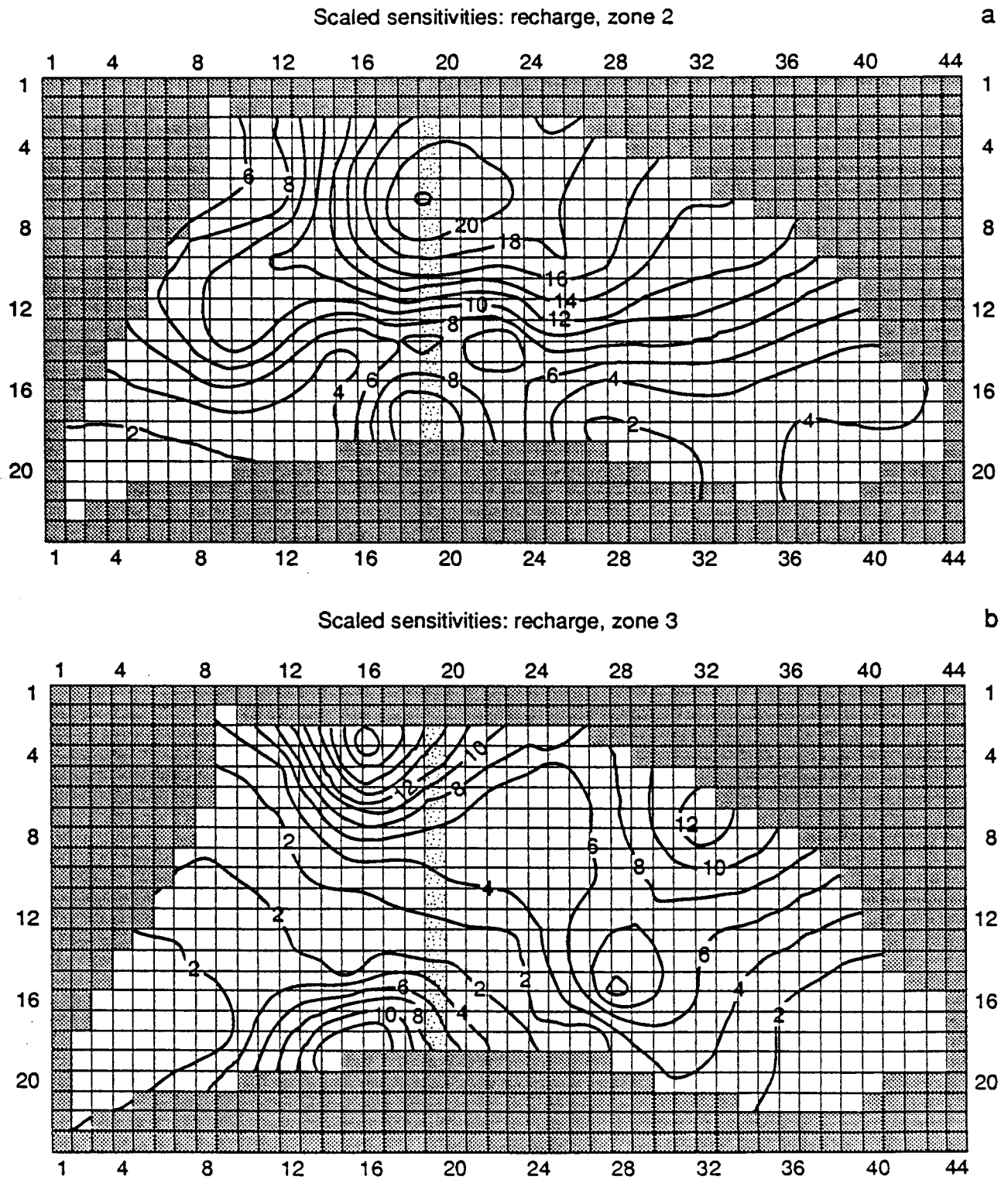


Figure 55. Areal variation in transient-state model scaled recharge sensitivities for the (a) intermediate (zone 2) and (b) high (zone 3) recharge zones.

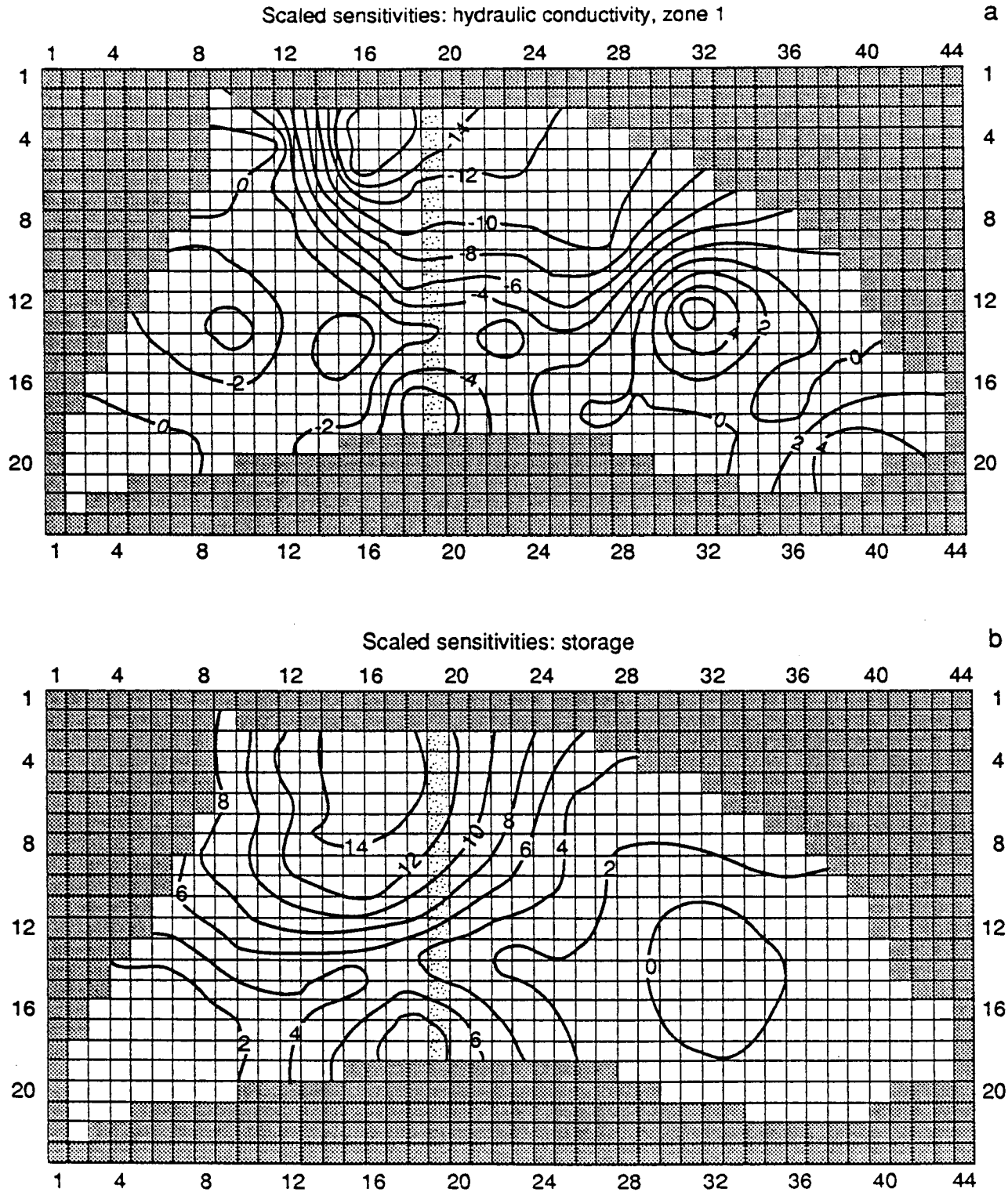


Figure 56. Areal variation in transient-state model scaled hydraulic conductivity sensitivities for the (a) intermediate zone (zone 1) and (b) scaled storativity sensitivities.

sensitive to recharge in the low-recharge areas (lowest recharge zone) and to hydraulic conductivities in the low and high K zones.

To better visualize the effect of high sensitivity areas on the simulated ground-water levels or drawdowns, we display in fig. 57 the water table declines or rises for the next 20 years (assuming constant present-day climatic and pumping conditions, base case b) along a model cell column (column 19, marked in stippled pattern in figs. 54 and 55, passing northeast of St. John and crossing the Rattlesnake Creek at row 14) for varying [increasing (c) and decreasing (a)] recharge values by 50%. The reader should compare the contoured recharge scaled sensitivities (fig. 55a) along all the model grid rows of column 19 with the corresponding water table changes (drawdown) shown in fig. 57.

Refined-grid modeling of the Quivira National Wildlife Refuge

The immediate vicinity of the Quivira NWR (a 12 mi \times 12 mi square area) was also modeled using a finer grid (1/2 mi \times 1/2 mi) than the one used for the lower Rattlesnake Creek model to obtain a more detailed spatial resolution of hydrologic variables. The procedure and results of this simulation are presented in Appendix 6.

VIII. Management alternatives

The predictive capabilities of the calibrated model permit hypothetical conditions to be explored by simply changing the data input to emulate the desired situations. The following general set of scenarios have been tested:

1. Effects of climatic fluctuations and changing incoming Rattlesnake Creek streamflows (climatic fluctuations set).
2. Effects of changing pumping patterns, establishing protective stream corridors and achieving specified desired Rattlesnake Creek streamflows (stream corridor set).

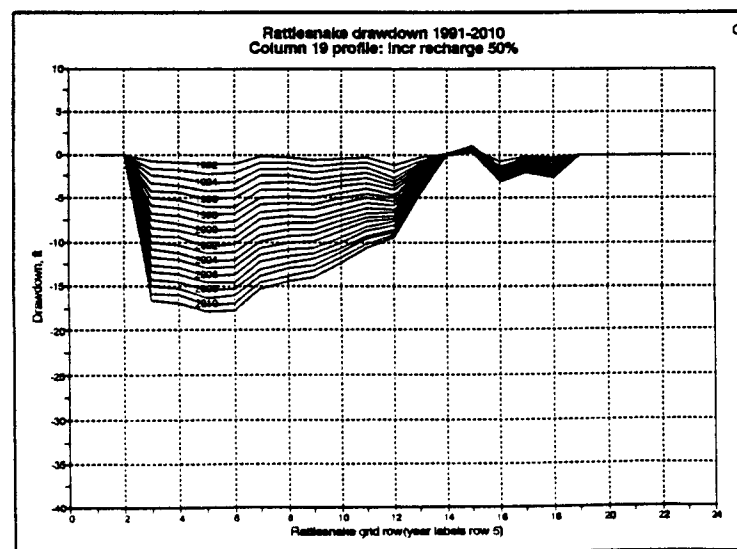
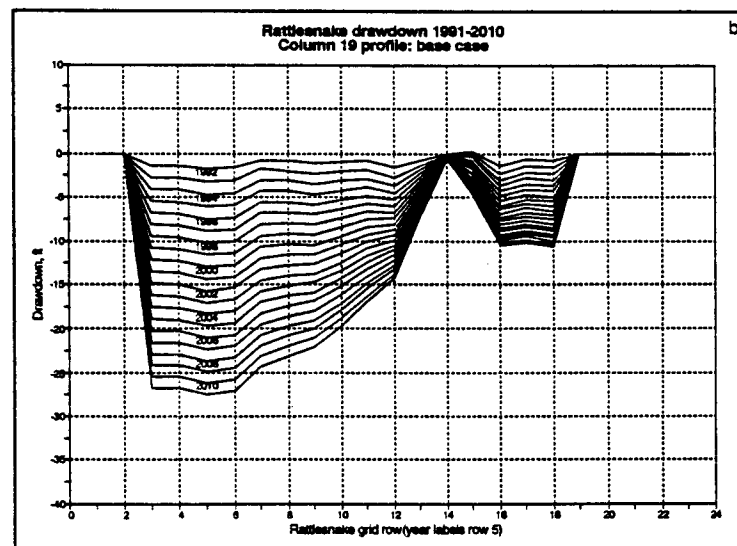
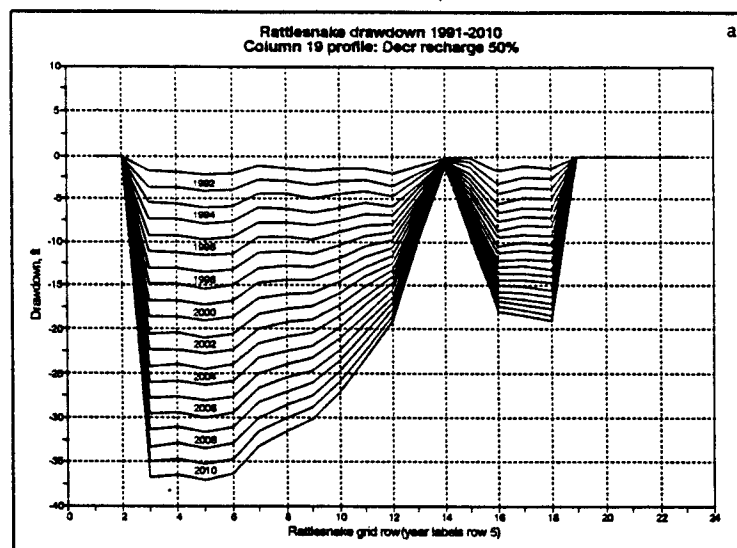


Figure 57. Base-case water table drawdown versus time (b) along column 29 of model grid shown in stippled pattern in fig. 55, and its sensitivity after (a) a 50% decrease and (c) 50% increase in recharge relative to the base case.

Climatic fluctuations set of scenarios

To simulate flood-drought cycles and their effects on the stream-aquifer system, we examined the entire Rattlesnake Creek streamflow record to identify annual flood and drought flows. The largest flood on record was the 1973 annual streamflow of 154.6 cfs, and the lowest flow, representing drought conditions, was the 1991 water-year streamflow of 1.5 cfs. The average annual streamflow during the 1988–1990 period of 9.3 cfs was taken as the normal streamflow (base case). Therefore a 10-year cycle of the above-mentioned flood-drought or drought-flood streamflows of 5-year duration each was simulated, followed by normal streamflows for the last 10 years of a 20-year total simulation run. During flooding periods, recharge was increased by 100% and actual pumping (i.e., 70% of appropriations) was reduced by 50%. During droughts, recharge was reduced by 100% and pumpage was increased to the nominal appropriated amounts. Figure 58 displays both the flood-drought and drought-flood cycle streamflows at the model entry point and at the Zenith streamgaging station.

The effect of these climatic fluctuations on the aquifer is shown in fig. 59 for an area near St. John [node (16, 15)] and Hudson [node (12, 24)]. The results show that the effects of droughts on ground-water levels are more severe when the ground-water levels are high than when they are low and that the sequence drought-flood-normal ends up in higher ground-water levels by the end of the climatic fluctuation cycle than the flood-drought-normal cycle. Figure 60 shows the response of the same grid cells as those in fig. 59 to climatic fluctuations but without the effects of pumpage (i.e., assuming all wells are shut down for the next 20 years), where the maximum expected water-level recovery can be seen.

Stream corridor set of scenarios

The cause and effect of various management alternatives under this set of scenarios are outlined in table 12 and are summarized in what follows.

The Rattlesnake Creek streamflows entering the Quivira marsh under different management scenarios are displayed in fig. 61. The lower curve of fig. 61 represents the base-case scenario,

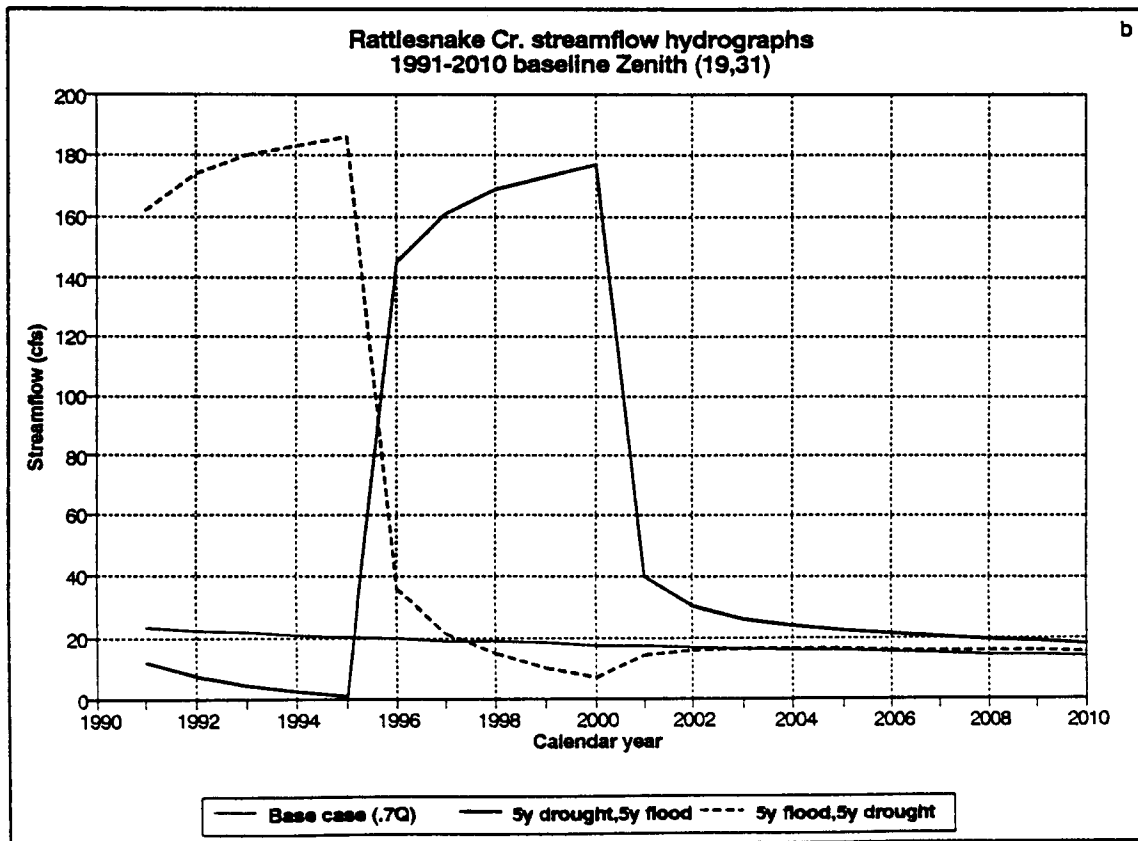
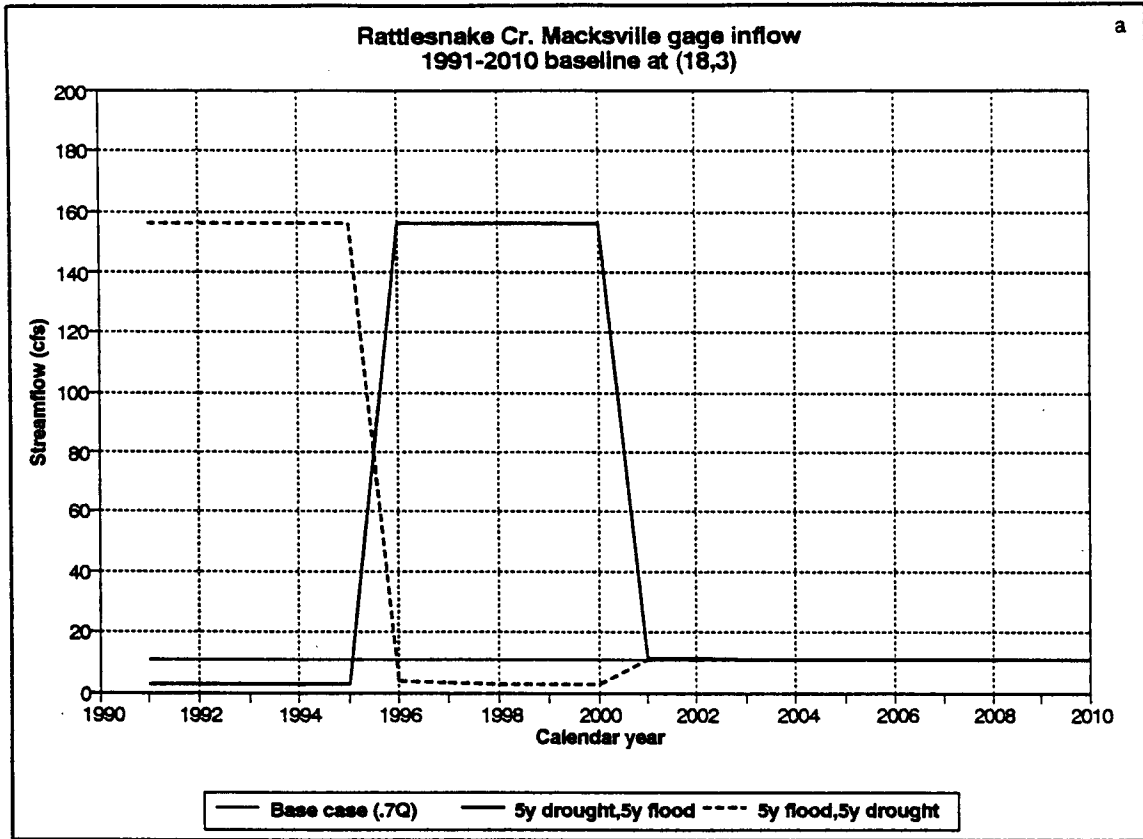


Figure 58. Flood-drought and drought-flood cycle streamflows at (a) the model entry point and (b) the Zenith stream-gaging station. Each flood or dry period lasts 5 years. Base case consists of 1988–1990 average incoming streamflows remaining constant throughout projection period.

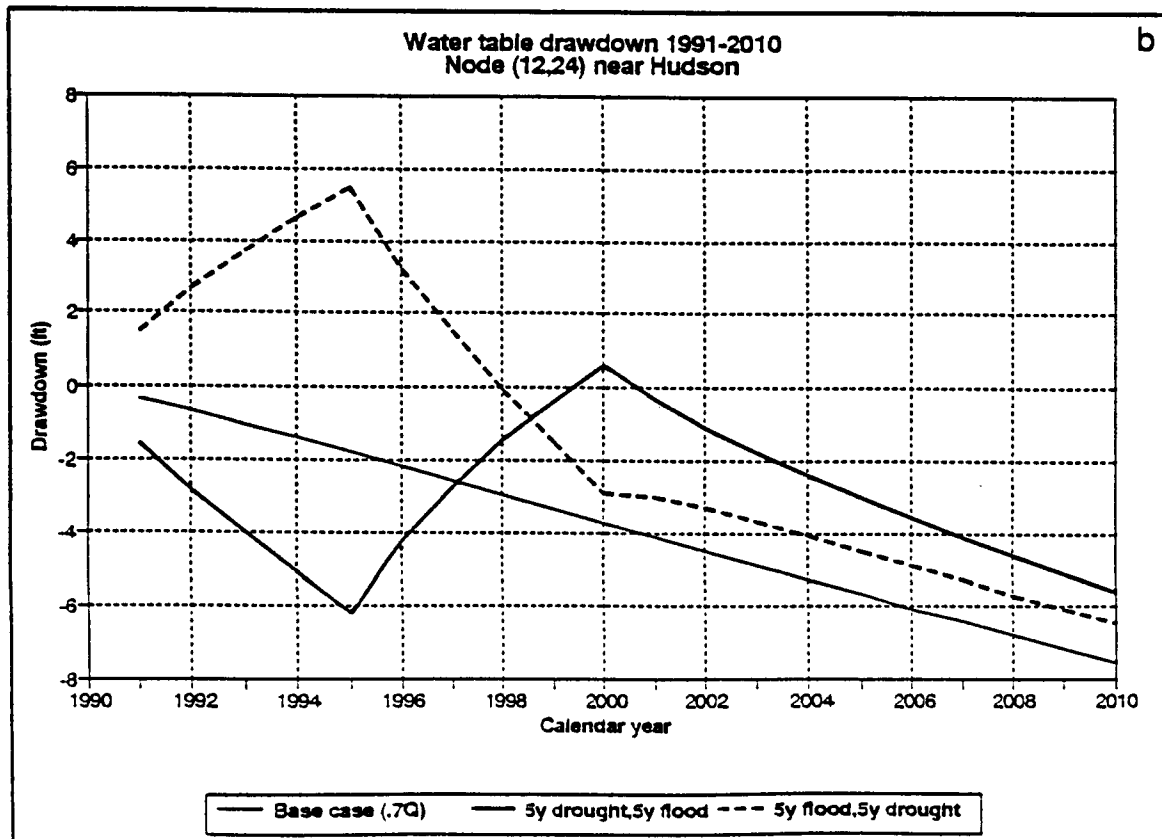
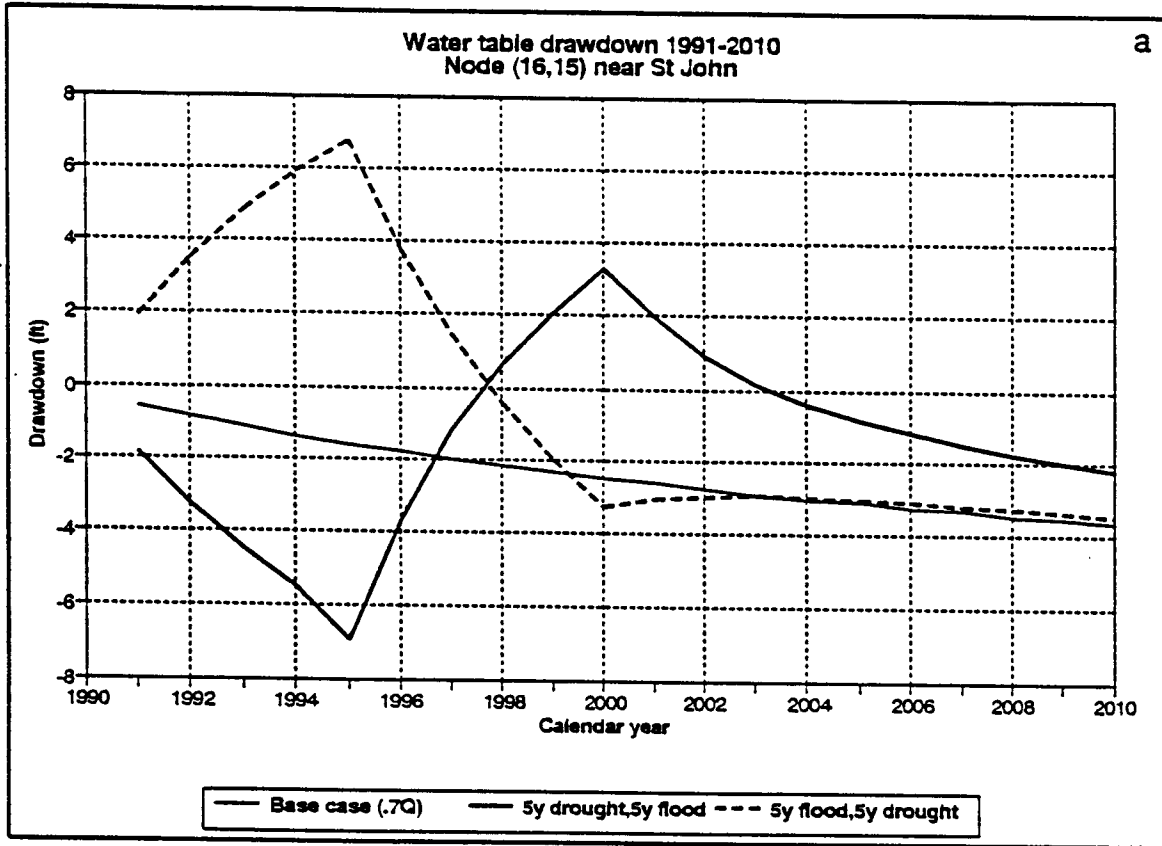


Figure 59. Effect of streamflow climatic cycles shown in fig. 58 on aquifer near (a) St. John and (b) Hudson.

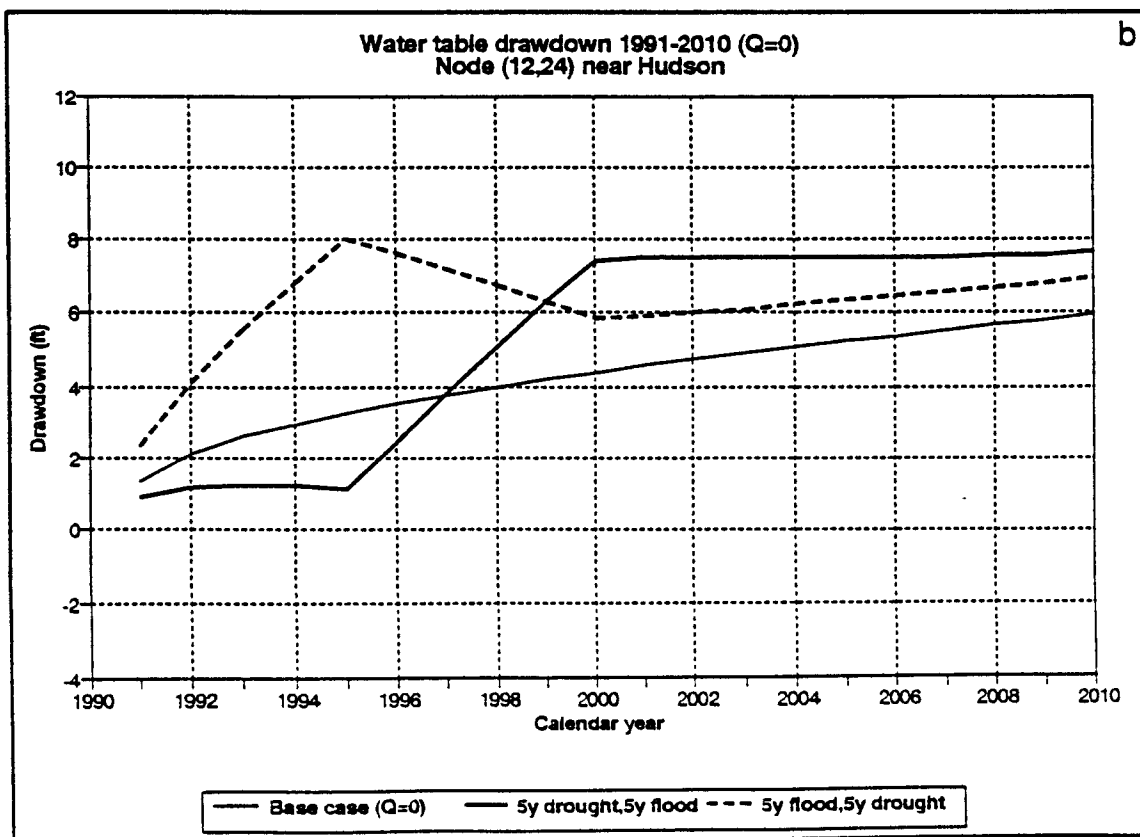
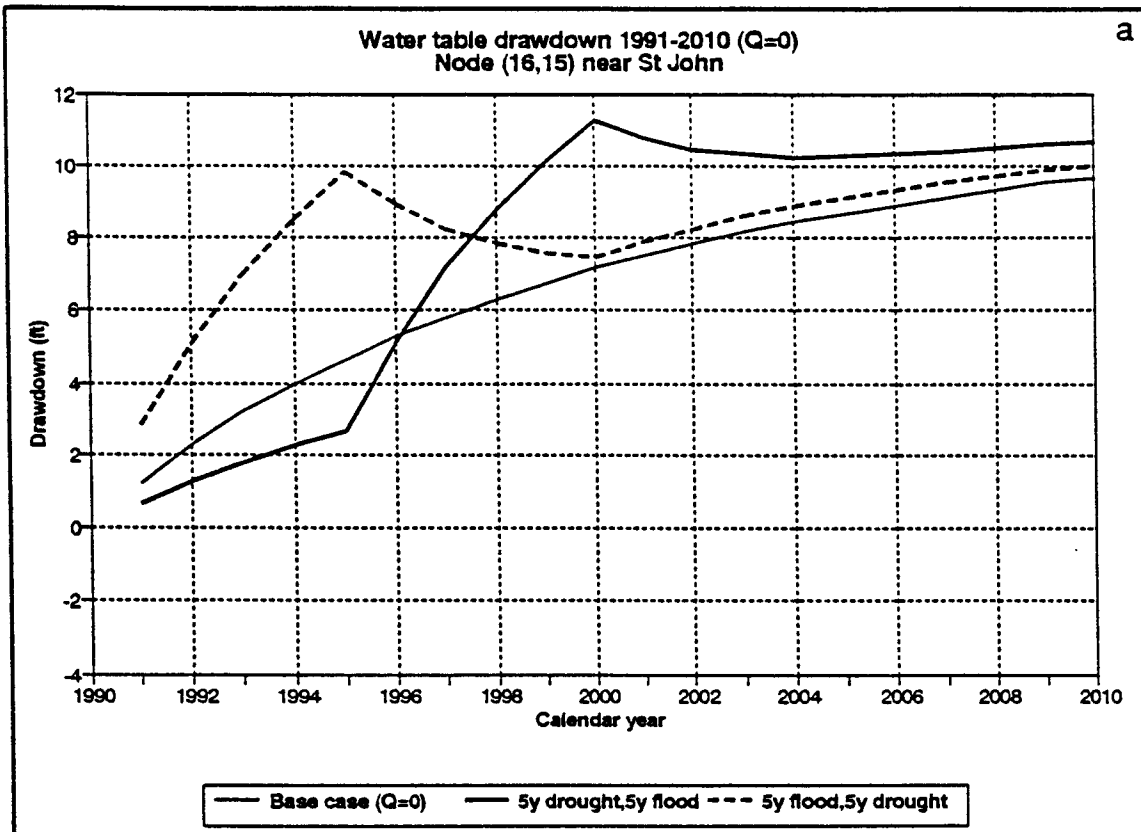


Figure 60. Effect of streamflow climatic cycles shown in fig. 58 on aquifer near (a) St. John and (b) Hudson, assuming complete pumping moratorium for the next 20 years.

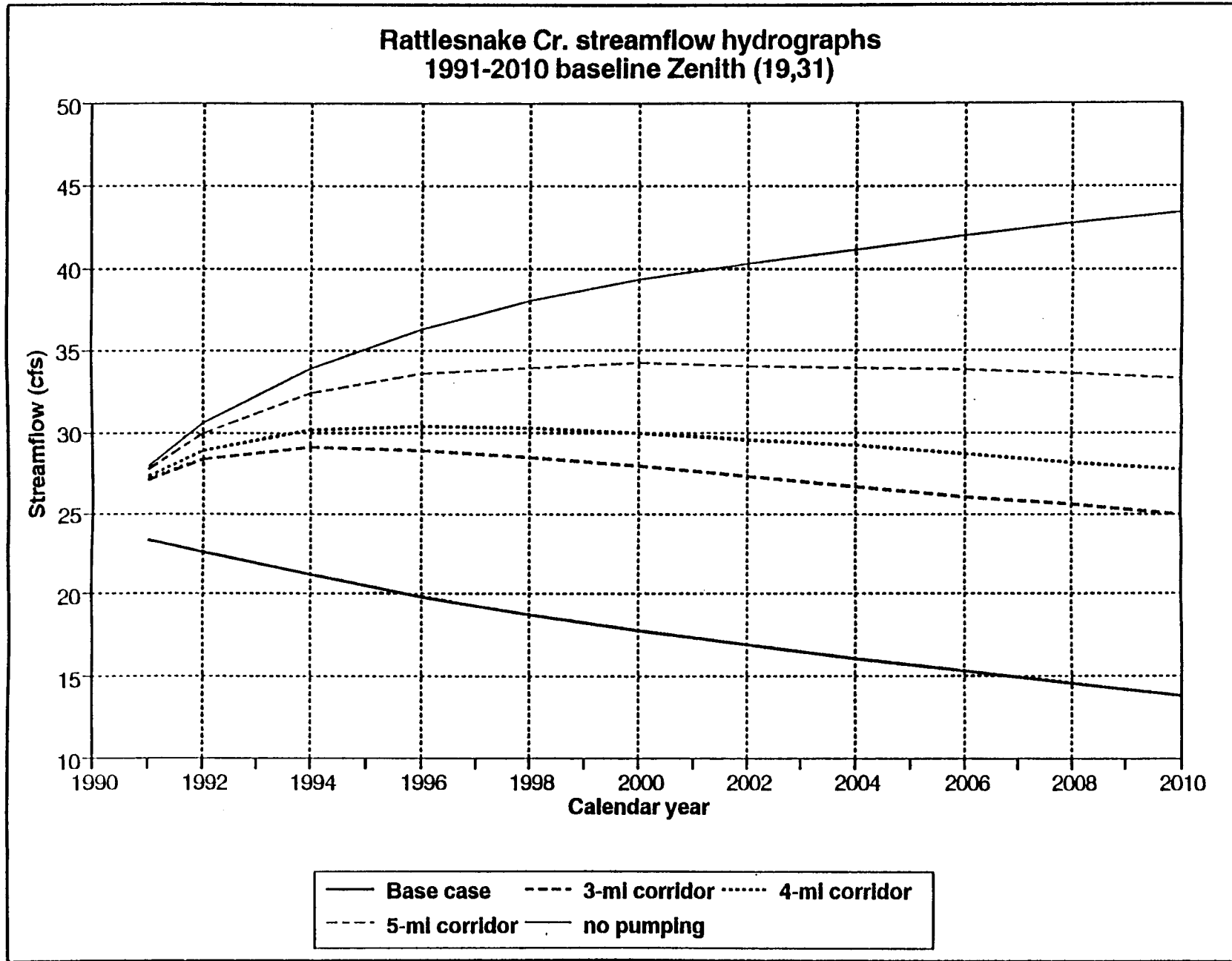


Figure 61. Predicted effect of different management scenarios on Rattlesnake Creek streamflows at Zenith gaging station. Refer to text for explanation of curves.

Table 12. Management alternatives considered for the lower Rattlesnake Creek model area.

Pumping patterns	Effects	Results in figure
1. Base case: 1990 "status quo" maintained (pumpage 70% of appropriations)	40% streamflow decline by 2010 at the Zenith streamgaging station	61, 64a
2. Complete pumpage moratorium throughout model area	Increased streamflows throughout Rattlesnake Creek. Maximum streamflow gain	61, 62
3. 3- to 5-mi stream corridors with pumping moratoria	Only 4-mi stream corridor or larger would maintain present-day streamflows or stabilize flow	61, 64b, 64c
4. Time varying stream corridors with pumping moratoria during a 20-year planning horizon		
a. 3-mi (first decade) followed by 4-mi (next decade)	Present-day streamflows are maintained	65/1 ^a
b. 3-mi (first decade) followed by 5-mi (next decade)	Increased streamflow at the entrance to Quivira NWR	65/3
5. Meeting 30 cfs streamflow target within 3 years by employing a 3-mi stream corridor with pumping moratorium, plus ~29% pumpage reduction throughout model area	Streamflows at entrance to Quivira NWR increase to more than 30 cfs in 3 years	65/4
6. 50% pumpage reduction throughout model area	Streamflows stabilized, with flow at Quivira NWR higher than incoming streamflow at upstream model boundary	65/2

a. Numbers following a slash indicate curve in figure.

that is, the predicted Rattlesnake Creek streamflows at the Zenith gaging station for the next 20 years assuming that present-day conditions of pumpage, recharge, ground-water evapotranspiration, and incoming streamflows at the Macksville gaging station persist throughout the 1991–2010 period. The uppermost curve in fig. 61 represents the maximum expected Rattlesnake Creek streamflows at the Zenith gaging station if all irrigation wells within the model area are completely shut down for the entire 1991–2010 period while recharge, evapotranspiration, and incoming streamflows at the Macksville gaging station are frozen at the present-day levels.

The reach-by-reach streamflow recovery in the Rattlesnake Creek for this case is shown in fig. 62. The rest of the curves in fig. 61 represent predicted streamflows at the Zenith gaging station under various pumpage-moratorium corridors around Rattlesnake Creek. Figure 63 displays 3- and 5-mi stream corridors around Rattlesnake Creek. For a 20-year planning horizon, only stream corridors greater than 4 mi (i.e., 2 mi on either side of the streambanks) with complete pumping shutdown would be effective in stabilizing or increasing streamflows at the entrance to the Quivira marsh, provided present-day (1988–1991) climatic conditions remain constant over the next 20 years. Figure 64 displays the reach-by-reach streamflow gains or losses with time for the base case and for 3-mi and 5-mi corridors with pumping moratoria. Table 13 depicts the relative decreases in pumpage and corresponding gains in streamflows for the different scenarios in the Rattlesnake Creek model area.

Figure 65 displays additional temporally varying management options. For example, a 3-mi corridor around Rattlesnake Creek with a complete irrigation-well pumping moratorium up to the year 2000, followed by a 4-mi corridor thereafter until the year 2010 would approximately maintain present-day streamflows (curve 1, fig. 65); however, if a 5-mi corridor of irrigation-well pumping moratorium followed after the year 2000, Rattlesnake Creek streamflow at the entrance to the Quivira NWR (Zenith gaging station) would have increased by almost 4 cfs from present-day streamflows (curve 3, fig. 65).

Table 13. Management scenarios for enhancing streamflows in Rattlesnake Creek.

	Present-day conditions (base case)	3-mi corridor ^a	4-mi corridor ^a	5-mi corridor ^a	Complete pumpage shutdown ^a
Ground-water pumpage (acre-ft/yr) ^b	69,655	59,889 [-14.0%]	56,531 [-18.8%]	50,719 [-27.2%]	0
Stream leakage gains (acre-ft/yr)	10,702	16,447 [+53.7%]	18,898 [+76.6%]	22,418 [+109.5%]	30,424 [+184.3%]

a. Brackets indicate percent change in ground-water pumpage or stream gains relative to the base case.

b. 70% of appropriations.

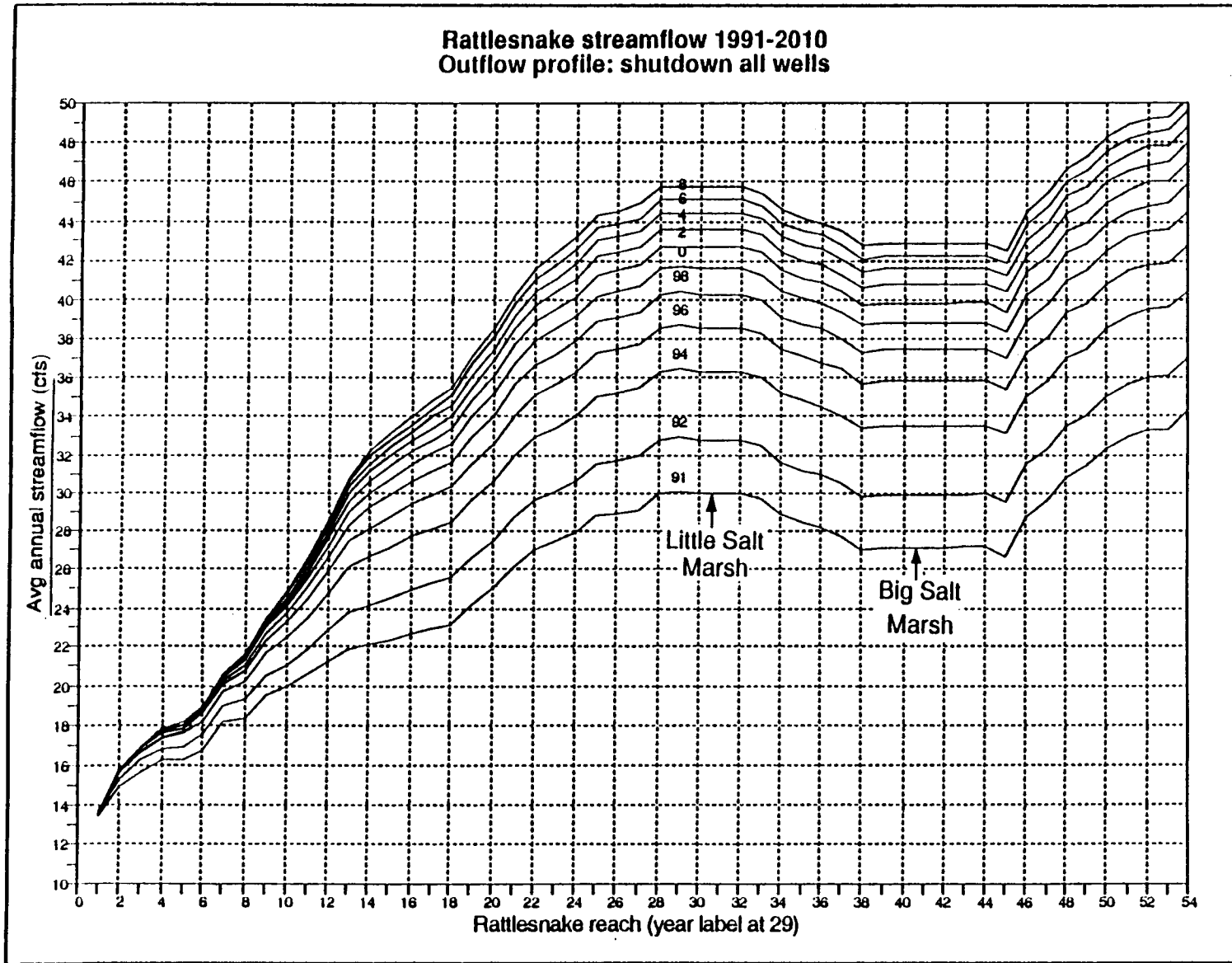


Figure 62. Predicted effect of reach-by-reach Rattlesnake Creek streamflow recovery for the case of complete pumpage moratorium for the 1991-2010 period.

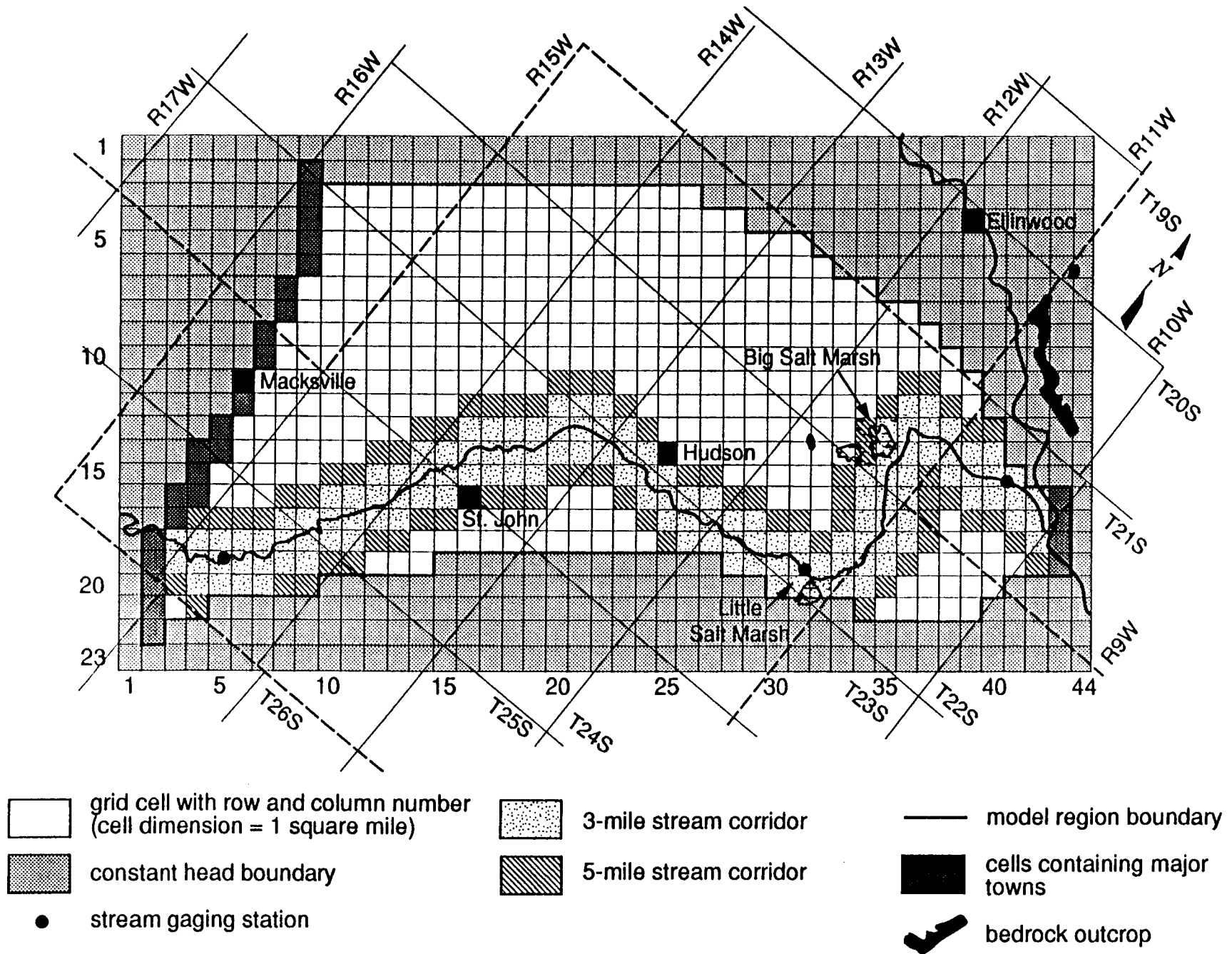


Figure 63. Three-mile and 5-mile stream corridors around Rattlesnake Creek within the model area.

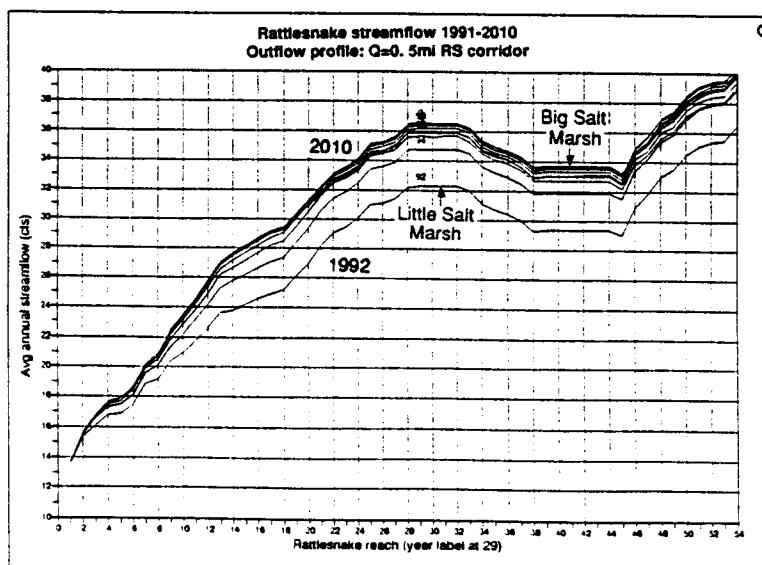
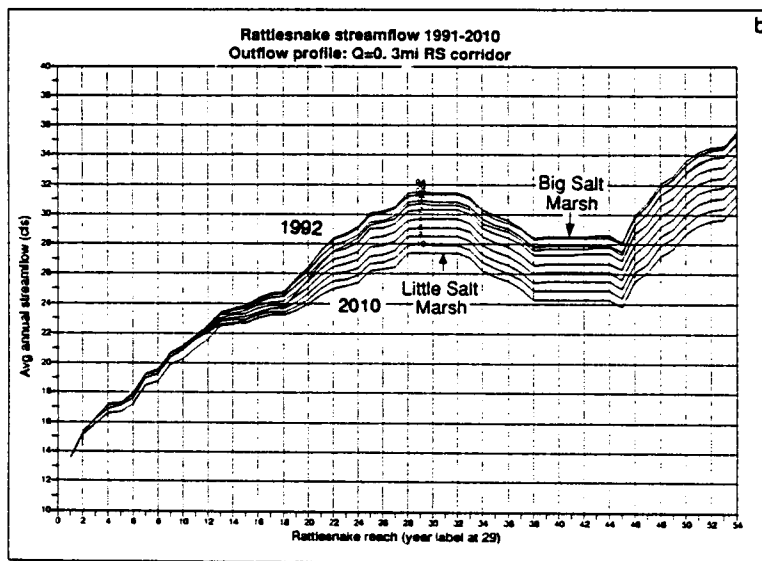
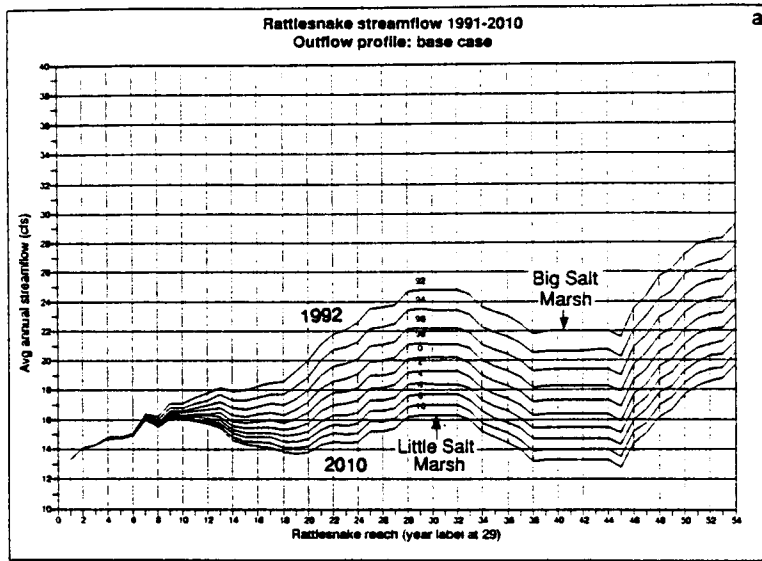


Figure 64. Predicted reach-by-reach Rattlesnake Creek streamflow gains or losses with time for the (a) base case, (b) 3-mile, and (c) 5-mile stream corridors with pumping moratoria.

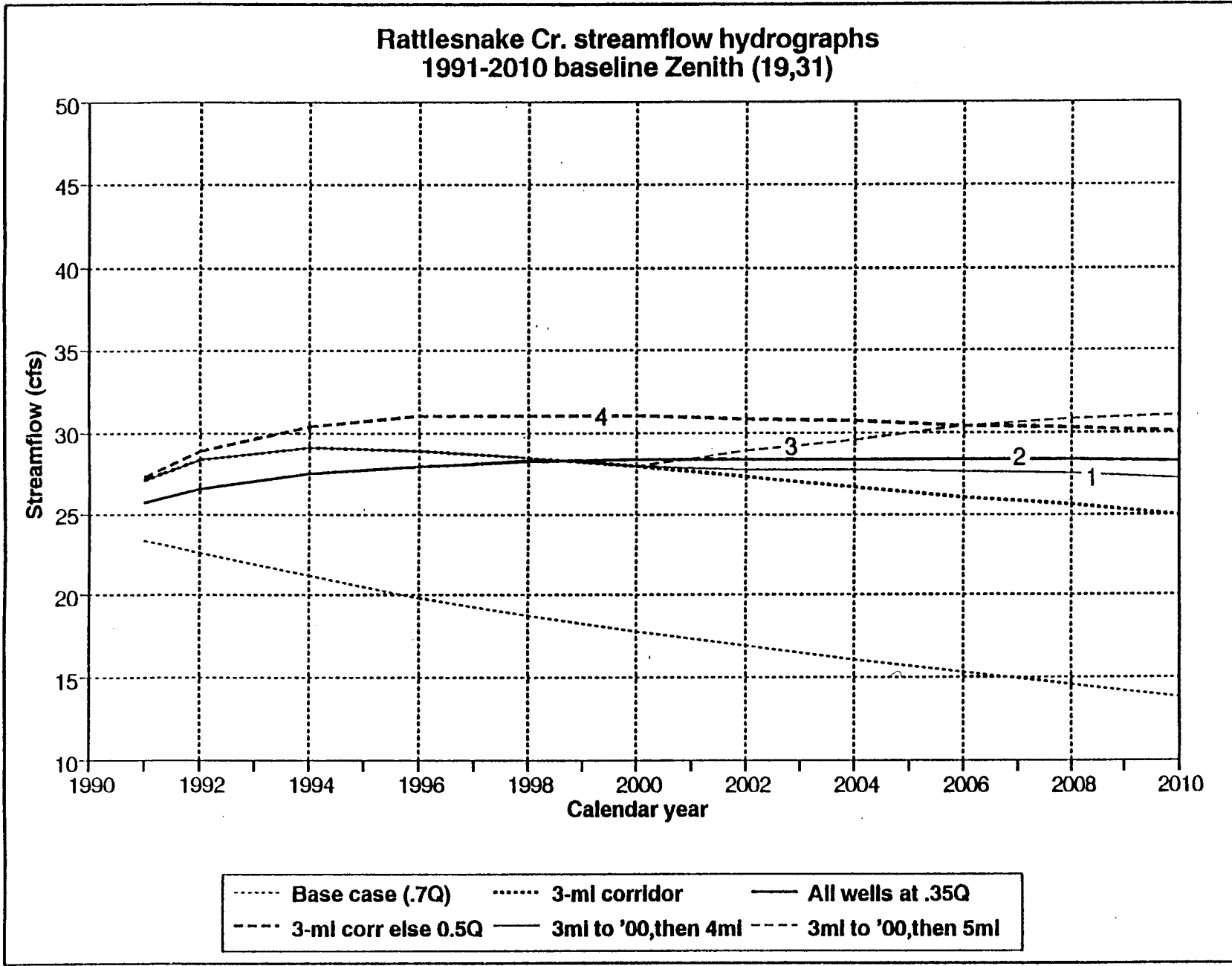


Figure 65. Predicted effect of additional management options, including temporally varying ones, on Rattlesnake Creek streamflows at Zenith gaging station. Refer to text for explanation of curves.

If a target of 30 cfs or more is set for streamflow at the Zenith gaging station over a 20-year planning period, this goal could be achieved within the next 3 or 4 years if a 3-mi corridor of irrigation-well pumping moratorium is adopted in combination with a 50% reduction in appropriated pumpage throughout the model area (curve 4, fig. 65). That 50% reduction in appropriated pumpage corresponds to only a 28.6% decrease in actual pumpage, assuming that the irrigators are actually using only 70% of their water rights appropriations. Finally, if all irrigation wells are permitted to pump only half of what they normally pump, this would definitely stabilize and improve streamflows at a level of more than 3 cfs over present-day streamflows from 1997 to the end of the planning horizon (2010) (curve 2, fig 65).

IX. Summary and conclusions

This study was undertaken to address concerns with declining streamflows and to explore possible management options to remedy this situation. The approach we followed was to analyze the stream-aquifer system as a unit in the lower Rattlesnake Creek watershed. A two-dimensional stream-aquifer model coupled with parameter estimation and optimization modeling was implemented in the study area and proved to be an effective and efficient approach in addressing the stream-aquifer problem. The model was field calibrated for both predevelopment and development periods and was given a limited validation using stresses different from those used in the calibration.

Hydrologic budgets for both predevelopment and developed conditions indicate significant differences in the hydrologic components resulting from development. Such computer simulations provide insight into the changes in recharge and discharge resulting from development. The predevelopment budgets give us an estimate of natural recharge, that is, water moving through the ground-water system under the boundary conditions imposed by natural topography, geology, and climate, whereas the developed-conditions budgets give us an estimate of induced recharge, that is, water added to the natural ground-water system in response to artificial boundary conditions imposed at well fields, farm ponds, drains, reservoirs, and other boundary conditions. Natural

recharge balances natural discharge as baseflow of streams or outflow to springs and wetlands and does not enter the water account for artificial ground-water diversions. Induced recharge and ground-water storage are the two sources of water to balance artificial ground-water withdrawals. The effects of concern to water policy are primarily aquifer drawdown and surface-water depletion. Both are functionally related to pumping rate, aquifer diffusivity, location, and time of pumpage. Thus the natural recharge rate is not directly related to any parameters controlling these primary water policy concerns and should not be used as a measure of the magnitude of ground-water development that will lead to stable, nondepleting ground-water levels. As Bredehoeft et al. (1982) noted, the suggestion that the safe yield of a ground-water basin be defined as the annual extraction of water that does not exceed the average annual ground-water recharge is misleading. As the comparison of the steady-state and transient-state water budgets for both model areas shows, major ground-water development, such as the one in the GMD5 region, significantly changes the recharge-discharge regime with time. The yield of the ground-water basin depends on both the manner in which the effects of withdrawal are transmitted through the aquifer and the changes in rates of recharge and discharge induced by the withdrawals.

We used sensitivity analysis to identify parameters to which the transient-state model is most sensitive. Ground-water pumpage has the largest effect on aquifer water levels and streamflows, followed by recharge, aquifer storativity, and hydraulic conductivity, in order of decreasing sensitivity. These parameters are much more sensitive than stream-related parameters (streambed conductance, Manning's roughness coefficient, stream slope, and stream width).

The calibrated models provide a predictive tool that explains the connections between well field withdrawals and surface-water depletion. Such causal hydrologic models also link proposed actions to hydrologic effects, as clearly demonstrated by the effects of various management alternatives on the streamflows of Rattlesnake Creek. The hydrologic effectiveness of protective stream corridors with restricted ground-water extraction is demonstrated for the study area, thus providing a possible means of restoring specified streamflows in the Rattlesnake Creek.

The results from this study indicate that the present level of ground-water pumpage in the area is not sustainable over the long term and that desirable streamflows cannot be maintained unless severe measures along the lines indicated in this study are taken to protect and conserve the water resources of the region. In view of the possible significant impact such studies might have on water management policies in the GMD5 region, the irrigators of the area were organized to protect their rights and contest any unfavorable results from this study. It is hoped that hydrologic studies such as this one will raise people's awareness of hydrologic reality and will encourage open discussion and improve understanding concerning the important issues we are addressing and their significance to all concerned.

Acknowledgments

U.S. Fish and Wildlife Service funding of this project is gratefully acknowledged. The valuable field assistance of Quivira National Wildlife Refuge personnel Dan Schaad, Pat Gonzales, and Gary Meggers is gratefully appreciated. The support and assistance of Groundwater Management District No. 5 in providing hydrologic data for the area is also gratefully appreciated. All chemical analyses were performed at the Kansas Geological Survey Chemistry Lab under the direction of Larry Hathaway. Bob Buddemeier, Tom McClain, and Frank Cherry of the Kansas Geological Survey provided administrative support for the project. Tain-Shing Ma, a graduate student assistant, provided field and data processing assistance for the project. Alan Stern, a graduate student assistant, provided GIS cartographic support. Jim Mitchell provided GIS-related advice and assisted with computer data retrievals. Anna Kraxner and Shan Chen typed and assembled the manuscript. Mimi Braverman edited the typescript.

References

- Anderson, M. S., Lakin, H. W., Beeson, K. C., Smith, F. F., and Tacker, E., 1961. Selenium in agriculture. Agricultural Handbook 200, U. S. Department of Agriculture, 65 p.
- Bark, L. D., 1961. Rainfall patterns in Kansas. Reprint 9, Kansas Agricultural Experiment Station, Manhattan, 4 p.
- Bark, L. D., 1978. Climate. In: Soil survey of Stafford County, Kansas, D. A. Dodge et al., eds. US Department of Agriculture, Soil Conservation Service, p. 55–57.
- Bidleman, L. A., 1983. An investigation into the source of chlorides in the Arkansas River and related drainage between Great Bend and Wichita. Mimeograph Reports. Equus Beds Groundwater Management District, Halstead, Kansas, 19 p.
- Bredehoeft, J. D., Papadopulos, S. S., and Cooper, H. H., Jr., 1982. Groundwater—the water-budget myth. In, Fiering, M. (ed.), Scientific Basis of Water Resource Management, p. 51–57, National Academy Press, Washington, D. C.
- Chow, V. T., 1959. Open-channel hydraulics. McGraw-Hill, New York, 680 p.
- Cobb, P. M., 1979. Description and analysis of aquifer tests conducted by the Kansas Geological Survey in Stafford and Pawnee counties, Kansas. Open-File Report 79-6, Kansas Geological Survey, 78 p.
- Cobb, P. M., 1980. The distribution and mechanisms of saltwater intrusion in the freshwater aquifer and in Rattlesnake Creek, Stafford Co., Kansas. MS thesis, Department of Civil Engineering, University of Kansas, Lawrence, 176 p.
- Cooley, R. L., 1979. A method of estimating parameters and assessing reliability for models of steady state groundwater flow. 2. Application of statistical analysis. Water Resources Research 15(3):603–617.
- Cooley, R. L., and Naff, R. L., 1985. Regression modeling of ground-water flow. Open-File Report 85-180. US Geological Survey, Lakewood, Colorado, 450 p.
- Doherty, J., 1990. MODINV, MODFLOW parameter optimization manual, version 1.05. Australian Center for Tropical Freshwater Research, 258 p.
- Draper, N. R., and Smith, H., 1981. Applied regression analysis (2d ed.). John Wiley, New York, 709 p.
- Fader, S. W., and Stullken, L. E., 1978. Geohydrology of the Great Bend Prairie, south-central Kansas, Irrigation Series 4, Kansas Geological Survey, 19 p.
- Fent, O. S., 1950. Pleistocene drainage history of central Kansas. Transactions of the Kansas Academy of Science 53(1):81–90.
- Fromm, C., and Wilk, S. (eds.), 1988. Kansas water quality assessment, 1986–87. Report 305b. Kansas Department of Health and Environment, Bureau of Water Protection.
- Frye, J. C., and Leonard, A. B., 1952. Pleistocene geology of Kansas. Bulletin 99, Kansas Geological Survey, 230 p.

- Hansen, C. V., 1991. Estimates of freshwater storage and potential natural recharge for principal aquifers in Kansas. Water Resources Investigations Report 87-4230. U.S. Geological Survey, Lawrence, Kansas, 100 p.
- Latta, B., 1950. Geology and ground-water resources of Barton and Stafford counties, Kansas. Kansas Geological Survey, Bulletin 88, 228 p.
- McDonald, M. G., and Harbaugh, A. W., 1988. A modular three-dimensional finite difference ground-water flow model. Techniques of Water-Resources Investigations, US Geological Survey, Book 6, Chapter A1, 586 p.
- Morris, D. A., and Johnson, A. I., 1967. Summary of hydrologic and physical properties of rock and soil materials as analyzed by the Hydrologic Laboratory of the U.S. Geological Survey 1948-1960. Water Supply Paper 1839-D, U.S. Geological Survey, 74 p.
- Ohlendorf, H.M., 1989. Bioaccumulation and effects of selenium in wildlife. In Selenium in agriculture and the environment. Special Publication 23. Soil Science Society of America, p. 133-177.
- Prudic, D. E., 1989. Documentation of a computer program to simulate stream-aquifer relations using a modular, finite-difference, ground-water flow model. Open-File Report 88-729. U.S. Geological Survey, Carson City, Nevada, 113 p.
- Ray, J., and Coslett, G., 1972. Rattlesnake Creek fish investigation. Kansas Forestry, Fish and Game Commission Report, 28 p.
- Rosner, M. L., 1988. The stratigraphy of the Quaternary alluvium in the Great Bend Prairie, Kansas. MS thesis, Department of Geology, University of Kansas, Lawrence, 183 p.
- Roth, W. E., 1973. Soil survey of Edwards County, Kansas. U.S. Department of Agriculture, Soil Conservation Service, 64 p.
- Saiki, M. K., and Lowe, T. P., 1987. Selenium in aquatic organisms from subsurface agricultural drainage water, San Joaquin Valley, California. Arch. Environ. Contam. Toxicol. 16:657-670.
- Sophocleous, M. A., 1981. The declining ground-water resources of alluvial valleys: a case study. Ground Water 19(2):214-226.
- Sophocleous, M. A., 1983. Groundwater observation network design for the Kansas Groundwater Management Districts USA. Journal of Hydrology 61:371-389.
- Sophocleous, M. A., 1984. Groundwater flow parameter estimation and quality modeling of the Equus Beds aquifer in Kansas. Journal of Hydrology 69:197-222.
- Sophocleous, M. A., 1991a. Recharge estimation for the Groundwater Management District No. 5: A six-year record. Open-File Report 91-1. Kansas Geological Survey, 14 p.
- Sophocleous, M. A., 1991b. Stream floodwave propagation through the Great Bend alluvial aquifer, Kansas: field measurements and numerical simulations. Journal of Hydrology 124:207-228.

- Sophocleous, M. A., 1992a. Groundwater recharge estimation and regionalization: the Great Bend Prairie of central Kansas and its recharge statistics. *Journal of Hydrology*, 137(1-4):113-140.
- Sophocleous, M. A., 1992b. Modifications and improvements on the lower Rattlesnake Creek-Quivira Marsh stream-aquifer numerical model. Open-File Report 92-37. Kansas Geological Survey, 14 p.
- Sophocleous, M. A., 1992c. A quarter-century of ground-water recharge estimates for the Great Bend Prairie aquifer of Kansas (1967-1992). Open-File Report 92-17. Kansas Geological Survey, 22 p.
- Sophocleous, M. A., and Birdie, T., 1990. Documentation and testing of a computer program to simulate stream-aquifer interaction and single-fluid flow using the Mercer et al. (1980) model for areal flow of saltwater and freshwater separated by an interface. Open-File Report 90-31. Kansas Geological Survey, 95 p.
- Sophocleous, M. A., and McAllister, J. A., 1987. Basinwide water-balance modeling with emphasis on spatial distribution of ground-water recharge. *Water Resources Bulletin*, 23(6):997-1010.
- Sophocleous, M. A., and McAllister, J. A., 1990. Hydrologic-balance modeling of the Rattlesnake Creek watershed, Kansas. *Ground Water Series 11*. Kansas Geological Survey, 72 p.
- Sophocleous, M. A., Arnold, W., and McClain, T., 1990. Pre-Cenozoic bedrock and predevelopment water-level maps and data bases for the Great Bend Prairie of Kansas. Open-File Report 90-15. Kansas Geological Survey, 119 p.
- Sophocleous, M. A., Townsend, M. A., Vogler, L. D., McClain, T. J., Marks, E. T., and Coble, G. R., 1987. Stream-aquifer interaction along the Arkansas River in central Kansas: field testing and analysis. Open-File Report 87-2. Kansas Geological Survey, 90 p.
- Sophocleous, M. A., Townsend, M. A., Vogler, L. D., McClain, T. J., Marks, E. T., and Coble, G. R., 1988. Experimental studies in stream-aquifer interaction along the Arkansas River in central Kansas: field testing and analysis. *Journal of Hydrology* 98:249-273.
- Stramel, G. J., 1967. Rattlesnake Creek study. Mimeograph report. Wichita Water Department, 31 p.
- U.S. Army Corps of Engineers, Tulsa District, 1966. Water quality control study: Texas-Oklahoma-Kansas, v. 1, Main Report. U.S. Army Corps of Engineers, Tulsa, Oklahoma.
- U.S. Environmental Protection Agency, 1987. Ambient aquatic life water quality criteria for selenium—1987. Report EPA-440/5-87-006. U.S. Environmental Protection Agency.
- White, F. M. (ed.), 1979. *Fluid mechanics*. McGraw-Hill, New York, 701 p.
- White, K. E., and Sloto, R. A., 1990. Base-flow-frequency characteristics of selected Pennsylvania streams. U.S. Geological Survey, Water-Resources Investigation Report 90-4160, 67 p.

Yager, R. M., 1991. Estimation of hydraulic conductivity of a riverbed and aquifer system on the Susquehanna River in Broome County, New York. Open-File Report 91-457. U.S. Geological Survey, 54 p.

Appendix 1. Ground-water rights in the Rattlesnake Creek study area

Appendix 1. Ground-water rights in the Rattlesnake Creek study area (1990)

Key to Table Columns:

- (a) Location of each well (or grid corner) using the Public Land Survey System. Well identification number is listed first, followed by county abbreviation, township number (all south of the 40th parallel), range, section number, and quarter-section identifier.
- (b) Pumpage rate in gallons per minute.
- (c) Water rights appropriation amount in acre-feet per year.
- (d, e) Well-use codes: (1) domestic, (2) industrial, (3) irrigation, (4) municipal, (5) recreation, (6) stock watering. G = ground-water right, V = vested right, A . . = appropriated right and year established (e.g., A54 = appropriated 1954).
- (f, g) Conversion to longitude, latitude (deg) from legal coordinates (a) automated by LEO I-PC written by C. G. Ross, KGS Open-File Report 91-37, September 1991.
- (h, i) Albers projection (x, y) coordinates are with respect to origin (0, 0) located at 36.8750° N latitude, 98.3125° W longitude. Albers projection is based on meridian at 98.3215° W, parallels at 34.0° N and 44.0° N, and earth radius 6,371,007 m (weighted average based on the geodetic reference spheroid WGS-72).
- (j, k) Wells are located on a 23 mi × 44 mi rectangle with a regular 1-mile grid of rows and columns. The study-area rectangle's corners are listed at the beginning of the table.
- (l, m) Integer values for row and column denote the cell in which the well lies.
- (n) Cell activity: 0 = outside model area; -1 = constant-head cell; 1 = active model cell.

Study-area grid corners

Township, range, section, quarter-section	Longitude (deg)	Latitude (deg)	Albers x (m)	Albers:y (m)	Grid row	Grid column
<i>SW corners</i>						
23 17W 23 CCC	-99.1672	38.0299	-74591.	129201.	0	0
26 14W 19 BCC	-98.9021	37.7704	-51645.	100055.	23	0
<i>NE corners</i>						
19 11W 3BDB	-98.5299	38.4302	-18863.	173546	0	44
22 9W 1BDC	-98.2645	38.1672	4183.	144172.	23	44

Appendix 1. Well data

(a) Well ID, township, range, section, quarter-section	(b) Rate (gpm)	(c) Approp (ac-ft)	(d) Use code	(e) Year	(f, g) Longitude (deg)	(f, g) Latitude (deg)	(h, i) Albers x (m)	(h, i) Albers y (m)	(j, k) Grid row/col. (mi)	(l, m) Grid index row/col	(n) cell activ.
BT0002-BT 19 11W 31 CAAB	177.00	82.86	4 G V		-98.5826	38.3545	-23465.	165107.	2.19 38.61	3 39	1
RC0012-RC20 10W 21 CDCC	2.00	3.22	2 G V		-98.4376	38.2897	-10880.	157857.	10.55 41.94	11 42	1
038126-BT 20 12W 10 BDBB	900.00	147.00	3 G V		-98.6403	38.3295	-28487.	162336.	1.60 35.11	2 36	1
038126-BT 20 12W 10 BDBB	900.00	65.00	2 G V		-98.6403	38.3295	-28487.	162336.	1.60 35.11	2 36	1
030718-SF 21 12W 9 BADC	1000.00	20.00	3 G V		-98.6483	38.2431	-29215.	152703.	6.01 31.07	7 32	1
030718-SF 21 12W 9 BADC	.00	96.00	5 G V		-98.6483	38.2431	-29215.	152703.	6.01 31.07	7 32	1
033973-PN 22 15W 33 AACB	300.00	72.00	3 G V		-98.9713	38.0997	-57437.	136845.	2.88 11.29	3 12	1
036564-SF 23 13W 29 CDAA	450.00	5.00	5 G V		-98.7755	38.0173	-40416.	127551.	13.94 15.99	14 16	1
036563-SF 23 13W 29 CDAD	450.00	5.00	5 G V		-98.7755	38.0164	-40416.	127450.	13.99 15.95	14 16	1
PN0071-PN 23 15W 26 DCBB	350.00	10.00	3 G V		-98.9396	38.0181	-54737.	127726.	8.35 9.11	9 10	1
PN0072-PN 23 16W 12 BDC	1000.00	210.00	3 G V		-99.0342	38.0664	-62954.	133170.	2.54 7.21	3 8	1
SF0001-SF 24 12W 11 CDC	850.00	214.82	4 G V		-98.6127	37.9702	-26218.	122233.	21.99 20.84	22 21	1
036203-SF 24 12W 14 CADA	50.00	10.50	3 G V		-98.6098	37.9598	-25967.	121072.	22.65 20.52	23 21	1
SF0002-SF 24 13W 4 ABAD	1340.00	245.51	4 G V		-98.7521	37.9980	-38380.	125388.	15.78 16.15	16 17	1
SF0010-SF 24 13W 7 BDC	2050.00	210.00	3 G V		-98.7966	37.9789	-42277.	123273.	15.31 13.45	16 14	1
SF0004-SF 24 14W 9 BDBB	1000.00	265.00	3 G V		-98.8708	37.9813	-48754.	123578.	12.67 10.42	13 11	1
019757-SF 24 15W 8 CDCD	1025.00	120.00	3 G V		-98.9979	37.9715	-59861.	122558.	8.89 4.64	9 5	1
SF0003-SF 24 15W 15 CCCA	350.00	18.41	4 G V		-98.9658	37.9580	-57069.	121029.	10.71 5.41	11 6	1
009364-PR 26 14W 9 BBB	228.00	20.00	3 G V		-98.8663	37.8052	-48480.	103924.	22.33 3.02	23 4	1
001586-RC 20 10W 35 ABD	700.00	140.00	3 G A53		-98.3935	38.2722	-7042.	155892.	12.98 43.05	13 44	1
001790-RC 21 9W 27 BCDA	550.00	104.00	3 G A53		-98.3031	38.1966	814.	147452.	20.11 43.62	21 44	1
001180-SF 23 14W 23 DDBB	450.00	89.00	3 G A53		-98.8248	38.0322	-44711.	129228.	11.47 14.55	12 15	1
001592-PN 23 15W 12 ABA	180.00	18.00	2 G A53		-98.9184	38.0719	-52842.	133717.	6.16 12.32	7 13	1
002065-PN 23 16W 31 DBBB	510.00	71.00	3 G A53		-99.1221	38.0067	-70680.	126574.	2.78 .93	3 1	1
001978-ED 24 16W 13 CBDD	360.00	126.00	3 G A53		-99.0363	37.9606	-63224.	121368.	8.18 2.55	9 3	1
001600-SF 25 14W 30 CDBB	715.00	266.00	3 G A53		-98.9069	37.8430	-52012.	108164.	18.91 2.93	19 3	1
001228-PR 26 15W 2 BABB	480.00	150.00	3 G A53		-98.9347	37.8248	-54451.	106145.	18.96 .97	19 1	1
002149-SF 23 13W 7 CACC	750.00	128.00	3 G A54		-98.7972	38.0618	-42283.	132527.	10.80 16.99	11 17	1
003399-BT 19 11W 26 BDAB	400.00	90.00	3 G A55		-98.5095	38.3723	-17112.	167078.	3.67 42.45	4 43	1
004119-SF 22 14W 27 ACC	685.00	34.00	3 G A55		-98.8470	38.1098	-46594.	137901.	6.53 16.96	7 17	1
003426-PN 22 15W 11 ABC	920.00	222.00	3 G A55		-98.9385	38.1573	-54536.	143252.	.87 15.16	1 16	1
003425-PN 22 15W 11 BDB	1000.00	83.00	3 G A55		-98.9431	38.1555	-54935.	143055.	.82 14.89	1 15	1
004654-SF 23 13W 15 ADB	1500.00	180.00	3 G A55		-98.7322	38.0530	-36616.	131511.	13.47 19.35	14 20	1
003664-PN 23 16W 16 BAB	85.00	12.00	3 G A55		-99.0895	38.0571	-67785.	132179.	1.17 4.49	2 5	1
003500-SF 24 12W 13 BAC	410.00	30.00	3 G A55		-98.5944	37.9666	-24625.	121824.	22.80 21.46	23 22	1

Appendix 1. Well data (cont.)

(a) Well ID, township, range, section, quarter-section	(b) Rate (gpm)	(c) Approp (ac-ft)	(d) Use code	(e) Year	(f, g) Longitude (deg)	(f, g) Latitude (deg)	(h, i) Albers x (m)	(h, i) Albers y (m)	(j, k) Grid row/col. (mi)	(l, m) Grid index row/col	(n) cell activ.
004570-SF 24 14W 3 DDA	700.00	185.00	3 G A55		-98.8402	37.9880	-46083.	124312.	13.34 12.00	14 12	1
003633-SF 24 15W 6 BABB	955.00	207.00	3 G A55		-99.0169	37.9998	-61502.	125730.	6.72 5.06	7 6	1
004191-SF 25 13W 11 ACDD	1230.00	480.00	3 G A55		-98.7149	37.8907	-35189.	113396.	22.84 13.10	23 14	1
004623-SF 25 13W 21 CBA	1400.00	257.00	3 G A55		-98.7618	37.8606	-39302.	110050.	22.88 9.82	23 10	1
004752-SF 25 13W 30 CAB	1500.00	480.00	3 G A55		-98.7962	37.8462	-42324.	108466.	22.49 7.75	23 8	1
005345-BT 19 11W 31 CAAB	.00	33.68	4 G A56		-98.5826	38.3545	-23465.	165107.	2.19 38.61	3 39	1
006460-SF 21 13W 23 DBBB	2500.00	240.00	3 G A56		-98.7196	38.2092	-35435.	148945.	5.45 26.61	6 27	1
005905-PN 22 15W 19 DCDC	1090.00	135.00	3 G A56		-99.0100	38.1170	-60796.	138797.	.63 10.41	1 11	1
005809-SF 23 13W 5 AACC	1000.00	190.00	3 G A56		-98.7696	38.0836	-39859.	134938.	10.56 19.09	11 20	1
005168-SF 23 14W 19 ACAA	755.00	104.00	3 G A56		-98.8995	38.0398	-51224.	130120.	8.54 11.73	9 12	1
005936-SF 24 12W 9 CDBB	755.00	230.00	3 G A56		-98.6496	37.9729	-29446.	122548.	20.59 19.39	21 20	1
005573-SF 24 12W 21 DCBB	690.00	171.00	3 G A56		-98.6451	37.9438	-29057.	119293.	22.32 18.33	23 19	1
005999-SF 24 14W 1 CCB	850.00	210.00	3 G A56		-98.8195	37.9879	-44277.	124291.	14.04 12.87	15 13	1
007165-BT 19 11W 30 ACB	1000.00	294.00	3 G A57		-98.5800	38.3720	-23233.	167068.	1.32 39.48	2 40	1
007324-BT 19 11W 34 BBCC	300.00	63.00	3 G A57		-98.5344	38.3586	-19280.	165553.	3.58 40.81	4 41	1
007322-SF 21 13W 5 CBDC	570.00	117.00	3 G A57		-98.7816	38.2507	-40815.	153600.	1.12 25.78	2 26	1
007286-PN 22 15W 25 ADBB	1180.00	213.00	3 G A57		-98.9164	38.1124	-52638.	138228.	4.05 14.15	5 15	1
007009-SF 23 14W 3 ADBC	700.00	240.00	3 G A57		-98.8430	38.0820	-46267.	134802.	8.16 15.93	9 16	1
007564-PN 23 16W 2 DACB	800.00	240.00	3 G A57		-99.0440	38.0778	-63795.	134447.	1.60 7.29	2 8	1
006649-SF 24 13W 25 CDBB	1100.00	192.00	3 G A57		-98.7044	37.9297	-34251.	117745.	21.08 15.22	22 16	1
006774-ED 24 16W 12 DBCC	900.00	120.00	3 G A57		-99.0305	37.9752	-62711.	122987.	7.59 3.42	8 4	1
007822-BT 19 11W 19 BCC	428.00	136.00	3 G A58		-98.5890	38.3849	-24009.	168508.	.32 39.65	1 40	1
007705-SF 22 14W 35 DDBB	770.00	226.00	3 G A58		-98.8246	38.0902	-44657.	135702.	8.35 17.06	9 18	1
007965-SF 25 14W 13 ACC	1700.00	40.00	5 G A58		-98.8101	37.8771	-43518.	111919.	20.35 8.49	21 9	1
008032-SF 21 13W 9 DBC	615.00	111.00	3 G A59		-98.7558	38.2365	-38573.	152001.	2.75 26.26	3 27	1
008256-SF 22 13W 17 CBA	1400.00	351.00	5 G A59		-98.7810	38.1369	-40822.	140891.	7.29 20.91	8 21	1
008113-SF 23 13W 14 ADBB	910.00	138.00	3 G A59		-98.7144	38.0534	-35063.	131546.	14.06 20.12	15 21	1
008303-SF 22 13W 4 CBD	367.00	80.00	5 G A60		-98.7627	38.1639	-39220.	143898.	6.45 22.84	7 23	1
008328-PN 22 15W 22 DABC	275.00	119.00	3 G A60		-98.9529	38.1224	-55813.	139369.	2.27 13.05	3 14	1
008348-SF 24 13W 10 BDAB	1200.00	405.00	3 G A60		-98.7392	37.9807	-37263.	123448.	17.15 15.95	18 16	1
008634-SF 23 12W 35 ADBB	1000.00	247.00	3 G A61		-98.6042	38.0088	-25461.	126534.	20.18 22.86	21 23	1
009596-SF 22 13W 9 CDBB	1090.00	195.00	3 G A63		-98.7609	38.1480	-39064.	142124.	7.37 22.23	8 23	1
009416-SF 23 12W 25 DCCB	575.00	135.00	3 G A63		-98.5905	38.0141	-24267.	127128.	20.35 23.66	21 24	1
010470-SF 21 13W 31 DCCB	655.00	31.00	3 G A64		-98.7930	38.1755	-41845.	145210.	4.80 22.07	5 23	1
009737-SF 22 14W 16 BDBB	2500.00	378.00	3 G A64		-98.8708	38.1412	-48645.	141416.	4.03 17.31	5 18	1

Appendix 1. Well data (cont.)

(a) Well ID, township, range, section, quarter-section	(b) Rate (gpm)	(c) Approp (ac-ft)	(d) Use code	(e) Year	(f, g) Longitude (deg)	(f, g) Latitude (deg)	(h, i) Albers x (m)	(h, i) Albers y (m)	(j, k) Grid row/col. (mi)	(l, m) Grid index row/col	(n) cell activ.
010269-SF 22 14W 36 CDBB	869.00	160.00	3 G	A64	-98.8154	38.0901	-43855.	135693.	8.66 17.44	9 18	1
009781-SF 23 13W 27 DDBB	800.00	196.00	3 G	A64	-98.7326	38.0170	-36670.	127499.	15.41 17.79	16 18	1
009816-SF 25 13W 3 ACDA	265.00	118.00	3 G	A64	-98.7334	37.9063	-36792.	115142.	21.37 12.99	22 13	1
010458-SF 25 14W 19 ACA	1187.00	200.00	3 G	A64	-98.8996	37.8644	-51355.	110546.	18.01 4.16	19 5	1
011303-RC 21 9W 33 CACB	905.00	211.00	3 G	A65	-98.3203	38.1786	-678.	145441.	20.51 42.13	21 43	1
011492-SF 21 13W 14 CBD	2500.00	237.00	3 G	A65	-98.7258	38.2216	-35976.	150330.	4.57 26.88	5 27	1
010931-SF 23 13W 28 CABB	790.00	177.00	3 G	A65	-98.7604	38.0209	-39097.	127939.	14.26 16.78	15 17	1
010754-SF 24 12W 11 BDBB	1600.00	240.00	3 G	A65	-98.6133	37.9797	-26268.	123294.	21.45 21.22	22 22	1
011363-SF 24 14W 11 BDBB	735.00	195.00	3 G	A65	-98.8339	37.9811	-45533.	123539.	13.93 11.97	14 12	1
011266-SF 25 15W 23 CDBB	885.00	192.00	3 G	A65	-98.9437	37.8575	-55222.	109806.	16.88 2.00	17 3	1
011903-BT 19 11W 31 DBDC	.00	107.80	4 G	A66	-98.5780	38.3516	-23069.	164791.	2.49 38.68	3 39	1
011866-SF 21 13W 1 BCB	390.00	86.00	3 G	A66	-98.7094	38.2563	-34528.	154189.	3.25 29.06	4 30	1
012106-SF 22 12W 30 BDBB	740.00	129.00	3 G	A66	-98.6872	38.1114	-32660.	138009.	11.83 23.76	12 24	1
012313-PN 22 15W 26 ADAB	450.00	119.00	3 G	A66	-98.9322	38.1124	-54022.	138239.	3.51 13.49	4 14	1
011559-SF 23 12W 7 DBA	1365.00	120.00	3 G	A66	-98.6795	38.0636	-32011.	132680.	14.68 22.03	15 23	1
012479-PN 23 15W 23 DBA	680.00	90.00	3 G	A66	-98.9368	38.0357	-54474.	129682.	7.50 9.99	8 10	1
012143-PN 23 16W 23 ACA	1000.00	227.00	3 G	A66	-99.0458	38.0392	-63983.	130145.	3.62 5.55	4 6	1
012042-SF 24 12W 17 CAB	1500.00	438.00	3 G	A66	-98.6672	37.9617	-30982.	121301.	20.61 18.17	21 19	1
012023-SF 24 14W 29 CDBB	700.00	233.00	3 G	A66	-98.8890	37.9304	-50384.	117911.	14.80 7.46	15 8	1
013062-BT 20 11W 6 CCCB	1270.00	166.00	3 G	A67	-98.5894	38.3349	-24064.	162928.	3.02 37.49	4 38	1
013032-RC 21 9W 31 ADBB	795.00	223.00	3 G	A67	-98.3478	38.1842	-3071.	146072.	19.29 41.21	20 42	1
013557-SF 21 13W 26 ACBB	3000.00	396.00	3 G	A67	-98.7196	38.1983	-35443.	147726.	6.04 26.14	7 27	1
012998-SF 21 13W 33 DCAD	400.00	85.00	3 G	A67	-98.7530	38.1760	-38367.	145244.	6.12 23.77	7 24	1
013246-SF 21 14W 32 ADBB	1215.00	180.00	3 G	A67	-98.8800	38.1848	-49420.	146292.	1.36 18.81	2 19	1
013518-SF 22 13W 5 CBC	400.00	40.00	5 G	A67	-98.7834	38.1641	-41015.	143937.	5.74 21.98	6 22	1
012967-SF 22 13W 21 BBDD	810.00	165.00	3 G	A67	-98.7619	38.1271	-39164.	139791.	8.47 21.29	9 22	1
013238-SF 22 13W 22 CACC	1690.00	240.00	3 G	A67	-98.7423	38.1198	-37459.	138970.	9.52 21.80	10 22	1
013554-SF 22 14W 6 DCAA	975.00	221.00	3 G	A67	-98.8993	38.1631	-51116.	143880.	1.88 17.06	2 18	1
013553-SF 22 14W 7 ADBB	905.00	214.00	3 G	A67	-98.8982	38.1558	-51024.	143066.	2.31 16.79	3 17	1
013260-SF 22 14W 15 DDBC	610.00	150.00	3 G	A67	-98.8432	38.1328	-46246.	140472.	5.41 18.12	6 19	1
013084-PN 22 15W 17 DCBB	1700.00	176.00	3 G	A67	-98.9942	38.1342	-59409.	140714.	.24 11.82	1 12	1
012526-SF 23 13W 4 ABDD	1225.00	234.00	3 G	A67	-98.7524	38.0835	-38364.	134927.	11.14 19.81	12 20	1
012922-SF 23 13W 32 CDBB	1200.00	237.00	3 G	A67	-98.7788	38.0028	-40707.	125930.	14.62 15.23	15 16	1
012524-SF 23 14W 15 CDBB	950.00	162.00	3 G	A67	-98.8524	38.0468	-47105.	130878.	9.75 14.02	10 15	1
014010-SF 24 13W 16 ABB	1215.00	215.00	3 G	A67	-98.7548	37.9694	-38630.	122194.	17.23 14.80	18 15	1

Appendix 1. Well data (cont.)

(a) Well ID, township, range, section, quarter-section	(b) Rate (gpm)	(c) Approp (ac-ft)	(d) Use code	(e) Year	(f, g) Longitude (deg) Latitude (deg)		(h, i) Albers x (m) Albers y (m)		(j, k) GrID row/col. (mi)		(l, m) GrID index row/col		(n) cell activ.
013336-SF 24 14W 17 ADBB	680.00	158.00	3 G	A67	-98.8800	37.9668	-49573.	121966.	13.14	9.41	14	10	1
013861-SF 24 14W 24 CDBB	330.00	120.00	3 G	A67	-98.8155	37.9448	-43949.	119474.	16.51	11.18	17	12	1
013812-SF 24 14W 24 DDBB	960.00	190.00	3 G	A67	-98.8063	37.9449	-43144.	119476.	16.82	11.57	17	12	1
012812-SF 24 15W 32 DBCA	1030.00	95.00	3 G	A67	-98.9928	37.9177	-59465.	116550.	11.97	2.53	12	3	1
013092-SF 25 13W 9 DDBB	985.00	240.00	3 G	A67	-98.7508	37.8865	-38327.	112937.	21.85	11.40	22	12	1
013432-SF 25 14W 20 DDBB	920.00	216.00	3 G	A67	-98.8795	37.8576	-49602.	109776.	19.06	4.72	20	5	1
014314-BT 20 11W 9 CABB	1765.00	231.00	3 G	A68	-98.5481	38.3258	-20475.	161901.	4.90	38.83	5	39	1
014678-BT 20 13W 24 DCBB	4000.00	240.00	3 G	A68	-98.7090	38.2931	-34478.	158304.	1.26	30.66	2	31	1
014619-SF 21 13W 27 CDBC	800.00	120.00	3 G	A68	-98.7427	38.1904	-37457.	146854.	5.69	24.83	6	25	1
015780-SF 22 13W 18 DBCC	2000.00	236.00	3 G	A68	-98.7928	38.1346	-41854.	140649.	7.02	20.31	8	21	1
014620-SF 22 13W 28 BBDD	965.00	195.00	3 G	A68	-98.7617	38.1125	-39155.	138170.	9.26	20.67	10	21	1
014442-SF 22 14W 29 BABB	1195.00	117.00	3 G	A68	-98.8891	38.1159	-50262.	138609.	4.78	15.45	5	16	1
014633-PN 22 15W 20 CDCC	1895.00	240.00	3 G	A68	-98.9988	38.1170	-59817.	138794.	1.01	10.89	2	11	1
015053-PN 22 15W 27 CBBB	200.00	66.00	3 G	A68	-98.9666	38.1088	-57022.	137861.	2.54	11.89	3	12	1
014674-PN 22 15W 29 ACA	1665.00	240.00	3 G	A68	-98.9913	38.1120	-59169.	138232.	1.54	10.99	2	11	1
015459-SF 23 11W 4 DDAD	305.00	50.00	3 G	A68	-98.5279	38.0731	-18787.	133697.	19.27	28.84	20	29	1
015976-SF 23 11W 22 BCCB	.00	90.00	3 G	A68	-98.5266	38.0359	-18684.	129547.	21.32	27.30	22	28	1
015975-SF 23 11W 22 BCCB	975.00	60.00	3 G	A68	-98.5266	38.0359	-18684.	129547.	21.32	27.30	22	28	1
015010-SF 23 12W 21 ACAB	1250.00	180.00	3 G	A68	-98.6432	38.0383	-28859.	129836.	17.27	22.47	18	23	1
014774-SF 23 12W 25 CDC	670.00	114.00	3 G	A68	-98.5945	38.0137	-24615.	127081.	20.24	23.48	21	24	1
015174-SF 23 12W 36 BBCC	2500.00	266.00	3 G	A68	-98.5996	38.0096	-25062.	126629.	20.29	23.09	21	24	1
015562-SF 23 13W 16 CCAA	790.00	221.00	3 G	A68	-98.7616	38.0463	-39187.	130773.	12.85	17.82	13	18	1
014602-SF 23 13W 35 BDBB	1760.00	234.00	3 G	A68	-98.7234	38.0097	-35869.	126681.	16.11	17.86	17	18	1
014966-SF 23 13W 35 CDBB	780.00	240.00	3 G	A68	-98.7233	38.0025	-35868.	125870.	16.51	17.55	17	18	1
015945-SF 23 14W 26 ADBB	730.00	73.00	3 G	A68	-98.8249	38.0249	-44720.	128418.	11.86	14.23	12	15	1
015685-PN 23 16W 35 ADBB	2500.00	473.00	3 G	A68	-99.0441	38.0106	-63865.	126951.	5.22	4.38	6	5	1
014329-SF 24 12W 17 ADBB	1025.00	224.00	3 G	A68	-98.6587	37.9657	-30238.	121747.	20.68	18.70	21	19	1
015138-SF 24 13W 5 BACD	880.00	221.00	3 G	A68	-98.7775	37.9964	-40604.	125217.	15.00	15.00	16	16	1
015682-SF 24 13W 20 BCAA	975.00	204.00	3 G	A68	-98.7799	37.9519	-40833.	120249.	17.33	12.99	18	13	1
015312-SF 24 14W 10 ADBB	690.00	90.00	3 G	A68	-98.8431	37.9812	-46335.	123549.	13.61	11.58	14	12	1
014773-SF 24 14W 22 BBCB	750.00	131.00	3 G	A68	-98.8570	37.9541	-47571.	120530.	14.61	9.83	15	10	1
015762-SF 24 14W 25 ADBB	840.00	221.00	3 G	A68	-98.8063	37.9376	-43149.	118665.	17.21	11.26	18	12	1
015761-SF 24 14W 25 BDBB	815.00	221.00	3 G	A68	-98.8155	37.9375	-43953.	118664.	16.90	10.87	17	11	1
015611-SF 24 15W 10 BABA	1225.00	203.00	3 G	A68	-98.9612	37.9853	-56651.	124074.	9.39	6.78	10	7	1
015648-SF 24 15W 27 ADBB	1080.00	120.00	3 G	A68	-98.9530	37.9378	-55969.	118765.	12.24	5.08	13	6	1

Appendix 1. Well data (cont.)

(a) Well ID, township, range, section, quarter-section	(b) Rate (gpm)	(c) Approp (ac-ft)	(d) Use code	(e) Year	(f, g) Longitude (deg)	(f, g) Latitude (deg)	(h, i) Albers x (m)	(h, i) Albers y (m)	(j, k) Grid row/col. (mi)	(j, k) Grid index row/col	(n) cell activ.
015952-ED 24 16W 12 CCBB	1220.00	150.00	3 G	A68	-99.0396	37.9742	-63505.	122887.	7.33 3.00	8 3	1
014931-ED 24 16W 15 ADBB	745.00	162.00	3 G	A68	-99.0626	37.9668	-65519.	122077.	6.95 1.71	7 2	1
015781-SF 25 14W 17 CDBC	820.00	149.00	3 G	A68	-98.8887	37.8712	-50394.	111305.	18.01 4.92	19 5	1
016540-RC 20 10W 32 ACB	450.00	71.00	3 G	A69	-98.4523	38.2705	-12163.	155707.	11.10 40.49	12 41	1
016686-BT 20 12W 5 DACB	855.00	192.00	3 G	A69	-98.6678	38.3383	-30876.	163327.	.20 34.33	1 35	1
016747-BT 20 12W 30 BCAA	780.00	182.00	3 G	A69	-98.6963	38.2858	-33372.	157485.	2.09 30.88	3 31	1
016169-SF 22 13W 12 CACB	610.00	113.00	3 G	A69	-98.7057	38.1494	-34255.	142262.	9.15 24.62	10 25	1
016032-SF 22 14W 9 BCAC	1200.00	222.00	3 G	A69	-98.8731	38.1548	-48838.	142938.	3.22 17.80	4 18	1
016594-SF 22 14W 22 BAD	44.00	47.20	2 G	A69	-98.8495	38.1279	-46796.	139924.	5.47 17.64	6 18	1
016276-PN 22 15W 13 ADBB	900.00	240.00	3 G	A69	-98.9163	38.1414	-52608.	141468.	2.48 15.41	3 16	1
016600-PN 22 15W 13 DDBB	900.00	240.00	3 G	A69	-98.9163	38.1341	-52619.	140658.	2.87 15.09	3 16	1
016238-PN 22 15W 32 CDB	1200.00	236.00	3 G	A69	-98.9982	38.0901	-59793.	135794.	2.48 9.75	3 10	1
016237-PN 22 15W 32 DBD	1200.00	240.00	3 G	A69	-98.9913	38.0919	-59191.	135995.	2.62 10.12	3 11	1
016762-SF 23 13W 27 CBBB	14.48	6.79	6 G	A69	-98.7465	38.0208	-37877.	127921.	14.74 17.36	15 18	1
016669-SF 23 13W 32 ADCC	1765.00	225.50	3 G	A69	-98.7696	38.0073	-39903.	126428.	14.68 15.81	15 16	1
016623-SF 23 13W 34 ADBB	1105.00	221.00	3 G	A69	-98.7326	38.0098	-36670.	126688.	15.80 17.48	16 18	1
016624-SF 23 14W 15 ADDC	900.00	104.00	3 G	A69	-98.8409	38.0513	-46100.	131367.	9.90 14.70	10 15	1
016137-SF 23 14W 36 ABCB	1300.00	126.00	3 G	A69	-98.8112	38.0121	-43530.	126981.	13.02 14.26	14 15	1
016578-PN 23 15W 26 DCBB	.00	101.00	3 G	A69	-98.9396	38.0181	-54737.	127726.	8.35 9.11	9 10	1
016844-PN 23 16W 24 CDBB	1200.00	240.00	3 G	A69	-99.0348	38.0324	-63035.	129376.	4.36 5.72	5 6	1
016355-PN 23 16W 25 ADBB	4800.00	960.00	3 G	A69	-99.0256	38.0251	-62238.	128562.	5.06 5.79	6 6	1
016335-PN 23 16W 35 BDBB	1100.00	233.00	3 G	A69	-99.0533	38.0106	-64668.	126958.	4.91 4.00	5 4	1
016334-PN 23 16W 35 CDBB	1100.00	240.00	3 G	A69	-99.0533	38.0033	-64675.	126149.	5.30 3.68	6 4	1
016750-SF 24 12W 14 BBBB	400.00	153.44	4 G	A69	-98.6178	37.9688	-26662.	122080.	21.89 20.56	22 21	1
016678-SF 24 13W 17 BDBB	870.00	204.00	3 G	A69	-98.7787	37.9664	-40725.	121872.	16.58 13.66	17 14	1
016200-SF 24 13W 27 BCBB	44.00	70.89	2 G	A69	-98.7460	37.9371	-37880.	118586.	19.28 13.78	20 14	1
016775-SF 25 13W 11 CBCB	475.00	106.00	3 G	A69	-98.7275	37.8881	-36293.	113110.	22.55 12.45	23 13	1
017344-BT 19 11W 28 ABCC	1225.00	234.00	3 G	A70	-98.5439	38.3731	-20101.	167183.	2.47 41.04	3 42	1
017313-BT 19 11W 28 BCBD	1000.00	228.00	3 G	A70	-98.5520	38.3713	-20798.	166984.	2.30 40.63	3 41	1
017672-BT 20 11W 32 AACC	900.00	203.00	3 G	A70	-98.5572	38.2726	-21285.	155961.	7.47 36.16	8 37	1
017670-BT 20 11W 33 CDBB	855.00	188.00	3 G	A70	-98.5481	38.2644	-20493.	155052.	8.22 36.20	9 37	1
017046-RC 21 9W 28 DDBB	775.00	198.00	3 G	A70	-98.3112	38.1912	116.	146854.	20.13 43.05	21 44	1
017047-RC 21 9W 33 ACAB	1000.00	207.00	3 G	A70	-98.3134	38.1840	-80.	146047.	20.45 42.65	21 43	1
017048-RC 21 9W 33 DDBB	1000.00	210.00	3 G	A70	-98.3111	38.1767	123.	145236.	20.92 42.44	21 43	1
017704-SF 22 13W 17 DDBB	625.00	221.00	3 G	A70	-98.7700	38.1335	-39869.	140515.	7.84 21.23	8 22	1

Appendix 1. Well data (cont.)

(a) Well ID, township, range, section, quarter-section	(b) Rate (gpm)	(c) Approp (ac-ft)	(d) Use code	(e) Year	(f, g) Longitude (deg) Latitude (deg)		(h, i) Albers x (m) Albers y (m)		(j, k) Grid row/col. (mi)		(l, m) Grid index row/col		(n) cell activ.
017705-SF 22 13W 20 ACAA	640.00	216.00	3 G	A70	-98.7711	38.1263	-39967.	139704.	8.20	20.87	9	21	1
017153-SF 22 14W 24 ADBD	825.00	82.00	3 G	A70	-98.8051	38.1255	-42932.	139641.	7.09	19.40	8	20	1
017030-SF 22 14W 34 ADBB	820.00	224.00	3 G	A70	-98.8430	38.0975	-46253.	136526.	7.33	16.60	8	17	1
017129-PN 22 15W 10 ADBB	2000.00	233.00	3 G	A70	-98.9528	38.1560	-55782.	143116.	.46	14.50	1	15	1
017017-PN 22 15W 36 BDBB	1600.00	240.00	3 G	A70	-98.9256	38.0979	-53452.	136617.	4.52	13.14	5	14	1
017085-PN 22 16W 25 DDBB	2000.00	414.00	3 G	A70	-99.0256	38.1051	-62164.	137481.	.75	9.25	1	10	1
016953-SF 23 13W 27 CDBB	1000.00	203.00	3 G	A70	-98.7418	38.0171	-37475.	127510.	15.09	17.40	16	18	1
017154-SF 23 14W 11 DDDB	280.00	49.00	3 G	A70	-98.8224	38.0593	-44483.	132260.	10.09	15.82	11	16	1
017140-PN 23 15W 6 BDBB	800.00	140.00	3 G	A70	-99.0167	38.0832	-61408.	135039.	2.23	8.68	3	9	1
016892-PN 23 16W 36 ADBB	1000.00	240.00	3 G	A70	-99.0257	38.0107	-62253.	126948.	5.84	5.16	6	6	1
017560-PN 23 16W 36 CDBB	1500.00	240.00	3 G	A70	-99.0349	38.0034	-63070.	126141.	5.92	4.46	6	5	1
017516-SF 24 12W 14 CBBA	305.00	36.00	3 G	A70	-98.6166	37.9617	-26564.	121279.	22.32	20.31	23	21	1
017473-SF 24 13W 26 AAD	100.00	28.00	3 G	A70	-98.7108	37.9384	-34807.	118714.	20.40	15.32	21	16	1
017194-SF 24 15W 17 BADA	1400.00	119.00	3 G	A70	-98.9956	37.9688	-59662.	122254.	9.12	4.62	10	5	1
016975-SF 24 15W 18 ADCB	1075.00	74.00	3 G	A70	-99.0081	37.9652	-60760.	121864.	8.89	3.94	9	4	1
017443-SF 25 13W 17 DACC	1245.00	240.00	3 G	A70	-98.7693	37.8728	-39950.	111423.	21.97	10.03	22	11	1
017146-SF 25 14W 14 CACC	1340.00	170.00	3 G	A70	-98.8335	37.8731	-45571.	111477.	19.78	7.33	20	8	1
017577-SF 25 15W 25 BCBA	1000.00	108.00	3 G	A70	-98.9288	37.8503	-53920.	108985.	17.78	2.32	18	3	1
017252-SF 25 15W 34 ADBB	990.00	221.00	3 G	A70	-98.9528	37.8358	-56033.	107381.	17.75	.68	18	1	1
018105-BT 20 11W 26 ADBB	1000.00	221.00	3 G	A71	-98.5019	38.2858	-16470.	157425.	8.61	39.06	9	40	1
018106-BT 20 11W 26 DACC	900.00	195.00	3 G	A71	-98.5019	38.2794	-16473.	156716.	8.96	38.79	9	39	1
018675-RC 21 10W 2 DDBB	730.00	195.00	3 G	A71	-98.3841	38.2496	-6232.	153371.	14.52	42.47	15	43	1
018004-SF 21 11W 5 ADBB	620.00	149.00	3 G	A71	-98.5494	38.2571	-20613.	154229.	8.58	35.83	9	36	1
018421-SF 21 13W 13 ADBC	890.00	101.00	3 G	A71	-98.6964	38.2265	-33413.	150866.	5.29	28.33	6	29	1
018388-SF 21 14W 32 BACC	1350.00	180.00	3 G	A71	-98.8892	38.1857	-50219.	146401.	1.00	18.46	2	19	1
018039-SF 22 13W 21 DBDD	800.00	221.00	3 G	A71	-98.7526	38.1198	-38361.	138976.	9.17	21.37	10	22	1
018129-SF 22 14W 14 CACC	900.00	195.00	3 G	A71	-98.8340	38.1346	-45444.	140666.	5.63	18.58	6	19	1
018003-PN 22 15W 13 CDBB	680.00	178.00	3 G	A71	-98.9255	38.1342	-53418.	140665.	2.56	14.71	3	15	1
018611-PN 22 15W 16 BDBB	1420.00	225.00	3 G	A71	-98.9805	38.1415	-58204.	141513.	.31	12.71	1	13	1
017839-PN 22 15W 26 BAD	1500.00	240.00	3 G	A71	-98.9408	38.1138	-54766.	138397.	3.15	13.19	4	14	1
018209-SF 23 12W 25 DBDD	865.00	75.00	3 G	A71	-98.5871	38.0168	-23968.	127430.	20.32	23.92	21	24	1
018270-SF 23 12W 35 DDCD	440.00	53.00	3 G	A71	-98.6030	37.9988	-25360.	125418.	20.77	22.48	21	23	1
018058-SF 23 14W 3 AACB	700.00	120.00	3 G	A71	-98.8430	38.0848	-46264.	135107.	8.02	16.05	9	17	1
018040-SF 23 14W 15 CABB	605.00	58.00	3 G	A71	-98.8524	38.0504	-47103.	131280.	9.56	14.18	10	15	1
018669-PN 23 15W 1 ABBB	780.00	221.00	3 G	A71	-98.9211	38.0870	-53071.	135397.	5.26	12.86	6	13	1

Appendix 1. Well data (cont.)

(a) Well ID, township, range, section, quarter-section	(b) Rate (gpm)	(c) Approp (ac-ft)	(d) Use code	(e) Year	(f, g) Longitude (deg)	(f, g) Latitude (deg)	(h, i) Albers x (m)	(h, i) Albers y (m)	(j, k) GrID row/col. (mi)	(l, m) GrID index row/col	(n) cell activ.
018670-PN 23 15W 1 BBDD	1000.00	214.00	3 G	A71	-98.9268	38.0842	-53572.	135095.	5.21 12.50	6 13	1
017917-PN 23 15W 8 DDBB	785.00	221.00	3 G	A71	-98.9898	38.0615	-59078.	132594.	4.31 8.87	5 9	1
017901-PN 23 15W 9 ADBB	1015.00	221.00	3 G	A71	-98.9715	38.0687	-57481.	133392.	4.54 9.95	5 10	1
018304-PN 23 15W 18 DDBB	1045.00	221.00	3 G	A71	-99.0077	38.0470	-60657.	130985.	4.49 7.49	5 8	1
018671-PN 23 15W 19 BABC	750.00	172.00	3 G	A71	-99.0166	38.0424	-61436.	130482.	4.43 6.92	5 7	1
018119-PN 23 16W 11 CCDC	350.00	82.00	3 G	A71	-99.0555	38.0587	-64815.	132325.	2.24 5.98	3 6	1
018321-PN 23 16W 26 CDBB	1000.00	240.00	3 G	A71	-99.0533	38.0178	-64660.	127768.	4.52 4.31	5 5	1
018322-PN 23 16W 36 BDBB	1200.00	240.00	3 G	A71	-99.0349	38.0106	-63059.	126947.	5.53 4.77	6 5	1
018267-SF 24 13W 6 ACB	1200.00	240.00	3 G	A71	-98.7920	37.9952	-41865.	125084.	14.58 14.34	15 15	1
017828-SF 24 13W 25 ADBB	560.00	173.00	3 G	A71	-98.6951	37.9370	-33434.	118548.	21.00 15.93	22 16	1
017829-SF 24 13W 25 BDBB	925.00	224.00	3 G	A71	-98.7044	37.9370	-34249.	118556.	20.69 15.53	21 16	1
018060-SF 24 13W 30 CDAB	925.00	195.00	3 G	A71	-98.7949	37.9303	-42155.	117845.	17.99 11.42	18 12	1
018059-SF 24 13W 31 BDBB	845.00	195.00	3 G	A71	-98.7971	37.9230	-42357.	117036.	18.31 11.02	19 12	1
017909-SF 24 14W 2 DDBB	730.00	165.00	3 G	A71	-98.8247	37.9884	-44729.	124348.	13.84 12.67	14 13	1
018183-ED 24 16W 12 ACCC	1000.00	120.00	3 G	A71	-99.0305	37.9788	-62706.	123395.	7.39 3.58	8 4	1
018278-ED 24 16W 12 CCBB	.00	120.00	3 G	A71	-99.0396	37.9742	-63505.	122887.	7.33 3.00	8 3	1
018080-SF 25 14W 29 BDBB	825.00	152.00	3 G	A71	-98.8887	37.8503	-50411.	108966.	19.14 4.02	20 5	1
017830-PR 26 14W 2 ABBA	1190.00	267.00	3 G	A71	-98.8198	37.8247	-44402.	106080.	22.85 5.82	23 6	1
017827-PR 26 15W 2 CABB	1000.00	240.00	3 G	A71	-98.9347	37.8149	-54460.	105048.	19.49 .55	20 1	1
019518-BT 19 11W 34 CCBA	650.00	122.00	3 G	A72	-98.5332	38.3504	-19173.	164645.	4.06 40.52	5 41	1
018886-BT 20 11W 32 DAAB	20.00	10.03	6 G	A72	-98.5549	38.2681	-21087.	155458.	7.80 36.07	8 37	1
019615-SF 21 12W 5 DDBB	920.00	195.00	3 G	A72	-98.6598	38.2495	-30217.	153414.	5.28 30.85	6 31	1
019482-SF 21 14W 21 ABCC	1295.00	192.00	3 G	A72	-98.8662	38.2148	-48198.	149633.	.21 20.68	1 21	1
019576-SF 22 13W 23 CDBB	840.00	176.00	3 G	A72	-98.7238	38.1188	-35849.	138856.	10.20 22.54	11 23	1
019115-PN 22 15W 3 DCDB	935.00	166.00	3 G	A72	-98.9551	38.1614	-55975.	143725.	.09 14.64	1 15	1
019427-PN 22 15W 10 BACC	1140.00	206.00	3 G	A72	-98.9620	38.1569	-56582.	143223.	.10 14.16	1 15	1
019906-PN 22 15W 28 BDBB	920.00	195.00	3 G	A72	-98.9804	38.1125	-58217.	138278.	1.88 11.47	2 12	1
019443-PN 22 15W 34 ADDD	715.00	175.00	3 G	A72	-98.9496	38.0952	-55547.	136327.	3.85 12.01	4 13	1
019024-SF 23 12W 22 BCCB	910.00	99.00	3 G	A72	-98.6364	38.0364	-28260.	129622.	17.61 22.68	18 23	1
019898-SF 23 13W 28 DDBB	965.00	156.00	3 G	A72	-98.7511	38.0172	-38284.	127522.	14.77 17.01	15 18	1
019431-SF 23 14W 29 ADBB	1200.00	229.50	3 G	A72	-98.8800	38.0253	-49532.	128488.	9.98 11.93	10 12	1
019430-SF 23 14W 29 BDBB	1200.00	240.00	3 G	A72	-98.8892	38.0253	-50333.	128497.	9.67 11.54	10 12	1
019377-PN 23 16W 2 BAAB	645.00	170.00	3 G	A72	-99.0509	38.0868	-64390.	135466.	.87 7.39	1 8	1
019168-PN 23 16W 31 CBBB	975.00	184.00	3 G	A72	-99.1313	38.0066	-71483.	126575.	2.47 .54	3 1	1
019351-PN 23 17W 25 DABB	965.00	185.00	3 G	A72	-99.1358	38.0212	-71857.	128206.	1.53 .99	2 1	1

Appendix 1. Well data (cont.)

(a) Well ID, township, range, section, quarter-section	(b) Rate (gpm)	(c) Approp (ac-ft)	(d) Use code	(e) Year	(f, g) Longitude (deg)	(f, g) Latitude (deg)	(h, i) Albers x (m)	(h, i) Albers y (m)	(j, k) GrID row/col. (mi)	(l, m) GrID index row/col	(n) cell activ.	
019029-SF 24 13W 7 AAAD	860.00	209.00	3 G	A72	-98.7845	37.9837	-41222.	123804.	15.45	14.16	16 15	1
019028-SF 24 13W 18 ADBD	1800.00	240.00	3 G	A72	-98.7869	37.9656	-41435.	121785.	16.35	13.28	17 14	1
019438-SF 24 13W 24 CDDD	865.00	224.00	3 G	A72	-98.7009	37.9415	-33942.	119060.	20.56	15.88	21 16	1
019694-SF 24 13W 30 BDBB	905.00	221.00	3 G	A72	-98.7971	37.9376	-42350.	118659.	17.52	11.64	18 12	1
018696-SF 24 13W 31 CDBB	1090.00	189.00	3 G	A72	-98.7971	37.9158	-42358.	116226.	18.70	10.71	19 11	1
019405-SF 24 13W 36 ACBB	810.00	221.00	3 G	A72	-98.6998	37.9224	-33848.	116927.	21.63	15.10	22 16	1
019429-SF 24 14W 3 ADBB	785.00	220.00	3 G	A72	-98.8432	37.9959	-46341.	125195.	12.81	12.21	13 13	1
018848-SF 24 14W 3 DDA	800.00	289.00	3 G	A72	-98.8402	37.9880	-46083.	124312.	13.34	12.00	14 12	1
018925-SF 24 14W 5 DACC	830.00	195.00	3 G	A72	-98.8800	37.9896	-49552.	124510.	11.91	10.39	12 11	1
018924-SF 24 14W 9 CACC	865.00	189.00	3 G	A72	-98.8708	37.9750	-48761.	122868.	13.01	10.15	14 11	1
019025-SF 24 14W 32 CDBB	860.00	187.00	3 G	A72	-98.8889	37.9159	-50380.	116283.	15.59	6.84	16 7	1
019151-ED 24 16W 14 BCBB	1600.00	240.00	3 G	A72	-99.0580	37.9668	-65118.	122076.	7.11	1.91	8 2	1
019923-SF 25 14W 30 DACC	945.00	209.00	3 G	A72	-98.8978	37.8439	-51211.	108261.	19.17	3.36	20 4	1
019925-SF 25 15W 25 ADBB	955.00	221.00	3 G	A72	-98.9162	37.8503	-52818.	108980.	18.21	2.85	19 3	1
019924-PR 26 14W 6 ADBB	965.00	195.00	3 G	A72	-98.8894	37.8198	-50494.	105565.	20.76	2.67	21 3	1
019922-PR 26 15W 1 BABB	965.00	195.00	3 G	A72	-98.9164	37.8247	-52850.	106129.	19.58	1.74	20 2	1
020511-BT 20 11W 27 DBCC	935.00	200.00	3 G	A73	-98.5249	38.2797	-18476.	156749.	8.17	37.83	9 38	1
021240-BT 20 11W 32 DDBB	730.00	162.00	3 G	A73	-98.5572	38.2644	-21286.	155052.	7.92	35.81	8 36	1
019985-BT 20 11W 33 DCAA	715.00	178.00	3 G	A73	-98.5401	38.2644	-19798.	155050.	8.49	36.54	9 37	1
020182-BT 20 12W 18 CCAA	800.00	234.00	3 G	A73	-98.6963	38.3076	-33363.	159912.	.91	31.82	1 32	1
021679-RC 21 9W 7 ABDD	885.00	192.00	3 G	A73	-98.3489	38.2432	-3168.	152657.	16.05	43.69	17 44	1
021135-RC 21 9W 34 BDBB	900.00	240.00	3 G	A73	-98.3019	38.1839	919.	146041.	20.84	43.13	21 44	1
021134-RC 21 9W 34 CDBB	900.00	240.00	3 G	A73	-98.3019	38.1767	924.	145232.	21.23	42.83	22 43	1
021033-SF 21 12W 15 CDBB	1200.00	240.00	3 G	A73	-98.6321	38.2204	-27816.	150154.	7.79	30.77	8 31	1
021139-SF 21 13W 6 BDBB	835.00	184.50	3 G	A73	-98.7974	38.2570	-42185.	154312.	.24	25.39	1 26	1
021140-SF 21 13W 6 CDBB	665.00	167.00	3 G	A73	-98.7975	38.2500	-42193.	153524.	.62	25.09	1 26	1
019938-SF 21 14W 25 ADBB	785.00	195.00	3 G	A73	-98.8064	38.1992	-43005.	147861.	3.06	22.52	4 23	1
019939-SF 21 14W 25 DDBB	1000.00	240.00	3 G	A73	-98.8064	38.1919	-43009.	147049.	3.46	22.21	4 23	1
020841-PN 21 15W 36 DCAA	805.00	195.00	3 G	A73	-98.9171	38.1777	-52659.	145518.	.49	16.94	1 17	1
020566-RN 22 9W 3 BCAA	730.00	201.00	3 G	A73	-98.3030	38.1694	827.	144420.	21.59	42.47	22 43	1
020181-SF 22 13W 8 CDBB	925.00	221.00	3 G	A73	-98.7792	38.1482	-40664.	142158.	6.74	21.47	7 22	1
020180-SF 22 13W 8 DACC	1110.00	193.00	3 G	A73	-98.7701	38.1490	-39864.	142243.	7.01	21.89	8 22	1
021159-SF 22 14W 1 CDBB	1000.00	240.00	3 G	A73	-98.8156	38.1628	-43826.	143802.	4.72	20.57	5 21	1
021303-SF 22 14W 5 BDA	3000.00	474.00	3 G	A73	-98.8863	38.1699	-49979.	144628.	1.96	17.90	2 18	1
020211-SF 22 14W 24 CDBB	810.00	195.00	3 G	A73	-98.8154	38.1192	-43834.	138933.	7.09	18.70	8 19	1

Appendix 1. Well data (cont.)

(a) Well ID, township, range, section, quarter-section	(b) Rate (gpm)	(c) Approp (ac-ft)	(d) Use code	(e) Year	(f, g) Longitude (deg)	(f, g) Latitude (deg)	(h, i) Albers x (m)	(h, i) Albers y (m)	(j, k) Grid row/col. (mi)	(l, m) Grid index row/col	(n) cell activ.
021172-SF 22 14W 26 CDBB	765.00	195.00	3 G	A73	-98.8338	38.1047	-45446.	137329.	7.25 17.30	8 18	1
019930-SF 22 14W 30 BDBB	1000.00	240.00	3 G	A73	-98.9073	38.1124	-51850.	138221.	4.35 14.53	5 15	1
020839-PN 22 15W 1 ACAA	740.00	195.00	3 G	A73	-98.9172	38.1704	-52668.	144708.	.88 16.62	1 17	1
020840-PN 22 15W 1 DCAA	795.00	195.00	3 G	A73	-98.9173	38.1631	-52681.	143893.	1.28 16.30	2 17	1
020816-PN 22 15W 24 CCAA	605.00	195.00	3 G	A73	-98.9265	38.1196	-53521.	139045.	3.31 14.04	4 15	1
021651-PN 22 15W 35 AACC	550.00	138.00	3 G	A73	-98.9347	38.0988	-54245.	136723.	4.16 12.80	5 13	1
019942-PN 22 15W 36 CDBB	660.00	177.00	3 G	A73	-98.9256	38.0906	-53463.	135805.	4.91 12.82	5 13	1
020221-PN 22 16W 26 DCDC	705.00	116.00	3 G	A73	-99.0462	38.1023	-63968.	137185.	.20 8.26	1 9	1
021198-SF 23 12W 16 DABB	1200.00	351.00	3 G	A73	-98.6410	38.0491	-28663.	131047.	16.76 23.03	17 24	1
020744-SF 23 13W 23 DDBB	1000.00	195.00	3 G	A73	-98.7143	38.0315	-35069.	129109.	15.24 19.18	16 20	1
021154-SF 23 13W 26 CDBB	835.00	221.00	3 G	A73	-98.7234	38.0170	-35870.	127492.	15.72 18.17	16 19	1
019961-SF 23 13W 33 BBB	500.00	79.97	2 G	A73	-98.7645	38.0132	-39453.	127084.	14.54 16.28	15 17	1
019937-SF 23 14W 20 CDBB	800.00	195.00	3 G	A73	-98.8892	38.0326	-50328.	129306.	9.28 11.85	10 12	1
020309-SF 23 14W 21 ADCC	810.00	221.00	3 G	A73	-98.8616	38.0369	-47917.	129777.	9.97 13.20	10 14	1
020308-SF 23 14W 21 DDBB	800.00	221.00	3 G	A73	-98.8616	38.0324	-47922.	129272.	10.22 13.01	11 14	1
020605-SF 23 14W 27 ADAA	605.00	189.00	3 G	A73	-98.8398	38.0250	-46023.	128433.	11.36 13.61	12 14	1
021309-SF 23 14W 36 DCC	1300.00	150.00	3 G	A73	-98.8105	38.0007	-43475.	125716.	13.66 13.80	14 14	1
019935-PN 23 15W 1 DDDA	740.00	195.00	3 G	A73	-98.9132	38.0742	-52392.	133968.	6.21 12.64	7 13	1
020980-PN 23 15W 2 BCAA	710.00	182.00	3 G	A73	-98.9452	38.0834	-55173.	135010.	4.64 11.69	5 12	1
020571-PN 23 15W 2 CDBB	1040.00	158.00	3 G	A73	-98.9441	38.0761	-55082.	134197.	5.07 11.42	6 12	1
020979-PN 23 15W 10 CCAA	695.00	160.00	3 G	A73	-98.9636	38.0615	-56797.	132580.	5.20 9.97	6 10	1
021021-PN 23 15W 12 CDDD	280.00	80.00	3 G	A73	-98.9224	38.0588	-53206.	132248.	6.74 11.59	7 12	1
021117-PN 23 15W 24 CACB	475.00	132.00	3 G	A73	-98.9259	38.0343	-53527.	129524.	7.94 10.39	8 11	1
021310-PN 23 16W 4 DDBB	550.00	147.00	3 G	A73	-99.0808	38.0759	-67006.	134260.	.45 5.66	1 6	1
020568-PN 23 16W 17 ADC	550.00	53.00	3 G	A73	-99.0987	38.0517	-68594.	131580.	1.15 3.86	2 4	1
020608-SF 24 13W 3 CACC	1145.00	312.00	3 G	A73	-98.7416	37.9889	-37466.	124360.	16.63 16.20	17 17	1
021324-SF 24 13W 4 DCAA	840.00	225.00	3 G	A73	-98.7520	37.9880	-38375.	124266.	16.32 15.72	17 16	1
020787-SF 24 13W 8 BCAA	940.00	191.00	3 G	A73	-98.7799	37.9810	-40818.	123494.	15.76 14.24	16 15	1
021333-SF 24 13W 10 CBDD	915.00	195.00	3 G	A73	-98.7426	37.9744	-37566.	122742.	17.38 15.53	18 16	1
020745-SF 24 13W 15 BDBB	895.00	195.00	3 G	A73	-98.7414	37.9662	-37468.	121832.	17.86 15.23	18 16	1
020746-SF 24 13W 15 CDBB	980.00	182.00	3 G	A73	-98.7414	37.9590	-37471.	121021.	18.25 14.92	19 15	1
021672-SF 24 13W 17 ADBB	700.00	195.00	3 G	A73	-98.7693	37.9663	-39904.	121856.	16.91 14.05	17 15	1
020424-SF 24 13W 17 DDBB	745.00	190.00	3 G	A73	-98.7693	37.9591	-39904.	121048.	17.30 13.74	18 14	1
021673-SF 24 13W 18 CDBB	1500.00	240.00	3 G	A73	-98.7971	37.9594	-42332.	121091.	16.35 12.58	17 13	1
020861-SF 24 13W 19 ADBB	1500.00	240.00	3 G	A73	-98.7880	37.9520	-41541.	120261.	17.05 12.65	18 13	1

Appendix 1. Well data (cont.)

(a) Well ID, township, range, section, quarter-section					(b) Rate (gpm)	(c) Approp (ac-ft)	(d) Use code	(e) Year	(f, g) Longitude (deg) Latitude (deg)		(h, i) Albers x (m) Albers y (m)		(j, k) Grid row/col. (mi)		(l, m) Grid index row/col		(n) cell activ.	
020121-SF	24	13W	19	BDBB	865.00	183.00	3	G	A73	-98.7971	37.9521	-42336.	120278.	16.74	12.27	17	13	1
020122-SF	24	13W	29	CDBB	900.00	195.00	3	G	A73	-98.7787	37.9302	-40745.	117828.	18.54	12.10	19	13	1
020227-SF	24	14W	11	ADBB	735.00	195.00	3	G	A73	-98.8247	37.9811	-44730.	123531.	14.24	12.36	15	13	1
020792-SF	24	14W	35	ADBB	2000.00	480.00	3	G	A73	-98.8246	37.9230	-44759.	117048.	17.38	9.86	18	10	1
020346-SF	24	14W	36	BDBB	800.00	195.00	3	G	A73	-98.8155	37.9230	-43959.	117043.	17.69	10.24	18	11	1
021203-SF	24	15W	21	CCBB	1800.00	240.00	3	G	A73	-98.9850	37.9452	-58762.	119610.	10.75	4.04	11	5	1
020845-ED	24	16W	3	BBDD	600.00	145.00	3	G	A73	-99.0728	37.9969	-66381.	125443.	4.98	2.58	5	3	1
021006-ED	24	16W	26	AACC	1145.00	210.00	3	G	A73	-99.0442	37.9387	-63941.	118925.	9.09	1.27	10	2	1
021162-ED	24	16W	35	DBDD	845.00	195.00	3	G	A73	-99.0454	37.9168	-64064.	116488.	10.23	.28	11	1	1
020798-SF	25	13W	4	BDAA	900.00	195.00	3	G	A73	-98.7566	37.9083	-38820.	115371.	20.48	12.09	21	13	1
020348-SF	25	13W	8	DCAA	800.00	221.00	3	G	A73	-98.7705	37.8866	-40047.	112956.	21.18	10.57	22	11	1
020334-SF	25	13W	16	BBDD	925.00	195.00	3	G	A73	-98.7612	37.8801	-39242.	112234.	21.84	10.69	22	11	1
020667-SF	25	13W	16	DDBB	995.00	240.00	3	G	A73	-98.7508	37.8719	-38339.	111313.	22.64	10.77	23	11	1
020347-SF	25	14W	4	ADBB	380.00	88.00	3	G	A73	-98.8612	37.9086	-47967.	115456.	16.92	7.69	17	8	1
020791-SF	25	14W	12	ADBB	1000.00	195.00	3	G	A73	-98.8062	37.8939	-43167.	113795.	19.57	9.38	20	10	1
020977-SF	25	14W	24	ADBB	790.00	195.00	3	G	A73	-98.8060	37.8648	-43170.	110548.	21.15	8.14	22	9	1
020547-SF	25	14W	24	CDBB	780.00	220.00	3	G	A73	-98.8151	37.8576	-43968.	109742.	21.24	7.44	22	8	1
020451-SF	25	14W	27	CACC	815.00	195.00	3	G	A73	-98.8518	37.8439	-47191.	108237.	20.73	5.30	21	6	1
020161-SF	25	14W	36	ADBB	800.00	240.00	3	G	A73	-98.8060	37.8358	-43183.	107307.	22.72	6.89	23	7	1
020160-SF	25	14W	36	BDBB	955.00	195.00	3	G	A73	-98.8151	37.8358	-43983.	107307.	22.42	6.50	23	7	1
020507-PR	26	15W	1	DABB	1200.00	195.00	3	G	A73	-98.9072	37.8149	-52054.	105031.	20.42	1.71	21	2	1
022728-RC	20	10W	35	DCBB	825.00	156.00	3	G	A74	-98.3965	38.2639	-7307.	154965.	13.33	42.56	14	43	1
021924-BT	20	11W	9	AACC	1200.00	240.00	3	G	A74	-98.5388	38.3303	-19669.	162400.	4.96	39.42	5	40	1
021998-BT	20	11W	33	BCAA	915.00	195.00	3	G	A74	-98.5492	38.2717	-20587.	155861.	7.79	36.46	8	37	1
023276-BT	20	12W	1	CDBB	830.00	195.00	3	G	A74	-98.6033	38.3367	-25272.	163126.	2.46	36.98	3	37	1
021931-RC	21	10W	2	BDBB	745.00	195.00	3	G	A74	-98.3934	38.2568	-7039.	154173.	13.82	42.39	14	43	1
021915-RC	21	10W	2	DDBB	.00	37.00	3	G	A74	-98.3841	38.2496	-6232.	153371.	14.52	42.47	15	43	1
022449-SF	21	12W	2	CDBB	1000.00	246.00	3	G	A74	-98.6137	38.2496	-26203.	153414.	6.82	32.80	7	33	1
022407-SF	21	12W	28	ADBB	900.00	240.00	3	G	A74	-98.6417	38.1983	-28666.	147701.	8.66	29.42	9	30	1
021775-SF	21	14W	31	ADBB	3000.00	480.00	3	G	A74	-98.8982	38.1849	-51004.	146308.	.75	18.04	1	19	1
022304-SF	21	14W	34	CDBB	1600.00	465.00	3	G	A74	-98.8524	38.1775	-47018.	145463.	2.69	19.65	3	20	1
021791-SF	22	13W	34	DCCC	815.00	195.00	3	G	A74	-98.7375	38.0871	-37059.	135323.	11.45	20.60	12	21	1
021777-SF	22	14W	7	CDBB	785.00	195.00	3	G	A74	-98.9072	38.1486	-51810.	142267.	2.40	16.10	3	17	1
022367-SF	22	14W	8	DDBB	1300.00	240.00	3	G	A74	-98.8800	38.1485	-49442.	142236.	3.33	17.24	4	18	1
021778-SF	22	14W	18	AACC	725.00	195.00	3	G	A74	-98.8982	38.1422	-51038.	141547.	3.05	16.20	4	17	1

Appendix 1. Well data (cont.)

(a) Well ID, township, range, section, quarter-section	(b) Rate (gpm)	(c) Approp (ac-ft)	(d) Use code	(e) Year	(f, g) Longitude (deg) Latitude (deg)		(h, i) Albers x (m) Albers y (m)		(j, k) Grid row/col. (mi)		(l, m) Grid index row/col		(n) cell activ.
021884-SF 22 14W 22 CACC	900.00	195.00	3	G A74	-98.8522	38.1202	-47042.	139072.	5.79	17.19	6	18	1
022256-SF 22 14W 36 BDBB	885.00	187.00	3	G A74	-98.8154	38.0974	-43848.	136504.	8.27	17.76	9	18	1
022097-PN 22 15W 10 CBDD	850.00	197.00	3	G A74	-98.9632	38.1496	-56693.	142414.	.45	13.79	1	14	1
022031-PN 22 15W 22 DDBB	275.00	72.00	3	G A74	-98.9528	38.1197	-55811.	139066.	2.42	12.94	3	13	1
021776-PN 23 15W 24 DDBB	735.00	195.00	3	G A74	-98.9167	38.0325	-52730.	129319.	8.35	10.69	9	11	1
022489-PN 23 16W 13 CDBB	670.00	195.00	3	G A74	-99.0348	38.0469	-63021.	131000.	3.57	6.35	4	7	1
021898-PN 23 16W 22 ADBB	810.00	192.00	3	G A74	-99.0625	38.0396	-65440.	130200.	3.03	4.86	4	5	1
022390-PN 23 16W 27 DDBB	800.00	192.00	3	G A74	-99.0625	38.0178	-65462.	127772.	4.20	3.92	5	4	1
022611-SF 24 12W 21 DCBB	1010.00	183.00	3	G A74	-98.6451	37.9438	-29057.	119293.	22.32	18.33	23	19	1
022934-SF 24 13W 7 DDAA	1000.00	240.00	3	G A74	-98.7846	37.9738	-41231.	122696.	15.99	13.73	16	14	1
021905-SF 24 13W 24 DDBB	1200.00	236.00	3	G A74	-98.6951	37.9442	-33432.	119359.	20.61	16.24	21	17	1
022590-SF 24 13W 35 CCAA	695.00	181.00	3	G A74	-98.7241	37.9153	-35979.	116143.	21.20	13.77	22	14	1
022007-SF 24 14W 21 ABB	2500.00	386.00	3	G A74	-98.8657	37.9554	-48328.	120687.	14.24	9.52	15	10	1
023303-ED 24 16W 12 BCBB	1220.00	141.00	3	G A74	-99.0396	37.9815	-63495.	123703.	6.94	3.32	7	4	1
021843-ED 24 16W 25 BDBB	750.00	195.00	3	G A74	-99.0351	37.9378	-63144.	118820.	9.45	1.62	10	2	1
023096-ED 24 16W 25 CDBB	1000.00	240.00	3	G A74	-99.0351	37.9305	-63148.	118011.	9.84	1.30	10	2	1
023097-ED 24 16W 35 ADBB	1000.00	240.00	3	G A74	-99.0443	37.9232	-63956.	117204.	9.92	.60	10	1	1
023250-ED 24 16W 36 ACAA	685.00	195.00	3	G A74	-99.0271	37.9232	-62455.	117188.	10.51	1.32	11	2	1
023249-ED 24 16W 36 DDBB	1000.00	240.00	3	G A74	-99.0260	37.9159	-62363.	116372.	10.94	1.06	11	2	1
022654-SF 25 13W 15 BDBB	1000.00	240.00	3	G A74	-98.7415	37.8791	-37522.	112115.	22.56	11.48	23	12	1
023055-SF 25 14W 31 BDBB	1000.00	221.00	3	G A74	-98.9069	37.8358	-52012.	107354.	19.31	2.62	20	3	1
022136-SF 25 15W 35 CDBB	1000.00	204.00	3	G A74	-98.9436	37.8285	-55228.	106570.	18.45	.76	19	1	1
023138-PR 26 15W 12 BDBB	800.00	240.00	3	G A74	-98.9164	37.8016	-52868.	103554.	20.83	.75	21	1	1
024009-BT 20 11W 3 AB BB	525.00	88.00	3	G A75	-98.5251	38.3468	-18476.	164237.	4.53	40.70	5	41	1
025175-BT 20 11W 19 CCAA	895.00	234.00	3	G A75	-98.5860	38.2932	-23779.	158266.	5.39	35.84	6	36	1
023884-BT 20 12W 3 DACC	850.00	197.00	3	G A75	-98.6310	38.3374	-27680.	163217.	1.49	35.84	2	36	1
023883-BT 20 12W 10 ADBB	785.00	167.00	3	G A75	-98.6310	38.3294	-27679.	162322.	1.92	35.50	2	36	1
023882-BT 20 12W 10 CCAA	755.00	198.00	3	G A75	-98.6413	38.3223	-28582.	161536.	1.96	34.76	2	35	1
023885-BT 20 12W 10 DDBB	740.00	198.00	3	G A75	-98.6309	38.3222	-27677.	161525.	2.31	35.20	3	36	1
024035-BT 20 12W 13 ACDC	805.00	179.00	3	G A75	-98.5963	38.3123	-24673.	160402.	4.01	36.22	5	37	1
023927-BT 20 12W 35 CCAA	935.00	203.00	3	G A75	-98.6228	38.2642	-26988.	155047.	5.73	33.05	6	34	1
023952-BT 20 13W 36 BACC	880.00	195.00	3	G A75	-98.7136	38.2723	-34884.	155975.	2.24	29.57	3	30	1
024129-RC 21 9W 28 CBAA	650.00	181.00	3	G A75	-98.3215	38.1949	-783.	147266.	19.59	42.78	20	43	1
024128-RC 21 9W 29 ADDB	670.00	155.00	3	G A75	-98.3272	38.1968	-1283.	147472.	19.29	42.61	20	43	1
023778-SF 21 12W 15 BDBB	900.00	240.00	3	G A75	-98.6320	38.2277	-27809.	150971.	7.39	31.09	8	32	1

Appendix 1. Well data (cont.)

(a) Well ID, township, range, section, quarter-section	(b) Rate (gpm)	(c) Approp (ac-ft)	(d) Use code	(e) Year	(f, g) Longitude (deg) Latitude (deg)		(h, i) Albers x (m) Albers y (m)		(j, k) Grid row/col. (mi)		(l, m) Grid index row/col		(n) cell activ.
023716-SF 21 12W 27 CDBB	1000.00	240.00	3	G A75	-98.6327	38.1910	-27881.	146875.	9.36	29.48	10	30	1
024910-SF 21 13W 31 BDBB	865.00	195.00	3	G A75	-98.7974	38.1846	-42229.	146231.	4.16	22.27	5	23	1
024860-SF 21 14W 24 DDBB	795.00	195.00	3	G A75	-98.8064	38.2065	-43000.	148673.	2.67	22.83	3	23	1
025105-SF 21 14W 32 DCBC	1620.00	240.00	3	G A75	-98.8846	38.1767	-49825.	145387.	1.65	18.26	2	19	1
024995-SF 21 14W 33 CDBB	1820.00	240.00	3	G A75	-98.8708	38.1775	-48623.	145475.	2.07	18.88	3	19	1
024927-SF 22 14W 1 ACBB	925.00	198.00	3	G A75	-98.8110	38.1701	-43423.	144614.	4.48	21.07	5	22	1
024877-SF 22 14W 4 DBC	1200.00	228.00	3	G A75	-98.8656	38.1643	-48179.	143997.	2.96	18.53	3	19	1
023612-SF 22 14W 9 CCCB	1000.00	216.00	3	G A75	-98.8754	38.1466	-49043.	142030.	3.58	17.36	4	18	1
025079-SF 22 14W 20 DDBB	1200.00	240.00	3	G A75	-98.8799	38.1195	-49459.	139001.	4.89	15.99	5	16	1
025292-SF 22 14W 21 ADBB	800.00	240.00	3	G A75	-98.8615	38.1266	-47848.	139787.	5.13	17.08	6	18	1
025078-SF 22 14W 21 CDBB	1200.00	240.00	3	G A75	-98.8707	38.1194	-48654.	138991.	5.21	16.38	6	17	1
025194-SF 22 14W 25 CDCB	525.00	63.00	3	G A75	-98.8154	38.1028	-43844.	137112.	7.97	17.99	8	18	1
025002-PN 22 15W 33 DDDC	630.00	192.00	3	G A75	-98.9691	38.0879	-57256.	135526.	3.59	10.88	4	11	1
024998-PN 22 16W 36 DCAA	665.00	173.00	3	G A75	-99.0268	38.0905	-62284.	135858.	1.49	8.57	2	9	1
024554-SF 23 12W 7 DBA	500.00	225.00	3	G A75	-98.6795	38.0636	-32011.	132680.	14.68	22.03	15	23	1
025176-SF 23 13W 5 CDBB	1000.00	240.00	3	G A75	-98.7789	38.0754	-40674.	134033.	10.69	18.35	11	19	1
024455-SF 23 13W 36 DBC	850.00	240.00	3	G A75	-98.6997	38.0038	-33805.	126006.	17.23	18.60	18	19	1
024274-SF 23 14W 7 ADBB	1000.00	228.00	3	G A75	-98.8984	38.0687	-51104.	133348.	7.01	13.03	8	14	1
024321-SF 23 14W 8 BCAA	960.00	195.00	3	G A75	-98.8904	38.0687	-50405.	133340.	7.28	13.36	8	14	1
024757-SF 23 14W 16 BDBB	865.00	221.00	3	G A75	-98.8708	38.0541	-48711.	131703.	8.73	13.56	9	14	1
024452-SF 23 14W 19 BDBB	850.00	240.00	3	G A75	-98.9076	38.0398	-51926.	130121.	8.27	11.39	9	12	1
024675-SF 23 14W 20 BDBB	1200.00	240.00	3	G A75	-98.8892	38.0398	-50322.	130112.	8.89	12.17	9	13	1
023734-PN 23 15W 4 CCAA	625.00	181.00	3	G A75	-98.9816	38.0760	-58353.	134212.	3.80	9.84	4	10	1
024954-PN 23 15W 12 BDBB	65.00	17.00	3	G A75	-98.9258	38.0688	-53492.	133366.	6.08	11.87	7	12	1
024705-PN 23 16W 9 CBDC	480.00	180.00	3	G A75	-99.0924	38.0621	-68033.	132739.	.80	4.58	1	5	1
025342-PN 23 16W 17 DACC	640.00	192.00	3	G A75	-99.0993	38.0476	-68645.	131126.	1.35	3.66	2	4	1
024586-PN 23 17W 23 ADAA	620.00	195.00	3	G A75	-99.1506	38.0395	-73133.	130254.	.05	1.15	1	2	1
024710-SF 24 12W 6 ADBB	745.00	195.00	3	G A75	-98.6772	37.9950	-31843.	125022.	18.47	19.18	19	20	1
024668-SF 24 13W 16 BDBB	950.00	198.00	3	G A75	-98.7600	37.9663	-39088.	121845.	17.23	14.45	18	15	1
024669-SF 24 13W 16 CBCC	915.00	198.00	3	G A75	-98.7646	37.9600	-39494.	121143.	17.41	13.98	18	14	1
024711-SF 24 13W 33 DDBB	965.00	195.00	3	G A75	-98.7507	37.9154	-38306.	116170.	20.29	12.65	21	13	1
024126-SF 24 14W 8 DDBB	900.00	222.00	3	G A75	-98.8800	37.9741	-49564.	122778.	12.75	9.72	13	10	1
024513-SF 24 14W 12 BABB	1200.00	212.00	3	G A75	-98.8155	37.9848	-43925.	123934.	14.35	12.90	15	13	1
024278-SF 24 14W 28 BDBB	900.00	240.00	3	G A75	-98.8707	37.9377	-48778.	118710.	15.03	8.54	16	9	1
023520-SF 24 14W 34 BBAA	925.00	221.00	3	G A75	-98.8533	37.9267	-47261.	117478.	16.21	8.81	17	9	1

Appendix 1. Well data (cont.)

(a) Well ID, township, range, section, quarter-section					(b) Rate (gpm)	(c) Approp (ac-ft)	(d) Use code	(e) Year	(f, g) Longitude (deg) Latitude (deg)		(h, i) Albers x (m) Albers y (m)		(j, k) GrID row/col. (mi)		(l, m) GrID index row/col		(n) cell activ.
025094-SF	24	14W	36	ADBB	820.00	195.00	3	G A75	-98.8063	37.9230	-43157.	117042.	18.00	10.63	18	11	1
023666-SF	24	15W	12	BCBB	840.00	195.00	3	G A75	-98.9303	37.9817	-53953.	123652.	10.63	7.93	11	8	1
024933-SF	24	15W	20	DABB	1000.00	240.00	3	G A75	-98.9897	37.9488	-59165.	120021.	10.40	4.01	11	5	1
023860-SF	24	15W	23	BDBB	1000.00	240.00	3	G A75	-98.9439	37.9524	-55164.	120397.	11.75	6.09	12	7	1
023411-SF	24	15W	31	BDBB	2400.00	480.00	3	G A75	-99.0168	37.9232	-61559.	117180.	10.86	1.76	11	2	1
024272-SF	24	15W	36	DCAA	745.00	195.00	3	G A75	-98.9173	37.9159	-52868.	116308.	14.62	5.64	15	6	1
024442-ED	24	16W	1	ABBD	750.00	150.00	3	G A75	-99.0292	37.9989	-62577.	125635.	6.35	4.50	7	5	1
023617-ED	24	16W	3	BBDD	120.00	31.00	3	G A75	-99.0728	37.9969	-66381.	125443.	4.98	2.58	5	3	1
023811-ED	24	16W	4	CACC	735.00	173.00	3	G A75	-99.0901	37.9895	-67898.	124635.	4.79	1.54	5	2	1
025037-SF	25	13W	3	DADD	905.00	233.00	3	G A75	-98.7287	37.9017	-36386.	114632.	21.77	12.99	22	13	1
023390-SF	25	13W	6	CCAA	955.00	221.00	3	G A75	-98.7982	37.9012	-42464.	114602.	19.45	10.03	20	11	1
024650-SF	25	14W	2	DDBB	1000.00	240.00	3	G A75	-98.8245	37.9012	-44763.	114618.	18.56	8.92	19	9	1
023924-SF	25	14W	28	BDBB	860.00	159.00	3	G A75	-98.8703	37.8503	-48799.	108959.	19.76	4.79	20	5	1
023925-SF	25	14W	28	CBDD	660.00	104.00	3	G A75	-98.8714	37.8439	-48900.	108247.	20.07	4.47	21	5	1
023500-SF	25	14W	31	ADBB	1000.00	221.00	3	G A75	-98.8977	37.8358	-51209.	107349.	19.62	3.01	20	4	1
024774-PR	26	14W	18	CDBB	775.00	180.00	3	G A75	-98.8982	37.7799	-51296.	101115.	22.62	.58	23	1	1
023468-PR	26	15W	11	DABB	1000.00	195.00	3	G A75	-98.9255	37.7980	-53672.	103152.	20.71	.20	21	1	1
027763-BT	20	11W	27	ADBB	890.00	151.00	3	G A76	-98.5203	38.2860	-18070.	157451.	7.99	38.29	8	39	1
026149-BT	20	11W	29	DDBB	900.00	180.00	3	G A76	-98.5573	38.2789	-21285.	156663.	7.13	36.43	8	37	1
025868-BT	20	11W	30	BCAA	725.00	189.00	3	G A76	-98.5860	38.2859	-23782.	157459.	5.79	35.53	6	36	1
027511-BT	20	11W	30	CCAA	890.00	186.00	3	G A76	-98.5860	38.2787	-23783.	156656.	6.18	35.22	7	36	1
025961-BT	20	12W	2	CDBC	510.00	23.00	3	G A76	-98.6218	38.3356	-26876.	163016.	1.89	36.16	2	37	1
026301-BT	20	12W	3	CACC	690.00	140.00	3	G A76	-98.6404	38.3375	-28489.	163227.	1.17	35.45	2	36	1
027731-BT	20	12W	25	ACBA	900.00	183.00	3	G A76	-98.5975	38.2860	-24779.	157467.	5.40	35.05	6	36	1
027801-BT	20	12W	25	CCAA	845.00	185.00	3	G A76	-98.6043	38.2788	-25379.	156666.	5.56	34.45	6	35	1
026051-BT	20	12W	25	DDBB	770.00	192.00	3	G A76	-98.5940	38.2787	-24481.	156659.	5.91	34.88	6	35	1
027802-BT	20	12W	26	DABB	815.00	186.00	3	G A76	-98.6124	38.2824	-26080.	157074.	5.09	34.26	6	35	1
026162-BT	20	12W	30	CDBB	585.00	160.00	3	G A76	-98.6951	38.2786	-33276.	156675.	2.52	30.62	3	31	1
025989-BT	20	12W	34	DDBB	985.00	186.00	3	G A76	-98.6309	38.2642	-27692.	155046.	5.46	32.70	6	33	1
027866-BT	20	12W	36	ACAA	830.00	192.00	3	G A76	-98.5951	38.2715	-24581.	155853.	6.26	34.52	7	35	1
026163-BT	20	13W	22	DCAA	875.00	180.00	3	G A76	-98.7425	38.2931	-37390.	158318.	.14	29.25	1	30	1
028067-BT	20	13W	23	ADBB	960.00	198.00	3	G A76	-98.7229	38.3004	-35682.	159118.	.40	30.39	1	31	1
026161-BT	20	13W	23	CDBB	700.00	192.00	3	G A76	-98.7322	38.2932	-36490.	158314.	.48	29.69	1	30	1
027931-BT	20	13W	26	BACC	710.00	149.00	3	G A76	-98.7322	38.2868	-36494.	157605.	.83	29.42	1	30	1
025873-BT	20	13W	34	BBDC	915.00	143.00	3	G A76	-98.7528	38.2722	-38294.	155987.	.92	27.92	1	28	1

Appendix 1. Well data (cont.)

(a) Well ID, township, range, section, quarter-section	(b) Rate (gpm)	(c) Approp (ac-ft)	(d) Use code	(e) Year	(f, g) Longitude (deg) Latitude (deg)		(h, i) Albers x (m) Albers y (m)		(j, k) GrID row/col. (mi)		(l, m) GrID index row/col		(n) cell activ.
026321-BT 20 13W 36 CACC	725.00	195.00	3 G	A76	-98.7135	38.2649	-34883.	155159.	2.64	29.26	3	30	1
027982-RC 21 9W 29 ACCC	995.00	278.00	3 G	A76	-98.3341	38.1959	-1883.	147374.	19.11	42.28	20	43	1
027525-RC 21 10W 1 CCAA	710.00	98.00	3 G	A76	-98.3760	38.2496	-5529.	153368.	14.79	42.81	15	43	1
028267-SF 21 12W 1 BDBB	2400.00	476.00	3 G	A76	-98.5952	38.2569	-24591.	154226.	7.05	33.89	8	34	1
026621-SF 21 12W 2 AACC	950.00	192.00	3 G	A76	-98.6044	38.2579	-25395.	154332.	6.69	33.55	7	34	1
026746-SF 21 12W 3 ADBB	1000.00	240.00	3 G	A76	-98.6228	38.2569	-26998.	154235.	6.12	32.73	7	33	1
026747-SF 21 12W 3 DDBB	1000.00	240.00	3 G	A76	-98.6229	38.2496	-27003.	153416.	6.51	32.41	7	33	1
026717-SF 21 12W 8 BBDD	810.00	195.00	3 G	A76	-98.6703	38.2431	-31130.	152700.	5.28	30.14	6	31	1
027306-SF 21 12W 11 ADBB	1000.00	240.00	3 G	A76	-98.6045	38.2422	-25406.	152590.	7.53	32.87	8	33	1
026562-SF 21 12W 11 CDBB	1000.00	240.00	3 G	A76	-98.6137	38.2350	-26212.	151779.	7.61	32.17	8	33	1
027800-SF 21 12W 12 DDBB	1100.00	240.00	3 G	A76	-98.5860	38.2348	-23801.	151755.	8.55	33.33	9	34	1
026476-SF 21 12W 15 DACB	1000.00	240.00	3 G	A76	-98.6230	38.2222	-27024.	150356.	7.99	31.23	8	32	1
027693-SF 21 12W 27 DDBB	1100.00	240.00	3 G	A76	-98.6235	38.1910	-27082.	146872.	9.67	29.87	10	30	1
027075-SF 21 13W 5 AACC	715.00	131.00	3 G	A76	-98.7700	38.2578	-39803.	154381.	1.12	26.57	2	27	1
025645-SF 21 13W 7 BDBB	880.00	185.00	3 G	A76	-98.7975	38.2428	-42196.	152722.	1.01	24.78	2	25	1
027509-SF 21 13W 27 BDBB	605.00	106.00	3 G	A76	-98.7427	38.1986	-37452.	147766.	5.25	25.18	6	26	1
025603-SF 21 13W 28 CDBB	720.00	189.00	3 G	A76	-98.7610	38.1916	-39056.	146987.	5.01	24.10	6	25	1
026320-SF 21 14W 11 ACA	1000.00	240.00	3 G	A76	-98.8267	38.2423	-44738.	152685.	.05	23.53	1	24	1
026516-SF 21 14W 12 BDBB	900.00	240.00	3 G	A76	-98.8158	38.2428	-43788.	152732.	.39	24.01	1	25	1
026258-SF 21 14W 13 BDBB	800.00	240.00	3 G	A76	-98.8157	38.2283	-43794.	151111.	1.18	23.38	2	24	1
026259-SF 21 14W 14 ADBB	800.00	231.00	3 G	A76	-98.8250	38.2283	-44598.	151115.	.87	22.99	1	23	1
026318-SF 21 14W 23 ACAA	820.00	195.00	3 G	A76	-98.8261	38.2137	-44703.	149494.	1.62	22.32	2	23	1
025758-SF 21 14W 24 ADBB	775.00	188.00	3 G	A76	-98.8064	38.2138	-42994.	149487.	2.28	23.15	3	24	1
025656-SF 21 14W 36 ADBB	1000.00	240.00	3 G	A76	-98.8064	38.1847	-43013.	146238.	3.85	21.89	4	22	1
026257-RN 22 10W 4 ADBB	600.00	90.00	3 G	A76	-98.4214	38.1691	-9481.	144393.	17.64	37.45	18	38	1
027399-SF 22 13W 18 CDBB	800.00	195.00	3 G	A76	-98.7973	38.1337	-42244.	140550.	6.91	20.09	7	21	1
025627-SF 22 13W 19 BDBB	675.00	165.00	3 G	A76	-98.7972	38.1265	-42243.	139739.	7.31	19.78	8	20	1
025714-SF 22 13W 20 CDBB	830.00	195.00	3 G	A76	-98.7790	38.1191	-40664.	138909.	8.32	20.22	9	21	1
027905-SF 22 13W 20 DBB	300.00	202.00	6 G	A76	-98.7739	38.1222	-40214.	139253.	8.33	20.57	9	21	1
027904-SF 22 13W 20 DDBB	800.00	158.00	3 G	A76	-98.7698	38.1190	-39858.	138889.	8.64	20.61	9	21	1
025985-SF 22 13W 25 CDBB	1000.00	195.00	3 G	A76	-98.7053	38.1042	-34248.	137221.	11.61	22.69	12	23	1
026084-SF 22 13W 29 CDBB	815.00	195.00	3 G	A76	-98.7788	38.1045	-40655.	137282.	9.11	19.60	10	20	1
026893-SF 22 13W 30 CDBB	780.00	193.00	3 G	A76	-98.7970	38.1046	-42240.	137301.	8.50	18.84	9	19	1
026105-SF 22 13W 31 AACB	495.00	87.00	3 G	A76	-98.7879	38.0991	-41453.	136683.	9.10	18.99	10	19	1
027616-SF 22 14W 14 ADBB	1000.00	240.00	3 G	A76	-98.8248	38.1409	-44638.	141368.	5.60	19.24	6	20	1

Appendix 1. Well data (cont.)

(a) Well ID, township, range, section, quarter-section	(b) Rate (gpm)	(c) Approp (ac-ft)	(d) Use code	(e) Year	(f, g) Longitude (deg)	(f, g) Latitude (deg)	(h, i) Albers x (m)	(h, i) Albers y (m)	(j, k) Grid row/col. (mi)	(l, m) Grid index row/col	(n) cell activ.
027617-SF 22 14W 14 DDBB	1000.00	240.00	3 G	A76	-98.8248	38.1337	-44643.	140556.	5.99 18.92	6 19	1
027588-SF 22 14W 15 BDBB	900.00	240.00	3 G	A76	-98.8523	38.1410	-47040.	141393.	4.66 18.08	5 19	1
026104-SF 22 14W 20 ADBB	750.00	188.00	3 G	A76	-98.8800	38.1267	-49455.	139808.	4.50 16.30	5 17	1
026151-SF 22 14W 21 BCAA	870.00	189.00	3 G	A76	-98.8719	38.1267	-48753.	139799.	4.78 16.64	5 17	1
026373-SF 22 14W 23 ADBB	930.00	195.00	3 G	A76	-98.8247	38.1264	-44643.	139746.	6.38 18.61	7 19	1
027023-SF 22 14W 23 DDBB	750.00	181.00	3 G	A76	-98.8246	38.1192	-44639.	138939.	6.78 18.31	7 19	1
026083-SF 22 14W 26 BDBB	1000.00	240.00	3 G	A76	-98.8338	38.1120	-45441.	138141.	6.86 17.61	7 18	1
026900-SF 22 14W 27 BBD	960.00	203.00	3 G	A76	-98.8539	38.1135	-47191.	138316.	6.10 16.83	7 17	1
026901-SF 22 14W 27 DDB	2600.00	690.00	3 G	A76	-98.8424	38.1043	-46197.	137286.	6.98 16.92	7 17	1
027824-SF 22 14W 28 ADBB	1000.00	240.00	3 G	A76	-98.8614	38.1121	-47847.	138171.	5.92 16.46	6 17	1
027825-SF 22 14W 28 BDBB	1000.00	240.00	3 G	A76	-98.8707	38.1122	-48658.	138182.	5.60 16.07	6 17	1
026528-PN 22 15W 2 CCBB	1800.00	237.00	3 G	A76	-98.9482	38.1632	-55373.	143923.	.23 15.01	1 16	1
026529-PN 22 15W 2 DCBB	1800.00	237.00	3 G	A76	-98.9391	38.1632	-54578.	143911.	.54 15.39	1 16	1
027957-PN 22 15W 9 DDBB	805.00	179.00	3 G	A76	-98.9713	38.1487	-57395.	142317.	.23 13.41	1 14	1
025979-PN 22 15W 13 BACC	855.00	195.00	3 G	A76	-98.9254	38.1423	-53407.	141575.	2.12 15.06	3 16	1
027844-PN 22 15W 20 ADCD	875.00	144.00	3 G	A76	-98.9885	38.1243	-58914.	139599.	.97 11.63	1 12	1
026291-PN 22 15W 25 BCAA	800.00	147.00	3 G	A76	-98.9266	38.1124	-53527.	138235.	3.70 13.72	4 14	1
026682-PN 22 15W 33 ADBB	165.00	55.00	3 G	A76	-98.9713	38.0979	-57440.	136642.	2.97 11.22	3 12	1
026448-SF 23 11W 7 BDBB	850.00	240.00	3 G	A76	-98.5771	38.0667	-23082.	132996.	17.96 26.49	18 27	1
026507-SF 23 11W 9 ADBB	900.00	240.00	3 G	A76	-98.5313	38.0668	-19085.	132989.	19.50 28.42	20 29	1
025801-SF 23 11W 16 CBDC	1000.00	240.00	3 G	A76	-98.5427	38.0458	-20087.	130654.	20.25 27.04	21 28	1
026789-SF 23 13W 13 BDBB	745.00	195.00	3 G	A76	-98.7052	38.0533	-34260.	131539.	14.37 20.51	15 21	1
026462-SF 23 14W 3 BDBB	745.00	169.00	3 G	A76	-98.8523	38.0830	-47071.	134914.	7.80 15.58	8 16	1
027988-SF 23 14W 4 CDBB	1100.00	240.00	3 G	A76	-98.8708	38.0758	-48690.	134124.	7.56 14.50	8 15	1
026079-SF 23 14W 7 BDBB	1250.00	240.00	3 G	A76	-98.9075	38.0688	-51901.	133355.	6.70 12.64	7 13	1
027072-SF 23 14W 13 CDBB	850.00	212.00	3 G	A76	-98.8156	38.0466	-43896.	130833.	11.01 15.56	12 16	1
026966-SF 23 14W 19 CDBB	900.00	240.00	3 G	A76	-98.9076	38.0326	-51931.	129316.	8.66 11.08	9 12	1
027419-SF 23 14W 20 DABC	820.00	188.00	3 G	A76	-98.8800	38.0352	-49524.	129598.	9.44 12.36	10 13	1
027418-SF 23 14W 21 CDBB	900.00	212.00	3 G	A76	-98.8708	38.0325	-48724.	129285.	9.90 12.62	10 13	1
026582-SF 23 14W 24 BDBB	885.00	195.00	3 G	A76	-98.8156	38.0393	-43903.	130025.	11.40 15.25	12 16	1
026500-SF 23 14W 24 CDB	700.00	56.00	3 G	A76	-98.8151	38.0316	-43861.	129165.	11.83 14.94	12 15	1
027987-SF 23 14W 25 CDBB	1100.00	240.00	3 G	A76	-98.8158	38.0176	-43928.	127597.	12.57 14.30	13 15	1
026106-SF 23 14W 34 CDDC	750.00	88.00	3 G	A76	-98.8502	38.0006	-46942.	125718.	12.32 12.12	13 13	1
027456-PN 23 15W 1 CBBB	690.00	195.00	3 G	A76	-98.9303	38.0797	-53876.	134588.	5.34 12.16	6 13	1
026147-PN 23 15W 4 DCAA	825.00	182.00	3 G	A76	-98.9726	38.0760	-57568.	134204.	4.11 10.22	5 11	1

Appendix 1. Well data (cont.)

(a) Well ID, township, range, section, quarter-section	(b) Rate (gpm)	(c) Approp (ac-ft)	(d) Use code	(e) Year	(f, g) Longitude (deg)	(f, g) Latitude (deg)	(h, i) Albers x (m)	(h, i) Albers y (m)	(j, k) Grid row/col. (mi)	(l, m) Grid index row/col	(n) cell activ.
025453-PN 23 15W 18 CDBB	920.00	180.00	3 G	A76	-99.0166	38.0469	-61432.	130988.	4.19 7.11	5 8	1
025845-PN 23 15W 25 ADBB	625.00	183.00	3 G	A76	-98.9168	38.0253	-52737.	128515.	8.74 10.38	9 11	1
025846-PN 23 15W 25 DDBB	720.00	195.00	3 G	A76	-98.9168	38.0181	-52743.	127711.	9.12 10.07	10 11	1
028185-PN 23 15W 31 DCCC	675.00	195.00	3 G	A76	-99.0126	38.0007	-61121.	125826.	6.82 5.28	7 6	1
026598-PN 23 16W 12 ABDD	570.00	162.00	3 G	A76	-99.0268	38.0696	-62304.	133522.	2.62 7.66	3 8	1
025866-PN 23 16W 20 BCDB	1095.00	227.00	3 G	A76	-99.1106	38.0376	-69647.	130018.	1.50 2.75	2 3	1
025406-PN 23 16W 36 DDBB	800.00	125.00	3 G	A76	-99.0258	38.0034	-62269.	126140.	6.23 4.85	7 5	1
026018-PN 23 17W 26 ADDD	785.00	177.00	3 G	A76	-99.1507	38.0222	-73154.	128323.	.98 .40	1 1	1
028046-PN 23 17W 36 ADBB	690.00	152.00	3 G	A76	-99.1359	38.0103	-71877.	126985.	2.12 .51	3 1	1
025788-SF 24 12W 17 BAC	.00	198.00	3 G	A76	-98.6672	37.9672	-30983.	121911.	20.31 18.40	21 19	1
026187-SF 24 12W 21 BDBB	1000.00	240.00	3 G	A76	-98.6496	37.9511	-29449.	120111.	21.78 18.46	22 19	1
026688-SF 24 13W 2 ACB	2000.00	388.00	3 G	A76	-98.7180	37.9947	-35409.	125006.	17.10 17.44	18 18	1
025596-SF 24 13W 8 ADBB	1105.00	195.00	3 G	A76	-98.7694	37.9808	-39899.	123476.	16.12 14.68	17 15	1
026810-SF 24 13W 20 CDD	900.00	228.00	3 G	A76	-98.7758	37.9424	-40482.	119190.	17.98 12.75	18 13	1
027146-SF 24 14W 1 CDCB	500.00	18.00	3 G	A76	-98.8155	37.9866	-43924.	124138.	14.25 12.98	15 13	1
025859-SF 24 14W 8 CDBB	760.00	106.00	3 G	A76	-98.8891	37.9742	-50358.	122789.	12.44 9.34	13 10	1
026049-SF 24 14W 14 CDBB	1000.00	240.00	3 G	A76	-98.8339	37.9593	-45547.	121100.	15.11 11.03	16 12	1
026153-SF 24 14W 25 CDBB	880.00	195.00	3 G	A76	-98.8155	37.9303	-43957.	117853.	17.30 10.55	18 11	1
026756-SF 24 15W 27 CDBB	900.00	216.00	3 G	A76	-98.9620	37.9305	-56764.	117957.	12.32 4.38	13 5	1
025809-SF 24 15W 28 BCBB	1500.00	240.00	3 G	A76	-98.9850	37.9378	-58762.	118792.	11.15 3.73	12 4	1
025811-SF 24 15W 28 CCBB	1500.00	218.00	3 G	A76	-98.9849	37.9305	-58763.	117969.	11.55 3.41	12 4	1
025810-SF 24 15W 29 ADBB	1000.00	240.00	3 G	A76	-98.9896	37.9378	-59165.	118794.	10.99 3.54	11 4	1
027396-ED 24 16W 4 BDBB	1000.00	195.00	3 G	A76	-99.0901	37.9959	-67898.	125346.	4.45 1.81	5 2	1
027397-ED 24 16W 5 ACAA	1000.00	195.00	3 G	A76	-99.1005	37.9959	-68800.	125349.	4.10 1.37	5 2	1
025910-ED 24 16W 5 CACC	795.00	195.00	3 G	A76	-99.1084	37.9894	-69495.	124638.	4.18 .76	5 1	1
027398-ED 24 16W 8 CACC	980.00	195.00	3 G	A76	-99.1083	37.9749	-69506.	123015.	4.96 .14	5 1	1
025971-ED 24 16W 11 CBDD	865.00	195.00	3 G	A76	-99.0545	37.9750	-64807.	122992.	6.78 2.41	7 3	1
025514-ED 24 16W 12 ADBB	850.00	233.00	3 G	A76	-99.0260	37.9816	-62307.	123701.	7.40 3.89	8 4	1
025621-ED 24 16W 16 ACAA	930.00	195.00	3 G	A76	-99.0821	37.9667	-67220.	122086.	6.29 .89	7 1	1
025637-SF 25 13W 7 BDBB	1035.00	195.00	3 G	A76	-98.7970	37.8939	-42366.	113788.	19.89 9.77	20 10	1
025473-SF 25 13W 8 CDBB	1000.00	240.00	3 G	A76	-98.7786	37.8866	-40755.	112964.	20.91 10.23	21 11	1
026015-SF 25 13W 10 ADBB	1200.00	231.00	3 G	A76	-98.7322	37.8936	-36695.	113726.	22.10 12.49	23 13	1
025638-SF 25 13W 16 ABDD	1050.00	195.00	3 G	A76	-98.7520	37.8801	-38433.	112227.	22.16 11.08	23 12	1
025692-SF 25 13W 19 ADBB	1000.00	231.00	3 G	A76	-98.7877	37.8648	-41565.	110533.	21.78 8.91	22 9	1
025693-SF 25 13W 19 BDBB	785.00	195.00	3 G	A76	-98.7969	37.8648	-42369.	110542.	21.46 8.52	22 9	1

Appendix 1. Well data (cont.)

(a) Well ID, township, range, section, quarter-section	(b) Rate (gpm)	(c) Approp (ac-ft)	(d) Use code	(e) Year	(f, g) Longitude (deg)	(f, g) Latitude (deg)	(h, i) Albers x (m)	(h, i) Albers y (m)	(j, k) GrID row/col. (mi)	(l, m) GrID index row/col	(n) cell activ.
026225-SF 25 13W 19 CACC	1100.00	195.00	3 G	A76	-98.7968	37.8585	-42368.	109832.	21.81 8.25	22 9	1
027032-SF 25 14W 2 CDBB	1000.00	240.00	3 G	A76	-98.8337	37.9013	-45567.	114625.	18.25 8.53	19 9	1
026344-SF 25 14W 15 DDBB	995.00	195.00	3 G	A76	-98.8427	37.8722	-46375.	111383.	19.52 6.90	20 7	1
025694-SF 25 14W 24 DDBB	900.00	195.00	3 G	A76	-98.8060	37.8576	-43171.	109737.	21.55 7.82	22 8	1
025520-SF 25 14W 30 BDBB	980.00	180.00	3 G	A76	-98.9070	37.8503	-52016.	108975.	18.52 3.24	19 4	1
025519-SF 25 14W 32 DDBB	915.00	195.00	3 G	A76	-98.8793	37.8284	-49608.	106522.	20.64 3.47	21 4	1
026894-SF 25 15W 17 ADBB	3200.00	960.00	3 G	A76	-98.9896	37.8795	-59215.	112281.	14.14 1.01	15 2	1
026398-SF 25 15W 21 BDBB	1800.00	480.00	3 G	A76	-98.9804	37.8648	-58425.	110638.	15.25 .77	16 1	1
026152-SF 25 15W 25 DCBB	915.00	195.00	3 G	A76	-98.9207	37.8430	-53214.	108170.	18.45 2.35	19 3	1
028044-ED 25 16W 1 CDBB	1000.00	240.00	3 G	A76	-99.0352	37.9013	-63182.	114748.	11.42 .04	12 1	1
026094-PR 26 14W 4 BACC	1175.00	198.00	3 G	A76	-98.8623	37.8211	-48117.	105697.	21.61 3.87	22 4	1
026853-PR 26 14W 5 AACC	1000.00	276.00	3 G	A76	-98.8714	37.8211	-48915.	105698.	21.30 3.49	22 4	1
025521-PR 26 14W 5 BABB	1000.00	201.00	3 G	A76	-98.8804	37.8247	-49706.	106102.	20.80 3.26	21 4	1
027245-PR 26 14W 7 BDBB	900.00	180.00	3 G	A76	-98.8983	37.8017	-51282.	103550.	21.44 1.52	22 2	1
026095-PR 26 15W 1 AABB	1125.00	201.00	3 G	A76	-98.9072	37.8247	-52044.	106123.	19.89 2.13	20 3	1
028493-BT 19 11W 19 BDD	1000.00	94.90	3 G	A77	-98.5824	38.3848	-23433.	168495.	.55 39.93	1 40	1
030299-RC 20 10W 29 CAC	1300.00	248.00	3 G	A77	-98.4555	38.2796	-12432.	156726.	10.51 40.75	11 41	1
028364-BT 20 11W 5 ABDC	1800.00	234.00	3 G	A77	-98.5595	38.3443	-21463.	163969.	3.51 39.15	4 40	1
028944-BT 20 11W 11 ACAA	690.00	195.00	3 G	A77	-98.5030	38.3288	-16559.	162221.	6.25 40.86	7 41	1
028436-BT 20 11W 19 ACDD	705.00	189.00	3 G	A77	-98.5768	38.2977	-22980.	158766.	5.46 36.42	6 37	1
029384-BT 20 11W 33 DDAA	785.00	155.00	3 G	A77	-98.5355	38.2644	-19401.	155048.	8.64 36.73	9 37	1
030874-BT 20 12W 1 ACBA	720.00	158.00	3 G	A77	-98.5975	38.3439	-24764.	163929.	2.26 37.53	3 38	1
028437-BT 20 12W 24 DDBB	715.00	189.00	3 G	A77	-98.5940	38.2932	-24478.	158271.	5.12 35.50	6 36	1
030962-BT 20 13W 24 ACAA	845.00	195.00	3 G	A77	-98.7055	38.3004	-34171.	159109.	.99 31.12	1 32	1
028359-BT 20 13W 25 ACAD	895.00	201.00	3 G	A77	-98.7055	38.2850	-34178.	157391.	1.82 30.46	2 31	1
030303-RC 21 9W 27 DACB	815.00	203.00	3 G	A77	-98.2928	38.1929	1718.	147043.	20.66 43.90	21 44	1
029463-RC 21 9W 35 BCAB	690.00	113.00	3 G	A77	-98.2859	38.1839	2321.	146036.	21.38 43.81	22 44	1
028807-RC 21 10W 1 BDBB	850.00	233.00	3 G	A77	-98.3750	38.2567	-5435.	154160.	14.44 43.16	15 44	1
031015-RC 21 10W 3 CACD	925.00	247.50	3 G	A77	-98.4108	38.2505	-8552.	153474.	13.58 41.39	14 42	1
030355-SF 21 12W 5 AACC	1000.00	97.50	3 G	A77	-98.6597	38.2577	-30204.	154332.	4.84 31.21	5 32	1
029385-SF 21 12W 11 BDBB	900.00	240.00	3 G	A77	-98.6137	38.2423	-26207.	152596.	7.22 32.49	8 33	1
028820-SF 21 12W 14 CACC	875.00	198.00	3 G	A77	-98.6139	38.2213	-26230.	150251.	8.35 31.58	9 32	1
028819-SF 21 12W 23 ABDD	810.00	195.00	3 G	A77	-98.6059	38.2139	-25537.	149429.	9.02 31.60	10 32	1
028818-SF 21 12W 23 BDBA	900.00	195.00	3 G	A77	-98.6128	38.2130	-26140.	149330.	8.83 31.27	9 32	1
028822-SF 21 12W 23 DBCC	900.00	201.00	3 G	A77	-98.6094	38.2066	-25846.	148608.	9.30 31.13	10 32	1

Appendix 1. Well data (cont.)

(a) Well ID, township, range, section, quarter-section	(b) Rate (gpm)	(c) Approp (ac-ft)	(d) Use code	(e) Year	(f, g) Longitude (deg)	(f, g) Latitude (deg)	(h, i) Albers x (m)	(h, i) Albers y (m)	(j, k) Grid row/col. (mi)	(l, m) Grid index row/col	(n) cell activ.
028821-SF 21 12W 26 BABA	760.00	195.00	3 G	A77	-98.6129	38.2020	-26154.	148098.	9.43 30.79	10 31	1
030697-SF 21 14W 13 ADBB	1000.00	240.00	3 G	A77	-98.8064	38.2283	-42987.	151106.	1.49 23.77	2 24	1
029947-SF 21 14W 22 DACC	765.00	195.00	3 G	A77	-98.8432	38.2074	-46202.	148795.	1.38 21.33	2 22	1
030458-SF 21 14W 23 DDBB	1200.00	240.00	3 G	A77	-98.8249	38.2065	-44607.	148681.	2.05 22.06	3 23	1
029269-SF 21 14W 28 ADBB	900.00	227.00	3 G	A77	-98.8616	38.1993	-47804.	147904.	1.20 20.21	2 21	1
029270-SF 21 14W 33 BCB	1200.00	120.00	3 G	A77	-98.8754	38.1848	-49019.	146288.	1.52 19.00	2 19	1
030431-RN 22 10W 4 CDBB	575.00	86.00	3 G	A77	-98.4305	38.1617	-10279.	143566.	17.74 36.75	18 37	1
030415-RN 22 10W 5 DDBB	1000.00	240.00	3 G	A77	-98.4398	38.1616	-11089.	143559.	17.43 36.36	18 37	1
030763-SF 22 12W 25 DCC	350.00	23.00	3 G	A77	-98.5904	38.1011	-24224.	136836.	15.65 27.40	16 28	1
028867-SF 22 13W 2 CAC	1200.00	200.00	3 G	A77	-98.7236	38.1635	-35807.	143844.	7.79 24.47	8 25	1
029067-SF 22 13W 3 DCCC	810.00	132.00	3 G	A77	-98.7380	38.1596	-37066.	143406.	7.52 23.69	8 24	1
029788-SF 22 13W 4 AACB	1000.00	156.00	3 G	A77	-98.7519	38.1714	-38268.	144735.	6.41 23.62	7 24	1
031102-SF 22 13W 10 DCAA	1500.00	240.00	3 G	A77	-98.7344	38.1478	-36757.	142091.	8.27 23.34	9 24	1
029417-SF 22 13W 20 BDBB	790.00	195.00	3 G	A77	-98.7792	38.1264	-40672.	139720.	7.92 20.53	8 21	1
028869-SF 22 13W 24 CCA	1200.00	200.00	3 G	A77	-98.7071	38.1183	-34398.	138794.	10.78 23.22	11 24	1
030652-SF 22 14W 7 BDBB	1000.00	225.00	3 G	A77	-98.9071	38.1558	-51802.	143075.	2.01 16.42	3 17	1
028592-SF 22 14W 8 ACBB	1600.00	240.00	3 G	A77	-98.8846	38.1558	-49837.	143052.	2.78 17.36	3 18	1
029811-SF 22 14W 11 BCAA	775.00	180.00	3 G	A77	-98.8351	38.1555	-45531.	143002.	4.46 19.43	5 20	1
029455-PN 22 15W 14 ACDA	700.00	117.00	3 G	A77	-98.9358	38.1396	-54309.	141279.	1.92 14.51	2 15	1
029271-PN 22 15W 16 CDBB	620.00	103.00	3 G	A77	-98.9805	38.1342	-58213.	140705.	.70 12.40	1 13	1
030086-PN 22 15W 28 CBC	800.00	198.00	3 G	A77	-98.9844	38.1065	-58575.	137618.	2.06 11.04	3 12	1
029334-SF 23 13W 13 ADBB	1100.00	240.00	3 G	A77	-98.6960	38.0533	-33456.	131533.	14.68 20.89	15 21	1
029825-SF 23 13W 26 BACC	800.00	195.00	3 G	A77	-98.7235	38.0252	-35872.	128403.	15.27 18.52	16 19	1
030385-SF 23 13W 27 ADBB	800.00	192.00	3 G	A77	-98.7327	38.0243	-36672.	128309.	15.01 18.10	16 19	1
028568-SF 23 13W 29 DDDD	1205.00	180.00	3 G	A77	-98.7662	38.0146	-39606.	127238.	14.40 16.26	15 17	1
028679-SF 23 14W 6 DDBB	1000.00	240.00	3 G	A77	-98.8984	38.0760	-51099.	134157.	6.62 13.34	7 14	1
028508-SF 23 14W 8 ACAA	860.00	195.00	3 G	A77	-98.8812	38.0686	-49602.	133328.	7.60 13.75	8 14	1
029631-PN 23 15W 3 CCAA	775.00	195.00	3 G	A77	-98.9635	38.0760	-56778.	134201.	4.42 10.60	5 11	1
028625-PN 23 15W 8 ADBB	710.00	178.00	3 G	A77	-98.9896	38.0687	-59059.	133404.	3.93 9.19	4 10	1
029633-PN 23 15W 9 BDBB	1200.00	240.00	3 G	A77	-98.9805	38.0687	-58269.	133399.	4.23 9.57	5 10	1
029186-PN 23 15W 23 ABAA	535.00	90.00	3 G	A77	-98.9362	38.0434	-54419.	130538.	7.10 10.34	8 11	1
029185-PN 23 15W 23 DCAA	675.00	173.00	3 G	A77	-98.9362	38.0325	-54426.	129330.	7.69 9.87	8 10	1
029135-PN 23 15W 26 CDBB	580.00	195.00	3 G	A77	-98.9442	38.0181	-55138.	127729.	8.19 8.92	9 9	1
029632-PN 23 16W 24 ADBB	1200.00	240.00	3 G	A77	-99.0256	38.0397	-62224.	130184.	4.28 6.42	5 7	1
030172-PN 23 16W 30 CCBC	770.00	239.00	3 G	A77	-99.1313	38.0167	-71467.	127694.	1.93 .98	2 1	1

Appendix 1. Well data (cont.)

	(a)				(b)	(c)	(d)	(e)	(f, g)		(h, i)		(j, k)		(l, m)		(n)		
	Well ID, township, range, section, quarter-section				Rate (gpm)	Approp (ac-ft)	Use code	Year	Longitude (deg)	Latitude (deg)	Albers x (m)	Albers y (m)	GrID row/col. (mi)		GrID index row/col		cell activ.		
	030407-PN	23	16W	34	CCAA	735.00	183.00	3	G	A77	-99.0728	38.0032	-66375.	126152.	4.64	2.86	5	3	1
	028388-SF	24	13W	36	DDBB	750.00	165.00	3	G	A77	-98.6951	37.9151	-33445.	116105.	22.19	14.98	23	15	1
	028768-SF	24	14W	31	BDBB	1000.00	240.00	3	G	A77	-98.9071	37.9232	-51972.	117109.	14.58	6.38	15	7	1
	028312-SF	24	15W	31	DDBB	900.00	240.00	3	G	A77	-99.0077	37.9160	-60770.	116366.	11.56	1.83	12	2	1
	029937-ED	24	16W	4	DDBB	850.00	126.00	3	G	A77	-99.0809	37.9887	-67095.	124532.	5.15	1.89	6	2	1
	030171-ED	24	16W	5	BDBB	915.00	195.00	3	G	A77	-99.1084	37.9958	-69493.	125351.	3.83	1.04	4	2	1
	028495-ED	24	16W	13	DBCC	1200.00	195.00	3	G	A77	-99.0306	37.9606	-62726.	121367.	8.37	2.79	9	3	1
	030453-ED	24	16W	24	BDBB	1000.00	240.00	3	G	A77	-99.0351	37.9524	-63133.	120452.	8.66	2.25	9	3	1
	031021-ED	24	16W	35	BDBB	.00	120.00	3	G	A77	-99.0534	37.9232	-64759.	117207.	9.61	.21	10	1	1
	031020-ED	24	16W	35	BDBB	1200.00	120.00	3	G	A77	-99.0534	37.9232	-64759.	117207.	9.61	.21	10	1	1
	030194-SF	25	15W	20	DBBB	865.00	204.00	3	G	A77	-98.9943	37.8611	-59641.	110241.	14.97	.03	15	1	1
	029953-SF	25	15W	26	DDCC	1500.00	240.00	3	G	A77	-98.9344	37.8402	-54418.	107871.	18.13	1.65	19	2	1
	029954-SF	25	15W	36	CCB	800.00	120.00	3	G	A77	-98.9292	37.8281	-53968.	106509.	18.97	1.35	19	2	1
	031251-BT	20	12W	13	CACC	645.00	145.00	3	G	A78	-98.6032	38.3086	-25274.	159999.	3.98	35.78	4	36	1
641	031418-BT	20	12W	31	BDBB	700.00	178.00	3	G	A78	-98.6951	38.2713	-33279.	155863.	2.91	30.31	3	31	1
	032253-SF	21	12W	1	ACAA	990.00	201.00	3	G	A78	-98.5871	38.2569	-23885.	154223.	7.32	34.24	8	35	1
	031196-SF	21	14W	1	DDB	2200.00	480.00	3	G	A78	-98.8060	38.2496	-42934.	153483.	.36	24.71	1	25	1
	032179-SF	21	14W	12	DDBB	1000.00	240.00	3	G	A78	-98.8065	38.2355	-42986.	151916.	1.10	24.08	2	25	1
	032463-SF	21	14W	15	ACAA	720.00	169.00	3	G	A78	-98.8444	38.2283	-46293.	151131.	.21	22.18	1	23	1
	031303-SF	21	14W	22	CDBB	1000.00	240.00	3	G	A78	-98.8524	38.2066	-46999.	148707.	1.12	20.91	2	21	1
	032122-SF	22	13W	25	BDBB	915.00	195.00	3	G	A78	-98.7054	38.1115	-34249.	138033.	11.21	23.00	12	24	1
	031294-SF	22	13W	26	ADBB	1000.00	240.00	3	G	A78	-98.7146	38.1116	-35049.	138042.	10.90	22.62	11	23	1
	031344-SF	22	13W	28	CDBB	865.00	195.00	3	G	A78	-98.7605	38.1044	-39056.	137258.	9.74	20.37	10	21	1
	032365-SF	22	14W	16	DDBB	1100.00	240.00	3	G	A78	-98.8616	38.1338	-47847.	140594.	4.74	17.39	5	18	1
	031946-PN	22	15W	15	CBCB	535.00	120.00	3	G	A78	-98.9667	38.1360	-57011.	140898.	1.07	13.06	2	14	1
	031217-PN	22	15W	16	DDBB	.00	120.00	3	G	A78	-98.9713	38.1342	-57414.	140699.	1.01	12.78	2	13	1
	031216-PN	22	15W	16	DDBB	1200.00	120.00	3	G	A78	-98.9713	38.1342	-57414.	140699.	1.01	12.78	2	13	1
	032016-PN	22	15W	34	CCAA	710.00	138.00	3	G	A78	-98.9634	38.0906	-56754.	135828.	3.63	11.24	4	12	1
	032015-PN	22	15W	35	CCAA	850.00	171.00	3	G	A78	-98.9451	38.0906	-55159.	135820.	4.25	12.01	5	13	1
	031830-PN	22	15W	35	DACC	.00	63.00	3	G	A78	-98.9348	38.0915	-54259.	135913.	4.55	12.48	5	13	1
031622-PN	22	15W	35	DACC	720.00	65.00	3	G	A78	-98.9348	38.0915	-54259.	135913.	4.55	12.48	5	13	1	
031436-SF	23	12W	22	CAD	1300.00	212.00	3	G	A78	-98.6289	38.0322	-27611.	129155.	18.08	22.82	19	23	1	
032151-SF	23	13W	32	ACCC	655.00	132.00	3	G	A78	-98.7742	38.0073	-40308.	126433.	14.53	15.61	15	16	1	
031733-SF	23	13W	34	CACA	600.00	30.00	3	G	A78	-98.7406	38.0044	-37375.	126088.	15.82	16.90	16	17	1	
032087-SF	23	14W	6	CDBB	600.00	144.00	3	G	A78	-98.9075	38.0760	-51894.	134166.	6.31	12.96	7	13	1	

Appendix 1. Well data (cont.)

(a) Well ID, township, range, section, quarter-section	(b) Rate (gpm)	(c) Approp (ac-ft)	(d) Use code	(e) Year	(f, g) Longitude (deg)	(f, g) Latitude (deg)	(h, i) Albers x (m)	(h, i) Albers y (m)	(j, k) GrID row/col. (mi)	(l, m) GrID index row/col	(n) cell activ.
032316-SF 23 14W 17 DDBB	1200.00	233.00	3 G	A78	-98.8800	38.0469	-49517.	130906.	8.81 12.86	9 13	1
031681-SF 23 14W 28 BACB	250.00	69.00	3 G	A78	-98.8708	38.0270	-48727.	128679.	10.20 12.39	11 13	1
031454-PN 23 15W 21 ABDD	400.00	89.00	3 G	A78	-98.9729	38.0406	-57621.	130255.	6.01 8.68	7 9	1
031458-PN 23 15W 21 DCAA	400.00	97.50	3 G	A78	-98.9729	38.0325	-57629.	129348.	6.45 8.33	7 9	1
031749-PN 23 15W 25 BDBC	495.00	136.00	3 G	A78	-98.9259	38.0244	-53533.	128419.	8.48 9.96	9 10	1
032106-PN 23 15W 26 DDBB	780.00	120.00	3 G	A78	-98.9350	38.0181	-54337.	127724.	8.51 9.30	9 10	1
032028-PN 23 15W 36 BDAA	550.00	121.00	3 G	A78	-98.9225	38.0109	-53245.	126909.	9.32 9.52	10 10	1
031425-PN 23 16W 8 ADAA	655.00	167.00	3 G	A78	-99.0958	38.0685	-68325.	133449.	.34 4.71	1 5	1
031623-PN 23 16W 11 BCAB	1000.00	240.00	3 G	A78	-99.0555	38.0686	-64804.	133438.	1.70 6.41	2 7	1
031430-PN 23 16W 23 BDBB	725.00	198.00	3 G	A78	-99.0533	38.0396	-64637.	130199.	3.34 5.25	4 6	1
031428-PN 23 16W 23 CCAA	725.00	198.00	3 G	A78	-99.0544	38.0324	-64743.	129389.	3.69 4.89	4 5	1
031429-PN 23 16W 23 DACC	645.00	198.00	3 G	A78	-99.0440	38.0333	-63837.	129483.	4.00 5.37	4 6	1
031972-PN 23 16W 36 DDBB	100.00	70.00	3 G	A78	-99.0258	38.0034	-62269.	126140.	6.23 4.85	7 5	1
032393-PN 23 17W 23 DDAA	410.00	121.00	3 G	A78	-99.1506	38.0322	-73142.	129444.	.44 .84	1 1	1
031556-SF 24 12W 19 CCC	950.00	234.00	3 G	A78	-98.6899	37.9419	-32978.	119100.	20.91 16.36	21 17	1
031318-SF 24 13W 26 AAD	500.00	26.00	3 G	A78	-98.7108	37.9384	-34807.	118714.	20.40 15.32	21 16	1
032348-SF 24 13W 28 ACBB	1380.00	150.00	3 G	A78	-98.7553	37.9372	-38692.	118602.	18.96 13.40	19 14	1
032530-SF 24 13W 28 DDBB	1200.00	240.00	3 G	A78	-98.7506	37.9300	-38291.	117789.	19.51 13.28	20 14	1
031157-SF 24 14W 2 BDBB	1065.00	195.00	3 G	A78	-98.8341	37.9959	-45538.	125183.	13.12 12.60	14 13	1
032415-SF 24 15W 2 ADBB	920.00	195.00	3 G	A78	-98.9350	37.9964	-54350.	125292.	9.68 8.36	10 9	1
031392-SF 24 15W 30 CDBB	1000.00	234.00	3 G	A78	-99.0169	37.9305	-61555.	117992.	10.46 2.07	11 3	1
031201-SF 25 13W 10 CCAA	835.00	195.00	3 G	A78	-98.7427	37.8864	-37616.	112928.	22.13 11.74	23 12	1
031535-SF 25 14W 1 ADBB	1000.00	240.00	3 G	A78	-98.8063	37.9085	-43163.	115420.	18.79 10.01	19 11	1
031200-SF 25 14W 1 BBD	1200.00	240.00	3 G	A78	-98.8171	37.9099	-44111.	115578.	18.34 9.61	19 10	1
032505-SF 25 14W 19 CDBB	865.00	155.00	3 G	A78	-98.9071	37.8576	-52015.	109787.	18.12 3.55	19 4	1
032772-RC 20 10W 35 DDDC	600.00	119.00	3 G	A79	-98.3894	38.2612	-6688.	154665.	13.72 42.75	14 43	1
032972-BT 20 11W 19 DDAB	28.00	7.70	6 G	A79	-98.5734	38.2931	-22681.	158261.	5.82 36.37	6 37	1
033696-BT 20 11W 31 CCAA	1010.00	170.00	3 G	A79	-98.5859	38.2643	-23780.	155041.	6.96 34.60	7 35	1
033447-SF 21 11W 6 ABBD	335.00	24.00	5 G	A79	-98.5710	38.2598	-22488.	154538.	7.70 35.03	8 36	1
033726-SF 21 12W 2 DDBB	1000.00	6.00	3 G	A79	-98.6044	38.2496	-25400.	153408.	7.13 33.19	8 34	1
033725-SF 21 12W 5 AACC	.00	97.50	3 G	A79	-98.6597	38.2577	-30204.	154332.	4.84 31.21	5 32	1
033520-SF 21 13W 4 BBB	1000.00	240.00	3 G	A79	-98.7648	38.2600	-39348.	154626.	1.18 26.89	2 27	1
033375-SF 21 13W 32 BDBB	980.00	198.00	3 G	A79	-98.7795	38.1845	-40667.	146212.	4.77 23.02	5 24	1
033195-SF 21 14W 26 DDBB	765.00	195.00	3 G	A79	-98.8249	38.1920	-44612.	147061.	2.84 21.43	3 22	1
033348-SF 21 14W 30 CDBB	1200.00	222.00	3 G	A79	-98.9070	38.1921	-51768.	147122.	.06 17.99	1 18	1

150

Appendix 1. Well data (cont.)

(a) Well ID, township, range, section, quarter-section	(b) Rate (gpm)	(c) Approp (ac-ft)	(d) Use code	(e) Year	(f, g) Longitude (deg) Latitude (deg)		(h, i) Albers x (m) Albers y (m)		(j, k) Grid row/col. (mi)		(l, m) Grid index row/col		(n) cell activ.
032764-SF 22 13W 16 BDBB	1200.00	240.00	3	G A79	-98.7608	38.1407	-39064.	141312.	7.77	21.92	8	22	1
033044-SF 22 14W 6 CDBB	1000.00	240.00	3	G A79	-98.9071	38.1631	-51794.	143885.	1.62	16.73	2	17	1
032732-SF 22 14W 8 CDBB	1200.00	240.00	3	G A79	-98.8892	38.1485	-50242.	142246.	3.01	16.86	4	17	1
032643-SF 22 14W 35 CACC	800.00	195.00	3	G A79	-98.8338	38.0911	-45457.	135808.	7.99	16.71	8	17	1
033350-PN 22 15W 34 DCAA	840.00	194.00	3	G A79	-98.9542	38.0906	-55957.	135824.	3.94	11.62	4	12	1
033066-SF 23 13W 16 BDBB	1130.00	180.00	3	G A79	-98.7604	38.0535	-39079.	131584.	12.49	18.18	13	19	1
032997-SF 23 13W 20 ACC	1200.00	191.00	3	G A79	-98.7738	38.0368	-40257.	129722.	12.95	16.90	13	17	1
033456-SF 23 14W 4 ADBB	1000.00	240.00	3	G A79	-98.8615	38.0830	-47878.	134925.	7.48	15.20	8	16	1
033266-SF 23 14W 18 BDBB	1000.00	225.00	3	G A79	-98.9076	38.0543	-51916.	131737.	7.48	12.02	8	13	1
032642-SF 23 14W 23 DDBB	365.00	128.00	3	G A79	-98.8248	38.0322	-44711.	129228.	11.47	14.55	12	15	1
033440-SF 23 14W 30 DCBB	1000.00	240.00	3	G A79	-98.9030	38.0181	-51542.	127700.	9.59	10.65	10	11	1
032992-PN 23 15W 12 DAA	1200.00	240.00	3	G A79	-98.9138	38.0647	-52454.	132904.	6.71	12.20	7	13	1
033064-PN 23 15W 25 CABB	270.00	35.00	3	G A79	-98.9259	38.0217	-53535.	128118.	8.62	9.84	9	10	1
033483-SF 24 12W 4 CDBB	900.00	198.00	3	G A79	-98.6497	37.9875	-29448.	124174.	19.80	20.02	20	21	1
033014-SF 24 13W 13 CBDA	1000.00	65.00	3	G A79	-98.7056	37.9606	-34342.	121192.	19.37	16.50	20	17	1
033513-SF 24 14W 1 BDBB	1000.00	240.00	3	G A79	-98.8156	37.9958	-43927.	125161.	13.75	13.37	14	14	1
032934-SF 24 15W 28 DDBB	1100.00	198.00	3	G A79	-98.9712	37.9305	-57564.	117962.	12.01	3.99	13	4	1
032561-ED 24 16W 10 DDBB	865.00	181.00	3	G A79	-99.0626	37.9741	-65510.	122890.	6.56	2.03	7	3	1
033244-SF 25 13W 30 ADCC	705.00	135.00	3	G A79	-98.7876	37.8475	-41568.	108609.	22.71	8.17	23	9	1
033494-SF 25 14W 19 DDBB	1000.00	240.00	3	G A79	-98.8979	37.8576	-51213.	109782.	18.43	3.94	19	4	1
033011-SF 25 14W 23 DDBB	1200.00	237.00	3	G A79	-98.8243	37.8576	-44769.	109747.	20.93	7.05	21	8	1
034303-BT 19 11W 27 DBCA	365.00	47.00	3	G A80	-98.5243	38.3667	-18400.	166465.	3.47	41.59	4	42	1
034302-BT 19 11W 27 DBCC	455.00	58.00	3	G A80	-98.5255	38.3658	-18498.	166363.	3.49	41.50	4	42	1
034014-RC 20 10W 26 CCB	90.00	19.95	4	G A80	-98.4051	38.2775	-8055.	156482.	12.31	42.78	13	43	1
034094-BT 20 11W 9 ADDB	1000.00	240.00	3	G A80	-98.5365	38.3276	-19471.	162098.	5.19	39.40	6	40	1
034368-BT 20 12W 4 BDBB	1000.00	228.00	3	G A80	-98.6586	38.3436	-30075.	163916.	.23	34.95	1	35	1
034785-BT 20 12W 22 DDBB	1000.00	237.00	3	G A80	-98.6309	38.2933	-27686.	158293.	3.88	33.95	4	34	1
033857-BT 20 12W 31 ADBB	1000.00	240.00	3	G A80	-98.6860	38.2713	-32481.	155858.	3.22	30.69	4	31	1
034747-BT 20 13W 23 DCAA	345.00	99.00	3	G A80	-98.7241	38.2932	-35788.	158312.	.76	30.03	1	31	1
034128-BT 20 13W 35 BDBB	1000.00	240.00	3	G A80	-98.7320	38.2713	-36490.	155877.	1.67	28.75	2	29	1
034192-BT 20 13W 36 DACC	920.00	209.00	3	G A80	-98.7043	38.2649	-34078.	155156.	2.95	29.65	3	30	1
034008-SF 21 12W 9 CDBB	1100.00	240.00	3	G A80	-98.6506	38.2350	-29425.	151793.	6.37	30.62	7	31	1
033885-SF 21 12W 28 DDBB	1000.00	120.00	3	G A80	-98.6419	38.1910	-28681.	146879.	9.05	29.09	10	30	1
034459-SF 21 12W 34 ADC	1100.00	240.00	3	G A80	-98.6231	38.1813	-27046.	145795.	10.21	29.47	11	30	1
033849-SF 21 14W 14 DDBB	900.00	240.00	3	G A80	-98.8249	38.2210	-44600.	150305.	1.26	22.68	2	23	1

Appendix 1. Well data (cont.)

(a) Well ID, township, range, section, quarter-section	(b) Rate (gpm)	(c) Approp (ac-ft)	(d) Use code	(e) Year	(f, g) Longitude (deg) Latitude (deg)		(h, i) Albers x (m) Albers y (m)		(j, k) Grid row/col. (mi)		(l, m) Grid index row/col		(n) cell activ.
034468-SF 22 13W 30 DDBB	1000.00	135.00	3 G	A80	-98.7880	38.1046	-41451.	137294.	8.80	19.22	9	20	1
033895-SF 22 14W 19 CDBB	1000.00	240.00	3 G	A80	-98.9073	38.1196	-51844.	139030.	3.96	14.85	4	15	1
034607-SF 22 14W 21 DDBC	1000.00	240.00	3 G	A80	-98.8614	38.1185	-47844.	138880.	5.57	16.73	6	17	1
034028-PN 22 15W 30 CDBB	605.00	169.00	3 G	A80	-99.0166	38.1051	-61382.	137478.	1.05	9.62	2	10	1
034029-PN 22 16W 36 CDBB	620.00	164.00	3 G	A80	-99.0348	38.0905	-62984.	135864.	1.22	8.23	2	9	1
034676-SF 23 11W 21 BDAA	750.00	75.00	3 G	A80	-98.5370	38.0377	-19588.	129747.	20.88	26.94	21	27	1
034661-SF 23 11W 21 DABB	1000.00	240.00	3 G	A80	-98.5312	38.0341	-19085.	129346.	21.27	27.03	22	28	1
033825-SF 23 11W 22 BCCB	.00	120.00	3 G	A80	-98.5266	38.0359	-18684.	129547.	21.32	27.30	22	28	1
033744-SF 23 12W 15 BDBB	1000.00	236.00	3 G	A80	-98.6319	38.0527	-27868.	131438.	16.87	23.57	17	24	1
034463-SF 23 13W 14 ADBB	290.00	102.00	3 G	A80	-98.7144	38.0534	-35063.	131546.	14.06	20.12	15	21	1
034469-SF 23 13W 14 BCAA	995.00	195.00	3 G	A80	-98.7247	38.0534	-35964.	131556.	13.70	19.69	14	20	1
034657-SF 23 13W 23 CDBB	1000.00	203.00	3 G	A80	-98.7235	38.0315	-35870.	129113.	14.93	18.79	15	19	1
034472-SF 23 13W 28 CDBA	1000.00	44.00	3 G	A80	-98.7593	38.0172	-38995.	127533.	14.50	16.67	15	17	1
034713-SF 23 13W 34 BDDB	1000.00	90.00	3 G	A80	-98.7395	38.0080	-37274.	126492.	15.66	17.11	16	18	1
034664-SF 23 13W 34 CBD	1000.00	158.00	3 G	A80	-98.7435	38.0039	-37626.	126039.	15.75	16.76	16	17	1
033803-SF 23 13W 36 BDA	1000.00	192.00	3 G	A80	-98.7021	38.0092	-34012.	126618.	16.86	18.74	17	19	1
034684-SF 23 14W 9 CDBB	1200.00	218.00	3 G	A80	-98.8708	38.0614	-48706.	132509.	8.34	13.87	9	14	1
034115-SF 23 14W 34 DBAB	595.00	165.00	3 G	A80	-98.8456	38.0069	-46537.	126418.	12.14	12.59	13	13	1
034752-PN 23 15W 30 ADBB	910.00	175.00	3 G	A80	-99.0082	38.0251	-60715.	128550.	5.65	6.52	6	7	1
034844-PN 23 15W 34 DDCD	765.00	152.00	3 G	A80	-98.9521	38.0009	-55845.	125811.	8.86	7.84	9	8	1
034678-PN 23 16W 4 CDBB	635.00	109.00	3 G	A80	-99.0900	38.0758	-67811.	134259.	.15	5.27	1	6	1
034065-PN 23 16W 11 BDB	.00	48.00	3 G	A80	-99.0526	38.0682	-64554.	133385.	1.82	6.52	2	7	1
034281-PN 23 16W 31 BDBB	740.00	195.00	3 G	A80	-99.1267	38.0103	-71076.	126981.	2.43	.90	3	1	1
034417-PN 23 16W 31 DBBB	625.00	159.00	3 G	A80	-99.1221	38.0067	-70680.	126574.	2.78	.93	3	1	1
033899-PN 23 16W 34 ADBB	1000.00	240.00	3 G	A80	-99.0625	38.0106	-65470.	126962.	4.60	3.61	5	4	1
034556-PN 23 17W 26 DDBB	640.00	189.00	3 G	A80	-99.1541	38.0176	-73458.	127814.	1.11	.06	2	1	1
034221-SF 24 12W 14 BBBB	200.00	55.23	4 G	A80	-98.6178	37.9688	-26662.	122080.	21.89	20.56	22	21	1
034702-SF 25 14W 31 CDBC	1000.00	195.00	3 G	A80	-98.9069	37.8276	-52016.	106444.	19.75	2.27	20	3	1
033896-SF 25 14W 33 BDBB	715.00	132.00	3 G	A80	-98.8702	37.8357	-48802.	107330.	20.55	4.17	21	5	1
033756-PR 26 14W 5 CACB	1145.00	204.00	3 G	A80	-98.8805	37.8126	-49717.	104753.	21.46	2.74	22	3	1
034576-PR 26 15W 2 DDBB	1000.00	195.00	3 G	A80	-98.9255	37.8100	-53663.	104493.	20.07	.72	21	1	1
034444-PR 26 15W 13 ADBB	1030.00	198.00	3 G	A80	-98.9072	37.7871	-52079.	101927.	21.92	.51	22	1	1
034443-PR 26 15W 13 DDBB	1200.00	240.00	3 G	A80	-98.9072	37.7798	-52086.	101115.	22.31	.19	23	1	1
035364-BT 19 11W 31 BCDB	200.00	13.50	3 G	A81	-98.5871	38.3564	-23859.	165321.	1.93	38.50	2	39	1
035363-BT 19 11W 31 CBBD	200.00	16.00	3 G	A81	-98.5883	38.3537	-23958.	165026.	2.04	38.34	3	39	1

Appendix 1. Well data (cont.)

(a) Well ID, township, range, section, quarter-section	(b) Rate (gpm)	(c) Approp (ac-ft)	(d) Use code	(e) Year	(f, g) Longitude (deg)	(f, g) Latitude (deg)	(h, i) Albers x (m)	(h, i) Albers y (m)	(j, k) GrID row/col. (mi)	(l, m) GrID index row/col	(n) cell activ.
035595-BT 19 11W 32 DCBB	350.00	6.75	2	G A81	-98.5619	38.3505	-21667.	164663.	3.09 39.31	4 40	1
035076-BT 20 12W 17 BBDB	500.00	60.00	3	G A81	-98.6792	38.3167	-31876.	160919.	.99 32.93	1 33	1
035033-BT 20 12W 19 CDBB	1200.00	238.00	3	G A81	-98.6951	38.2931	-33268.	158293.	1.73 31.24	2 32	1
035191-BT 20 13W 25 BDBB	1000.00	240.00	3	G A81	-98.7137	38.2859	-34884.	157498.	1.50 30.16	2 31	1
035193-BT 20 13W 25 CDBB	1000.00	240.00	3	G A81	-98.7136	38.2786	-34884.	156688.	1.89 29.84	2 30	1
035196-BT 20 13W 26 CDCB	805.00	201.00	3	G A81	-98.7321	38.2768	-36491.	156487.	1.37 28.99	2 29	1
035199-BT 20 13W 26 DDDD	815.00	203.00	3	G A81	-98.7194	38.2759	-35387.	156387.	1.85 29.48	2 30	1
035192-BT 20 13W 27 ADBB	1000.00	240.00	3	G A81	-98.7414	38.2859	-37295.	157505.	.57 28.99	1 29	1
035624-SF 21 14W 27 ADBB	1000.00	180.00	3	G A81	-98.8432	38.1992	-46207.	147883.	1.82 20.98	2 21	1
034975-SF 22 13W 5 ADBB	870.00	189.00	3	G A81	-98.7702	38.1698	-39868.	144567.	5.87 22.78	6 23	1
035043-SF 22 13W 10 DCAA	.00	51.00	3	G A81	-98.7344	38.1478	-36757.	142091.	8.27 23.34	9 24	1
035128-SF 22 13W 11 BCA	1500.00	233.00	3	G A81	-98.7258	38.1545	-36007.	142838.	8.20 23.99	9 24	1
034867-SF 22 13W 13 BBD	1000.00	200.00	3	G A81	-98.7073	38.1418	-34402.	141411.	9.51 24.22	10 25	1
035849-SF 22 13W 13 CACC	1000.00	200.00	3	G A81	-98.7055	38.1341	-34248.	140553.	9.99 23.97	10 24	1
035140-SF 22 13W 25 ADBB	1500.00	240.00	3	G A81	-98.6962	38.1114	-33451.	138020.	11.53 23.38	12 24	1
035111-PN 22 15W 11 CDDD	1000.00	240.00	3	G A81	-98.9403	38.1460	-54699.	141992.	1.42 14.60	2 15	1
034920-PN 22 15W 28 ABAB	500.00	120.00	3	G A81	-98.9734	38.1161	-57610.	138682.	1.92 11.92	2 12	1
034921-PN 22 15W 28 ABCB	500.00	120.00	3	G A81	-98.9757	38.1143	-57813.	138479.	1.94 11.74	2 12	1
035168-PN 22 15W 31 DDBB	1200.00	198.00	3	G A81	-99.0078	38.0905	-60630.	135848.	2.13 9.36	3 10	1
034918-PN 22 16W 34 DABB	755.00	195.00	3	G A81	-99.0624	38.0941	-65383.	136279.	.10 7.22	1 8	1
035112-PN 22 16W 36 ADBB	1100.00	240.00	3	G A81	-99.0256	38.0978	-62172.	136669.	1.14 8.93	2 9	1
035332-SF 23 13W 25 DDBB	800.00	153.00	3	G A81	-98.6958	38.0169	-33457.	127475.	16.65 19.34	17 20	1
035677-SF 23 14W 32 AACC	300.00	80.00	3	G A81	-98.8800	38.0117	-49542.	126968.	10.72 11.34	11 12	1
035676-SF 23 14W 32 ADBB	300.00	80.00	3	G A81	-98.8800	38.0107	-49543.	126867.	10.76 11.30	11 12	1
035675-SF 23 14W 32 ADBB	300.00	80.00	3	G A81	-98.8800	38.0107	-49543.	126867.	10.76 11.30	11 12	1
035806-PN 23 15W 29 BBBB	845.00	195.00	3	G A81	-99.0039	38.0288	-60336.	128951.	5.60 6.86	6 7	1
035807-PN 23 15W 29 CB BB	900.00	195.00	3	G A81	-99.0038	38.0215	-60338.	128144.	5.99 6.55	6 7	1
035226-PN 23 16W 1 AADA	1000.00	240.00	3	G A81	-99.0222	38.0850	-61890.	135245.	1.94 8.52	2 9	1
035103-SF 24 13W 28 CDBB	1500.00	230.00	3	G A81	-98.7600	37.9300	-39105.	117803.	19.19 12.89	20 13	1
035101-SF 24 15W 2 CABB	1200.00	240.00	3	G A81	-98.9441	37.9927	-55150.	124886.	9.57 7.82	10 8	1
035085-SF 24 15W 9 BDBB	1200.00	240.00	3	G A81	-98.9807	37.9816	-58351.	123669.	8.93 5.80	9 6	1
035102-SF 24 15W 12 DCCC	1200.00	240.00	3	G A81	-98.9211	37.9716	-53158.	122519.	11.49 7.88	12 8	1
035100-SF 24 15W 14 BBD	1000.00	177.00	3	G A81	-98.9457	37.9684	-55307.	122179.	10.83 6.71	11 7	1
035003-SF 24 15W 28 ADBB	1800.00	240.00	3	G A81	-98.9713	37.9378	-57565.	118782.	11.61 4.31	12 5	1
035098-SF 24 15W 33 ADBB	1200.00	240.00	3	G A81	-98.9711	37.9231	-57562.	117144.	12.41 3.68	13 4	1

Appendix 1. Well data (cont.)

(a) Well ID, township, range, section, quarter-section	(b) Rate (gpm)	(c) Approp (ac-ft)	(d) Use code	(e) Year	(f, g) Longitude (deg)	(f, g) Latitude (deg)	(h, i) Albers x (m)	(h, i) Albers y (m)	(j, k) Grid row/col. (mi)	(l, m) Grid index row/col	(n) cell activ.
035099-SF 24 15W 33 BDBB	1200.00	240.00	3 G	A81	-98.9803	37.9231	-58362.	117148.	12.10 3.29	13 4	1
035097-SF 24 15W 33 DAB	1200.00	240.00	3 G	A81	-98.9705	37.9190	-57511.	116683.	12.66 3.53	13 4	1
035689-ED 24 16W 14 DCBB	530.00	27.00	3 G	A81	-99.0489	37.9596	-64325.	121268.	7.81 1.98	8 2	1
034915-SF 25 15W 35 DDBB	1100.00	240.00	3 G	A81	-98.9343	37.8285	-54421.	106563.	18.77 1.15	19 2	1
035252-SF 25 15W 36 DCAB	1055.00	195.00	3 G	A81	-98.9183	37.8285	-53017.	106553.	19.31 1.83	20 2	1
035540-PR 26 14W 3 CDBB	1000.00	240.00	3 G	A81	-98.8439	37.8105	-46516.	104501.	22.81 4.19	23 5	1
035281-PR 26 14W 9 ADBB	1200.00	240.00	3 G	A81	-98.8530	37.8022	-47322.	103576.	22.95 3.45	23 4	1
035266-PR 26 15W 2 BABB	720.00	129.00	3 G	A81	-98.9347	37.8248	-54451.	106145.	18.96 .97	19 1	1
035237-PR 26 15W 2 CDCC	900.00	112.00	3 G	A81	-98.9347	37.8063	-54467.	104087.	19.95 .18	20 1	1
035989-RC 20 10W 29 BACB	500.00	81.00	3 G	A82	-98.4561	38.2873	-12484.	157589.	10.07 41.06	11 42	1
035908-SF 21 12W 6 ADBB	1000.00	240.00	3 G	A82	-98.6781	38.2568	-31801.	154231.	4.27 30.40	5 31	1
036169-SF 21 13W 13 ADBC	.00	100.00	3 G	A82	-98.6964	38.2265	-33413.	150866.	5.29 28.33	6 29	1
036382-SF 21 14W 22 ADBB	1200.00	230.00	3 G	A82	-98.8432	38.2138	-46198.	149504.	1.04 21.60	2 22	1
036266-SF 21 14W 29 ACAD	1000.00	246.00	3 G	A82	-98.8812	38.1984	-49513.	147814.	.59 19.34	1 20	1
035953-SF 22 14W 3 CDBB	1000.00	240.00	3 G	A82	-98.8523	38.1629	-47025.	143833.	3.48 19.03	4 20	1
036010-SF 22 14W 17 ADBB	1000.00	240.00	3 G	A82	-98.8800	38.1412	-49447.	141427.	3.72 16.93	4 17	1
036086-SF 22 14W 32 AACC	1200.00	240.00	3 G	A82	-98.8800	38.0986	-49477.	136674.	6.02 15.09	7 16	1
035903-SF 22 14W 32 BDCB	1000.00	240.00	3 G	A82	-98.8892	38.0959	-50284.	136380.	5.85 14.59	6 15	1
036077-SF 23 13W 36 DBBB	.00	120.00	3 G	A82	-98.7003	38.0061	-33857.	126261.	17.09 18.68	18 19	1
036147-SF 23 14W 15 ADDC	.00	94.00	3 G	A82	-98.8409	38.0513	-46100.	131367.	9.90 14.70	10 15	1
036202-PN 23 15W 6 ADBB	800.00	240.00	3 G	A82	-99.0078	38.0832	-60634.	135034.	2.53 9.05	3 10	1
036201-PN 23 15W 6 BDBB	.00	82.00	3 G	A82	-99.0167	38.0832	-61408.	135039.	2.23 8.68	3 9	1
036036-PN 23 15W 10 BDBB	1100.00	240.00	3 G	A82	-98.9624	38.0688	-56688.	133389.	4.84 10.33	5 11	1
035896-PN 23 16W 32 BBCC	1000.00	237.00	3 G	A82	-99.1129	38.0113	-69871.	127079.	2.85 1.52	3 2	1
035893-SF 24 13W 3 DDBB	1200.00	222.00	3 G	A82	-98.7323	37.9880	-36662.	124258.	16.99 16.55	17 17	1
036231-SF 25 13W 9 DDBB	.00	57.00	3 G	A82	-98.7508	37.8865	-38327.	112937.	21.85 11.40	22 12	1
036167-SF 25 14W 29 CDBB	1000.00	240.00	3 G	A82	-98.8886	37.8430	-50406.	108155.	19.54 3.71	20 4	1
036274-SF 25 14W 29 DDBB	1000.00	240.00	3 G	A82	-98.8794	37.8430	-49603.	108149.	19.85 4.09	20 5	1
036287-SF 25 15W 22 DACC	1200.00	155.00	3 G	A82	-98.9529	37.8584	-56022.	109911.	16.52 1.66	17 2	1
036405-PR 26 14W 4 CDBB	1200.00	240.00	3 G	A82	-98.8623	37.8103	-48124.	104495.	22.19 3.41	23 4	1
036589-BT 19 11W 22 CCAB	1500.00	240.00	3 G	A83	-98.5325	38.3795	-19108.	167890.	2.51 41.79	3 42	1
036574-BT 20 11W 28 DDBB	1000.00	240.00	3 G	A83	-98.5388	38.2789	-19684.	156659.	7.75 37.21	8 38	1
036926-BT 20 12W 29 CDBB	710.00	189.00	3 G	A83	-98.6767	38.2785	-31676.	156664.	3.14 31.39	4 32	1
036925-BT 20 12W 33 ADBB	790.00	198.00	3 G	A83	-98.6492	38.2714	-29286.	155856.	4.45 32.24	5 33	1
036865-SF 21 13W 28 ADBB	1000.00	240.00	3 G	A83	-98.7519	38.1987	-38254.	147783.	4.93 24.80	5 25	1

Appendix 1. Well data (cont.)

(a) Well ID, township, range, section, quarter-section	(b) Rate (gpm)	(c) Approp (ac-ft)	(d) Use code	(e) Year	(f, g) Longitude (deg)	(f, g) Latitude (deg)	(h, i) Albers x (m)	(h, i) Albers y (m)	(j, k) Grid row/col. (mi)	(l, m) Grid index row/col	(n) cell activ.
036505-SF 22 14W 15 ADBB	1000.00	240.00	3 G	A83	-98.8432	38.1410	-46241.	141384.	4.97 18.47	5 19	1
036521-PN 22 15W 22 DDAA	350.00	92.00	3 G	A83	-98.9494	38.1197	-55510.	139062.	2.54 13.08	3 14	1
036557-PN 22 15W 23 ADBB	800.00	240.00	3 G	A83	-98.9346	38.1269	-54219.	139861.	2.65 14.01	3 15	1
036452-PN 23 15W 7 DDBB	1000.00	240.00	3 G	A83	-99.0077	38.0615	-60643.	132604.	3.71 8.11	4 9	1
036940-PN 23 16W 13 ADBB	900.00	240.00	3 G	A83	-99.0256	38.0541	-62215.	131800.	3.49 7.04	4 8	1
036939-PN 23 16W 13 DDBB	900.00	240.00	3 G	A83	-99.0256	38.0469	-62219.	130994.	3.88 6.73	4 7	1
036836-SF 24 15W 22 BBAC	350.00	55.23	4 G	A83	-98.9646	37.9552	-56969.	120721.	10.90 5.34	11 6	1
036793-SF 25 14W 21 DDBB	1200.00	240.00	3 G	A83	-98.8611	37.8576	-47989.	109764.	19.68 5.50	20 6	1
036785-SF 25 14W 29 AACC	900.00	40.00	3 G	A83	-98.8795	37.8512	-49604.	109066.	19.40 4.44	20 5	1
036682-SF 25 14W 33 CDBB	1200.00	240.00	3 G	A83	-98.8702	37.8284	-48807.	106517.	20.95 3.85	21 4	1
036945-PR 26 14W 6 CDBB	1200.00	222.00	3 G	A83	-98.8982	37.8101	-51275.	104482.	20.99 1.88	21 2	1
037458-BT 20 11W 17 CCDD	800.00	240.00	3 G	A84	-98.5676	38.3049	-22180.	159568.	5.38 37.11	6 38	1
037146-BT 20 11W 29 CDBB	1100.00	240.00	3 G	A84	-98.5664	38.2788	-22085.	156657.	6.83 36.04	7 37	1
037500-BT 20 12W 7 ADBB	1000.00	240.00	3 G	A84	-98.6861	38.3293	-32469.	162334.	.07 33.18	1 34	1
037419-BT 20 12W 8 ADBB	1000.00	240.00	3 G	A84	-98.6678	38.3294	-30881.	162333.	.69 33.95	1 34	1
037261-BT 20 12W 13 DACC	.00	120.00	3 G	A84	-98.5940	38.3086	-24472.	159996.	4.29 36.16	5 37	1
037293-RC 21 10W 12 BDBB	1200.00	273.00	3 G	A84	-98.3748	38.2424	-5425.	152567.	15.22 42.56	16 43	1
037049-SF 21 11W 7 ABDA	1000.00	240.00	3 G	A84	-98.5689	38.2441	-22309.	152792.	8.62 34.45	9 35	1
037507-SF 21 12W 8 ADBB	1000.00	240.00	3 G	A84	-98.6599	38.2422	-30227.	152602.	5.67 30.54	6 31	1
037471-SF 21 12W 16 ADBB	1100.00	240.00	3 G	A84	-98.6413	38.2277	-28612.	150973.	7.08 30.70	8 31	1
037069-SF 21 13W 3 ADBB	1100.00	240.00	3 G	A84	-98.7331	38.2568	-36586.	154254.	2.42 28.09	3 29	1
037113-SF 21 14W 23 BACC	1200.00	240.00	3 G	A84	-98.8341	38.2146	-45401.	149597.	1.30 22.02	2 23	1
037029-PN 21 15W 36 ADBB	1200.00	240.00	3 G	A84	-98.9160	38.1849	-52554.	146322.	.14 17.30	1 18	1
037155-SF 22 12W 29 DDBD	120.00	19.88	2 G	A84	-98.6586	38.1029	-30174.	137054.	13.25 24.60	14 25	1
037152-SF 22 14W 33 CDBB	1200.00	473.00	3 G	A84	-98.8708	38.0904	-48681.	135752.	6.77 15.12	7 16	1
037156-PN 22 15W 12 DDBB	970.00	195.00	3 G	A84	-98.9162	38.1486	-52598.	142276.	2.09 15.73	3 16	1
037555-SF 23 13W 5 AACC	600.00	50.00	3 G	A84	-98.7696	38.0836	-39859.	134938.	10.56 19.09	11 20	1
037028-SF 23 13W 5 DDBB	1000.00	240.00	3 G	A84	-98.7696	38.0754	-39867.	134024.	11.00 18.74	12 19	1
037547-SF 23 13W 6 CDBB	1200.00	235.00	3 G	A84	-98.7971	38.0755	-42269.	134052.	10.07 17.58	11 18	1
037124-SF 23 13W 14 DDBB	1200.00	240.00	3 G	A84	-98.7143	38.0461	-35062.	130733.	14.45 19.81	15 20	1
037407-SF 23 13W 32 ACCC	.00	132.00	3 G	A84	-98.7742	38.0073	-40308.	126433.	14.53 15.61	15 16	1
037110-SF 23 13W 32 DCAD	130.00	34.06	4 G	A84	-98.7706	38.0018	-39998.	125818.	14.94 15.53	15 16	1
037109-SF 23 13W 33 BDBC	200.00	29.00	4 G	A84	-98.7603	38.0091	-39095.	126620.	14.90 16.27	15 17	1
037477-SF 23 14W 28 CDAA	400.00	107.00	3 G	A84	-98.8674	38.0179	-48433.	127659.	10.81 12.14	11 13	1
037251-SF 23 14W 28 CDBB	500.00	133.00	3 G	A84	-98.8708	38.0179	-48734.	127664.	10.69 12.00	11 12	1

Appendix 1. Well data (cont.)

(a) Well ID, township, range, section, quarter-section	(b) Rate (gpm)	(c) Approp (ac-ft)	(d) Use code	(e) Year	(f, g) Longitude (deg)	(f, g) Latitude (deg)	(h, i) Albers x (m)	(h, i) Albers y (m)	(j, k) Grid row/col. (mi)	(l, m) Grid index row/col	(n) cell activ.
036971-PN 23 15W 28 ADBB	500.00	120.00	3 G	A84	-98.9717	38.0252	-57537.	128539.	6.88 8.06	7 9	1
036970-PN 23 15W 28 ADBB	500.00	120.00	3 G	A84	-98.9717	38.0252	-57537.	128539.	6.88 8.06	7 9	1
036972-PN 23 16W 33 ADBB	1000.00	240.00	3 G	A84	-99.0809	38.0105	-67073.	126963.	3.98 2.83	4 3	1
037102-PN 23 17W 25 ACAA	895.00	176.00	3 G	A84	-99.1369	38.0249	-71950.	128614.	1.30 1.10	2 2	1
037516-SF 24 12W 31 BBDA	1200.00	237.00	3 G	A84	-98.6871	37.9241	-32736.	117115.	21.97 15.71	22 16	1
037526-SF 24 14W 18 CDBB	1000.00	237.00	3 G	A84	-98.9074	37.9597	-51965.	121182.	12.60 7.94	13 8	1
037531-SF 24 15W 33 CDBB	1000.00	240.00	3 G	A84	-98.9802	37.9158	-58360.	116331.	12.50 2.98	13 3	1
037103-ED 24 16W 10 CDBB	1000.00	240.00	3 G	A84	-99.0718	37.9740	-66313.	122890.	6.25 1.64	7 2	1
037499-ED 24 16W 13 CBDD	300.00	105.00	3 G	A84	-99.0363	37.9606	-63224.	121368.	8.18 2.55	9 3	1
037361-SF 25 13W 4 BCDB	600.00	60.00	3 G	A84	-98.7623	37.9065	-39326.	115176.	20.38 11.77	21 12	1
037521-SF 25 14W 23 ADBB	1000.00	240.00	3 G	A84	-98.8243	37.8648	-44765.	110556.	20.54 7.36	21 8	1
037515-SF 25 14W 24 BCAB	1000.00	240.00	3 G	A84	-98.8174	37.8648	-44165.	110552.	20.77 7.65	21 8	1
037349-SF 25 15W 35 BDBB	1200.00	240.00	3 G	A84	-98.9436	37.8357	-55228.	107375.	18.06 1.07	19 2	1
037496-PR 26 14W 18 ADBB	1000.00	240.00	3 G	A84	-98.8894	37.7872	-50513.	101928.	22.52 1.27	23 2	1
037490-PR 26 14W 18 BDBB	1000.00	228.00	3 G	A84	-98.8982	37.7872	-51291.	101926.	22.23 .89	23 1	1
037437-PR 26 15W 12 CACC	1100.00	180.00	3 G	A84	-98.9164	37.7953	-52873.	102844.	21.17 .47	22 1	1
037610-BT 20 11W 18 DBDA	800.00	240.00	3 G	A85	-98.5768	38.3094	-22977.	160081.	4.82 36.92	5 37	1
037834-RC 21 9W 17 BBAA	1200.00	120.00	3 G	A85	-98.3400	38.2314	-2394.	151338.	16.99 43.56	17 44	1
038073-RC 21 9W 18 AAAB	1200.00	240.00	3 G	A85	-98.3457	38.2315	-2890.	151345.	16.79 43.32	17 44	1
037609-SF 21 12W 7 ACDA	1000.00	120.00	3 G	A85	-98.6794	38.2403	-31925.	152394.	5.12 29.63	6 30	1
037613-SF 21 12W 7 BDAA	1200.00	115.50	3 G	A85	-98.6839	38.2421	-32316.	152598.	4.87 29.52	5 30	1
037899-SF 22 13W 14 DADB	400.00	23.93	5 G	A85	-98.7124	38.1351	-34846.	140662.	9.70 23.72	10 24	1
037960-SF 22 13W 33 CDBB	1200.00	240.00	3 G	A85	-98.7604	38.0899	-39057.	135641.	10.53 19.75	11 20	1
037710-SF 23 12W 5 CCBC	850.00	55.50	3 G	A85	-98.6733	38.0740	-31468.	133840.	14.32 22.74	15 23	1
037703-SF 23 12W 9 CDBB	1000.00	240.00	3 G	A85	-98.6503	38.0602	-29466.	132281.	15.85 23.12	16 24	1
037758-SF 23 12W 11 CDBB	1000.00	240.00	3 G	A85	-98.6137	38.0597	-26275.	132222.	17.10 24.64	18 25	1
037961-SF 23 13W 7 DDBB	1200.00	240.00	3 G	A85	-98.7881	38.0609	-41487.	132419.	11.16 17.34	12 18	1
037716-SF 23 14W 22 AABA	550.00	118.00	3 G	A85	-98.8420	38.0431	-46203.	130463.	10.30 14.30	11 15	1
037685-SF 23 14W 22 ADBB	550.00	119.00	3 G	A85	-98.8432	38.0395	-46308.	130058.	10.46 14.09	11 15	1
037624-PN 23 15W 21 ACCD	400.00	97.50	3 G	A85	-98.9752	38.0370	-57825.	129853.	6.13 8.43	7 9	1
037625-PN 23 15W 21 DCCD	400.00	97.50	3 G	A85	-98.9752	38.0298	-57833.	129046.	6.52 8.11	7 9	1
037595-SF 24 13W 33 BDBB	1200.00	240.00	3 G	A85	-98.7600	37.9228	-39111.	116994.	19.58 12.58	20 13	1
037894-SF 24 15W 1 AACC	200.00	203.00	3 G	A85	-98.9167	37.9972	-52756.	125381.	10.25 9.17	11 10	1
037642-SF 24 15W 11 BADA	900.00	240.00	3 G	A85	-98.9406	37.9835	-54854.	123861.	10.19 7.57	11 8	1
037574-ED 24 16W 15 CCAB	1200.00	240.00	3 G	A85	-99.0741	37.9595	-66530.	121277.	6.95 .91	7 1	1

Appendix 1. Well data (cont.)

(a) Well ID, township, range, section, quarter-section	(b) Rate (gpm)	(c) Approp (ac-ft)	(d) Use code	(e) Year	(f, g) Longitude (deg) Latitude (deg)		(h, i) Albers x (m) Albers y (m)		(j, k) Grid row/col. (mi)		(l, m) Grid index row/col		(n) cell activ.
037657-SF 25 14W 17 CDBC	.00	49.00	3 G	A85	-98.8887	37.8712	-50394.	111305.	18.01	4.92	19	5	1
037594-SF 25 14W 26 BDBB	1200.00	240.00	3 G	A85	-98.8334	37.8503	-45577.	108939.	21.01	6.35	22	7	1
037963-SF 25 15W 4 BDAA	1400.00	480.00	3 G	A85	-98.9767	37.9085	-58061.	115514.	13.01	2.81	14	3	1
038145-RC 21 9W 17 BBAA	800.00	120.00	3 G	A86	-98.3400	38.2314	-2394.	151338.	16.99	43.56	17	44	1
038396-SF 22 13W 1 DBDD	1000.00	210.00	3 G	A86	-98.6977	38.1629	-33557.	143763.	8.69	25.53	9	26	1
038150-SF 22 14W 36 DABD	1000.00	198.00	3 G	A86	-98.8051	38.0928	-42948.	135986.	8.86	18.00	9	18	1
038193-ED 24 16W 24 DDCB	1000.00	300.00	3 G	A86	-99.0260	37.9432	-62344.	119420.	9.47	2.23	10	3	1
038481-SF 21 12W 17 ADBB	1200.00	240.00	3 G	A87	-98.6600	38.2276	-30243.	150976.	6.46	29.91	7	30	1
038552-SF 21 12W 17 DDBB	1200.00	240.00	3 G	A87	-98.6600	38.2203	-30250.	150153.	6.85	29.59	7	30	1
038451-SF 21 13W 24 DDBB	1200.00	240.00	3 G	A87	-98.6966	38.2055	-33439.	148517.	6.42	27.41	7	28	1
038512-SF 22 12W 19 DBCD	600.00	26.00	2 G	A87	-98.6816	38.1195	-32170.	138915.	11.58	24.35	12	25	1
038646-SF 22 14W 12 DABB	1100.00	240.00	3 G	A87	-98.8064	38.1519	-43026.	142579.	5.63	20.48	6	21	1
038494-SF 23 13W 2 CABB	800.00	87.36	5 G	A87	-98.7237	38.0789	-35857.	134397.	12.36	20.83	13	21	1
038722-SF 24 14W 16 ADBB	1100.00	110.00	3 G	A87	-98.8616	37.9667	-47962.	121946.	13.77	10.18	14	11	1
038657-SF 24 15W 13 CBBC	11.67	18.81	2 G	A87	-98.9302	37.9625	-53961.	121509.	11.67	7.10	12	8	1
038612-ED 24 16W 16 DDBB	1200.00	240.00	3 G	A87	-99.0809	37.9595	-67129.	121281.	6.72	.63	7	1	1
038503-SF 25 14W 11 BDBB	1200.00	240.00	3 G	A87	-98.8337	37.8940	-45569.	113813.	18.64	8.22	19	9	1
038943-RC 21 9W 7 BACC	1000.00	220.50	3 G	A88	-98.3566	38.2432	-3839.	152661.	15.79	43.36	16	44	1
039056-SF 21 13W 1 CDBB	1200.00	240.00	3 G	A88	-98.7055	38.2494	-34191.	153420.	3.75	28.93	4	29	1
038743-SF 21 13W 10 DABB	800.00	120.00	3 G	A88	-98.7332	38.2386	-36610.	152226.	3.40	27.30	4	28	1
038833-SF 21 13W 10 DDBB	800.00	120.00	3 G	A88	-98.7333	38.2349	-36615.	151816.	3.60	27.14	4	28	1
039066-SF 21 13W 11 DDBB	1200.00	240.00	3 G	A88	-98.7148	38.2348	-35012.	151797.	4.22	27.91	5	28	1
039070-SF 21 13W 12 BDBB	1200.00	240.00	3 G	A88	-98.7056	38.2421	-34201.	152604.	4.14	28.61	5	29	1
039080-SF 21 13W 12 CDBB	1200.00	240.00	3 G	A88	-98.7056	38.2348	-34210.	151790.	4.53	28.29	5	29	1
038740-SF 21 13W 15 ACCC	800.00	120.00	3 G	A88	-98.7379	38.2249	-37028.	150705.	3.98	26.51	4	27	1
038840-SF 21 13W 15 ADBB	800.00	120.00	3 G	A88	-98.7333	38.2276	-36623.	151002.	3.99	26.82	4	27	1
038834-SF 21 13W 15 BDBB	800.00	120.00	3 G	A88	-98.7426	38.2277	-37427.	151017.	3.67	26.44	4	27	1
038742-SF 21 13W 15 BDCC	800.00	120.00	3 G	A88	-98.7426	38.2250	-37430.	150712.	3.82	26.32	4	27	1
038831-SF 21 13W 16 BDBB	800.00	120.00	3 G	A88	-98.7610	38.2279	-39031.	151047.	3.04	25.67	4	26	1
038955-SF 21 13W 22 ADBB	1200.00	240.00	3 G	A88	-98.7334	38.2131	-36635.	149376.	4.78	26.19	5	27	1
039132-SF 22 12W 19 DBCD	.00	127.20	2 G	A88	-98.6816	38.1195	-32170.	138915.	11.58	24.35	12	25	1
038921-SF 22 13W 34 CCCC	1200.00	229.50	3 G	A88	-98.7467	38.0872	-37867.	135330.	11.14	20.21	12	21	1
039131-SF 23 12W 33 CDBB	1100.00	240.00	3 G	A88	-98.6498	38.0021	-29447.	125804.	19.01	20.64	20	21	1
039092-SF 23 13W 7 ADBB	1000.00	240.00	3 G	A88	-98.7881	38.0682	-41482.	133231.	10.77	17.65	11	18	1
039077-SF 23 13W 7 BDBB	1000.00	195.00	3 G	A88	-98.7972	38.0682	-42277.	133239.	10.46	17.27	11	18	1

Appendix 1. Well data (cont.)

(a) Well ID, township, range, section, quarter-section	(b) Rate (gpm)	(c) Approp (ac-ft)	(d) Use code	(e) Year	(f, g) Longitude (deg)	(f, g) Latitude (deg)	(h, i) Albers x (m)	(h, i) Albers y (m)	(j, k) Grid row/col. (mi)	(l, m) Grid index row/col	(n) cell activ.
039061-SF 23 13W 18 BDBB	1000.00	236.00	3 G	A88	-98.7973	38.0537	-42294.	131615.	11.24 16.64	12 17	1
039114-SF 23 14W 1 CBDD	1000.00	240.00	3 G	A88	-98.8166	38.0765	-43966.	134172.	9.35 16.81	10 17	1
039093-SF 23 14W 1 DBDD	1000.00	205.00	3 G	A88	-98.8074	38.0765	-43165.	134163.	9.67 17.19	10 18	1
039142-SF 23 14W 10 ADCB	800.00	120.00	3 G	A88	-98.8431	38.0666	-46285.	133082.	8.99 15.26	9 16	1
039062-SF 23 14W 13 DDBB	1000.00	240.00	3 G	A88	-98.8065	38.0465	-43100.	130820.	11.32 15.94	12 16	1
038843-SF 23 14W 15 ACCC	1000.00	100.00	3 G	A88	-98.8478	38.0513	-46701.	131375.	9.66 14.41	10 15	1
039067-SF 23 14W 25 DDBB	1200.00	240.00	3 G	A88	-98.8066	38.0175	-43126.	127582.	12.88 14.69	13 15	1
039005-SF 23 14W 27 DACC	1200.00	240.00	3 G	A88	-98.8433	38.0186	-46327.	127728.	11.58 13.19	12 14	1
039163-SF 23 14W 34 B	1000.00	195.00	3 G	A88	-98.8530	38.0110	-47182.	126880.	11.67 12.45	12 13	1
039096-PN 23 15W 13 CDBB	1000.00	171.00	3 G	A88	-98.9259	38.0470	-53517.	130935.	7.26 10.93	8 11	1
039126-SF 24 12W 4 ACBC	1200.00	343.50	3 G	A88	-98.6452	37.9939	-29047.	124882.	19.61 20.48	20 21	1
038914-SF 24 12W 16 DDBB	1200.00	240.00	3 G	A88	-98.6406	37.9584	-28662.	120921.	21.68 19.15	22 20	1
039123-SF 24 12W 21 AABC	1200.00	228.75	3 G	A88	-98.6406	37.9538	-28664.	120414.	21.93 18.96	22 19	1
038925-SF 24 12W 29 ADAB	1000.00	222.00	3 G	A88	-98.6562	37.9366	-30036.	118492.	22.34 17.55	23 18	1
038727-SF 24 14W 16 DCAA	550.00	120.00	3 G	A88	-98.8628	37.9595	-48073.	121141.	14.12 9.82	15 10	1
038771-SF 24 14W 16 DDAA	550.00	120.00	3 G	A88	-98.8582	37.9595	-47669.	121138.	14.27 10.01	15 11	1
039049-SF 24 14W 18 DDBB	1000.00	240.00	3 G	A88	-98.8983	37.9596	-51177.	121172.	12.91 8.32	13 9	1
039045-SF 24 14W 29 DDBB	1000.00	120.00	3 G	A88	-98.8799	37.9305	-49583.	117906.	15.11 7.84	16 8	1
038975-SF 24 15W 8 BCDC	1100.00	225.00	3 G	A88	-99.0013	37.9788	-60154.	123380.	8.38 4.81	9 5	1
039168-SF 24 15W 12 CCAA	1000.00	240.00	3 G	A88	-98.9269	37.9743	-53657.	122830.	11.15 7.76	12 8	1
039057-SF 24 15W 15 ADBB	1000.00	212.00	3 G	A88	-98.9531	37.9671	-55959.	122034.	10.65 6.33	11 7	1
039053-SF 24 15W 15 DDBB	1000.00	258.00	3 G	A88	-98.9531	37.9598	-55961.	121221.	11.04 6.02	12 7	1
039047-SF 24 15W 22 ADCB	1000.00	240.00	3 G	A88	-98.9531	37.9506	-55966.	120199.	11.54 5.63	12 6	1
039046-SF 24 15W 22 DDBB	1000.00	240.00	3 G	A88	-98.9531	37.9451	-55969.	119583.	11.84 5.39	12 6	1
038971-SF 24 15W 26 ADBB	1100.00	240.00	3 G	A88	-98.9346	37.9378	-54365.	118754.	12.86 5.85	13 6	1
039118-SF 25 14W 22 DDBB	1000.00	240.00	3 G	A88	-98.8427	37.8576	-46378.	109755.	20.31 6.27	21 7	1
039541-BT 20 12W 3 CACC	310.00	55.00	3 G	A89	-98.6404	38.3375	-28489.	163227.	1.17 35.45	2 36	1
039288-BT 20 12W 17 BBDB	250.00	97.50	3 G	A89	-98.6792	38.3167	-31876.	160919.	.99 32.93	1 33	1
039248-BT 20 12W 23 CDBB	900.00	172.50	3 G	A89	-98.6217	38.2933	-26881.	158288.	4.19 34.34	5 35	1
039421-RC 21 9W 31 BDBB	900.00	195.00	3 G	A89	-98.3568	38.1842	-3859.	146072.	18.98 40.83	19 41	1
039545-SF 21 11W 8 ADBB	1000.00	203.00	3 G	A89	-98.5496	38.2420	-20630.	152549.	9.39 35.17	10 36	1
039446-SF 21 12W 4 AACC	1000.00	179.00	3 G	A89	-98.6413	38.2578	-28599.	154332.	5.45 31.99	6 32	1
039587-SF 21 12W 19 DDAB	1200.00	216.00	3 G	A89	-98.6763	38.2056	-31671.	148526.	7.10 28.27	8 29	1
039585-SF 21 12W 31 BDBB	1200.00	201.00	3 G	A89	-98.6876	38.1838	-32662.	146094.	7.90 26.86	8 27	1
039480-SF 21 12W 32 ADBB	950.00	195.00	3 G	A89	-98.6603	38.1838	-30291.	146080.	8.82 28.01	9 29	1

Appendix 1. Well data (cont.)

(a) Well ID, township, range, section, quarter-section	(b) Rate (gpm)	(c) Approp (ac-ft)	(d) Use code	(e) Year	(f, g) Longitude (deg)	(f, g) Latitude (deg)	(h, i) Albers x (m)	(h, i) Albers y (m)	(j, k) Grid row/col. (mi)	(l, m) Grid index row/col	(n) cell activ.
039753-SF 21 12W 33 BDBB	1000.00	190.00	3 G	A89	-98.6512	38.1837	-29492.	146071.	9.13 28.39	10 29	1
039426-SF 21 13W 10 BDAB	600.00	120.00	3 G	A89	-98.7401	38.2423	-37210.	152643.	2.97 27.17	3 28	1
039586-SF 21 13W 26 BDBB	1200.00	216.00	3 G	A89	-98.7242	38.1984	-35843.	147733.	5.88 25.95	6 26	1
039435-SF 21 13W 31 ACBB	1600.00	222.00	3 G	A89	-98.7930	38.1846	-41843.	146228.	4.31 22.46	5 23	1
039434-SF 21 13W 31 DDBB	1000.00	120.00	3 G	A89	-98.7885	38.1773	-41456.	145409.	4.85 22.33	5 23	1
039476-RN 22 9W 8 CDBB	900.00	195.00	3 G	A89	-98.3387	38.1476	-2280.	141984.	21.58 40.03	22 41	1
039602-SF 22 13W 5 ADDB	400.00	13.16	3 G	A89	-98.7679	38.1680	-39669.	144361.	6.05 22.80	7 23	1
039393-SF 23 13W 16 BDBB	.00	15.00	3 G	A89	-98.7604	38.0535	-39079.	131584.	12.49 18.18	13 19	1
039710-SF 23 14W 6 CDBC	715.00	181.00	3 G	A89	-98.9075	38.0751	-51895.	134065.	6.36 12.92	7 13	1
039218-PN 23 15W 14 A	800.00	180.00	3 G	A89	-98.9356	38.0547	-54355.	131800.	6.51 10.86	7 11	1
899028-PN 23 15W 30 CAAA	300.00	17.31	2 G	A89	-99.0135	38.0215	-61184.	128152.	5.66 6.14	6 7	1
039793-PN 23 16W 20 CDBB	1000.00	98.00	3 G	A89	-99.1084	38.0322	-69454.	129411.	1.87 2.61	2 3	1
039790-PN 23 16W 33 CDBB	1000.00	195.00	3 G	A89	-99.0902	38.0032	-67892.	126158.	4.06 2.13	5 3	1
039353-PN 23 17W 25 BACC	1000.00	240.00	3 G	A89	-99.1449	38.0258	-72649.	128726.	.98 .80	1 1	1
039419-SF 24 13W 22 BDBB	1000.00	195.00	3 G	A89	-98.7414	37.9517	-37474.	120208.	18.64 14.60	19 15	1
039192-SF 24 14W 31 CDBB	1200.00	201.00	3 G	A89	-98.9071	37.9159	-51973.	116303.	14.97 6.07	15 7	1
039321-SF 24 15W 3 BDBB	800.00	195.00	3 G	A89	-98.9625	37.9963	-56755.	125300.	8.75 7.20	9 8	1
039495-ED 24 16W 17 ADBB	900.00	198.00	3 G	A89	-99.0992	37.9668	-68713.	122101.	5.71 .17	6 1	1
039751-SF 25 14W 12 BDBB	1000.00	166.00	3 G	A89	-98.8153	37.8939	-43964.	113799.	19.27 9.00	20 9	1
900076-RC 21 10W 12 CB BB	60.00	1.07	2 G	A90	-98.3794	38.2388	-5826.	152161.	15.27 42.21	16 43	1
900119-SF 21 11W 18 BCDD	60.00	.92	2 G	A90	-98.5780	38.2248	-23108.	150630.	9.37 33.24	10 34	1
900075-SF 21 11W 18 CACB	60.00	1.07	2 G	A90	-98.5769	38.2220	-23011.	150325.	9.55 33.17	10 34	1
900157-SF 21 11W 18 DABC	60.00	1.07	2 G	A90	-98.5679	38.2230	-22227.	150434.	9.80 33.59	10 34	1
039914-SF 21 12W 18 CDDD	1000.00	195.00	3 G	A90	-98.6840	38.2174	-32337.	149844.	6.20 28.46	7 29	1
039894-SF 21 12W 19 BACC	1000.00	166.00	3 G	A90	-98.6874	38.2137	-32636.	149435.	6.29 28.15	7 29	1
039890-SF 21 12W 19 CDBB	1200.00	195.00	3 G	A90	-98.6875	38.2055	-32650.	148518.	6.73 27.80	7 28	1
039898-SF 21 12W 20 BDBB	1000.00	195.00	3 G	A90	-98.6693	38.2129	-31061.	149337.	6.94 28.88	7 29	1
039906-SF 21 12W 20 CDBB	1000.00	98.00	3 G	A90	-98.6694	38.2056	-31072.	148524.	7.33 28.56	8 29	1
900036-SF 21 12W 26 DDDD	50.00	.76	2 G	A90	-98.6015	38.1882	-25162.	146560.	10.56 30.68	11 31	1
039889-SF 21 12W 30 ADBB	1200.00	195.00	3 G	A90	-98.6786	38.1983	-31875.	147713.	7.42 27.86	8 28	1
039907-SF 21 12W 30 CDBB	1000.00	98.00	3 G	A90	-98.6876	38.1910	-32659.	146900.	7.51 27.17	8 28	1
900006-SF 21 13W 6 ADCB	100.00	.30	2 G	A90	-98.7884	38.2552	-41402.	154104.	.64 25.69	1 26	1
039912-SF 21 13W 15 AADA	800.00	120.00	3 G	A90	-98.7298	38.2294	-36318.	151199.	4.01 27.04	5 28	1
039913-SF 21 13W 15 BAAD	800.00	120.00	3 G	A90	-98.7391	38.2304	-37122.	151316.	3.65 26.70	4 27	1
900173-SF 21 13W 22 CACA	50.00	.76	2 G	A90	-98.7415	38.2077	-37345.	148780.	4.79 25.62	5 26	1

159

Appendix 1. Well data (cont.)

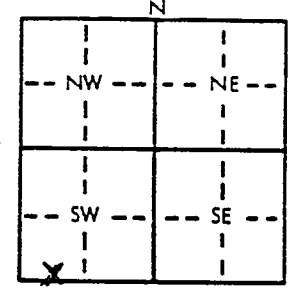
(a) Well ID, township, range, section, quarter-section				(b) Rate (gpm)	(c) Approp (ac-ft)	(d) Use code	(e) Year	(f, g) Longitude (deg) Latitude (deg)		(h, i) Albers x (m) Albers y (m)		(j, k) Grid row/col. (mi)		(l, m) Grid index row/col		(n) cell activ.		
039892-SF	21	13W	23	CCAA	1000.00	195.00	3	G	A90	-98.7253	38.2057	-35938.	148547.	5.45	26.21	6	27	1
039893-SF	21	13W	23	DDBB	1000.00	195.00	3	G	A90	-98.7150	38.2055	-35037.	148529.	5.80	26.64	6	27	1
039915-SF	21	13W	24	CDBB	1000.00	195.00	3	G	A90	-98.7058	38.2055	-34238.	148520.	6.11	27.03	7	28	1
900161-SF	22	11W	7	DCDA	85.00	.57	2	G	A90	-98.5695	38.1451	-22391.	141741.	13.97	30.17	14	31	1
900170-SF	22	11W	7	DDAA	85.00	.64	2	G	A90	-98.5649	38.1469	-21991.	141936.	14.03	30.44	15	31	1
900140-SF	22	11W	7	DDCD	120.00	.60	2	G	A90	-98.5672	38.1442	-22192.	141634.	14.10	30.23	15	31	1
900128-SF	22	11W	10	BBBD	100.00	.30	2	G	A90	-98.5259	38.1567	-18593.	143026.	14.80	32.51	15	33	1
900107-SF	22	11W	18	ABAD	100.00	.30	2	G	A90	-98.5695	38.1424	-22392.	141436.	14.12	30.06	15	31	1
900129-SF	22	11W	18	DDCD	100.00	.30	2	G	A90	-98.5672	38.1298	-22198.	140027.	14.87	29.61	15	30	1
900106-SF	22	12W	17	DAAD	100.00	.30	2	G	A90	-98.6564	38.1357	-29968.	140712.	11.55	26.10	12	27	1
900146-SF	22	12W	29	ACAD	60.00	.92	2	G	A90	-98.6609	38.1102	-30375.	137872.	12.78	24.82	13	25	1
039879-SF	22	13W	11	A	1200.00	186.00	3	G	A90	-98.7155	38.1553	-35107.	142928.	8.50	24.46	9	25	1
900150-SF	22	14W	27	BBCD	100.00	.30	2	G	A90	-98.8556	38.1130	-47342.	138267.	6.06	16.74	7	17	1
039867-SF	23	12W	16	CACB	1000.00	210.00	3	G	A90	-98.6502	38.0474	-29460.	130860.	16.54	22.57	17	23	1
039865-SF	23	13W	9	C	1250.00	126.00	3	G	A90	-98.7610	38.0613	-39123.	132446.	12.06	18.49	13	19	1
900165-SF	23	13W	14	CDCD	100.00	1.53	2	G	A90	-98.7224	38.0434	-35765.	130434.	14.33	19.35	15	20	1
900123-SF	23	13W	28	BCCD	50.00	.76	2	G	A90	-98.7639	38.0218	-39401.	128045.	14.09	16.67	15	17	1
900077-SF	23	14W	9	CABD	100.00	.30	2	G	A90	-98.8697	38.0640	-48602.	132810.	8.24	14.03	9	15	1
900178-SF	23	14W	9	CBAD	60.00	.92	2	G	A90	-98.8720	38.0641	-48803.	132813.	8.16	13.94	9	14	1
900002-SF	23	14W	13	CACA	100.00	1.53	2	G	A90	-98.8145	38.0484	-43794.	131034.	10.95	15.69	11	16	1
900113-SF	24	14W	15	DBCC	100.00	.85	2	G	A90	-98.8477	37.9603	-46757.	121221.	14.58	10.49	15	11	1
039881-SF	24	14W	34	C	1000.00	195.00	3	G	A90	-98.8526	37.9163	-47210.	116313.	16.80	8.39	17	9	1
039888-SF	25	14W	12	BDBB	1000.00	29.00	3	G	A90	-98.8153	37.8939	-43964.	113799.	19.27	9.00	20	9	1

Appendix 2. Well records for the Sittner and Figger sites

1 LOCATION OF WATER WELL: County: **STAFFORD** Fraction: **SW 1/4 SW 1/4 SW 1/4** Section Number: **1** Township Number: **T 23 S** Range Number: **R 12 E**

Distance and direction from nearest town or city street address of well if located within city?
7 miles North of Stafford, KS

2 WATER WELL OWNER: **LEE FIGGER/KANSAS GEOLOGICAL SURVEY**
 RR#, St. Address, Box #: **(STAFFORD, KS) 1930 CONSTANT AVE**
 City, State, ZIP Code: **LAURENCE, KS 66047**
 Board of Agriculture, Division of Water Resources
 Application Number:

3 LOCATE WELL'S LOCATION WITH AN "X" IN SECTION BOX:

 4 DEPTH OF COMPLETED WELL: **125** ft. ELEVATION: **1825** ft.
 Depth(s) Groundwater Encountered 1. ft. 2. ft. 3. ft.
 WELL'S STATIC WATER LEVEL **5.2** ft. below land surface measured on **mo/day/yr 07/03/90**
 Pump test data: Well water was ft. after hours pumping gpc
 Est. Yield gpm: Well water was ft. after hours pumping gpc
 Bore Hole Diameter **10** in. to ft., and in. to ft.
 WELL WATER TO BE USED AS:
 1 Domestic 3 Feedlot 6 Oil field water supply 9 Dewatering 12 Other (Specify below)
 2 Irrigation 4 Industrial 7 Lawn and garden only **10** Observation well
 Was a chemical/bacteriological sample submitted to Department? Yes.....No........; If yes, mo/day/yr sample was submitted
 Water Well Disinfected? Yes No

5 TYPE OF BLANK CASING USED:
 1 Steel 3 RMP (SR) 5 Wrought iron 8 Concrete tile CASING JOINTS: Glued Clamped
2 PVC 4 ABS 6 Asbestos-Cement 9 Other (specify below) Welded
 7 Fiberglass Threaded
 Blank casing diameter **5** in. to ft., Dia in. to ft., Dia in. to ft.
 Casing height above land surface **36** in., weight lbs./ft. Wall thickness or gauge No. **schedule 40**
 TYPE OF SCREEN OR PERFORATION MATERIAL:
 1 Steel 3 Stainless steel 5 Fiberglass 7 PVC 10 Asbestos-cement
 2 Brass 4 Galvanized steel 6 Concrete tile 8 RMP (SR) **11** Other (specify) **PVC screen**
 9 ABS 12 None used (open hole)
 SCREEN OR PERFORATION OPENINGS ARE:
 1 Continuous slot **3** Mill slot 5 Gauzed wrapped 8 Saw cut 11 None (open hole)
 2 Louvered shutter 4 Key punched 6 Wire wrapped 9 Drilled holes
 7 Torch cut 10 Other (specify)
 SCREEN-PERFORATED INTERVALS: From **15** ft. to **125** ft., From ft. to ft.
 From ft. to ft., From ft. to ft.
 GRAVEL PACK INTERVALS: From **14** ft. to **125** ft., From ft. to ft.
 From ft. to ft., From ft. to ft.

6 GROUT MATERIAL: 1 Neat cement 2 Cement grout 3 Bentonite 4 Other **bentonite pellets and baroid holes**
 Grout intervals: From **0** ft. to **14** ft., From **125** ft. to **138.5** ft., From ft. to ft.
 What is the nearest source of possible contamination:
 1 Septic tank 4 Lateral lines 7 Pit privy 10 Livestock pens 14 Abandoned water well
 2 Sewer lines 5 Cess pool 8 Sewage lagoon 11 Fuel storage **15** Oil well/Gas well
 3 Watertight sewer lines 6 Seepage pit 9 Feedyard 12 Fertilizer storage 16 Other (specify below)
 13 Insecticide storage
 Direction from well? How many feet?

FROM	TO	LITHOLOGIC LOG	FROM	TO	LITHOLOGIC LOG
0	5	Fine Sandy Loam			
5	14	Clay loam			
14	38	subrounded Fine Gravel and coarse sand with minor clay			
38	89	arkosic medium coarse and v. coarse sand with yellowish-brown clay stringers and carbonate nodules			
89	126	Fine Gravel and v. coarse sand with yellow clay stringers and carbonate nodules			
126	138.5	Permian red siltstone mixed (especially in upper depths) with F. Gravel and C. Sand probably cavings from above.			

7 CONTRACTOR'S OR LANDOWNER'S CERTIFICATION: This water well was (1) constructed, (2) reconstructed, or (3) plugged under my jurisdiction and was completed on (mo/day/year) **05/26/90** and this record is true to the best of my knowledge and belief. Kansas Water Well Contractor's License No. This Water Well Record was completed on (mo/day/yr) **07/11/90** under the business name of **KANSAS GEOL. SURVEY** by (signature) *[Signature]*

INSTRUCTIONS: Use typewriter or ball point pen. PLEASE PRESS FIRMLY and PRINT clearly. Please fill in blanks, underline or circle the correct answers. Send top three copies to Kansas Department of Health and Environment, Office of Oil Field and Environmental Geology, Regulation and Permitting Section, Topeka, Kansas 66620-7560, Telephone: 913-862-9360. Send one to WATER WELL OWNER and retain one for your records.

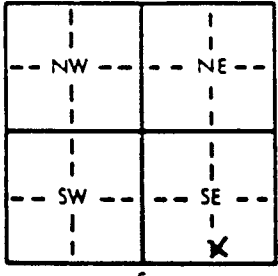
LOCATION OF WATER WELL: Fraction SW 1/4 SE 1/4 SE 1/4 Section Number 36 Township Number T 21 S Range Number R 12

Distance and direction from nearest town or city street address of well if located within city?

14 mi North of Stafford, KS

WATER WELL OWNER: MARYIN SITTNER/KANSAS GEOLOGICAL SURVEY
Address: (HUDSON, KS) 1930 CONSTANT AVE LAWRENCE, KS 66047
Board of Agriculture, Division of Water Resources
Application Number:

LOCATE WELL'S LOCATION WITH AN "X" IN SECTION BOX: DEPTH OF COMPLETED WELL: 111 ft. ELEVATION: 18.06 ft.



Depth(s) Groundwater Encountered 1... ft. 2... ft. 3... ft.
WELL'S STATIC WATER LEVEL ... 15.4 ft. below land surface measured on mo/day/yr 07/03/90
Pump test data: Well water was ... ft. after ... hours pumping
Est. Yield ... gpm: Well water was ... ft. after ... hours pumping
Bore Hole Diameter ... 10 in. to ... ft., and ... in. to ... ft.
WELL WATER TO BE USED AS: 5 Public water supply 8 Air conditioning 11 Injection well
1 Domestic 3 Feedlot 6 Oil field water supply 9 Dewatering 12 Other (Specify below)
2 Irrigation 4 Industrial 7 Lawn and garden only 10 Observation well
Was a chemical/bacteriological sample submitted to Department? Yes... No... [checked] If yes, mo/day/yr sample was submitted

TYPE OF BLANK CASING USED: 1 Steel 2 PVC 3 RMP (SR) 4 ABS 5 Wrought iron 6 Asbestos-Cement 7 Fiberglass 8 Concrete tile 9 Other (specify below) CASING JOINTS: Glued [checked] Clamped Welded Threaded
Blank casing diameter ... 5 in. to ... ft., Dia ... in. to ... ft., Dia ... in. to ... ft., Dia ... in. to ... ft.
Casing height above land surface ... 36 in., weight ... lbs./ft. Wall thickness or gauge No. schedule 40

TYPE OF SCREEN OR PERFORATION MATERIAL: 1 Steel 2 Brass 3 Stainless steel 4 Galvanized steel 5 Fiberglass 6 Concrete tile 7 PVC 8 RMP (SR) 9 ABS 10 Asbestos-cement 11 Other (specify) PVC screen 12 None used (open hole)

SCREEN OR PERFORATION OPENINGS ARE: 1 Continuous slot 2 Louvered shutter 3 Mill slot 4 Key punched 5 Gauzed wrapped 6 Wire wrapped 7 Torch cut 8 Saw cut 9 Drilled holes 10 Other (specify) 11 None (open hole)

SCREEN-PERFORATED INTERVALS: From ... 11 ft. to ... 111 ft. From ... ft. to ... ft. From ... ft. to ... ft. From ... ft. to ... ft.
GRAVEL PACK INTERVALS: From ... 10 ft. to ... 111 ft. From ... ft. to ... ft. From ... ft. to ... ft. From ... ft. to ... ft.

GROUT MATERIAL: 1 Neat cement 2 Cement grout 3 Bentonite 4 Other bentonite pellets and bandid hole
Grout intervals: From ... 0 ft. to ... 10 ft. From ... 111 ft. to ... 120.6 ft. From ... ft. to ... ft. From ... ft. to ... ft.

What is the nearest source of possible contamination: 1 Septic tank 2 Sewer lines 3 Watertight sewer lines 4 Lateral lines 5 Cess pool 6 Seepage pit 7 Pit privy 8 Sewage lagoon 9 Feedyard 10 Livestock pens 11 Fuel storage 12 Fertilizer storage 13 Insecticide storage 14 Abandoned water well 15 Oil well/Gas well 16 Other (specify below)

Direction from well? How many feet?

Table with columns: FROM, TO, LITHOLOGIC LOG. Rows describe geological layers: 0-4 Loomy sand, 4-20 Coarse sand and fine gravel, light brown to whitish, calcareous, with clay stringers, 20-30 Coarse sand, brown, calcareous, carbonaceous, granular with minor clay, 30-51 Coarse sand, whitish to light brown, granular, calcareous with minor clay, 51-85 Coarse sand, reddish brown, granular, not as calcareous with minor clay, 85-120 Coarse sand and F.G.M. gravel coarsening with depth with minor clays becoming prominent at 96-99' and 108-110', rounded, carbonaceous, 120-120.6 Permian red siltstone

CONTRACTOR'S OR LANDOWNER'S CERTIFICATION: This water well was: (1) constructed, (2) reconstructed, or (3) plugged under my jurisdiction and completed on (mo/day/year) ... 06/06/90 ... and this record is true to the best of my knowledge and belief. Kar ... later Well Contractor's License No. ... This Water Well Record was completed on (mo/day/yr) 07/10/90 ... under the business name of KANSAS GEOL. SURVEY by (signature)

INSTRUCTIONS: Use typewriter or ball point pen. PLEASE PRESS FIRMLY and PRINT clearly. Please fill in blanks, underline or circle the correct answers. Send top three copies to Kansas Department of Health and Environment, Office of Oil Field and Environmental Geology, Regulation and Permitting Section, Topeka, Kansas 66620-7500, Telephone: 913-862-9360. Send one to WATER WELL OWNER and retain one for your records.

Appendix 3. Chemical analyses of the waters of the Quivira National Wildlife Refuge

APPENDIX 3. QUIVIRA REFUGE WATER CHEMICAL ANALYSES

Location ^a	Date	Fld SpC ^b μS/cm	Lab SpC ^c μS/cm	Fld pH	Lab pH	SiO ₂ ppm	Ca ppm	Mg ppm	Na ppm	K ppm	Sr ppm	CO ₃ ppm	HCO ₃ ppm	SO ₄ ppm	Cl ppm	F ppm	NO ₃ ppm	NH ₄ ppm	PO ₄ ppb	Al ppb	As ppb	B ppb	Cr ppb	Cu ppb	Fe ppb	Mn ppb	Ni ppb	Pb ppb	Se ppb	Zn ppb	Ba ppb	
Rattl Entry	08/31/90	9,570	-	7.95	-	-	-	-	-	-	-	-	-	-	-	-	-	-	-	194	18	258	1.3	1.7	<29	62	2.4	14.0	1	<4	185	
L S Marsh	08/31/90	9,020	-	8.45	-	-	-	-	-	-	-	-	-	-	-	-	-	-	-	274	5	249	4.7	1.9	60	<4	2.9	5.9	14	31	277	
B S Marsh	08/31/90	14,460	-	8.90	-	-	-	-	-	-	-	-	-	-	-	-	-	-	-	425	9	265	1.4	0.8	<29	19	0.8	8.2	21	<4	193	
Rattl Exit	08/31/90	22,300	-	7.50	-	-	-	-	-	-	-	-	-	-	-	-	-	-	-	350	28	655	0.1	1.4	<29	247	0.7	6.3	51	21	119	
Rattl Entry	03/12/91	6,950	7,580	8.15	8.15	9.0	100	27	1,463	3.2	1.28	-	249	236	2,220	0.48	0.5	<0.1	80	47	0	187	0.2	0.5	<29	127	2.7	2.0	3	11	128	
L S Marsh	03/12/91	9,140	9,820	8.20	8.00	0.6	97	37	1,970	7.1	1.55	-	156	322	2,980	0.53	<0.1	0.1	70	54	2	215	0.3	0.4	<29	<4	1.2	1.0	4	27	199	
B S Marsh	03/12/91	15,100	16,500	8.25	8.05	10.0	103	79	3,455	14.0	2.26	-	278	571	5,250	1.00	<0.1	0.2	100	78	2	330	0.2	0.5	30	46	0.4	1.8	4	13	193	
Rattl Exit	03/12/91	20,600	22,600	7.25	7.95	12.0	223	122	4,840	10.0	4.32	-	327	927	7,480	0.60	<0.1	<0.1	20	59	15	552	0.2	0.1	<29	832	0.6	0.0	28	11	75	
165 Rattl Entry	06/21/91	7,020	7,130	8.70	8.55	6.1	79	25	1,362	8.8	1.08	5.9	173	217	2,110	0.54	0.5*	<0.1	50	<79	7	215	0.9	5.6	<21	14	12.0	2.4	5	<4	162	
L S Marsh	06/21/91	8,480	8,420	8.65	8.30	13.0	82	33	1,621	14.0	1.26	-	173	262	2,470	0.62	0.9*	0.1	80	<79	7	252	1.1	6.7	<21	4	8.4	4.1	5	14	208	
B S Marsh	06/21/91	20,000	18,400	9.95	9.65	9.2	52	79	3,903	22.0	1.85	53.0	46	578	6,020	0.96	3.2*	0.2	40	102	6	468	1.3	4.8	<21	4	5.8	4.0	11	5	158	
Rattl Exit	06/21/91	26,000	24,200	7.70	8.00	6.3	193	134	5,167	25.0	4.26	-	203	986	7,920	0.58	0.6*	<0.1	10	81	9	665	1.7	5.8	<21	93	12.0	4.0	8	6	93	
Rattl Entry	09/20/91	14,200	14,700	8.25	8.20	10.0	184	58	3,105	7.6	2.34	-	205	426	4,820	0.39	0.5*	-	30	75	4	314	0.7	8.0	<21	62	12.0	5.4	5	9	164	
L S Marsh	09/21/91	-	-	-	-	-	-	-	-	-	-	-	-	-	-	-	-	-	-	-	-	-	-	-	-	-	-	-	-	-	-	-
B S Marsh	09/20/91	54,400	49,900	8.70	8.40	25.0	212	228	13,100	37.0	6.28	8.1	253	1,830	19,700	1.05	11.0*	-	100	112	13	598	0.6	20.0	<21	7	5.1	4.0	19	6	873	
Rattl Exit	09/20/91	21,000	18,700	8.95	8.75	3.4	128	109	4,088	6.8	3.01	14.0	124	770	6,170	0.65	0.4*	-	30	130	10	523	0.9	19.0	34	15	11.0	4.6	15	<4	100	

a. Rattl = Rattlesnake Creek; L S = Little Salt Marsh; B S = Big Salt Marsh.

b. Field specific conductance.

c. Laboratory specific conductance

*UV screening value

**Appendix 4. X-ray analyses of rock and sediment samples
from the Big Salt Marsh and the bedrock outcrop**

ANALYTICAL REPORT
KANSAS GEOLOGICAL SURVEY X-RAY LABORATORY

KSG X-Ray Laboratory Sample Identification Numbers: 910538-910543

Samples Submitted by: Marios Sophocleous

Date collected (if not known, received): 6/20-6/21/91

Description of Samples:

#1	Bedrock outcrop - Kiowa shale black-gray with white nodules	ASL910538
#2	Bedrock outcrop - Pressure structures above Kiowa Sh.	ASL910539
#3	Bedrock outcrop - Capping rusty sandstone	ASL910540
#4	Stream bed of Salt Creek outlet from Big Salt Marsh black gooey stuff with sulfide smell	ASL910541
#5	Intermittent Big Salt Marsh by Marsh Road Salt crust	ASL910542
#6	Kiowa Shale - black fissile shale	ASL910543

Remarks:

abbr.: dom. - dominate, most or all of sample
maj. - major, more than 10%, usually more than 25%
min. - minor, 5% to 25%, usually 10%-20%
tr. - trace, less than 10%, usually less than 5%

XRF detection limit for Se is approximately 10ppm

Results

#1	XRF: Se below detection XRD: White nodules - Calcite dom., Quartz tr., clay tr. matrix - clay maj., Quartz maj.
#2	XRF: Se below detection XRD: Calcite dom., Quartz tr.
#3	XRF: Se below detection XRD: Goethite maj., Quartz maj.
#4	XRF: Se below detection XRD: Quartz maj., Feldspar maj.
#5	XRF: Se below detection XRD: white crust - Halite dom., Quartz tr. bulk sample - Halite maj., Quartz maj. water insoluble - Quartz maj., feldspar min., calcite min., clay min.
#6	XRF: Se below detection XRD: clay maj., Quartz maj.

Appendix 5. Revised model ground-water and streamflow sensitivities to varying stream-aquifer and input parameters (20 figures)

Aquifer drawdown: vary pumping
Node (12,24) at Hudson

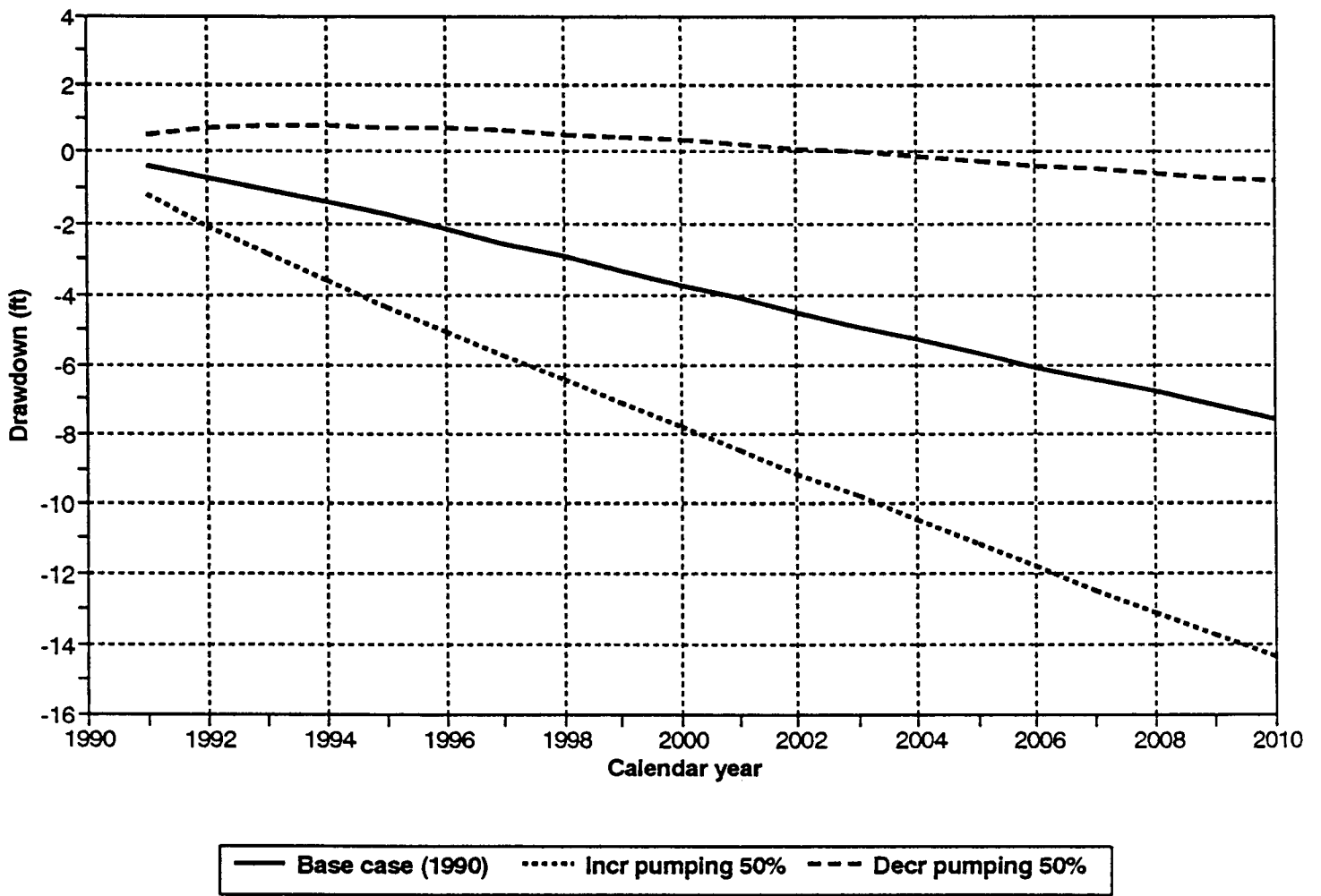


Figure A5-1.

Aquifer drawdown: vary recharge
Node (12,24) at Hudson

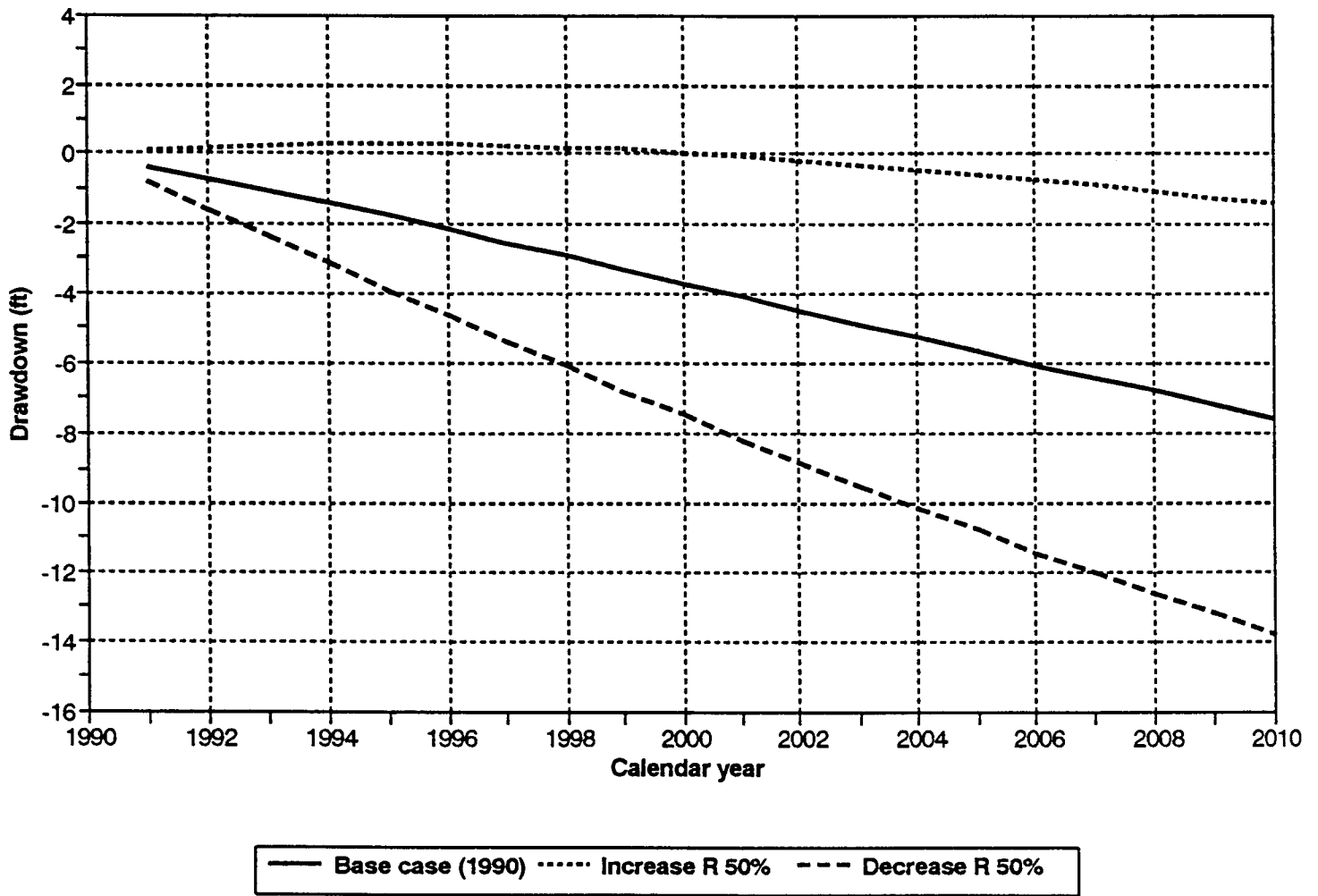


Figure A5-2.

**Aquifer drawdown: vary specific yield
Node (12,24) at Hudson**

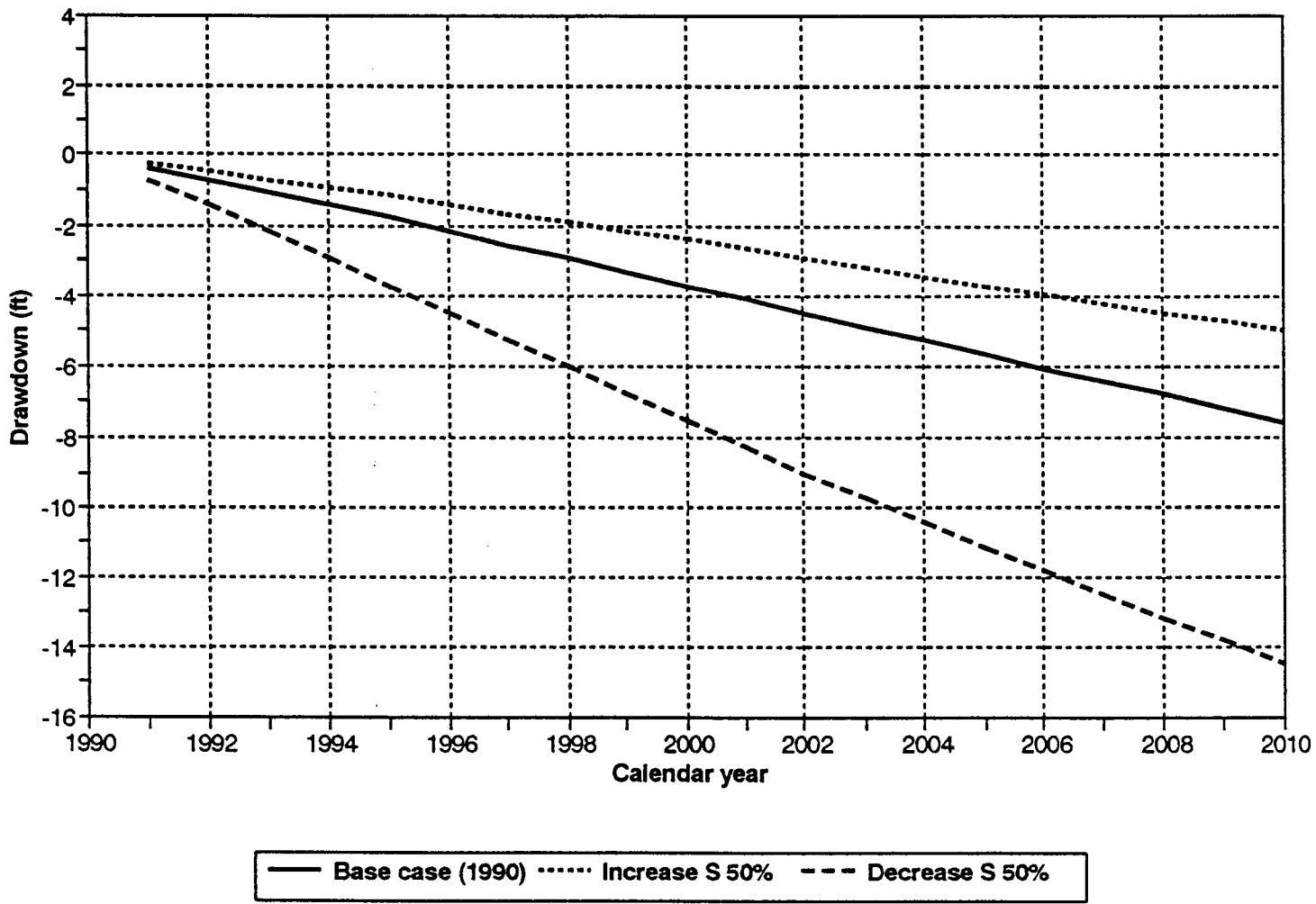


Figure A5-3.

Aquifer drawdown: vary hydraulic cond.
Node (12,24) at Hudson

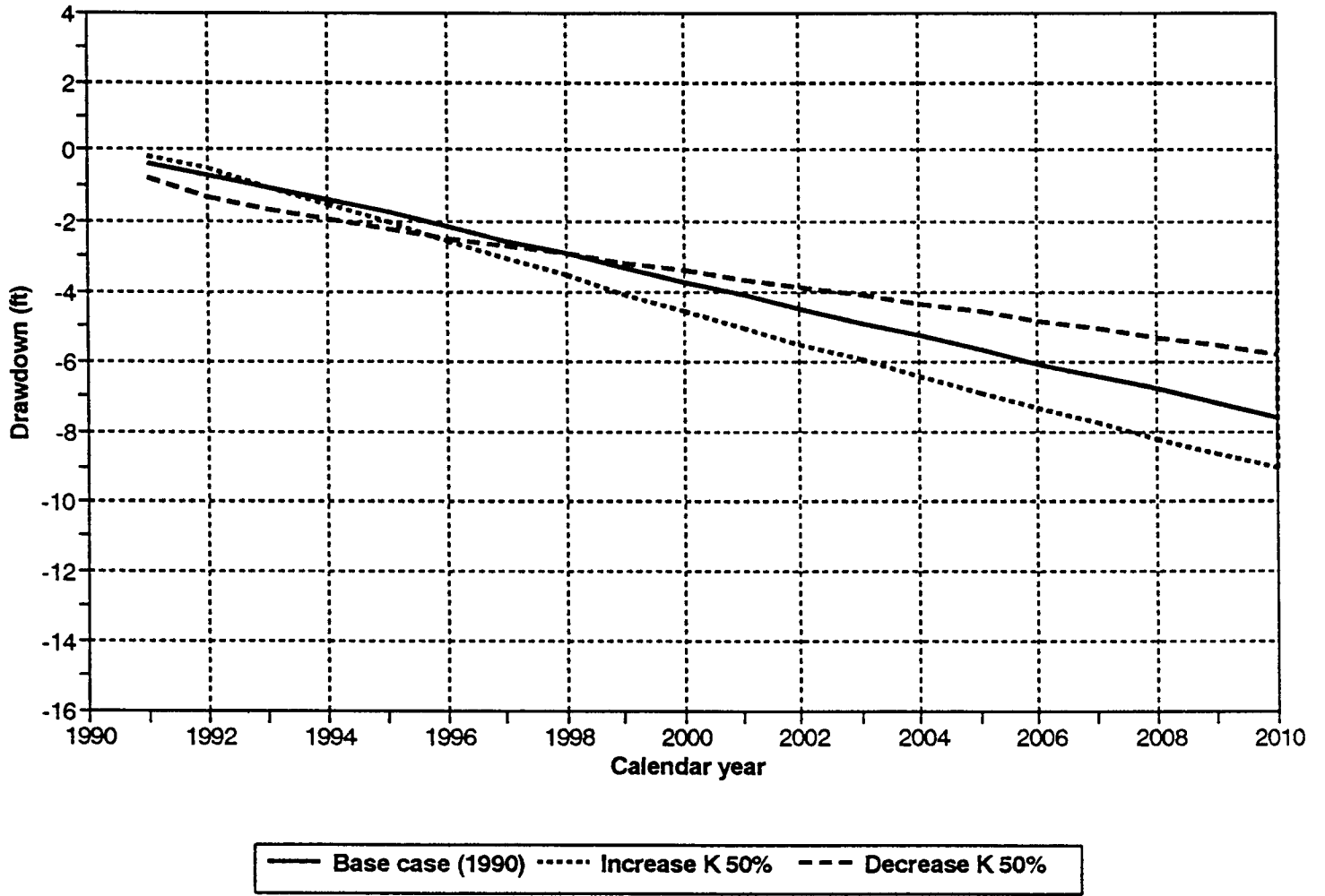


Figure A5-4.

Aquifer drawdown: vary evapotranspir.
Node (12,24) at Hudson

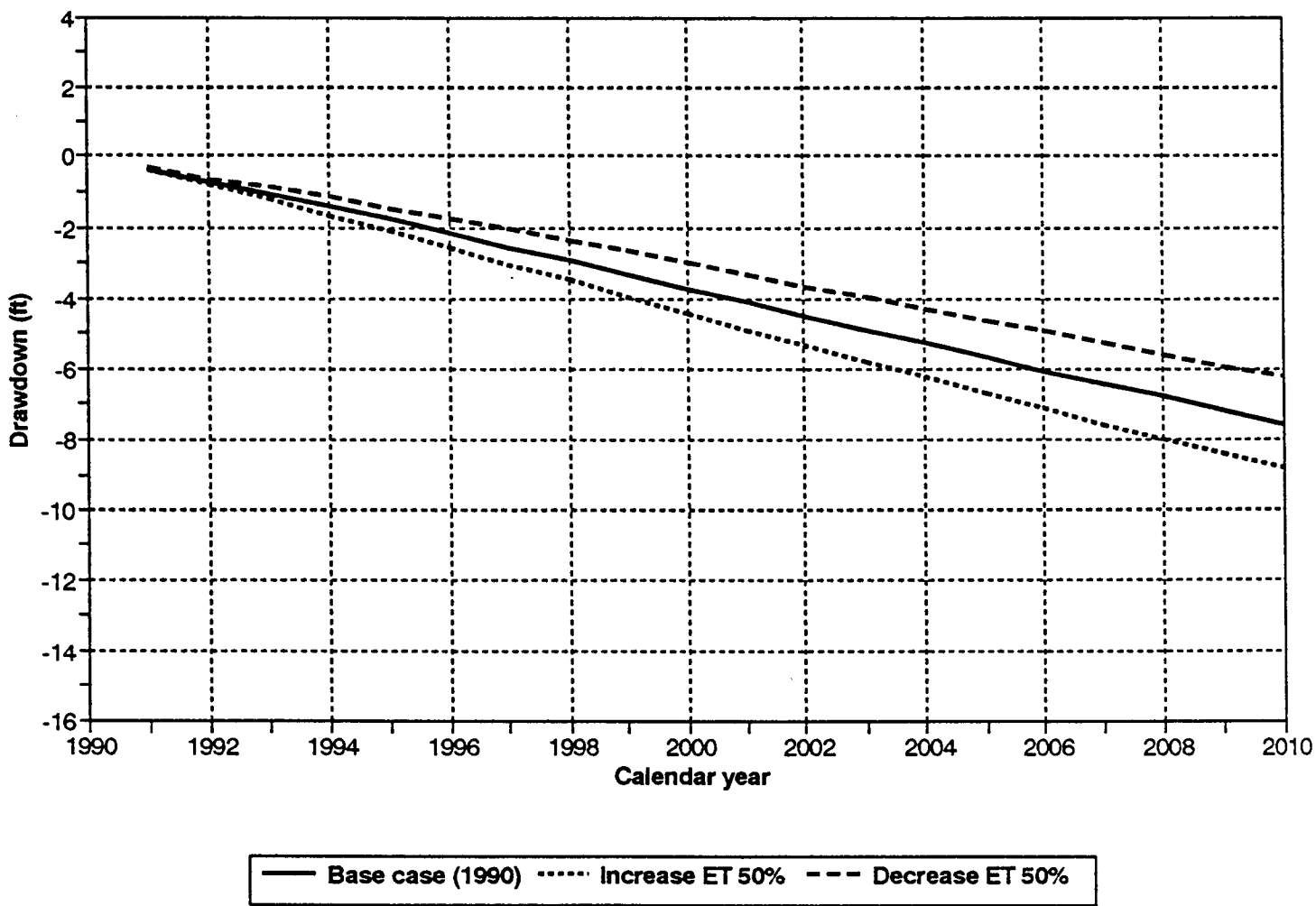


Figure A5-5.

**Rattlesnake streamflow: vary pumping
Node (19,31) at Zenith**

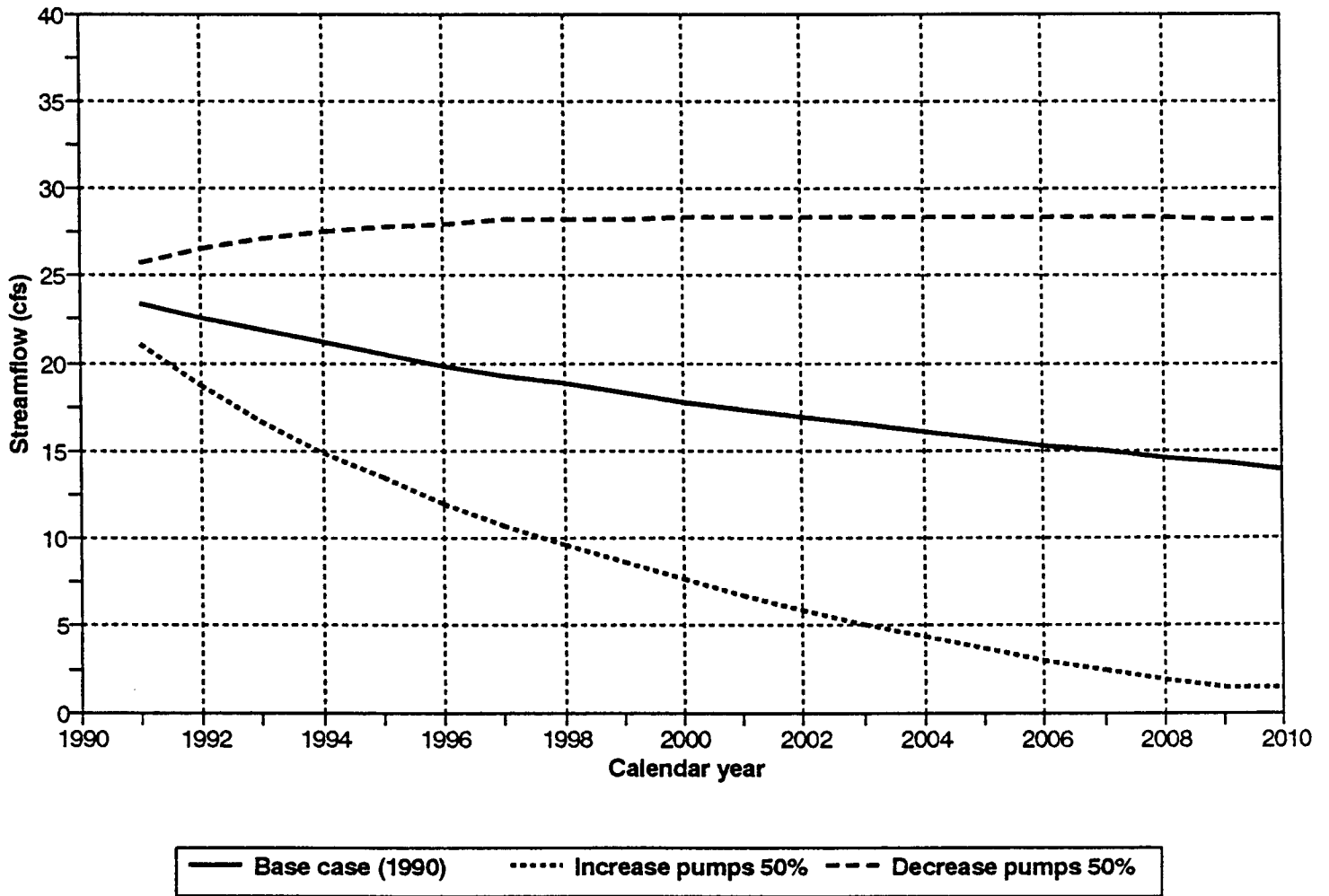


Figure A5-6.

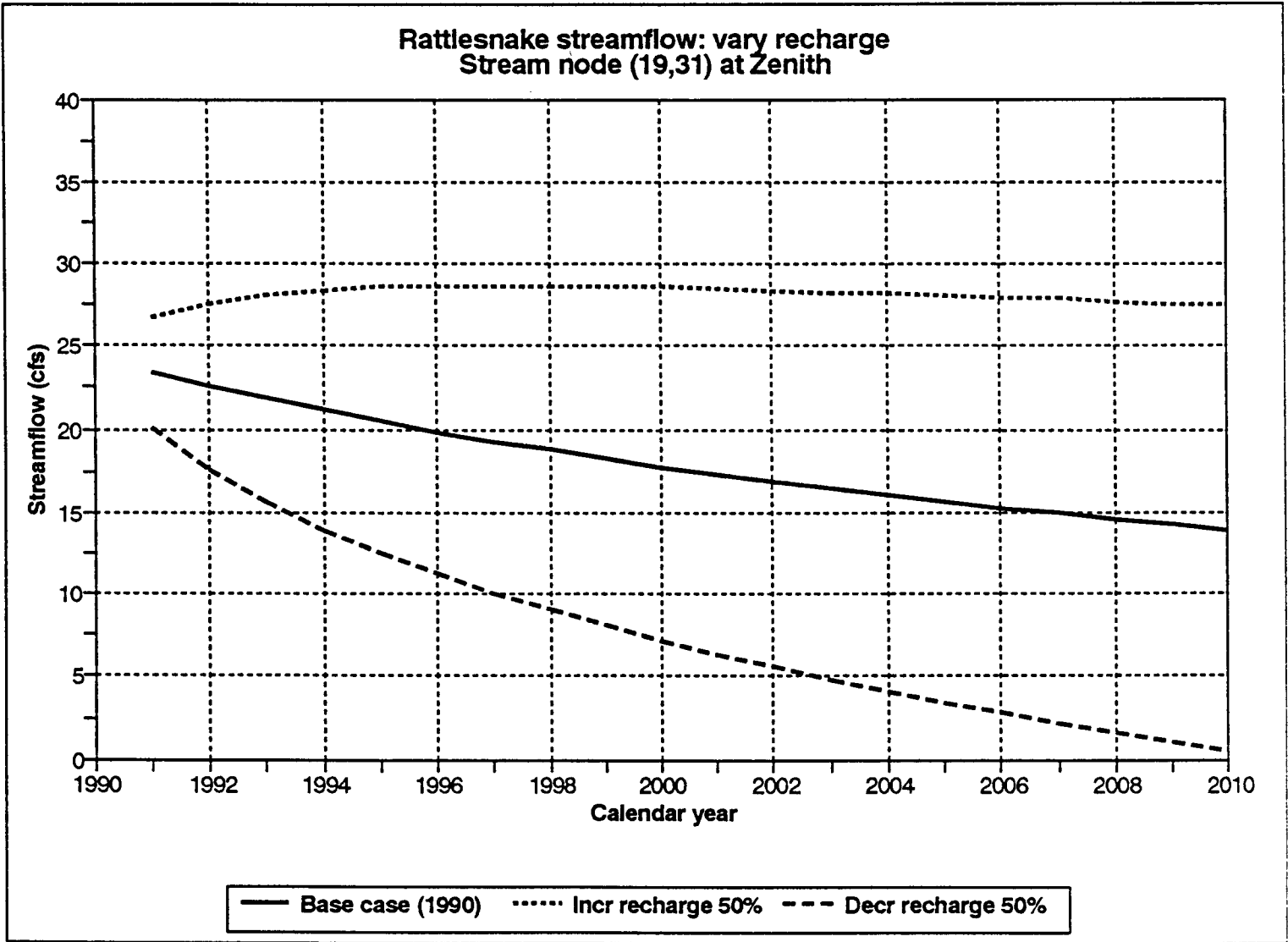


Figure A5-7.

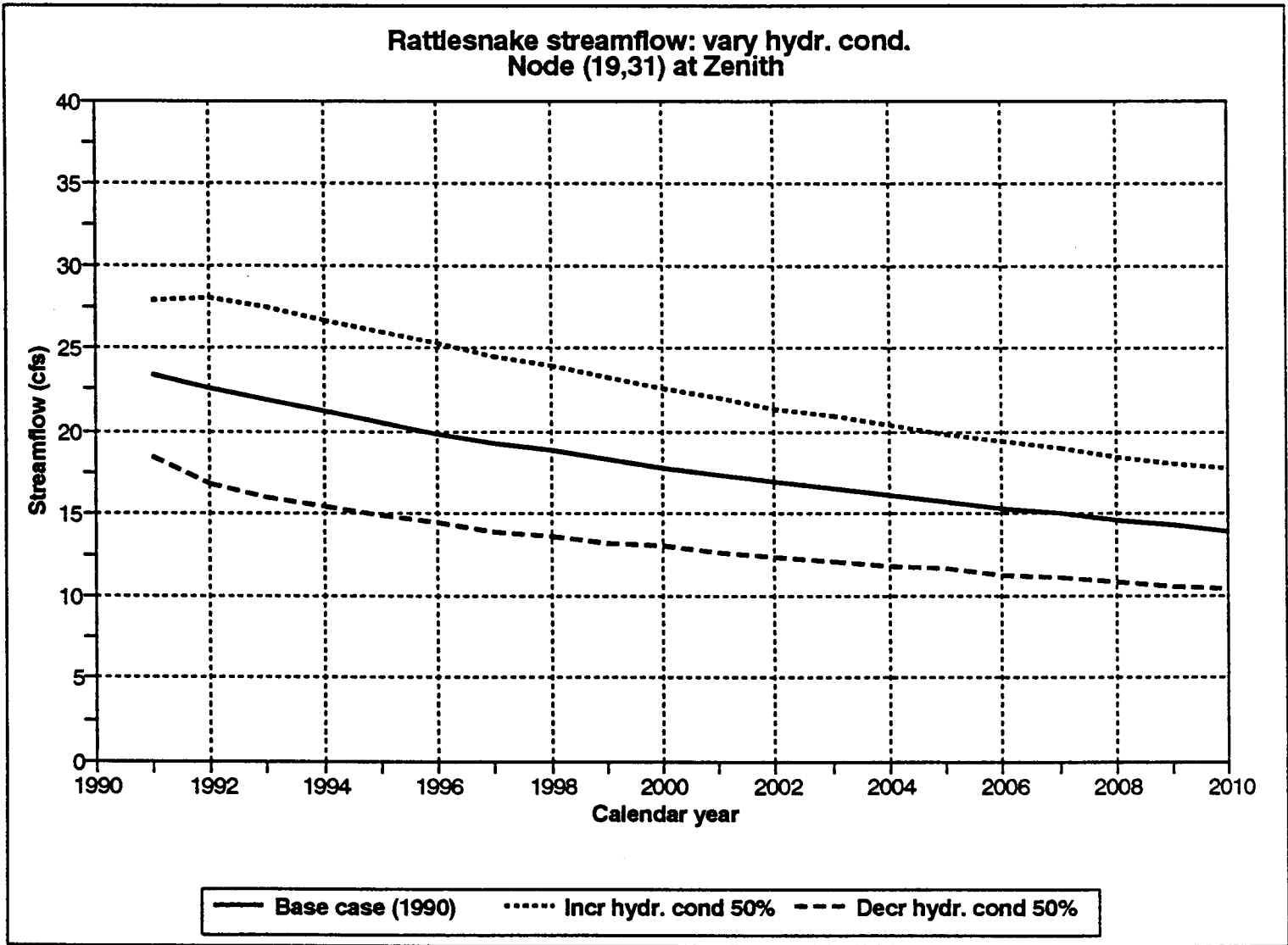


Figure A5-8.

Rattlesnake streamflow: vary storage
Node (19,31) at Zenith

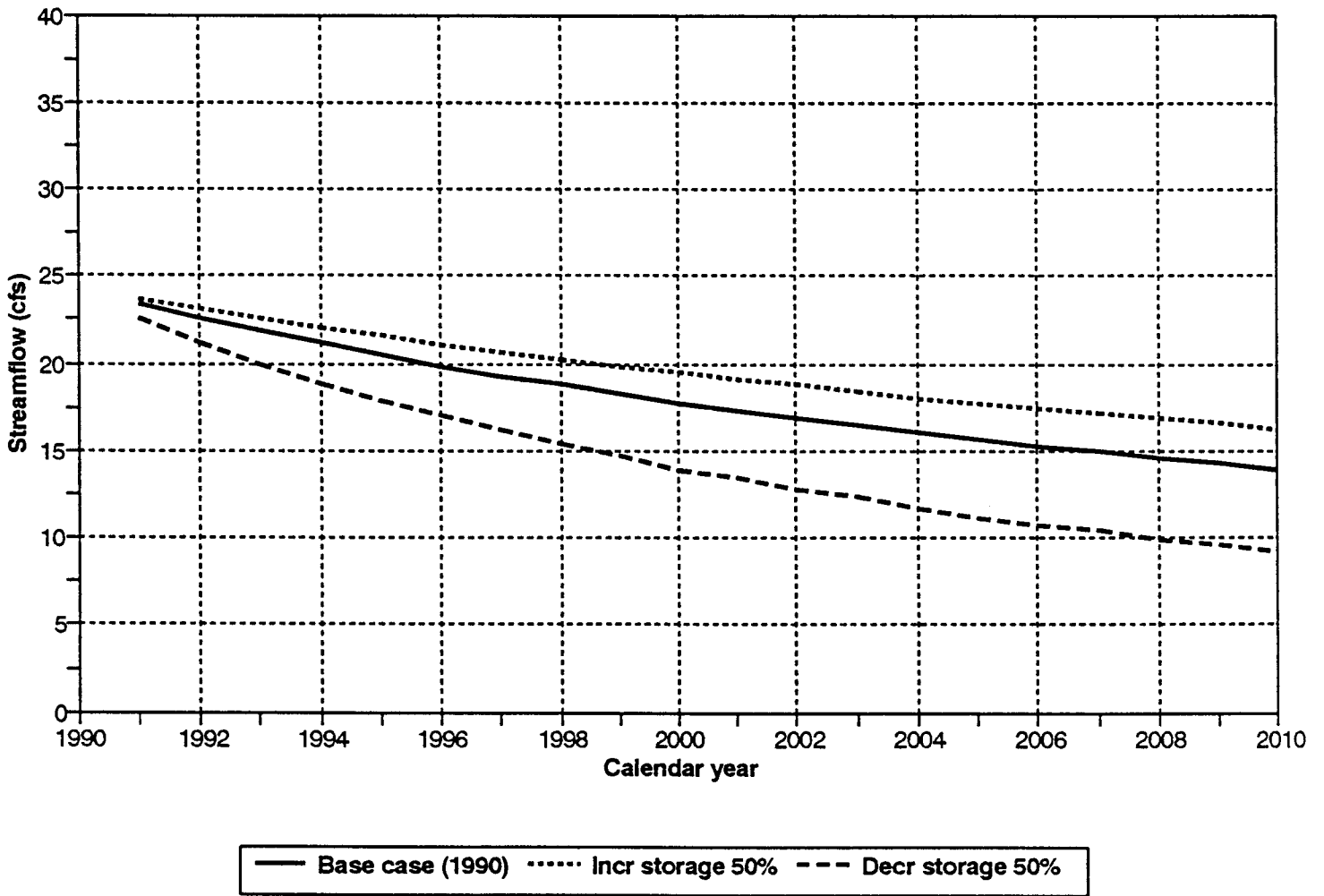


Figure A5-9.

Rattlesnake streamflow: vary evapotrans.
Node (19,31) at Zenith

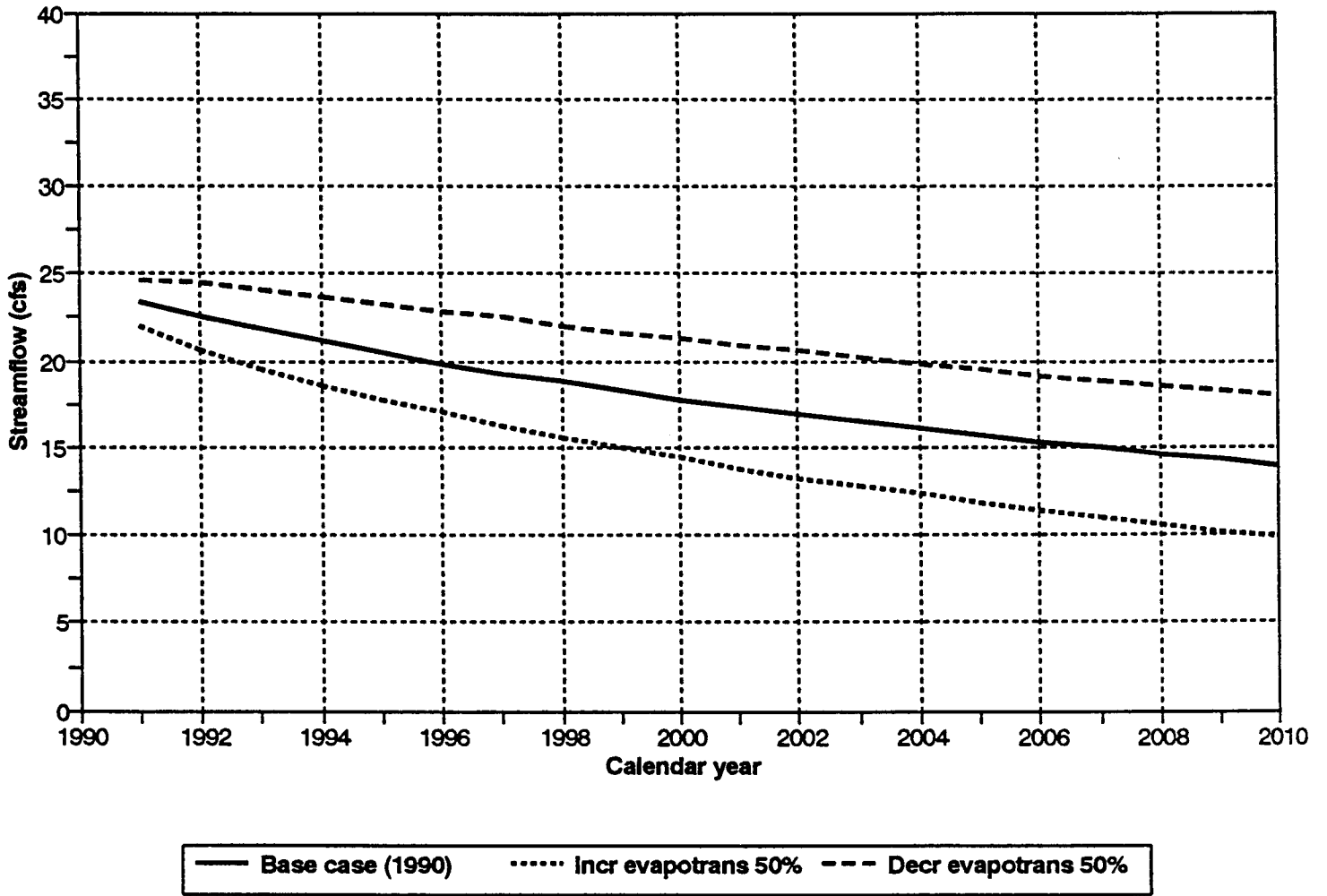
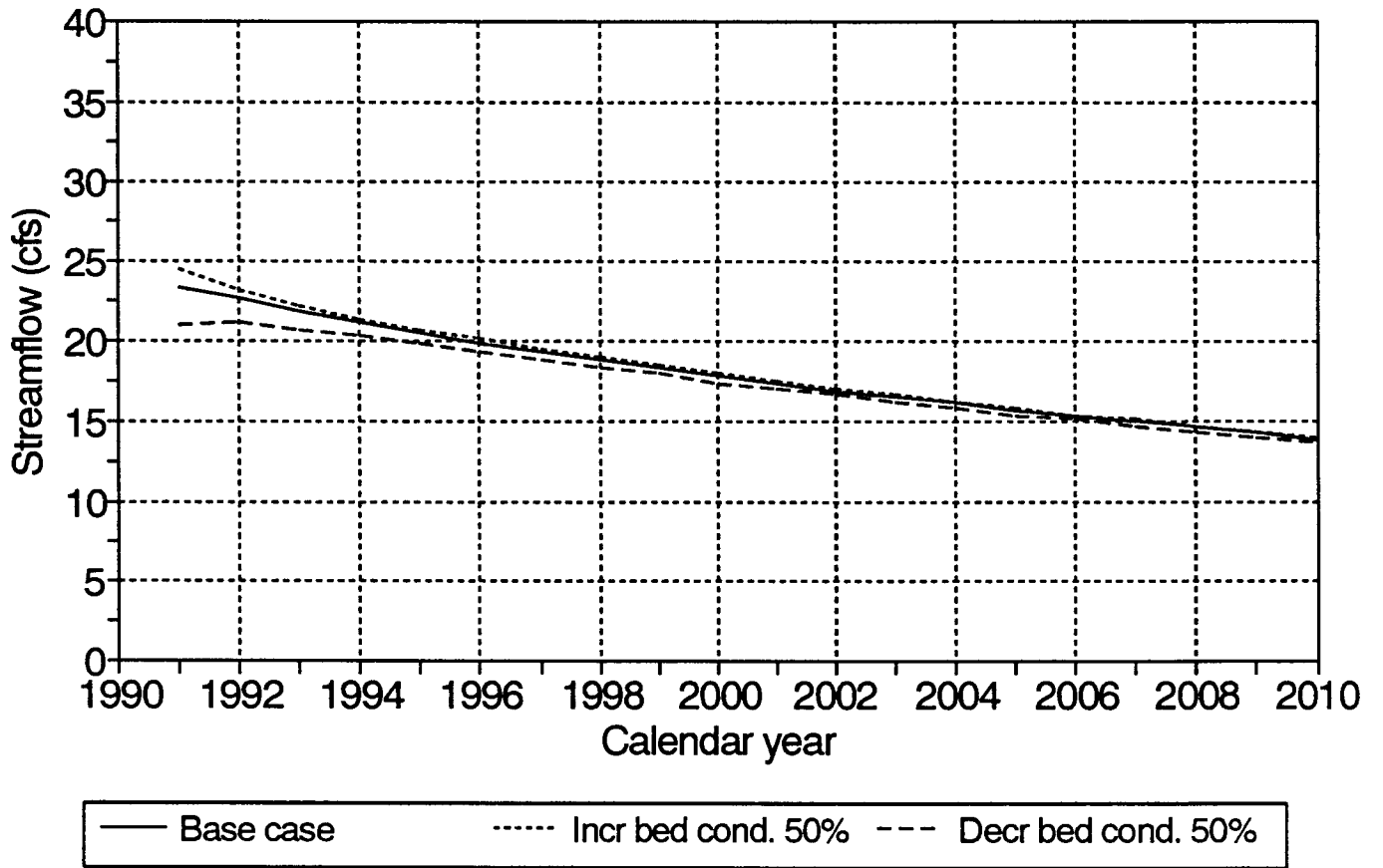


Figure A5-10.

Rattlesnake streamflow: vary bed cond
Node (19,31) at Zenith



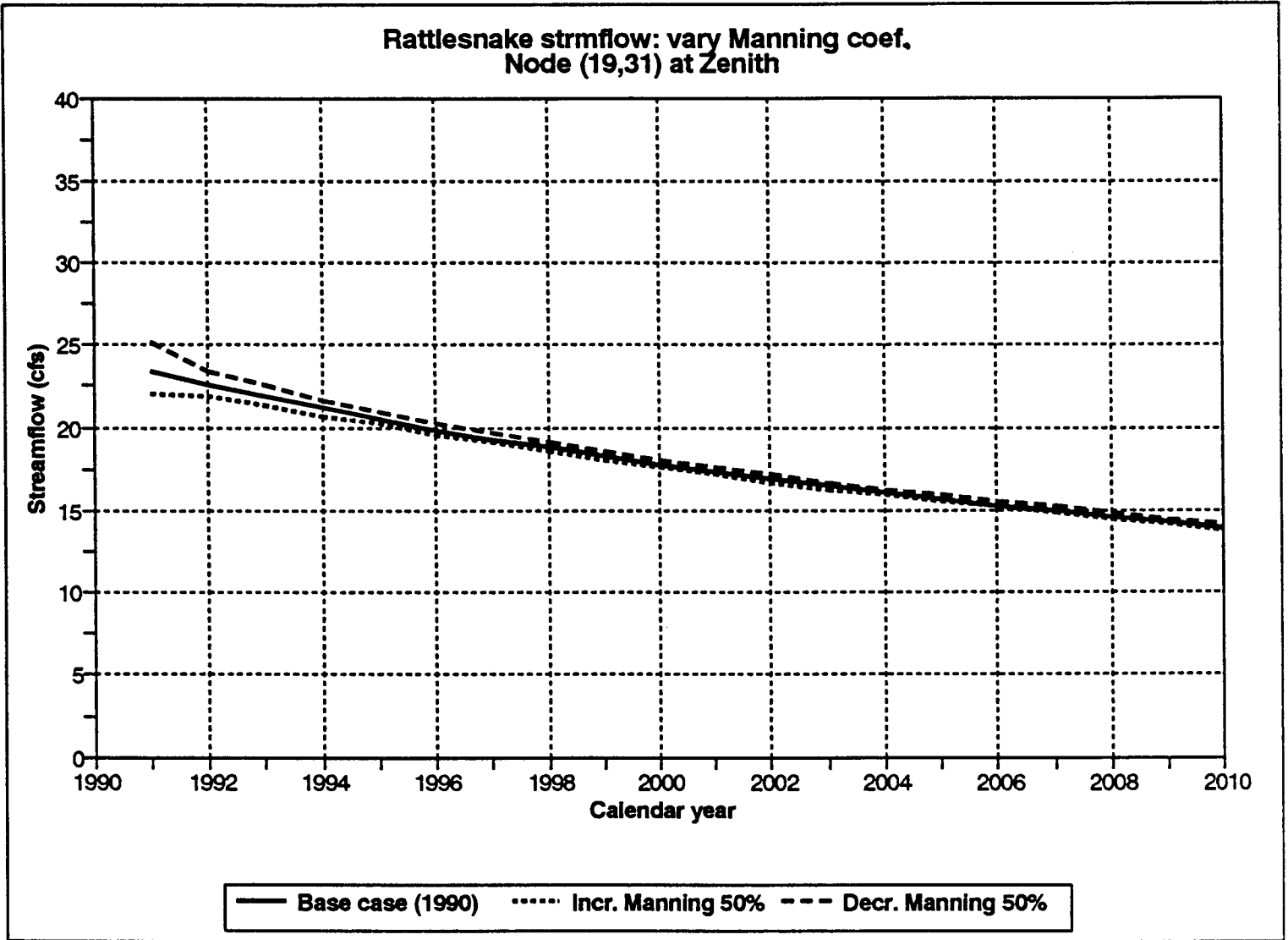


Figure A5-12.

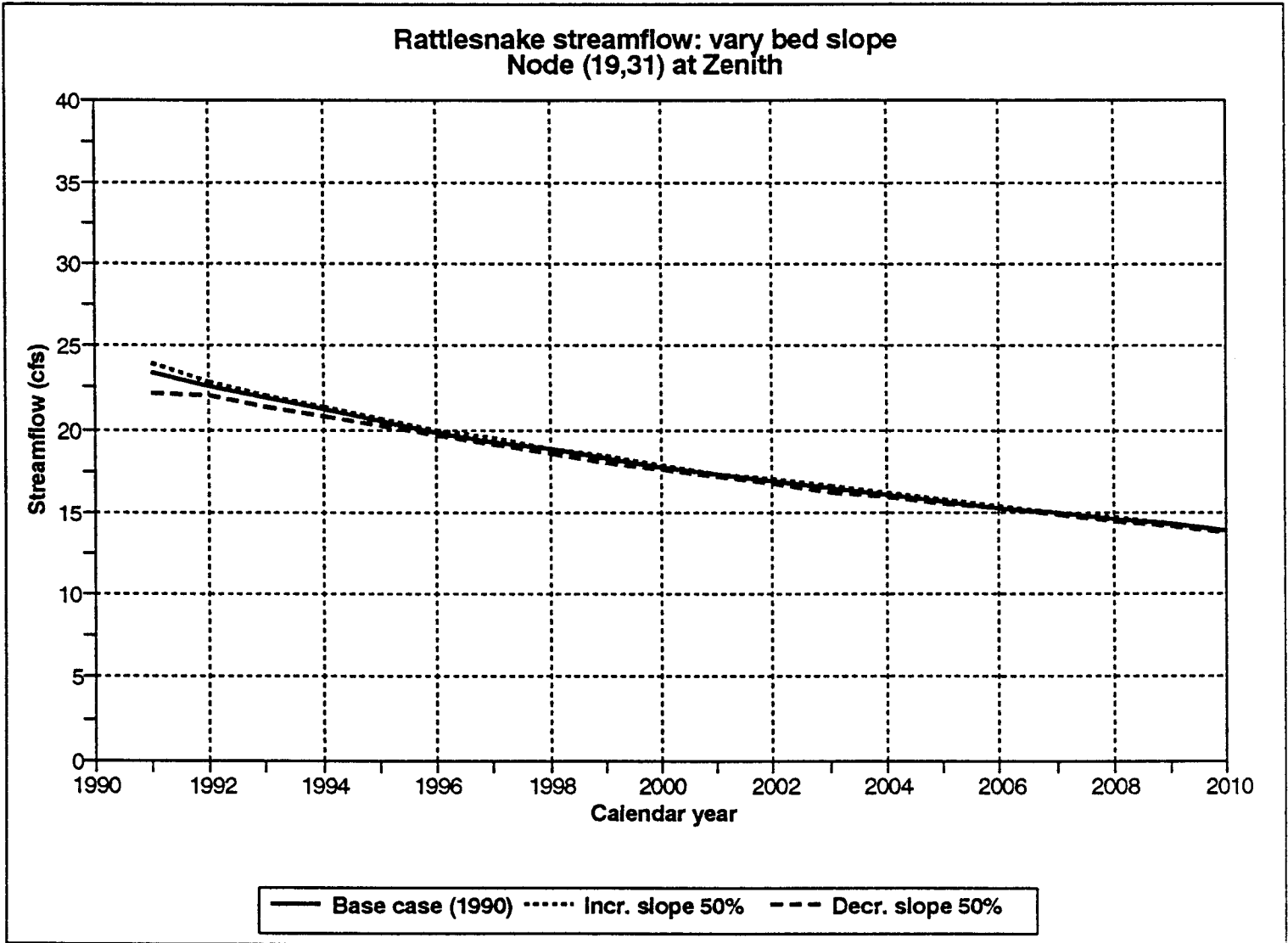


Figure A5-13.

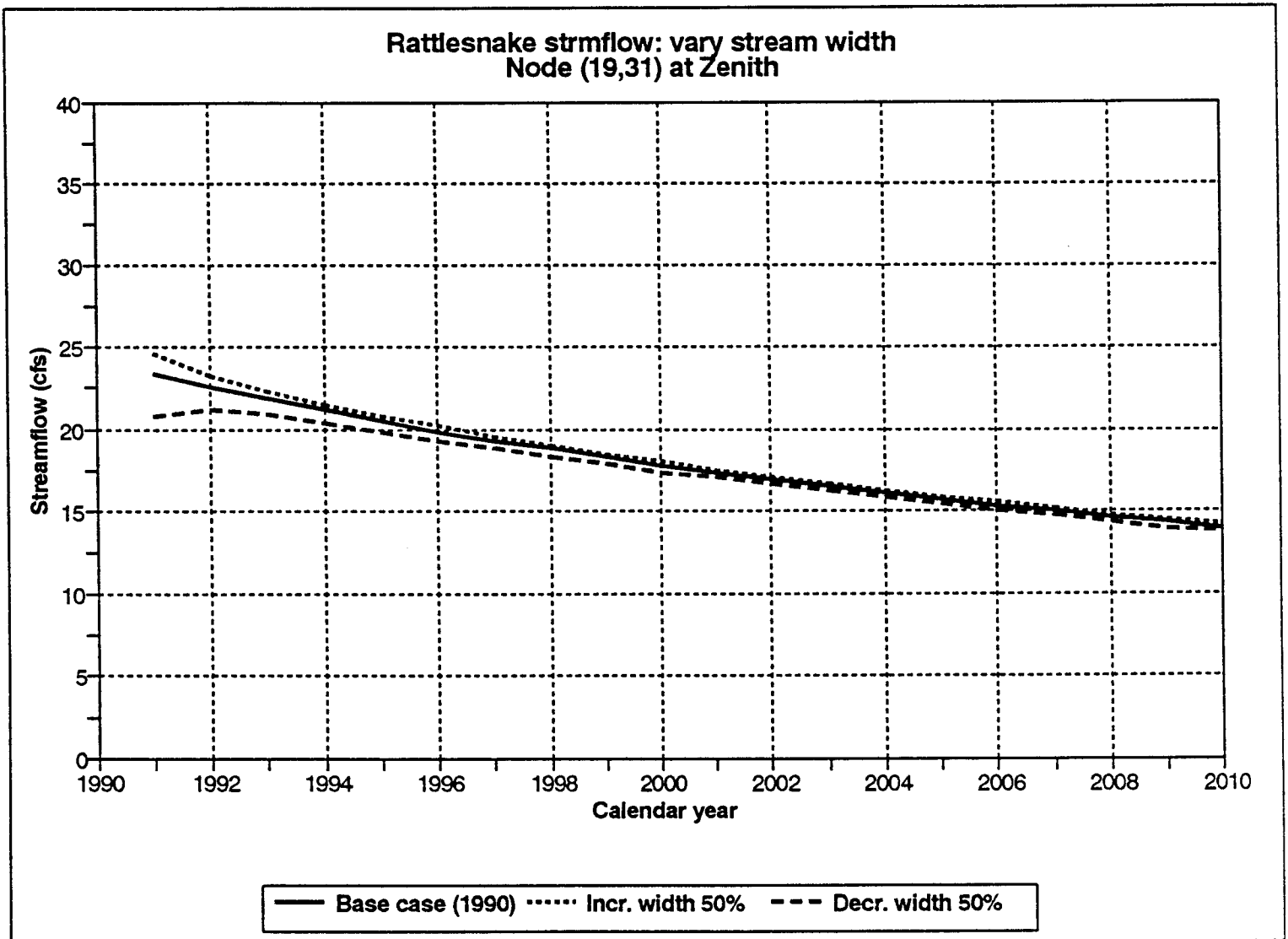


Figure A5-14.

Scaled sensitivities: hydraulic conductivity, zone 2

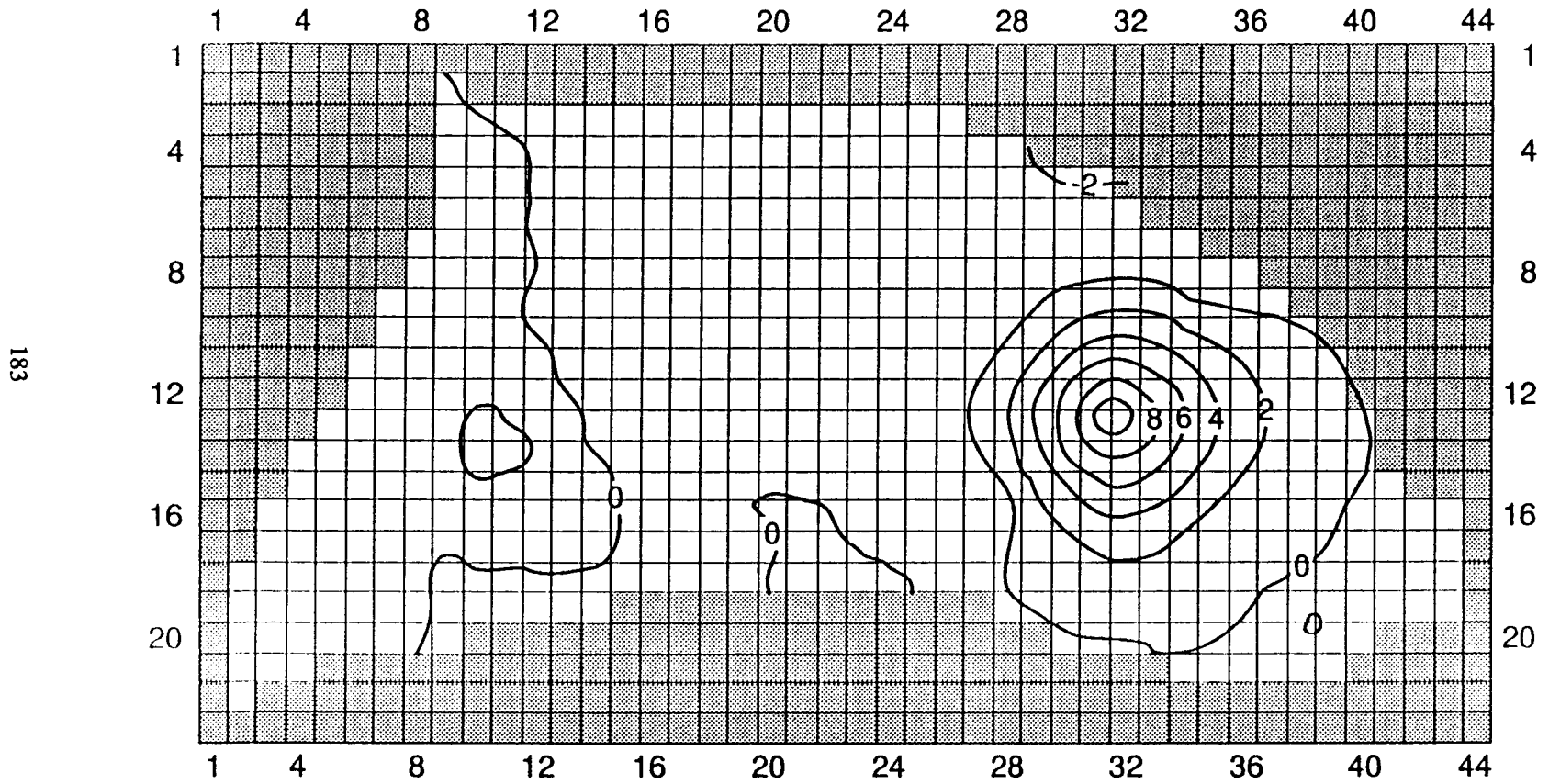
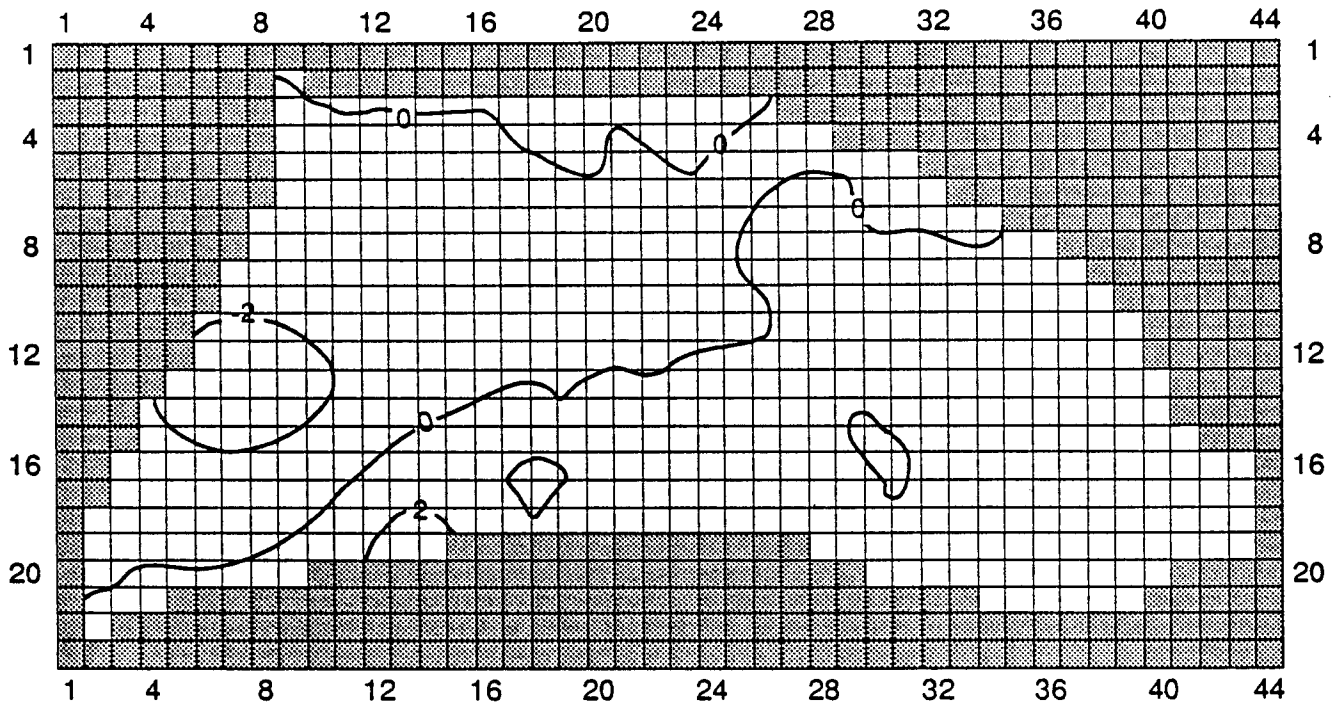


Figure A5-15.

Scaled sensitivities: hydraulic conductivity, zone 3

a



Scaled sensitivities: hydraulic conductivity, zone 3

b

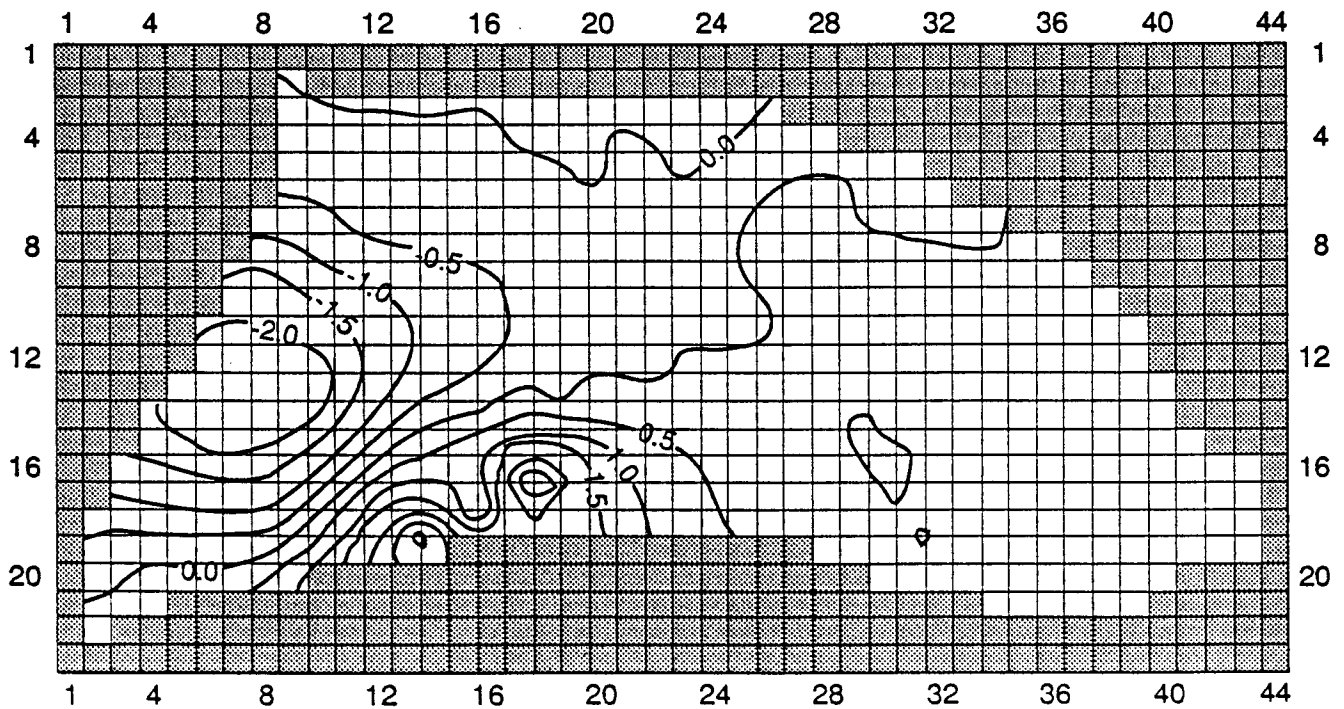


Figure A5-16.

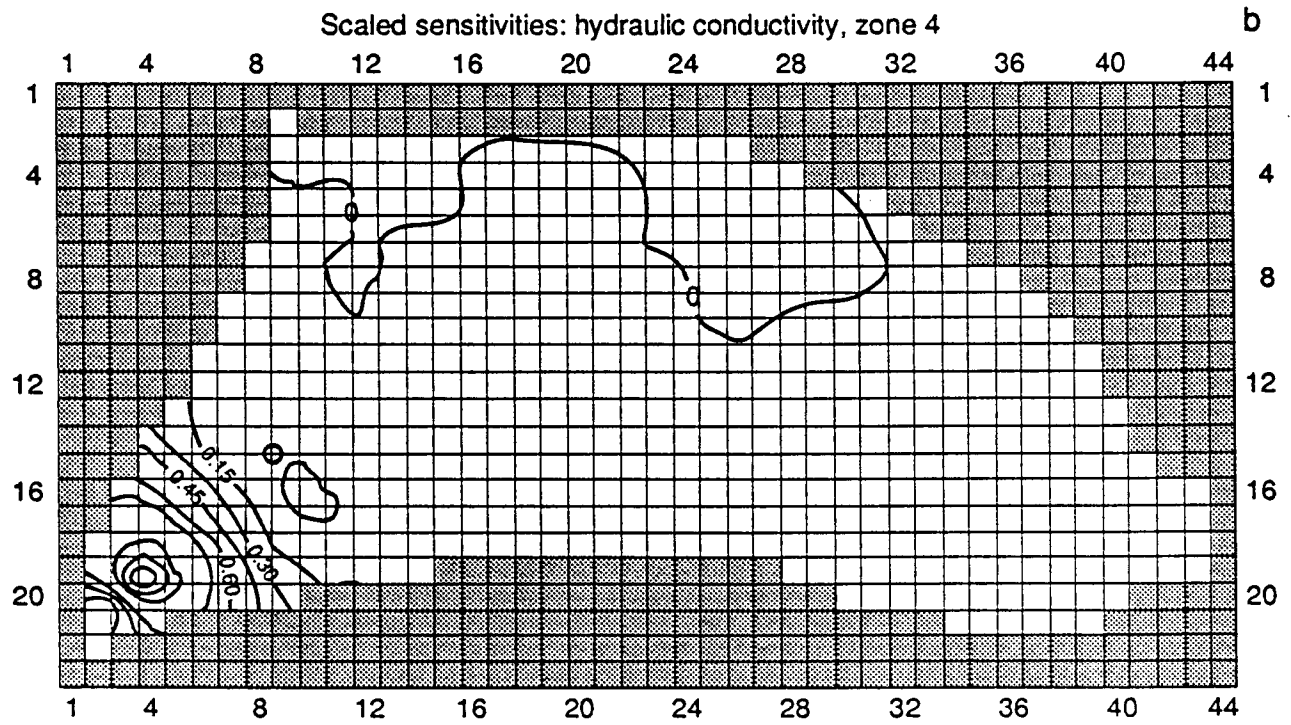
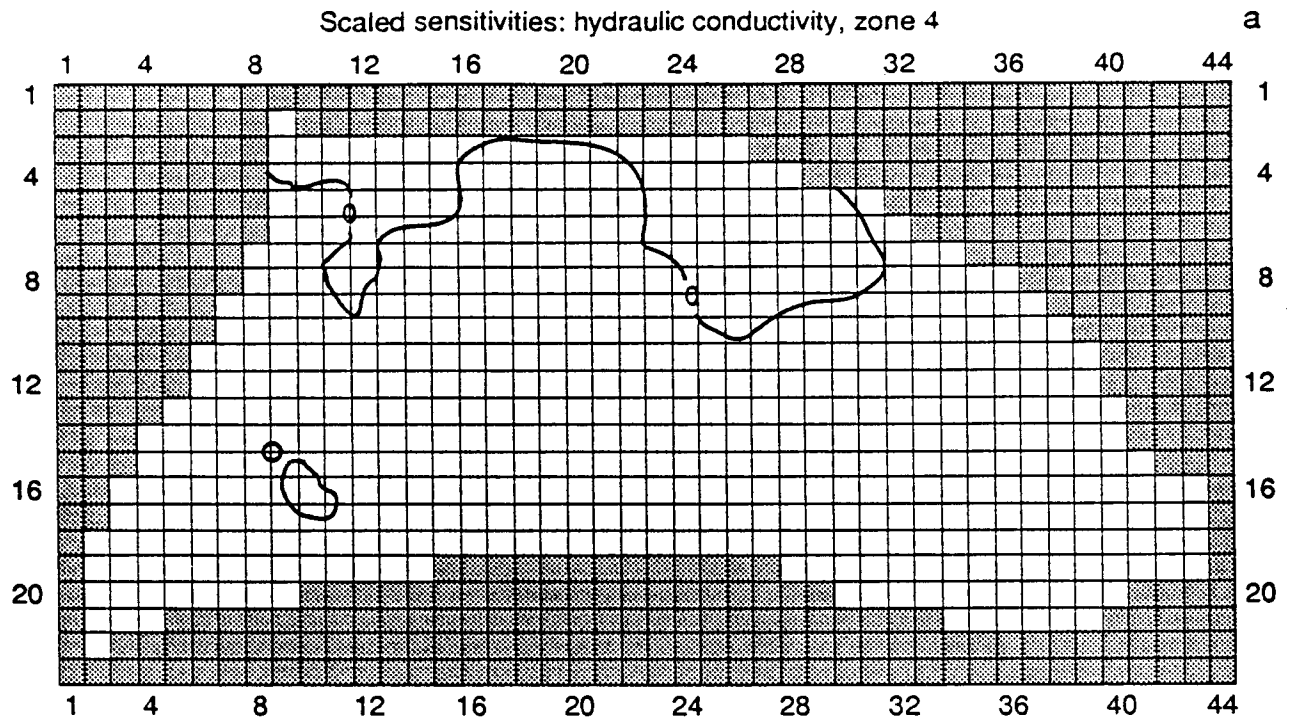


Figure A5-17.

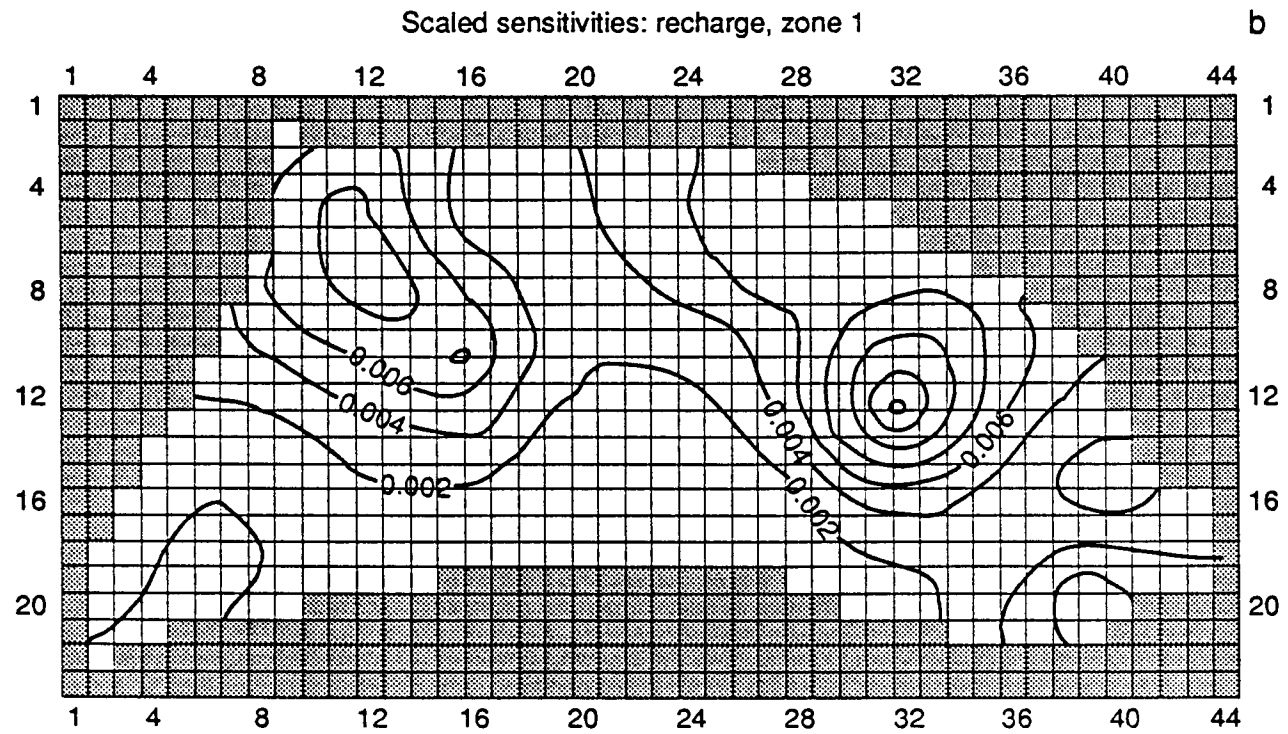
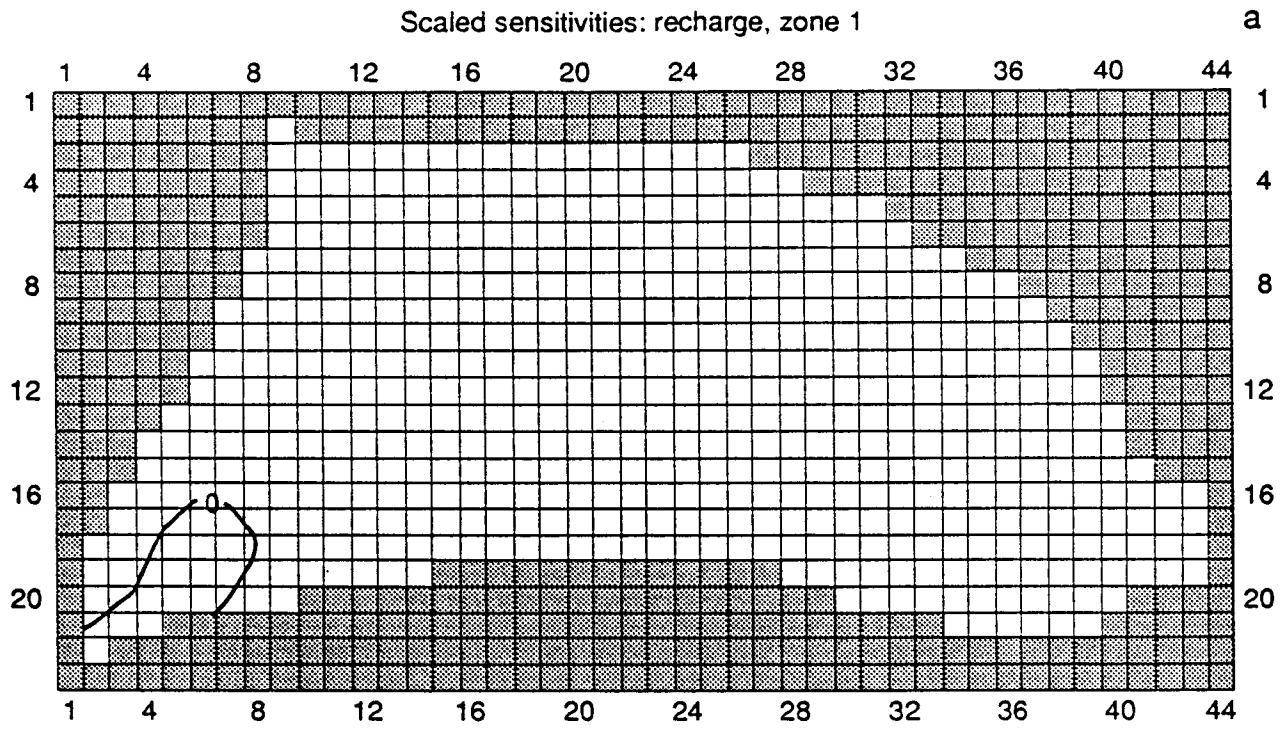


Figure A5-18.

Scaled sensitivities: evapotranspiration, zone 1

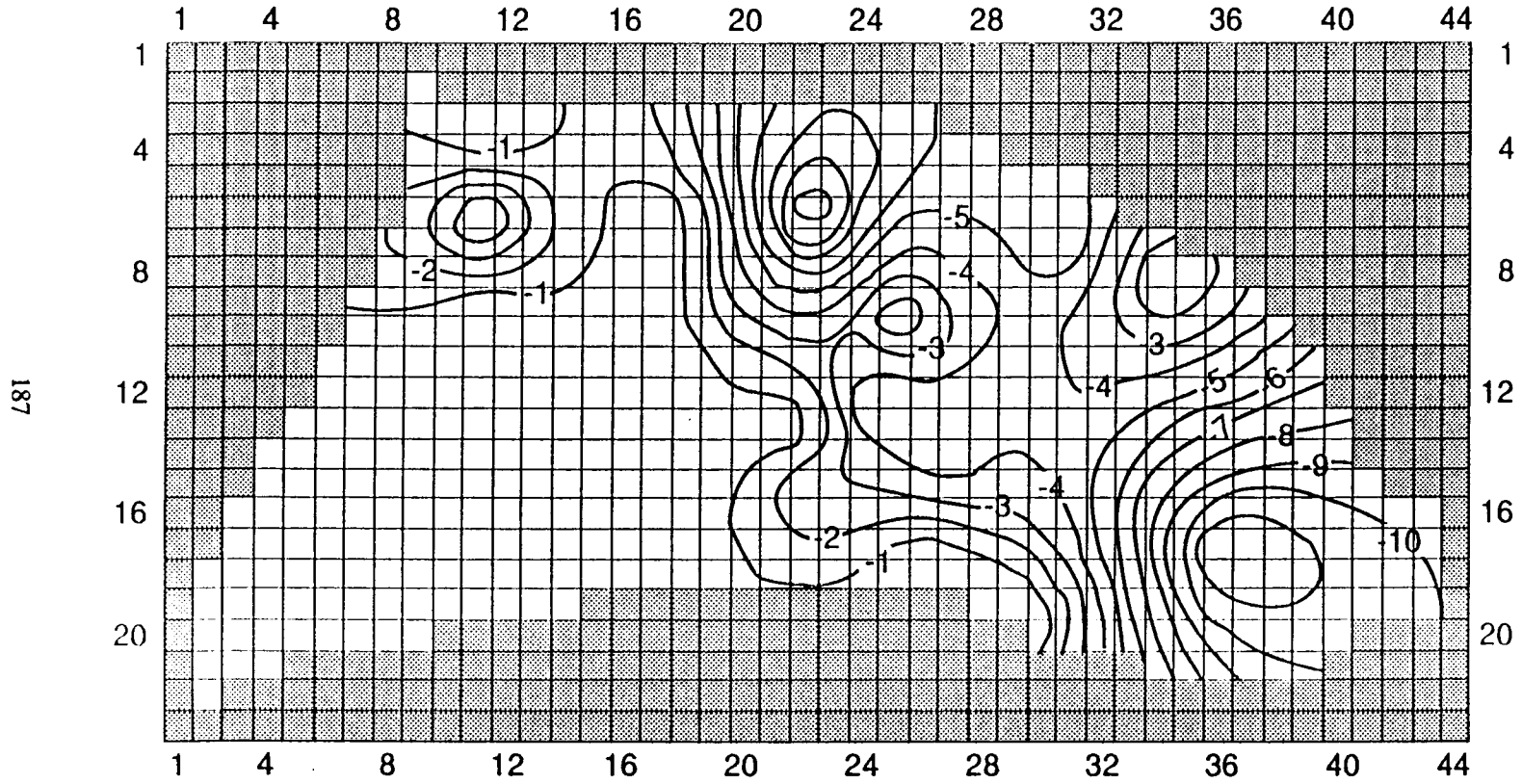


Figure A5-19.

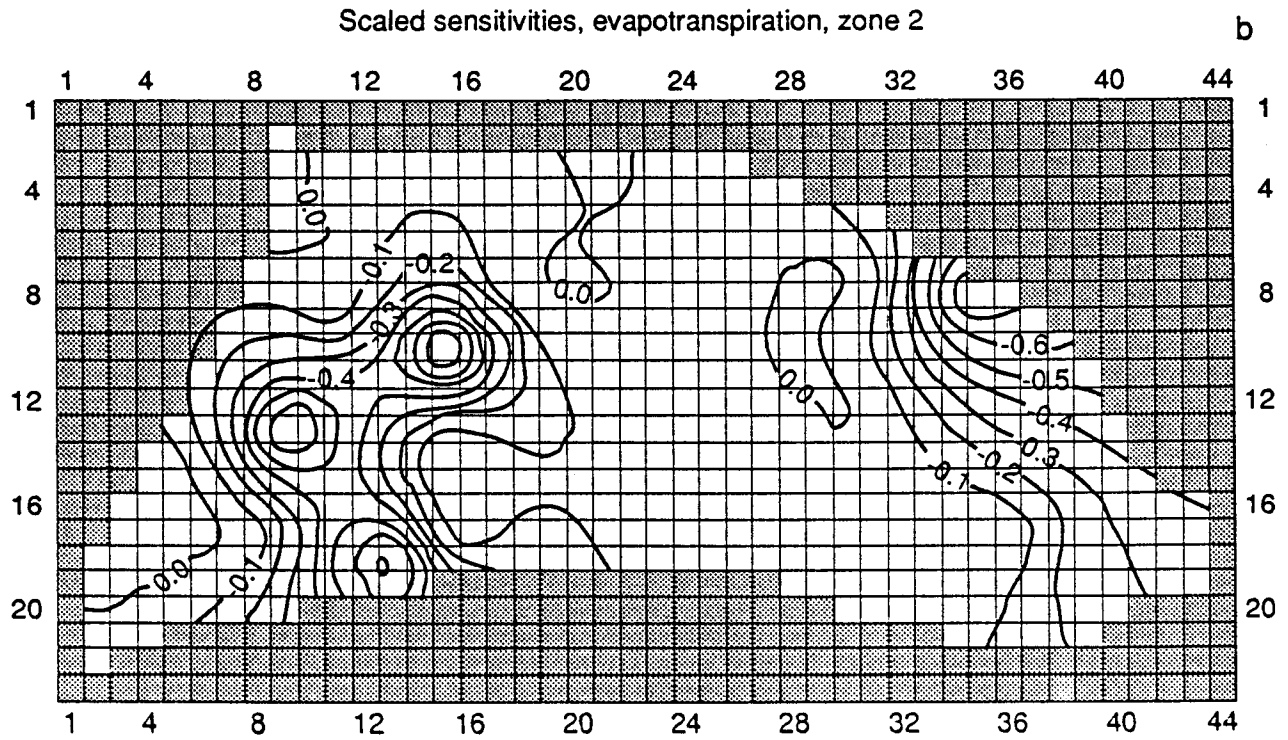
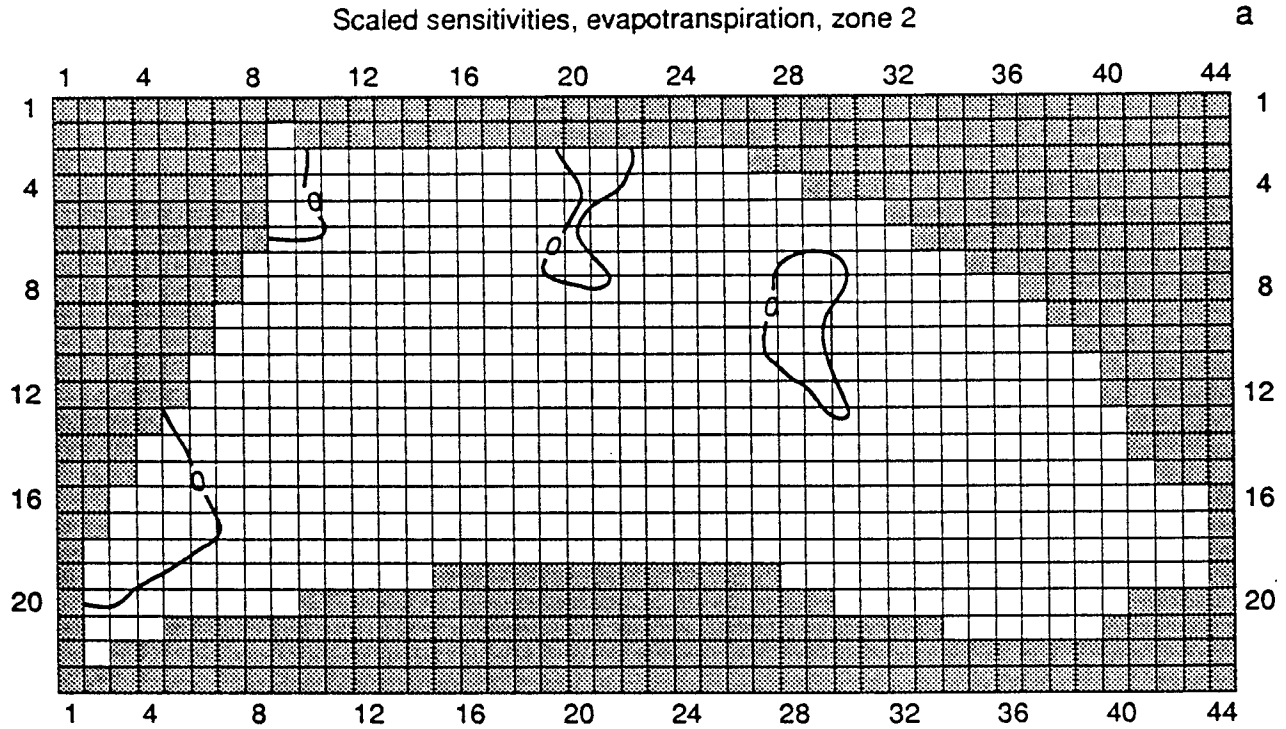


Figure A5-20.

**Appendix 6. Refined-grid modeling of the immediate vicinity of the Quivira National Wildlife Refuge
(8 figures)**

The immediate vicinity of the Quivira NWR (a 12 mi × 12 mi square area—Quivira square) was modeled using a finer grid (1/2 mi × 1/2 mi) than the one used for the lower Rattlesnake Creek model to obtain a more detailed spatial resolution of hydrologic variables. Figure A6-1 displays the two model areas. Geographic Information Systems (GIS) techniques were employed to grid and interpolate data values from the bedrock and from 1991 and 1992 water table maps (ARC-INFO coverages). Figures A6-2 through A6-8 display these gridding and interpolation steps.

The boundary conditions used for the detailed submodel were flux boundary (Neumann) conditions on three sides (left, upper, and right sides of the Quivira square; see fig. A6-1), and no flow boundary conditions for the lower side of the Quivira square. The boundary fluxes were obtained from the coarser lower Rattlesnake Creek model during 1990 (from the transient 1955–1990 simulations) and distributed along the three sides of the Quivira square. The same parameter zonation and parameters as those optimized in the coarser grid (with minor refinement) were employed for the finer grid as well. Average 1988–1990 annual Rattlesnake Creek streamflows at the Zenith gaging station (approximately 20 cfs) were used as incoming streamflows to the study area.

The resulting model-simulated 1991–1992 water balance for the Quivira square is shown in table A6-1. The largest ground-water inflow component to the Quivira NWR is recharge (1.8 in./yr), whereas the largest outflow component is ground-water evapotranspiration (2.3 in./yr), resulting in a net ground-water depletion from aquifer storage (0.6 in./yr).

Table A6-1. Volumetric water budget for 1991–1992 of the Quivira NWR and immediate vicinity^a

Water-balance component	Volumetric rate (acre-ft/yr)
<u>Inflows</u>	
Release from storage	7,136
Underflow into study area	4,368
Recharge	9,831
Stream leakage (losses)	4,041
Total inflows	25,376
<u>Outflows</u>	
Uptake to storage	3,944
Pumping and underflow out of area	3,054
Evapotranspiration	12,426
Stream leakage (gains)	5,952
Total outflows	25,376

Discrepancy = 0.00%

a. Active model grid area = 64,960 acres. Divide volumetric rate values by active model grid area to obtain water balance component expressed in length units

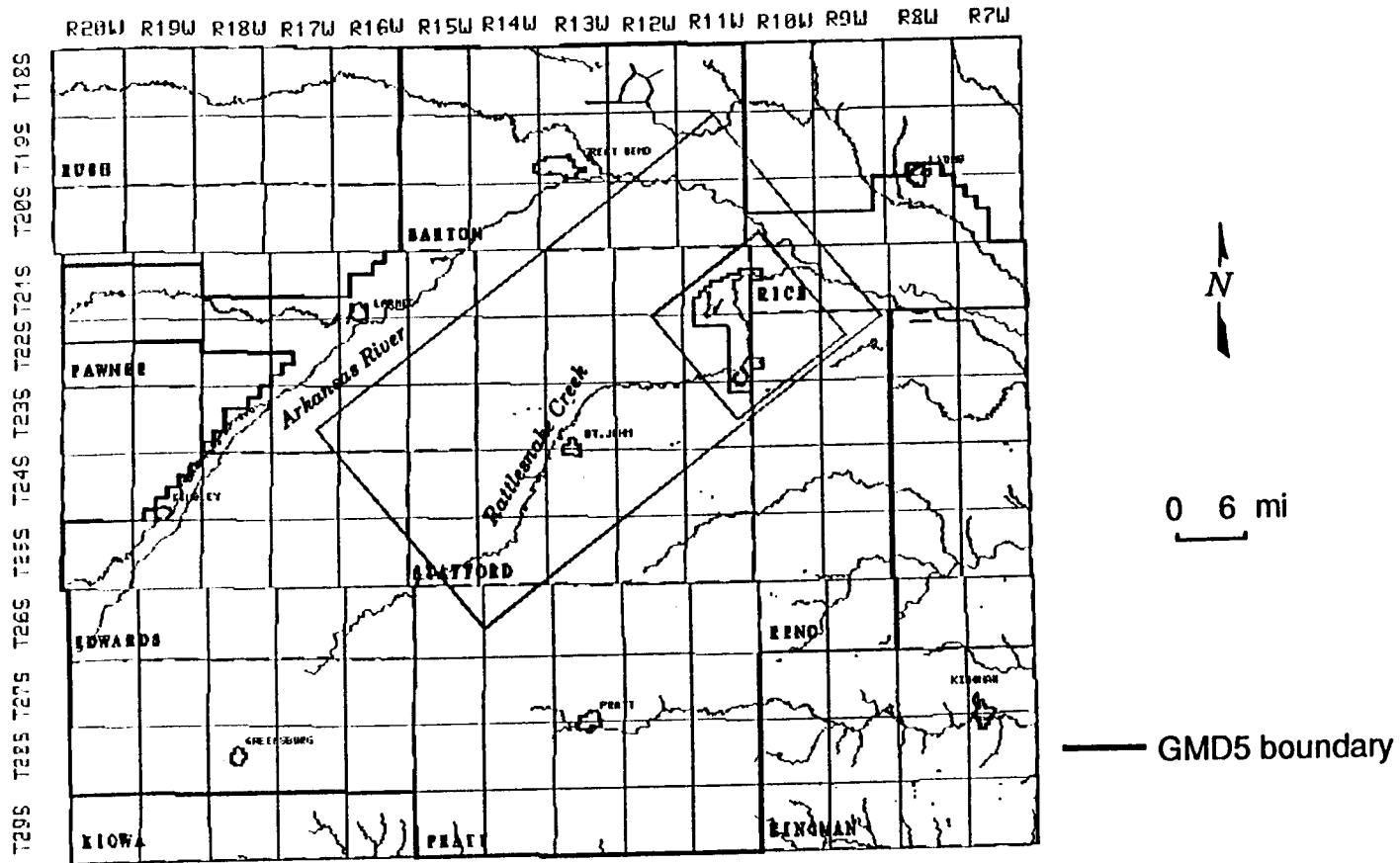


Figure A6-1. Location of study area.

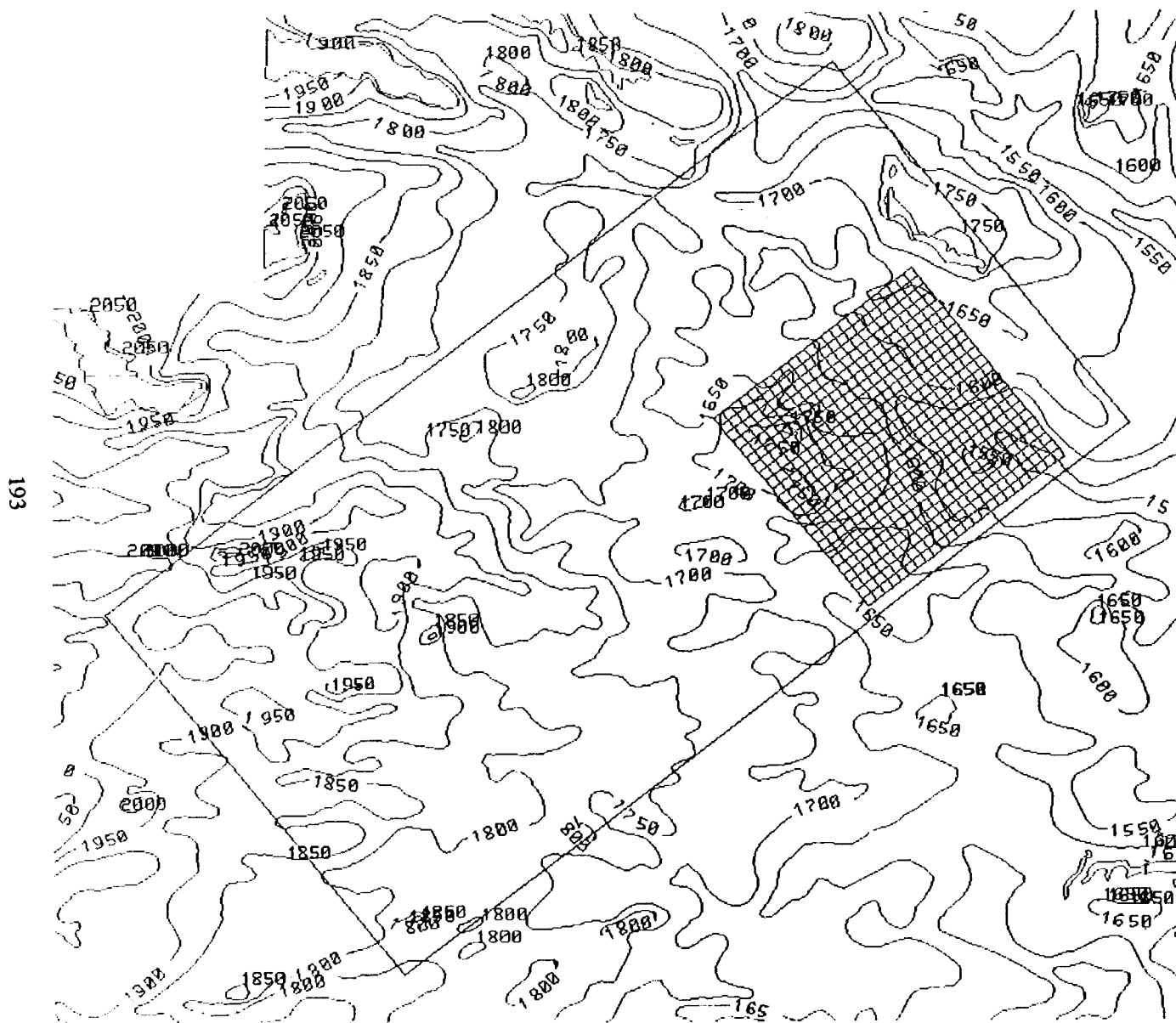


Figure A6-2. Bedrock contours in feet for lower Rattlesnake Creek model area and Quivira square grid (grid size: 0.5 mi x 0.5 mi).

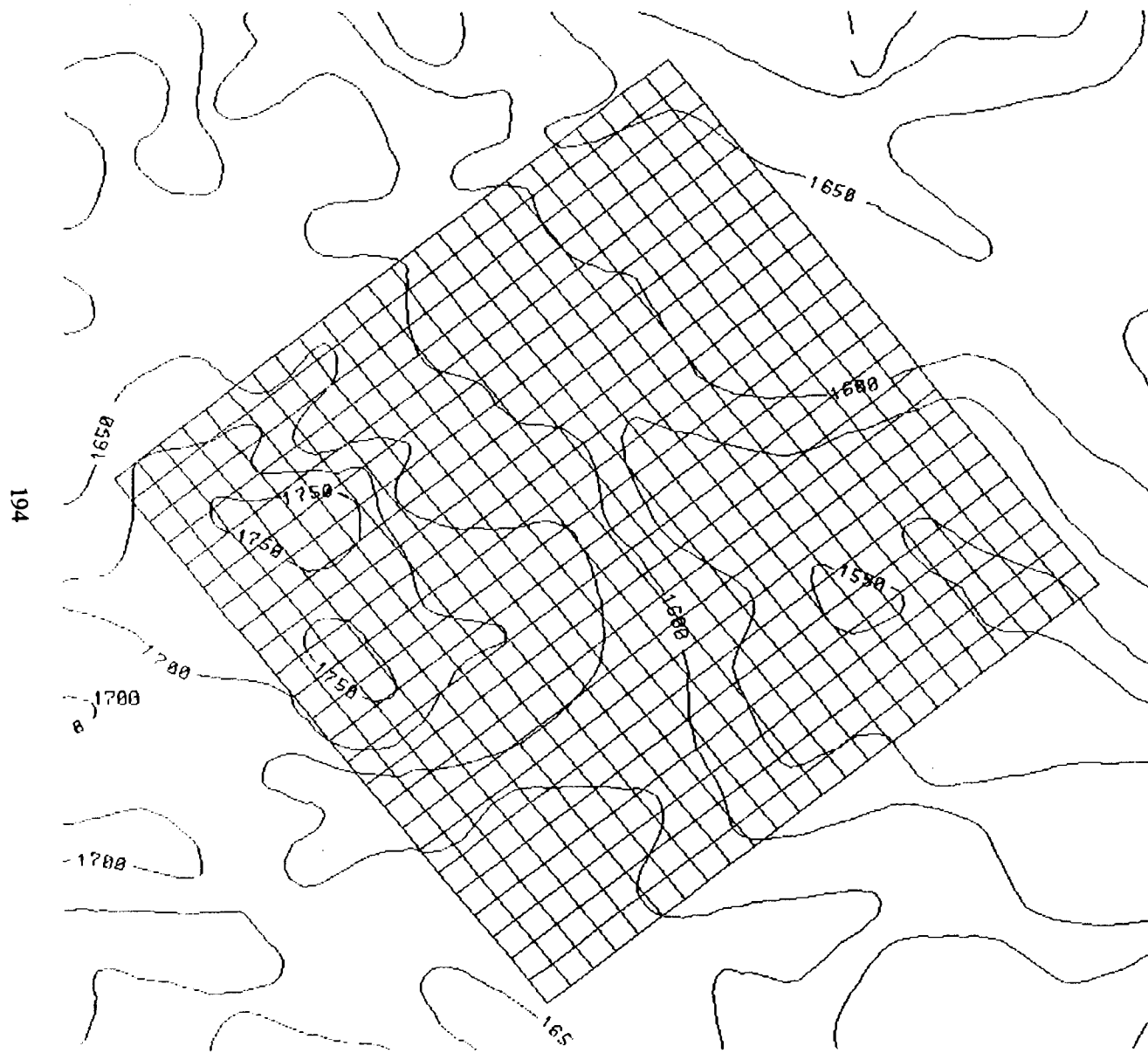


Figure A6-3. Quivira square grid bedrock contours detail (grid size: 0.5 mi x 0.5 mi).

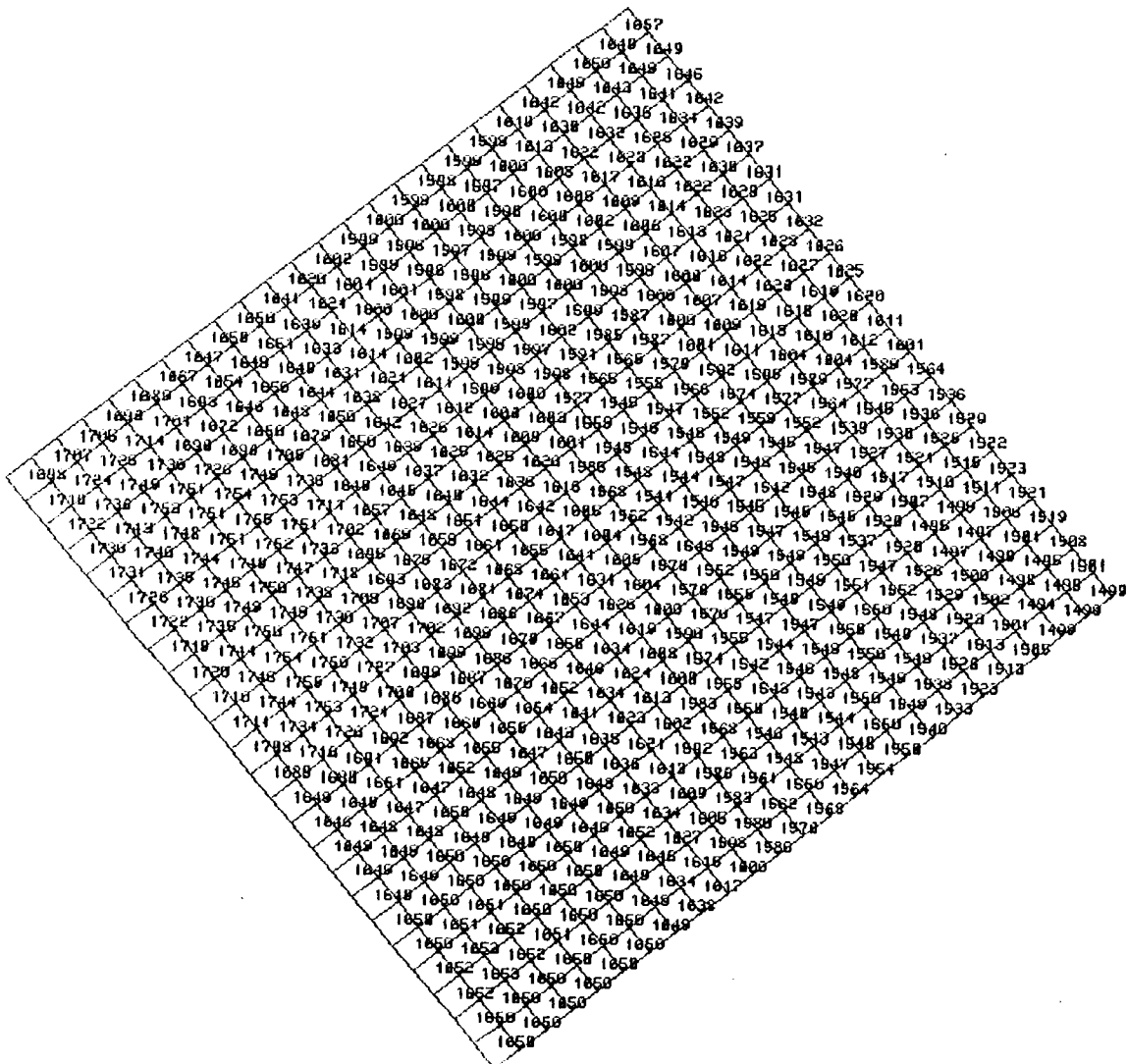


Figure A6-4. ARC-INFO gridded bedrock values for the Quivira square (grid size: 0.5 mi x 0.5 mi).

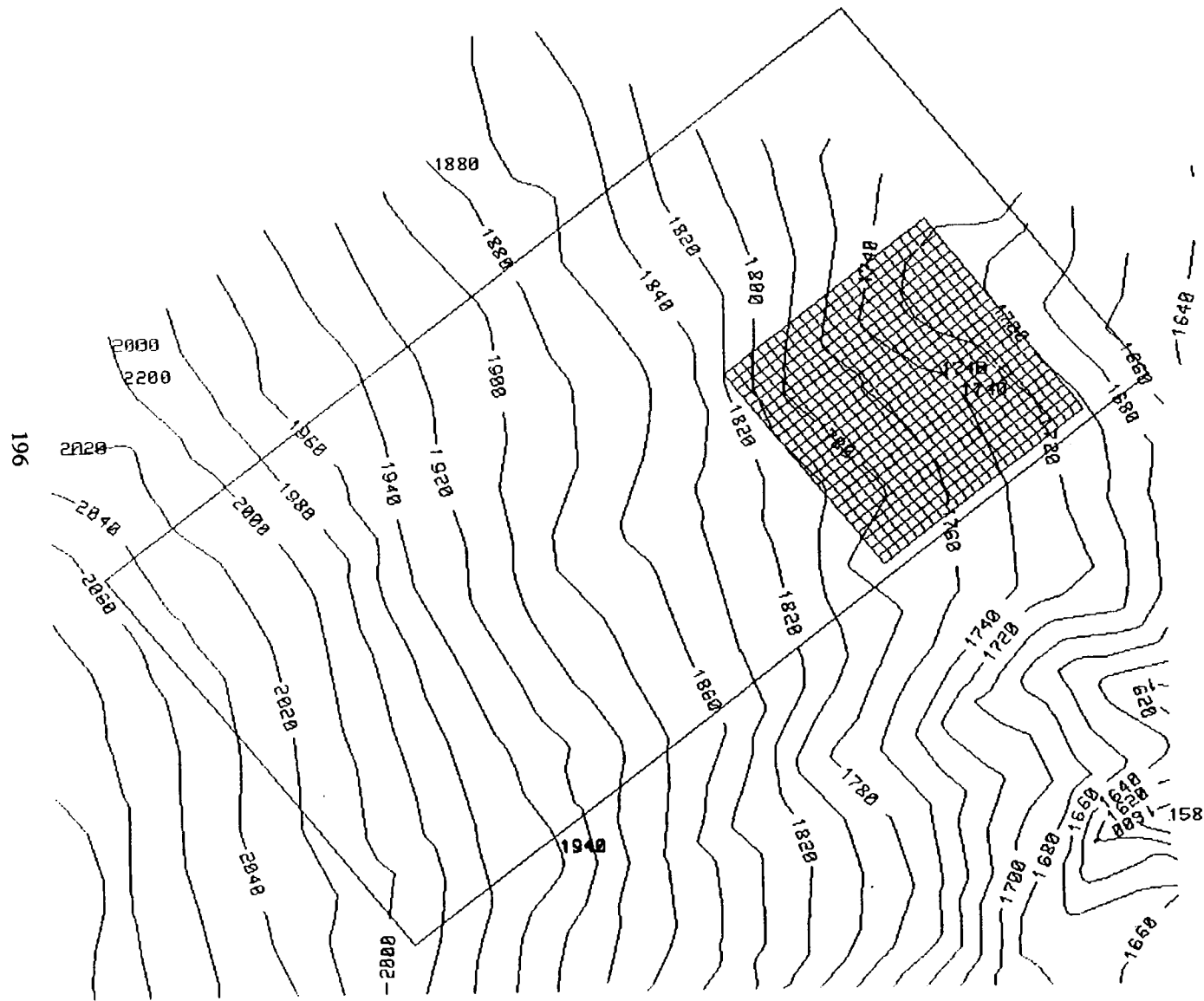


Figure A6-5. January 1991 water table contours for lower Rattlesnake Creek model area and Quivira square grid (grid size: 0.5 mi x 0.5 mi).

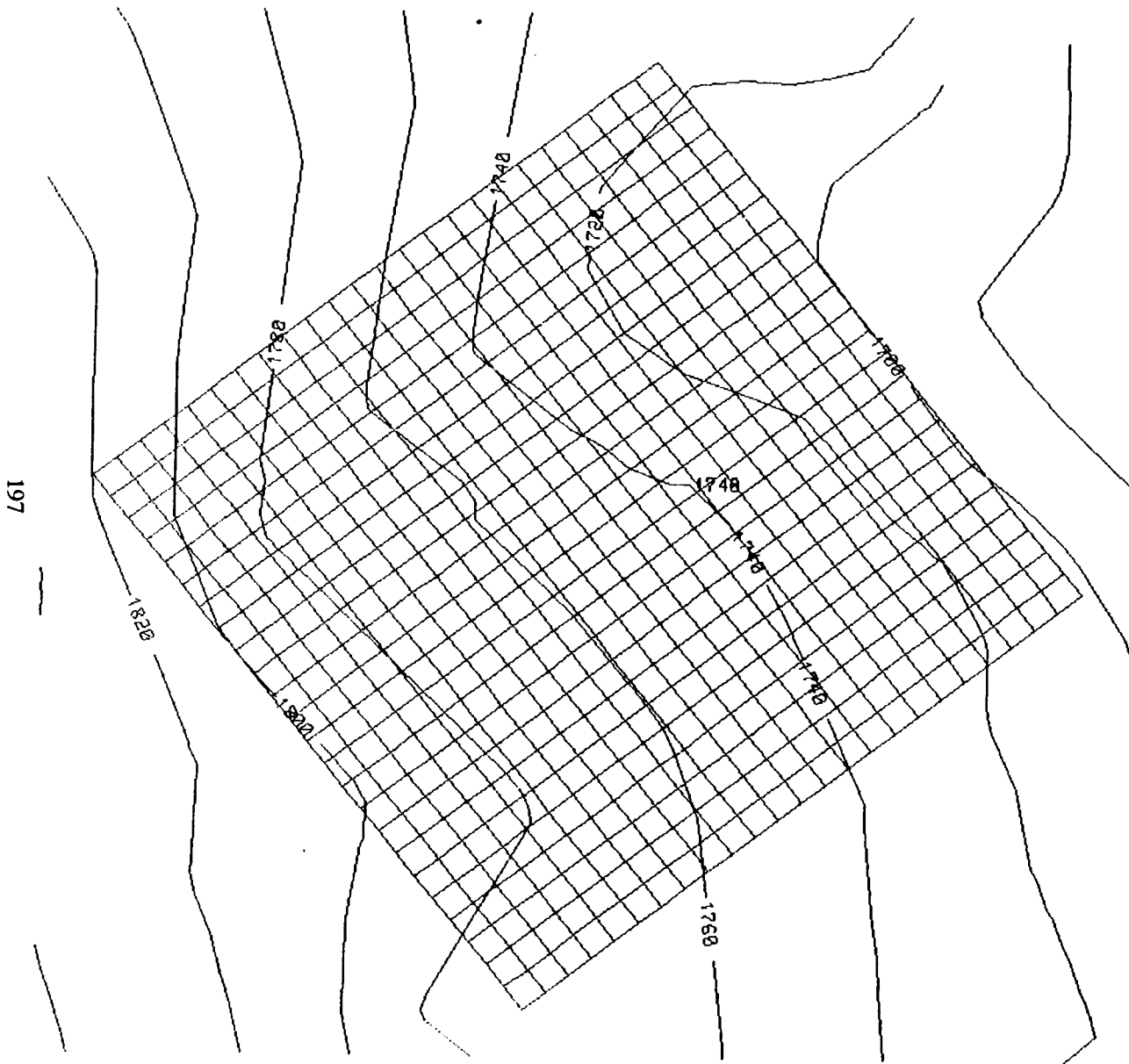


Figure A6-6. Quivira square grid 1991 water table contours detail (grid size: 0.5 mi \times 0.5 mi).

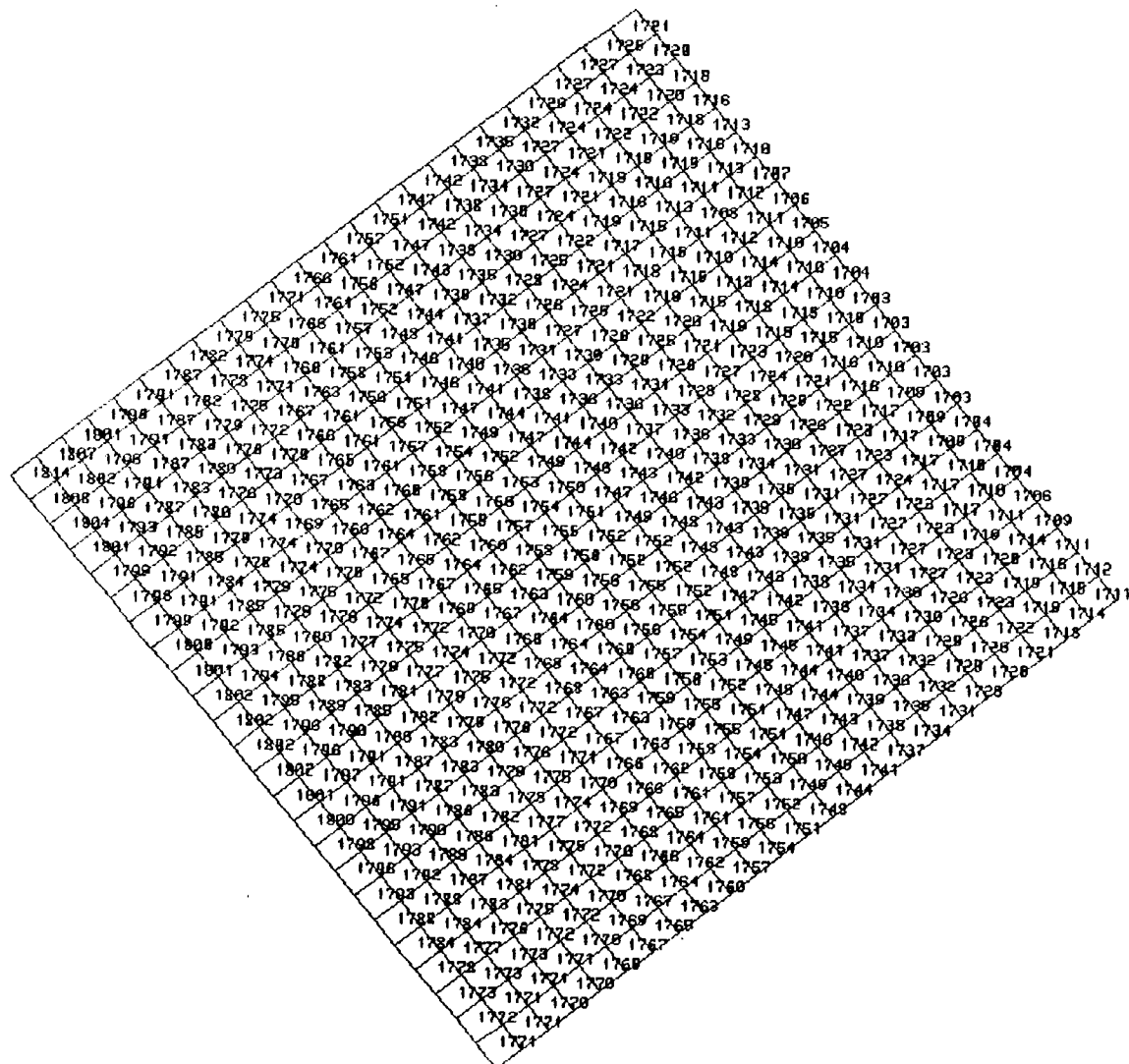


Figure A6-7. ARC-INFO gridded January 1991 water table values for the Quivira square (grid size: 0.5 mi \times 0.5 mi).

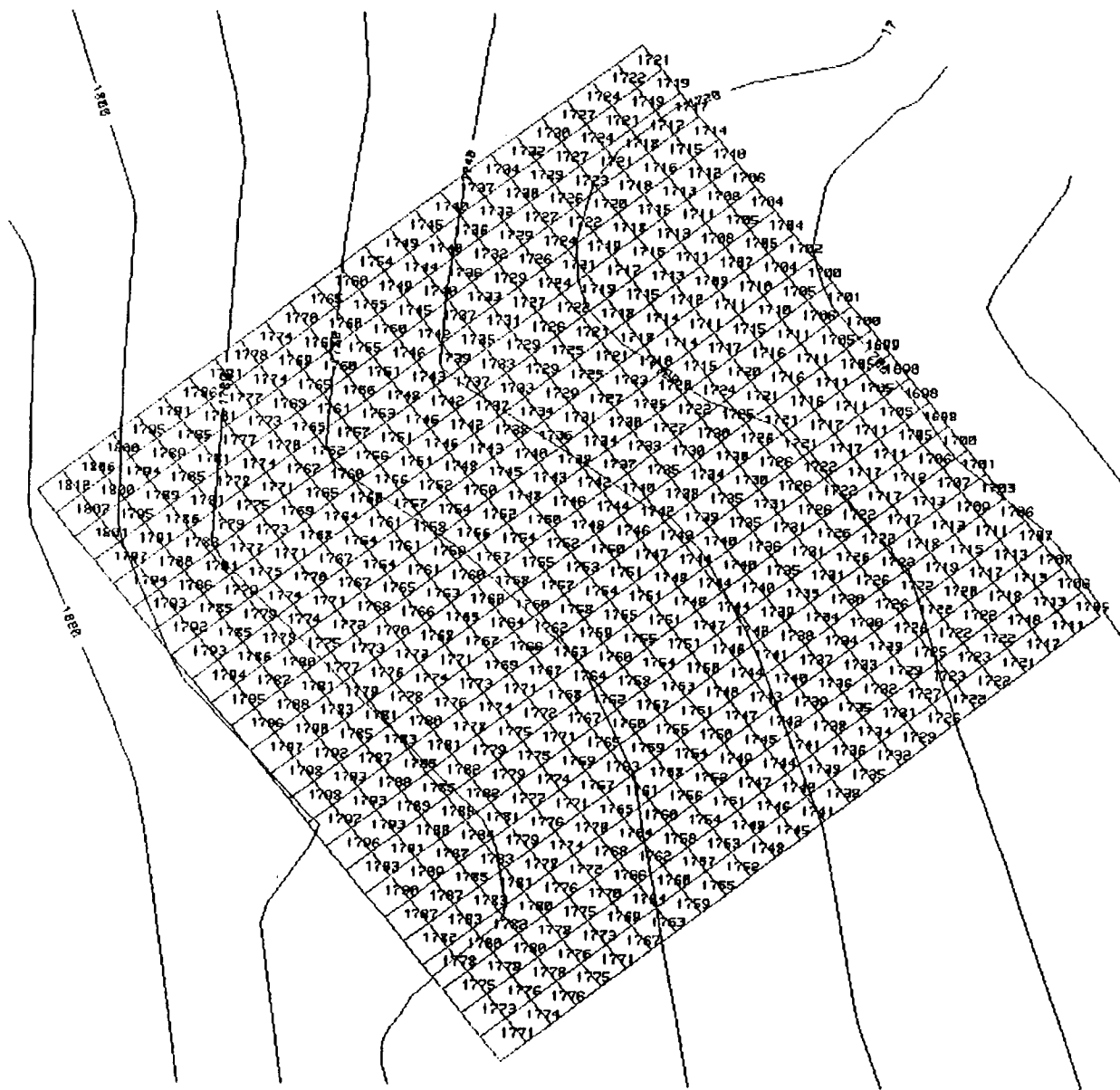


Figure A6-8. Quivira square grid January 1992 water table contours detail and ARC-INFO gridded values (grid size: 0.5 mi x 0.5 mi).